ABSTRACT

Title of dissertation: THE C PROTEINS OF HUMAN PARAINFLUENZA VIRUS TYPE 1 EXERT BROAD CONTROL OVER THE HOST INNATE IMMUNE RESPONSE

Jim Boonyaratanakornkit, Doctor of Philosophy, 2010

Dissertation directed by: Professor Peter Collins
National Institutes of Health

and

Professor Siba Samal
Veterinary Medical Sciences

Human parainfluenza virus type 1 (HPIV1) is an important pediatric respiratory pathogen, and its virulence *in vivo* can be attenuated by introducing mutations into the C gene, a strategy that has been used to design live attenuated candidate vaccines. By tracking gene expression over time, we found that a HPIV1 mutant with a single point mutation in the C gene, referred to as C^{F170S}, and a HPIV1 mutant with complete deletion of the C gene, referred to as P(C-), altered the expression of over 1000 genes, in sharp contrast to wild-type (WT) HPIV1. Using functional bioinformatics, we found that binding sites for the IRF and NF-κB family of transcription factors were over-represented in many of the C protein targeted pathways. By examining the activation of the major components of the type I interferon (IFN) enhanceosome, we found that the C mutant viruses, but not WT HPIV1, activated IRF3 phosphorylation and IκBβ degradation, steps integral to the formation of the interferon enhanceosome. To investigate the basis for the observed antagonism of the host response by the WT C proteins, which are expressed from the C open reading frame as a nested set of carboxy-coterminal proteins, we

searched for but were unable to identify C-interacting proteins among members of the RIG-I/MDA5 pathway. Furthermore, we also found that the WT C proteins supplied in trans could block IFNβ induced by P(C-) HPIV1 infection but not by heterologous inducers of RIG-I and MDA5, namely RSV and poly I:C, respectively. These two lines of evidence suggested that the HPIV1 C proteins do not directly block type I IFN production, such as by interacting with a host factor of the RIG-I/MDA5 pathway. Using knockout mouse embryonic fibroblasts, we found that HPIV1-induced IFNβ production relied mainly on MDA5. Consistent with this observation, a striking amount of intracellular dsRNA was detected during infection with the C mutant HPIV1 viruses but not with WT HPIV1. A marked increase in viral genome, antigenome, and mRNA as well as a decrease in viral protein accumulation provided compelling evidence for dysregulated viral RNA synthesis and an inhibition of viral protein synthesis in the absence of WT C proteins. We suggest that this resulted in an imbalance in the N protein-to-genomic RNA ratio, leading to incomplete encapsidation and an intracellular environment permissive for the generation of dsRNA. PKR activation followed the kinetics of dsRNA accumulation and contributed to both IFNβ induction and the reduction in viral protein levels. This study establishes the profound effects that the C proteins of wild-type HPIV1 play in evading the host response to HPIV1 infection, and it extends our current understanding of the innate immune response to HPIV1 infection.

THE C PROTEINS OF HUMAN PARAINFLUENZA VIRUS TYPE 1 EXERT BROAD CONTROL OVER THE HOST INNATE IMMUNE RESPONSE

By

Jim Boonyaratanakornkit

Dissertation submitted to the Faculty of the Graduate School of the
University of Maryland, College Park, in partial fulfillment
of the requirements for the degree of
Doctor of Philosophy
2010

Advisory Committee:
Professor Siba Samal, Chair
Professor Peter Collins
Professor Xiaoping Zhu
Professor Nathaniel Tablante
Professor Jeffrey DeStefano

Acknowledgements

I would like to thank, first and foremost, Peter Collins, Brian Murphy, Siba Samal, Alexander Schmidt, Emmalene Bartlett, and Henrick Schomacker for their guidance. I am grateful to Sonja Surman and Emerito Amaro-Carambot for their technical assistance.

I would also like to thank Shirin Munir and Christine Winter for providing the sucrose-purified GFP-tagged ΔNS1/NS2 RSV. I am grateful to Owen Schwartz, Juraj Kabat, Lily Koo, and Steven Becker (NIAID Biological Imaging Core) for assistance with confocal microscopy.

John Hiscott, McGill University, provided the VSV-GFP and Yasuhiko Ito, Mie University School of Medicine, provided the mouse anti-HPIV1 HN (8.2.2A and 4.5) antibodies.

J. B. B. was supported in part by funding from the Howard Hughes Medical Institute Research Scholars Program. This research was supported by the Intramural Research Program of the NIH, National Institute of Allergy and Infectious Diseases. This research was also supported in part by a CRADA between NIH and MedImmune, LLC, for the development of PIV and RSV vaccines.

Table of Contents

List of Abbreviations

293: human embryonic kidney cell line

A20: tumor necrosis factor alpha-induced protein 3

A549: human respiratory epithelial cell line

aa: amino acid

ADAR: adenosine deaminase, RNA-specific

AGM: African green monkey

AGT: angiotensinogen

AKT: v-akt murine thymoma viral oncogene homolog

ANOVA: analysis of variance

AP-1: activator protein 1

ATF: activating transcription factor

BAX: BCL2-associated X protein

BCL: B-cell leukemia/lymphoma

BHK: baby hamster kidney cell line

BIRC: Baculoviral inhibitor of apoptosis repeat-containing protein

bp: base pair

BSA: bovine serum albumin

C: C proteins, including C', C, Y1, and Y2.

cAMP: cyclic adenosine monophosphate

CARD: caspase recruitment domain

CASP: caspase

CCL: C-C motif chemokine

cpe: cytopathic effect

CTD: c-terminal domain

CXCL: C-X-C motif chemokine

DAPI: 4',6-diamidino-2-phenylindole

DIABLO: Direct inhibitor of apoptosis-binding protein with low pI

dsRNA: double stranded RNA

DTT: dithiothreitol

DUBA: deubiquitinating enzyme A

EDTA: ethylenediaminetetraacetic acid

EIF: eukaryotic translation initiation factor

ELISA: enzyme-linked immunosorbent assay

F: fusion protein

F170S: a recombinant HPIV1 with the C^{F170S} phenylalanine to serine substitution at amino acid 170 of the C proteins

FACS: fluorescence-activated cell sorting

FADD: Fas-associated via death domain

FBS: fetal bovine serum

FITC: fluorescein isothiocyanate

FLC: full-length antigenomic cDNA clone

FOX: forkhead box

GAPDH: glyceraldehyde-3-phosphate dehydrogenase

GFP: green fluorescent protein

h: hours

HA: hemagluttinin

HAE: Human airway epithelial

HEL: helicase domain

HEp-2: Human epithelial cell line (HeLa contaminant)

HLF: hepatic leukemia factor

HN: hemagluttinin/neuraminidase protein

HPIV: Human parainfluenza virus

IFI: interferon-induced protein

IFIT: IFN-induced protein with tetraicopeptide repeats

IFN: interferon

IFNAR: type 1 interferon receptor

Ig: immunoglobulin

IKK: IκB kinase

IL: interleukin

IP: immunoprecipitation

IPS1 (or IPS-1): interferon beta promoter stimulator protein 1

IRF: interferon regulatory factor

ISG: IFN-stimulated gene

ISGF: interferon-stimulated gene factor

ISRE: interferon-stimulated response elements

IU: international unit

IκB: inhibitor of of kappa light polypeptide gene enhancer in B-cells

JAK: Janus kinase

JNK: c-Jun N-terminal kinase

JUN: v-jun sarcoma virus 17 oncogene homolog

L: large polymerase protein

LD_{50}: 50% lethal dose

M: matrix protein

MAPK: mitogen-activated protein kinase

MAVS: mitochondrial antiviral signaling protein

MCL: myeloid cell leukemia

MDA5 (or MDA-5): melanoma differentiation-associated protein 5

MEF: mouse embryonic fibroblast

MEKK1: mitogen-activated protein kinase kinase kinase 1

MEM: minimum essential medium

MIAME: minimum information about a microarray experiment

min: minutes

MK2: Rhesus monkey kidney cell line

MOI: multiplicity of infection

MRC-5: normal human fetal lung cell line

MTC: multiple testing correction

MVA: Modified Vaccinia Ankara

MX: myxovirus (influenza virus) resistance

MYB: v-myb myeloblastosis viral oncogene homolog

n.s.: non-specific

N: nucleoprotein

nAb: neutralizing antibody

NEMO: NF-κB essential modulator

NF-κB: nuclear factor of kappa light polypeptide gene enhancer in B-cells 1

NS: nonstructural protein

NSm: medium segment nonstructural protein

NSs: small segment nonstructural protein

NU: neutralizing unit

OAS: oligoadenylate synthetase

ORF: open reading frame

P(C-): a recombinant HPIV1 that does not express any of the C proteins

p.i.: post-infection

P: phopho or phosphate or also HPIV1 phosphoprotein

P38: mitogen-activated protein kinase 14

PBS: phosphate buffered saline

PFA: paraformaldehyde

PFU: plaque forming unit

PI3K: phosphatidylinositol 3-kinase

PKR: double stranded RNA-dependent protein kinase

Poly I:C: polyinosinic:polycytidylic acid

PRD: positive-regulatory domain

PVDF: polyvinylidene fluoride

Rel: v-rel reticuloendotheliosis viral oncogene homolog

rHPIV: recombinant HPIV

RIG-I: retinoic acid-inducible gene-I

RLR: RIG-I-like receptors

RSV: respiratory syncytial virus

RT: room temperature or reverse transcription

RT-qPCR: reverse transcription-quantitative polymerase chain reaction

SDS-PAGE: sodium dodecyl sulfate polyacrylamide gel electrophoresis

SE (or S.E.): standard error

SeV: Sendai virus

sh: small hairpin

shCON: control small hairpin RNA

shPKR: PKR small hairpin RNA

SOCS: suppressor of cytokine signaling

SOX: sex determining region Y-box

SPIB: Spi-B transcription factor

ssRNA: single stranded RNA

STAT: signal transducer and activator of transcription

TAK1: TGFβ-activated kinase 1

TANK: TRAF family member-associated NF-κB activator

TBK1: TANK-binding kinase 1

TCF1: transcription factor 1, also known as hepatocyte nuclear factor 1α or IFN production regulator factor

$TCID_{50}$: 50% tissue culture infectious dose

TFBS: transcription factor-binding site

TFIIH: transcription factor II H

TIR: Toll-interleukin-1 receptor domain

TLR: Toll-like receptor

TM: transmembrane

TNF: tumor necrosis factor

TNFRSF: tumor necrosis factor receptor superfamily member

TNFSF: tumor necrosis factor ligand superfamily member

TRADD: TNFRSF1A-associated via death domain

TRAF: TNF receptor-associated factor

TRAIL: TNF-related apoptosis-inducing ligand

TRAIL-R: TRAIL receptor

TRIF: TIR domain-containing adapter protein inducing interferon beta

TRIM: tripartite motif-containing protein

Ub: ubiquitin

UDP: uridine diphosphosphate

Vero: African green monkey kidney cell line

VISA: virus-induced-signaling adapter

VP: viral protein

vRNA: viral RNA

VSV: vesicular stomatitis virus

WB: Western blot

WT (also wt): wild-type

ZNF: zinc finger

Chapter 1: General Introduction

Background and Rationale

Human parainfluenza virus type 1 (HPIV1) is an important and uncontrolled pediatric respiratory pathogen that causes a significant burden of disease, mainly in young children, the immunocompromised, and the elderly (30, 42, 58, 79, 134, 154). HPIV1 is the single most common cause of laryngotracheobronchitis or croup. Other clinical manifestations of HPIV1 range from mild disease, including rhinitis, pharyngitis, and otitis media, to severe lower respiratory disease, including bronchitis, bronchiolitis, and pneumonia (**Figure 1**) (30). In all, 4 major serotypes of human parainfluenza virus have been described, including HPIV1, 2, and 3 which, collectively, are the second most common cause of pediatric respiratory hospitalizations, only surpassed by respiratory syncytial virus (RSV) (42, 134). Disease caused by HPIV4 is less frequently diagnosed and typically less severe (13). Licensed vaccines are currently not available against any of the HPIVs but ongoing vaccine development efforts that employ cDNA derived live attenuated viruses have progressed to phase 1/2 clinical evaluation (89, 91, 93).

Figure 1. The clinical manifestations of HPIV1 infection.

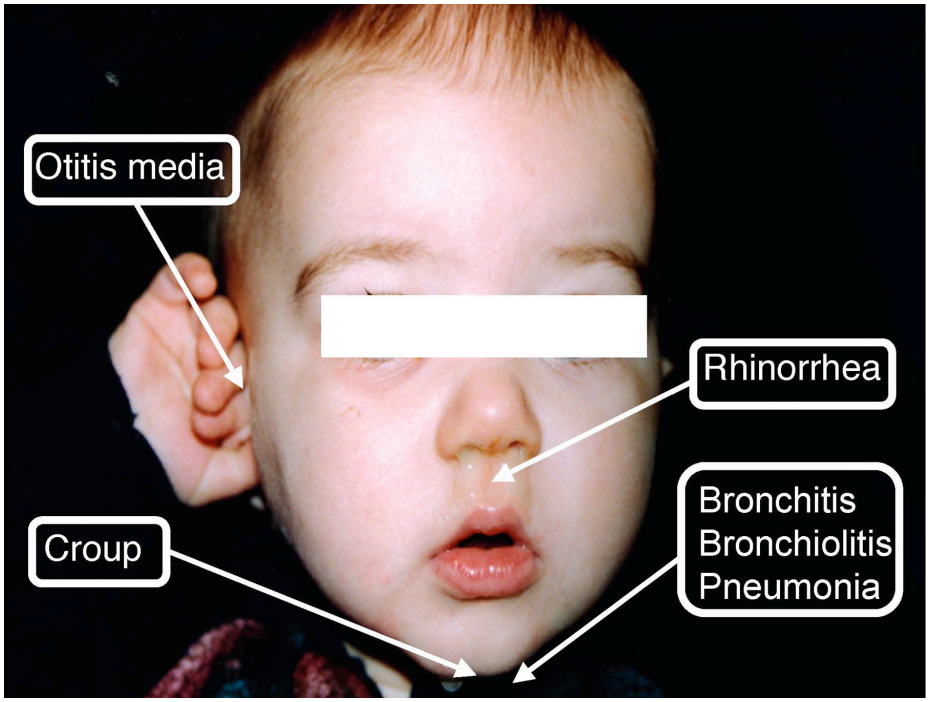

Viral Tropism, Animal Models, and Cell Culture

HPIV1 was first isolated from infants and children with lower respiratory tract disease (23). The virus infects and replicates in the epithelial cells that line the respiratory tract, including the mucus membranes of the nose and throat, larynx, trachea, bronchi, and lower airways (143). *In vivo*, HPIV1 is generally considered a pneumotropic virus since it buds from the apical surface instead of the basolateral surface (10, 136). The virus replicates well in the respiratory tract of hamsters, guinea pigs, cotton rats, ferrets, and non-human primates but infection is typically self-limited and asymptomatic with minimal pulmonary pathology (26, 37). In cell culture, HPIV1 replicates well in both simian and human kidney cells and human respiratory cells but trypsin must be supplied in the medium.

Viral Attachment and Entry

The hemagglutinin-neuraminidase (HN) transmembrane surface glycoprotein mediates attachment by binding sialic acid on cell surfaces. The HN protein also triggers fusion by interacting with the F protein (130, 151). The F protein promotes viral entry by mediating fusion between the viral envelope and the cell membrane. The inactive precursor F_0 protein is converted to the fusogenic F_1 and F_2 polypeptides after cleavage by a secretory protease, and a hydrophobic fusion peptide in F_1 initiates fusion (211). Together, the two surface glycoproteins HN and F constitute the major protective and the sole neutralizing antigens against infection (94, 153, 175).

Viral Replication and Transcription

HPIV1 is an enveloped, single stranded, negative sense, nonsegmented RNA virus in the Paramyxoviridae family (**Figure 2**). Upon attachment and fusion, the viral genome enters, replicates in the cytoplasm, and buds as pleomorphic, spherical virions through the plasma membrane (191). The viral genome, 15.6 kb in length, consists of 6 genes (3' – N-P/C-M-F-HN-L – 5') that encode the nucleoprotein (N), phosphoprotein (P), C proteins (C), matrix protein (M), fusion protein (F), hemagglutinin-neuraminidase protein (HN), and the large polymerase protein (L). Replication of the parainfluenza viral genome proceeds through an intermediate positive sense antigenome. Viral replication occurs in a nucleocapsid that consists of viral RNA-dependent RNA polymerase and P protein in association with N-bound genome and antigenomes. The L polymerase

catalyzes both RNA replication and transcription. The P protein binds to both the N and L proteins and serves as a polymerase cofactor that links the L protein to the N-RNA template (74). The N protein has traditionally been thought to function as a highly stable and ribonuclease resistant coat that protects the viral genome and antigenome from nuclease digestion (100). N encapsidation also leads to the formation of a helical structure that may align the major promoter at the 3' end of the viral genome and that may provide interaction sites for the assembly of nucleocapsids during viral budding (112, 186). The nucleotide length of the viral genome and antigenome must be an even multiple of six for efficient replication to occur. This "rule of six" is thought to arise from the need to fully encapsidate the entire length of the genome with a chain of N protein monomers that span exactly six nucleotides so that the phase or position of the nucleotides of the major promoter relative to each N monomer, i.e. positions 1 through 6, is conserved (102, 170, 194).

A single promoter at the 3' end of the genome promotes replication and leads to sequential transcription. Each gene is flanked by an upstream gene start region that directs viral polymerase initiation and mRNA capping and a downstream gene end that directs transcriptional termination and polyadenylation (138). Since polymerase reinitiation is imperfect, polymerase drop-off leads to a gradient of mRNA transcription that decreases with increasing distance from the 3' major promoter, i.e. N mRNA is more abundant than L mRNA (27).

Each gene of the HPIV1 genome encodes a single major protein with the exception of the P/C gene, which encodes the P protein in one open reading frame and a nested set of four carboxy-coterminal C proteins (C', C, Y1, and Y2) expressed from individual start sites in a second open reading frame. An unconventional GUG start codon for C' reduces translation initiation efficiency and thereby allows leaky scanning by the ribosome to initiate at the next downstream start codon for C. In contrast, the ribosome accesses the Y1 and Y2 start codons by discontinuous scanning-independent shunting from the 5' cap (32, 34). Recent studies, including the findings from this dissertation and from others in the lab, have shown that the C proteins play a critical role in HPIV1 virulence by inhibiting apoptosis, regulating type I interferon (IFN) production and signaling, and controlling the transcription of a large number of host genes (9, 17, 18, 192).

Figure 2. Diagrammatic representation of the HPIV1 virion (top) and its genome organization (bottom). The N gene and the N proteins encapsidating the viral genome are colored in green. The P gene and the P proteins associated with the viral polymerase are colored in yellow. The C ORF is colored in orange. The M gene and the M proteins located on the inner face of the viral envelope are colored in blue. The F gene and the F surface glycoproteins are colored in aqua. The HN gene and HN suface glycoproteins are colored in red. The L gene and the L polymerase are colored in purple.

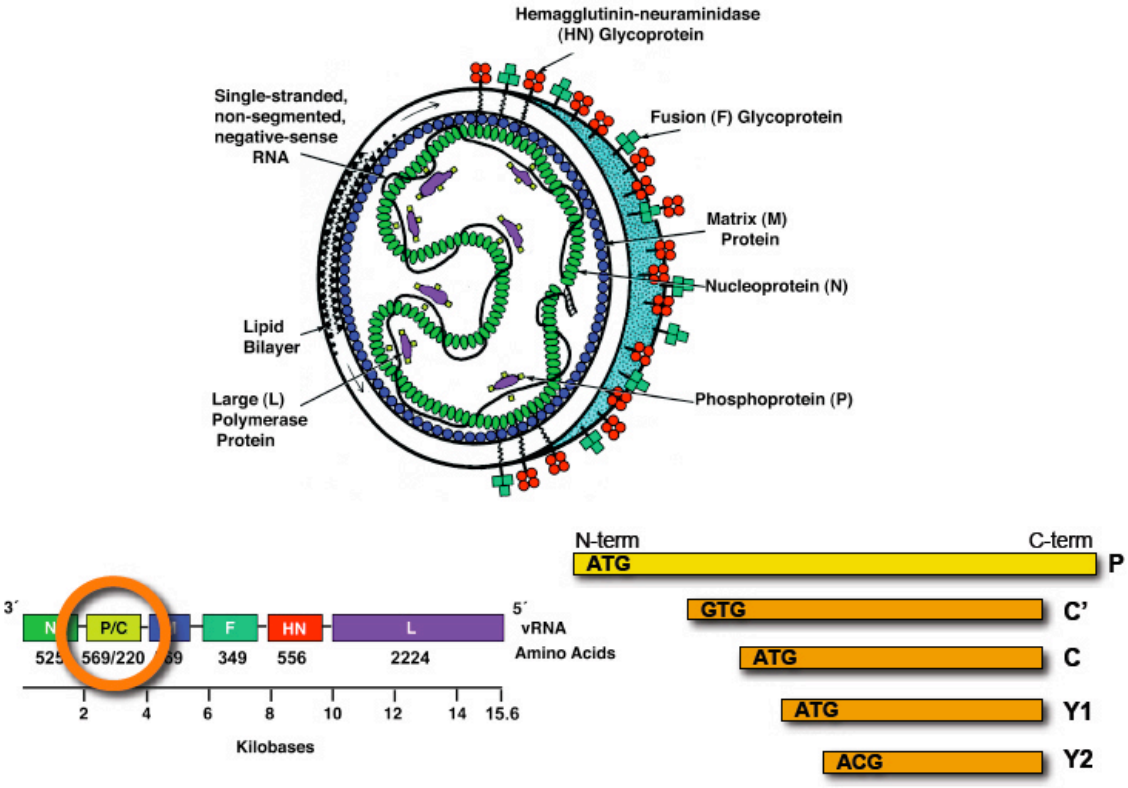

The Innate Immune Response and Type I IFN

Innate immunity, considered the front-line of host defense, comprises the early phases of the host response to infection and generally discriminates between groups of related

pathogens. The innate immune response also contributes, by antigen presentation and the secretion of cytokines, to the induction of effectors in the adaptive immune response, including cytotoxic T lymphocytes and secretory and serum neutralizing antibodies (77, 172, 184). An important component of the innate immune response to viral infection is the production of type I IFN, signaling through its receptor, and the subsequent establishment of an antiviral state. The induction of IFN synthesis following virus infection depends on a number of pattern-recognition receptors that recognize conserved pathogen-associated molecular patterns and initiate downstream signaling cascades (**Figure 3**). The presence of dsRNA, an intermediate of RNA viral replication, is recognized as a pathogen-associated molecular pattern by Toll-like receptor 3 (TLR3) and two caspase recruitment domain (CARD)-containing RNA helicases, retinoic acid-inducible gene I (RIG-I) and melanoma associated-differentiation gene 5 (MDA5), which act as intracytoplasmic sensors of dsRNA (2, 76, 147, 180, 212, 214). Whereas TLR3 mainly senses extracellular dsRNA on the surface and in the endosomal compartment of antigen-presenting cells, RIG-I and MDA5 are constitutively present and detect intracellular dsRNA (2, 214). RIG-I activation by dsRNA requires ubiquitination of its CARD domain by the ubiquitin ligase TRIM25 (45). The exact nature of the dsRNA ligands recognized by RIG-I and MDA5 is still controversial (203). Currently, it is thought that RIG-I binds to 5' triphosphorylated dsRNA, whereas MDA5 binds higher-order webs of dsRNA and ssRNA (148, 165). TLR3 signals through an adaptor called TIR domain-containing adaptor inducing IFNβ (TRIF), while RIG-I and MDA5 recruit another CARD-containing adaptor called mitochondrial antiviral signaling protein (MAVS, also referred to as IPS-1, Cardif, or VISA). MAVS contains a transmembrane

domain that targets the protein to the mitochondria, implicating a role for the mitochondria as a signaling platform for the innate immune response (167). MAVS relays the signal to two ubiquitin ligases TRAF3 and TRAF6. The deubiquitinases DUBA and A20 negatively regulate IFNβ induction by removing ubiquitin from TRAF3 and TRAF6, respectively. TRAF3 activates the kinases TBK1 and IKKε, which phosphorylate IRF3 (interferon regulatory factor 3) (41, 99, 140, 167, 207). Once activated, IRF3 translocates into the nucleus and binds the positive regulatory domain III (PRDIII) of the IFNβ promoter. TRAF6 activates IKKβ and induces the proteasome-mediated degradation of IκB which allows NF-κB to translocate into the nucleus and bind PRDII (167, 207). After the host cell recognizes and signals the presence of foreign RNA, IRF-3 and NF-κB, together with ATF-2/c-Jun (AP-1), form an enhanceosome that binds to the IFNβ promoter, inducing transcription of the IFNβ gene. Although crystal structures of ATF-2 and c-Jun bound to PRDIV of the IFNβ promoter are known, the viral triggers that activate the MAPK pathway leading to ATF-2 and c-Jun phosphorylation and dimerization are less well understood (142). Once type I IFN is produced and secreted, it binds to the type I IFN receptor on the surface of the infected and neighboring cells to induce a robust antiviral response (121, 183).

Figure 3. Diagrammatic representation of the cellular signal transduction pathways that can be activated by RNA virus infection and lead to IFNβ production. IFNβ expression relies on the activation of three transcription factors IRF3, NF-κB, and AP-1 that bind the IFNβ enhanceosome. Dotted lines represent protein-protein interactions. The dotted line with an arrowhead signifies binding of the AP-1 transcription factor to PRDIV. The dashed lines signify that the viral triggers that activate MEKK1 and the MAPK signal transduction pathway leading to ATF2 and JUN phopshorylation are not yet fully characterized.

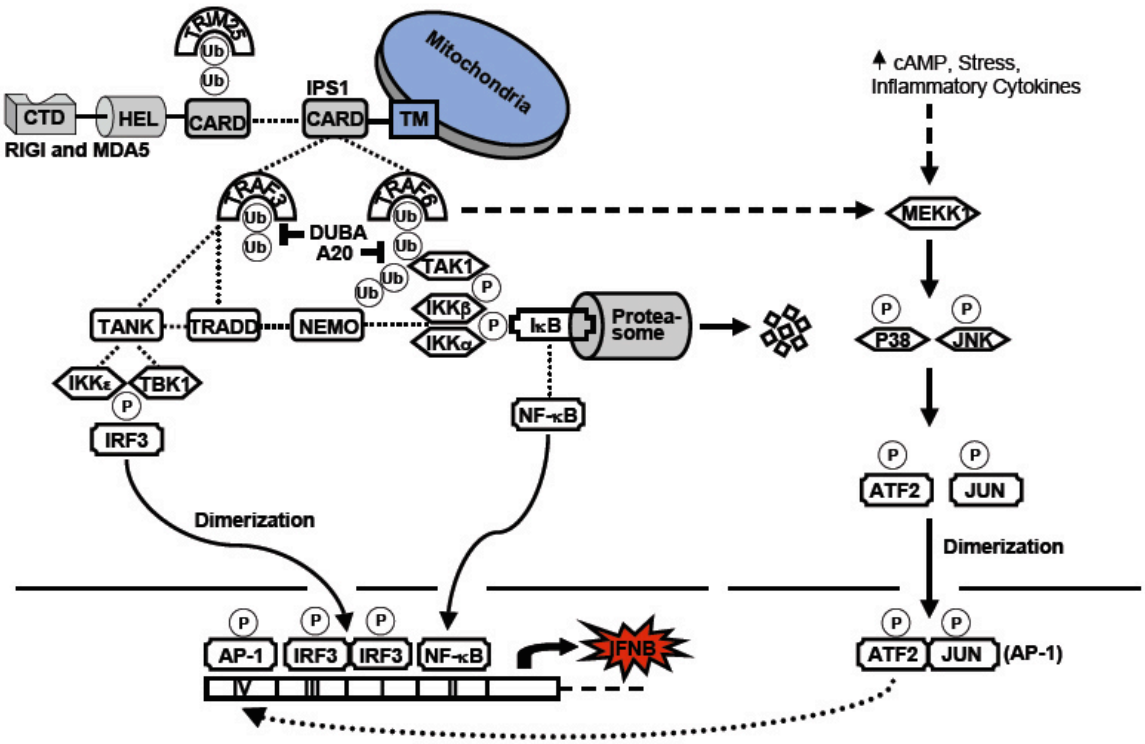

The transcriptional activation of type I IFN is biphasic. One gene encodes the prototypical IFNβ, while more than a dozen IFN species comprise the IFNα family (183). In humans, at least 23 gene loci on chromosome 9 correspond to the IFNα family, and at

least 14 are known to encode functional proteins (144). Recognition of viral infection results in phosphorylation of constitutively expressed IRF3 to induce IFNβ and IFNα1 expression in human cells as part of the early response to virus infection. Once early type I IFN is produced and secreted, it binds to the type I IFN receptor on the surface of the infected and neighboring cells and activates the JAK-STAT signal transduction cascade. The JAK1 and TYK2 kinases are activated by autophosphorylation and phosphorylate STAT1 and STAT2, inducing the formation of IFN-stimulated gene factor 3 (ISGF3) which consists of a heterotrimeric complex of STAT1, STAT2, and IRF9 (**Figure 4**). ISGF3 binds to the IFN-stimulated response elements (ISRE) within the promoter regions of several hundred IFN-inducible genes, including 2'-5'-oligoadenylate synthetase (OAS), dsRNA dependent protein kinase (PKR), and IRF7. The *de novo* produced IRF7, which is highly homologous to IRF3, can also undergo phosphorylation by TBK1, dimerize, translocate into the nucleus, and then activate production of additional type I IFNs. Unlike IRF3 though, IRF7 can form a homodimer or heterodimerize with IRF3 to efficienty activate the expression of both the IFNβ gene and the full set of IFNα genes (73, 163). Thus, immediate-early expression of IFNβ and IFNα1 occurs soon after viral infection is detected, while delayed expression of the entire type I IFN family, induced by IRF7, occurs only after IFNβ and IFNα1 secretion, receptor binding, and signaling to amplify a robust feed-forward antiviral response (121, 183).

Figure 4. Diagrammatic representation of the type 1 IFN signaling pathway from IFN receptor activation to the formation of the STAT1, STAT2, and IRF9 transcription factor complex (ISFG3).

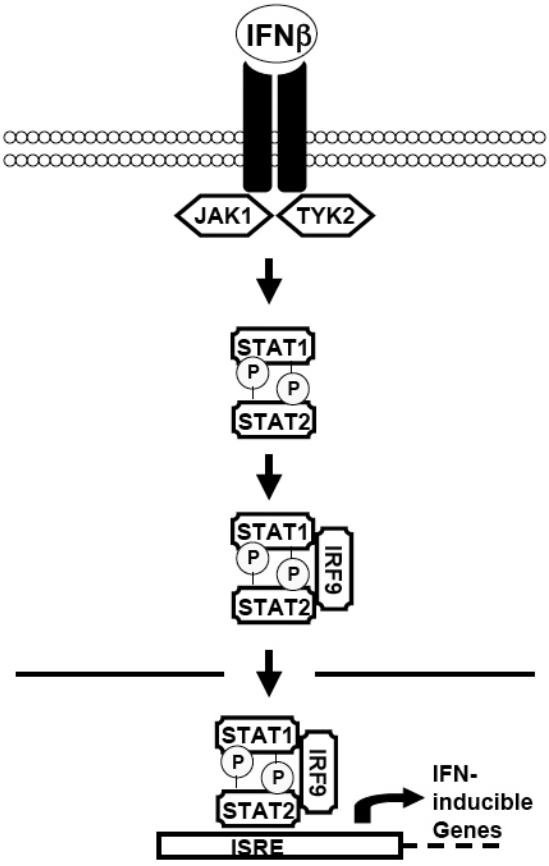

Apoptosis

Many viruses have evolved strategies to regulate host cell apoptotic responses to virus infection (reviewed in (127)). Apoptosis, a process of programmed cell death mediated by the activation of a group of caspases, results in systematic cellular self-destruction in response to a variety of stimuli (reviewed in (40)). There are two major apoptotic pathways, the extrinsic and intrinsic pathways, which converge at a step involving the activation of the effector caspase 3. The activation of effector caspases, nuclear

condensation and fragmentation, and cell death are the final steps in the apoptosis pathway. Viral proteins that are able to modulate the host apoptotic response include pro-apoptotic viral proteins such as West Nile virus capsid protein (208) and bunyavirus NSs proteins (28), and anti-apoptotic viral proteins such as RSV NS proteins (14), Bunyamwera virus NSs (101) and Rift Valley fever NSm protein (204). However, these studies are complex and some viral proteins such as influenza A virus NS1 have been reported to have both pro- and anti-apoptotic functions (166, 220). SeV C proteins have been implicated in the regulation of apoptosis but their role in this process remains incompletely defined (15, 71, 83, 105, 145). A role for HPIV1 proteins in apoptosis had not been investigated to date (9).

The HPIV1 C Proteins

The C proteins of SeV have been shown to have multiple functions that include inhibition of host innate immunity through antagonism of interferon (IFN) induction and/or signaling (51, 56, 104), regulation of viral mRNA synthesis by binding to the L polymerase protein (21, 33, 75, 110, 185), participation in virion assembly and budding via an interaction with AIP1/Alix, a cellular protein involved in apoptosis and endosomal membrane trafficking (66, 82, 156), and regulation of apoptosis. SeV mutants containing deletions of all four C proteins are viable, but are highly attenuated *in vitro* and in mice (55, 109, 110). To date, the HPIV1 C proteins have not been as extensively studied as those of SeV. However, the HPIV1 C proteins, like the SeV C proteins, are nonessential, play a role in evasion of host innate immunity through inhibition of type I IFN production and signaling, and regulate the host apoptotic response (9, 18, 192).

Reverse Genetics

Our laboratory has established a reverse genetics system for HPIV1 that allows the generation of infectious virus from cDNA (85, 137). In the reverse genetics system for HPIV1, a full length HPIV1 antigenomic cDNA, under the control of a T7 promoter, is transfected with support plasmids encoding the N, P, and L proteins into cells that constitutively express the T7 RNA polymerase, i.e. BHK-T7 cells, or into cells infected with the replication-deficient vaccinia virus MVA-T7 that encodes the T7 polymerase (206). HPIV1 can then be recovered from the supernatant. Using this system, we generated a number of HPIV1 mutants to investigate C protein function as well as to generate novel live virus vaccines that would be attenuated by disturbing the IFN antagonistic function of the C proteins, a strategy that has been shown to result in attenuation of replication *in vivo* (5, 6, 192). Previously, a phenylalanine to serine substitution of amino acid 170 of Sendai Virus (SeV, also referred to as murine PIV1) was shown to significantly attenuate a highly virulent SeV strain, increasing the lethal dose 50% (LD_{50}) 20,000-fold in mice (50). This C^{F170S} mutation was introduced into the P/C gene of recombinant HPIV1 by reverse genetics (85, 137). Whereas WT HPIV1 infection prevented IRF3 dimerization, its nuclear translocation, and IFNβ production, infection with HPIV1 containing the C^{F170S} mutation (F170S virus) led to IRF3 activation and IFNβ production (192). WT HPIV1, but not the F170S mutant virus, also inhibited the antiviral state induced by type I IFN, most likely due to inhibition of STAT1 nuclear translocation in human lung cells (18, 192). Not unexpectedly, the F170S mutant was attenuated for replication in the respiratory tract of hamsters and African green monkeys

(AGMs) (5, 192). We also constructed a HPIV1 mutant referred to as P(C-) that does not express any of the four C proteins due to point mutations that silence the C ORF, and this mutant was even more attenuated than F170S HPIV1 *in vivo* (9).

Current strategies to develop live attenuated vaccine candidates against this important pediatric pathogen include the introduction of attenuating mutations within the viral genome so that the vaccine strain causes little or no disease while, at the same time, confers protection from subsequent infections. The induction of IFN production, IFN signaling, and apoptosis that results from mutating or silencing the C gene may augment the establisment of an antiviral state, enhance antigen presentation and the adaptive immune response, and limit the spread of virus from infected cells. Interferon has been detected in the nasal washes of children infected with HPIV1 and likely contributes to host defense (63). The attenuation achieved by mutating or silencing the C gene underscores the importance of the HPIV1 C proteins as virulence factors during infection and as targets for developing candidate live attenuated virus vaccines.

Study Aims and Outline

This study addresses seven major aims: first, to create by reverse genetics a virus named P(C-) HPIV1 in which expression of the C proteins is silenced (this mutant virus was recovered by E. Bartlett); second, to compare the level of replication and of type I IFN induced *in vitro* during infection with P(C-) and WT HPIV1; third, to characterize the transcriptional response of human respiratory epithelial cells to infection with WT HPIV1 or HPIV1 in which the C gene is mutated or ablated; fourth, to examine the contribution

of IFNβ to this response; fifth, to determine the components of the type I interferon (IFN) response that are activated upon infection with C mutant HPIV1 viruses; sixth, to identify the stimuli that trigger host IFNβ production in response to these HPIV1 C mutants; and seventh, to examine the mechanisms by which the wild-type C proteins hold in check the induction of a potent host innate immune response. Aims one and two are described in chapter 2, aims three and four are described in chapter 3, and aims five through seven are described in chapter 4. Supplementary tables and figures are provided in the appendix.

Chapter 2: Human parainfluenza virus type 1 C proteins are nonessential proteins that inhibit the host interferon and apoptotic responses

Adapted from Journal of Virology 2008 Sep; 82(18): 8965–8977

Emmalene J. Bartlett,[1] Ann-Marie Cruz,[1] Janice Esker,[1] Adam Castaño,[1] Henrick Schomacker,[1] Sonja R. Surman,[1] Margaret Hennessey,[2,3] Jim Boonyaratanakornkit,[1] Raymond J. Pickles,[2,3] Peter L. Collins,[1] Brian R. Murphy,[1] and Alexander C. Schmidt[1]

[1]Laboratory of Infectious Diseases, RNA Viruses Section, National Institute of Allergy and Infectious Diseases, National Institutes of Health, Department of Health and Human Services. Bethesda, MD, 20892-2007, USA. [2]Cystic Fibrosis/Pulmonary Research and Treatment Center, University of North Carolina at Chapel Hill. Chapel Hill, NC, 27599-7248, USA. [3]Department of Microbiology and Immunology, University of North Carolina at Chapel Hill. Chapel Hill, NC, 27599-7248, USA.

Abstract

Recombinant human parainfluenza virus type 1 (rHPIV1) was modified to create rHPIV1-P(C-), a virus in which expression of the C proteins (C' , C, Y1, and Y2) was silenced without affecting the amino acid sequence of the P protein. Infectious rHPIV1-P(C-) was readily recovered from cDNA, indicating that the four C proteins were not essential for virus replication. Early during infection *in vitro*, rHPIV1-P(C-) replicated as efficiently as wild-type (wt) HPIV1, but its titer subsequently decreased coincident with the onset of an extensive cytopathic effect not observed with wt rHPIV1. rHPIV1-P(C-) infection, but not wt rHPIV1 infection, induced caspase 3 activation and nuclear fragmentation in LLC-MK2 cells, identifying the HPIV1 C proteins as inhibitors of apoptosis. In contrast to wt rHPIV1, rHPIV1-P(C-) and rHPIV1-C^{F170S}, a mutant encoding an F170S substitution in C, induced interferon (IFN) and did not inhibit IFN signaling *in vitro*. However, only rHPIV1-P(C-) induced apoptosis. Thus, the anti-IFN and antiapoptosis activities of HPIV1 were separable: both activities are disabled in rHPIV1-P(C-), whereas only the anti-IFN activity is disabled in rHPIV1-C^{F170S}. In primary human airway epithelial cell cultures, rHPIV1-P(C-) was considerably attenuated, suggesting that disabling the anti-IFN and antiapoptotic activities of HPIV1 had additive effects on attenuation. Its highly restricted replication in primary human airway epithelial cell cultures suggests that it might be overattenuated for use as a vaccine. Thus, the C proteins of HPIV1 are nonessential but have anti-IFN and antiapoptosis activities required for virulence.

Introduction

Human parainfluenza virus type 1 (HPIV1) is a member of the *Paramyxoviridae* family, which includes a number of other medically important human pathogens such as HPIV2 and 3, respiratory syncytial virus (RSV), measles virus, mumps virus, and human metapneumovirus (90). The HPIVs are enveloped, non-segmented, single-stranded, negative-sense RNA viruses that are classified in the genera *Respirovirus* (HPIV1 and HPIV3) and *Rubulavirus* (HPIV2). HPIV1, 2 and 3 are significant respiratory pathogens for infants and young children, with clinical manifestations ranging from mild disease, including rhinitis and pharyngitis, to more severe disease, including croup, bronchiolitis, and pneumonia (31, 68, 69, 90, 122, 154). The contribution of HPIV infections to pediatric respiratory hospitalizations varies between studies and ranges from 7-21% overall for HPIV1, 2 and 3. The HPIVs collectively are the second leading cause of pediatric hospitalizations for viral respiratory disease behind RSV and ahead of influenza (86, 90, 134). A licensed vaccine is currently not available for the prevention of HPIV disease, but experimental live attenuated candidate vaccines are under development for HPIV1, 2 and 3, with those for HPIV3 in clinical trials (8, 12, 61, 89, 92, 139).

The HPIV1 genome is 15,600 nucleotides in length and contains six genes in the order 3′-N-P/C-M-F-HN-L-5′ (138). Each gene encodes a single protein with the exception of the P/C gene that encodes the phosphoprotein P in one open reading frame (ORF) and up to four accessory C proteins, C', C, Y1 and Y2, in a second, overlapping ORF. The synthesis of the C proteins initiates at four separate translational start codons in the C ORF in the order C', C, Y1, and Y2, and the four proteins are carboxy co-terminal (90).

However, it is unclear whether the Y2 protein is actually expressed during HPIV1 infection (152). C proteins are expressed by members of the *Respirovirus*, *Morbillivirus* and *Henipavirus* genera but not by viruses that belong to the *Rubulavirus* and *Avulavirus* genera. The paramyxovirus C proteins studied to date are non-essential accessory proteins that contribute significantly to virus replication and virulence *in vivo* (5, 84, 109, 110). The C proteins of Sendai virus (SeV), a member of the *Respirovirus* genus and the closest homolog of HPIV1, are the most extensively characterized.

The C proteins of SeV have been shown to have multiple functions that include inhibition of host innate immunity through antagonism of interferon (IFN) induction and/or signaling (51, 56, 104), regulation of viral mRNA synthesis by binding to the L polymerase protein (21, 33, 75, 110, 185), participation in virion assembly and budding via an interaction with AIP1/Alix, a cellular protein involved in apoptosis and endosomal membrane trafficking (66, 82, 156), and regulation of apoptosis (see below). SeV mutants containing deletions of all four C proteins are viable, but are highly attenuated *in vitro* and in mice (55, 109, 110). To date, the HPIV1 C proteins have not been as extensively studied as those of SeV. However, the HPIV1 C proteins, like the SeV C proteins, play a role in evasion of host innate immunity through inhibition of type I IFN production and signaling (18, 192). Type I IFN was not detected during infection with HPIV1 wild type (wt) in A549 cells, a human epithelial lung carcinoma cell line, but was induced during infection with a recombinant HPIV1 (rHPIV1) mutant bearing a F170S amino acid substitution in C, designated rHPIV1-C^{F170S} (192). HPIV1 wt virus, but not the rHPIV1-C^{F170S} mutant virus, inhibited the antiviral state induced by type I IFN, most

likely due to inhibition of STAT1 nuclear translocation in human lung cells (18, 192).

Many viruses have evolved strategies to regulate host cell apoptotic responses to virus infection (reviewed in (127)). Apoptosis, a process of programmed cell death mediated by the activation of a group of caspases, results in systematic cellular self-destruction in response to a variety of stimuli (reviewed in (40)). There are two major apoptotic pathways, the extrinsic and intrinsic pathways, which converge at a step involving the activation of the effector caspase 3. The activation of effector caspases, nuclear condensation and fragmentation, and cell death are the final steps in the apoptosis pathway. Viral proteins that are able to modulate the host apoptotic response include pro-apoptotic viral proteins such as West Nile virus capsid protein (208) and bunyavirus NSs proteins (28), and anti-apoptotic viral proteins such as RSV NS proteins (14), Bunyamwera virus NSs (101) and Rift Valley fever NSm protein (204). However, these studies are complex and some viral proteins such as influenza A virus NS1 have been reported to have both pro- and anti-apoptotic functions (166, 220). SeV C proteins have been implicated in the regulation of apoptosis but their role in this process remains incompletely defined (15, 71, 83, 105, 145). A role for HPIV1 proteins in apoptosis has not been investigated to date.

In the present study, a rHPIV1 mutant was generated in which the C protein ORF was modified using reverse genetics to preclude expression of any of the four C proteins while maintaining expression of a wt P protein. This mutant, designated rHPIV1-P(C-), was evaluated for replication *in vitro* and *in vivo* in order to determine: i) whether C was

essential for HPIV1 replication; ii) what effect the deletion of C protein expression had on the host response to virus infection; and iii) whether a C protein deletion mutant had properties that warranted further development as a live attenuated HPIV1 candidate vaccine. In contrast to HPIV1 wt (but similar to rHPIV1-C^{F170S}), rHPIV1-P(C-) was found to induce a robust IFN response. Additionally, in contrast to HPIV1 wt (and also in contrast to rHPIV1-C^{F170S}), rHPIV1-P(C-) induced a potent apoptotic response. Both phenotypes appeared to contribute to attenuation in cultures of human ciliated airway epithelium.

Materials and Methods

Cells and Viruses

LLC–MK2 cells (ATCC CCL 7.1) and HEp–2 cells (ATCC CCL 23) were maintained in Opti–MEM I (Gibco–Invitrogen, Inc. Grand Island, NY) supplemented with 5% FBS and gentamicin sulfate (50 µg/ml). A549 cells (ATCC CCL-185) were maintained in F-12 nutrient mixture (HAM) (Gibco-Invitrogen, Inc.) supplemented with 10% FBS, gentamicin sulfate (50 µg/ml) and L-glutamine (4 mM). Vero cells (ATCC CCL-81) were maintained in MEM (Gibco-Invitrogen, Inc.) supplemented with 10% FBS, gentamicin sulfate (50 µg/ml) and L-glutamine (4 mM). BHK-T7 cells, which constitutively express T7 RNA polymerase (20), were kindly provided by Dr. Ursula Buchholz, NIAID, and were maintained in GMEM (Gibco-Invitrogen, Inc.) supplemented with 10% FBS, geneticin (1 mg/ml), MEM amino acids, and L-glutamine (2 mM). Human airway tracheobronchial epithelial (HAE) cells were isolated from airway specimens of patients without underlying lung disease provided by the National

Disease Research Interchange (NDRI, Philadelphia, PA) or from excess tissue obtained during lung transplantation, provided by the UNC Cystic Fibrosis Center Tissue Culture Core under protocols approved by the University of North Carolina at Chapel Hill (UNC) Institutional Review Board. Growth and differentiation of these cells on semi-permeable Transwell inserts at the air-liquid interface generated ciliated human airway epithelium, as previously described (149). All infections were incubated at 32ºC except where indicated otherwise.

Biologically-derived wt HPIV1 Washington/20993/1964, the parent of rHPIV1, was isolated from a clinical sample in primary AGM kidney (AGMK) cells, passaged 2 more times in primary AGMK cells (135) and once in LLC-MK2 cells (6). This preparation has a wt phenotype in AGMs, and will be referred to here as HPIV1 wt, but it was previously referred to as $HPIV1_{LLC1}$ (6). The rHPIV1 wt referred to in this study also contains a mutation in the HN gene, HN^{T553A}, that has previously been shown not to have an effect on virus replication (5) and is therefore considered the equivalent of wt virus. rHPIV1 wt was generated as previously described (6, 138, 192). The rHPIV1 wt was used in all experiments, with the exception that the biological HPIV1 wt was used for the hamster challenge and in the AGM studies, as indicated. The generation and characterization of the rHPIV1-C^{F170S} mutant also was described previously (6); this virus contains a single nucleotide substitution in the P/C gene that creates a phenylalanine-to-serine substitution at amino acid 170 (numbered relative to the C' protein) that affects all four C proteins and is silent in the P protein. Media used for propagation and infection of HPIV1 wt and rHPIV1 mutants in LLC–MK2 cells did not contain FBS but contained

1.2% TrypLE Select, a recombinant trypsin (Gibco-Invitrogen, Inc.), in order to cleave and activate the HPIV1 fusion (F) protein, as described previously (138). Purified virus stocks were obtained by infecting LLC-MK2 cells, followed by centrifugation and banding of virus containing supernatant in a discontinuous 30/60% (w/v) sucrose gradient, steps designed to minimize contamination with cellular factors, especially IFN. Recombinant vesicular stomatitis virus expressing the green fluorescent protein (VSV-GFP) was originally obtained from John Hiscott (176). Stocks of VSV were propagated in Vero cells and sucrose purified as indicated above.

Virus titers in samples were determined by 10-fold serial dilution of virus in 96-well LLC-MK2 monolayer cultures, using two or four wells per dilution. After 7 days of incubation, infected cultures were detected by hemadsorption with guinea pig erythrocytes, as described previously (169). Virus titers are expressed as $\log_{10}$ 50% tissue culture infectious dose per ml ($\log_{10}$ $TCID_{50}$/ml). VSV stock titers were determined by plaque assay on Vero cells under a 0.8% methyl cellulose overlay.

Antibodies

Polyclonal antisera directed against the HPIV1 C or P proteins were generated by repeated immunization of rabbits with the following KLH-conjugated peptides: (i) QMREDIRDQYLRMKTERW (amino acid (aa) residues 153-170 of HPIV1 C'; directed against the carboxyl terminal region of C', C, Y1 and Y2), for Skia-31; and (ii) RDPEAEGEAPRKQES (aa 10-24 of P), for Skia-2. Antisera were generated at Spring Valley Labs (Woodbine, MD). Two murine monoclonal antibodies directed against the

HPIV1 HN protein, designated 8.2.2.A and 4.5, were kindly provided by Dr. Yasuhiko Ito (103).

Construction of mutant rHPIV1-P(C-) cDNA

Nucleotide insertions, deletions and substitutions were introduced into the P/C gene of rHPIV1 wt (**Figure 1A**) (137) in order to silence the expression of the C', C, Y1, and Y2 proteins without affecting the P protein (**Figure 1B and C**). The 93 nucleotides between the P/C gene start signal and the P start codon, including the C' start codon, were deleted (**Figure 1B and C**, mutation 2) and replaced with a 6 nucleotide insertion to act as a "linker" (**Figure 1B and C**, mutation 1). The sequence immediately upstream of the P start codon was modified by the addition of the "linker": CGA(ATG) to AAC(ATG), making the P start site more efficient by Kozak's rules (106) and reducing translational initiation at the downstream start codons (**Figure 1B and C**, mutation 1). The C start codon was modified (ATG to ACG) (**Figure 1B and C**, mutation 3), and three codons were converted to stop codons, including one immediately downstream of the Y1 start codon (TCA to TGA), which will affect all of the C proteins except Y2, and two downstream of the Y2 start codon (TCG to TAG; TTG to TAG), which will affect all of the C proteins (**Figure 1B and C**, mutations 4, 5, and 6). All of the introduced changes are silent in the P protein. These changes were achieved using a modified PCR mutagenesis protocol described elsewhere (129) and the Advantage–HF PCR Kit (Clontech Laboratories, Palo Alto, CA). The entire PCR amplified gene product was sequenced using a Perkin–Elmer ABI 3100 sequencer with the Big Dye sequencing kit (Perkin–Elmer Applied Biosystems, Warrington, UK) to confirm amplification of the

desired sequence containing the introduced changes. Full–length antigenomic cDNA clones (FLCs) of HPIV1 containing the desired mutations were assembled in T7 polymerase-driven plasmids using standard molecular cloning techniques (138), and the region containing the introduced mutation in each FLC was sequenced as described above to confirm the presence of the introduced mutation and absence of adventitious changes. Each virus was designed to conform to the rule of six, i.e., the nucleotide length of each genome was designed to be an even multiple of six (102), a requirement for efficient replication of HPIV1.

Figure 1. Designing the HPIV1-P(C-) viral cDNA. (A) The HPIV1 wt genome, shown 3′ to 5′, includes the P/C gene that encodes the phosphoprotein P from one ORF and the four carboxy-coterminal C proteins, C', C, Y1 and Y2, from a second, overlapping ORF. The coding regions for these proteins are shown, with the initiation and termination codons numbered according to the P/C gene sequence. (B) Various mutations were introduced into the HPIV1 P/C gene to silence expression of the four C proteins without affecting the amino acid sequence of the P protein. Panel B shows the sequence of the upstream end of the P/C gene, with the transcription gene-start signal and the translational start signal for each protein boxed. Nucleotide (nt) substitutions and an insertion in the rHPIV1-P(C-) sequence are indicated in boldface, and a deletion is indicated with a dotted line. These mutations are identified with circled numbers that correspond with a description in panel (C) of the effect of each mutation. Briefly, 93 nt were deleted between the gene-start signal and P start codon and replaced with a 6-nt spacer CCCAAC (mutations 1 and 2), thus eliminating the first 11 codons of C' including

its start codon. The sequence immediately upstream of the P start codon was modified: CGA(ATG) to AAC(ATG), which will also optimize the Kozak sequence and reduce translational initiation at the downstream start codons (mutation 1). The methionine start codon of the C protein was converted to threonine (mutation 3), and one stop codon was introduced downstream of the Y1 start codon (mutation 4) and two stop codons were introduced downstream of the Y2 start codon (mutation 5 and 6). This cDNA was used to recover infectious rHPIV1-P(C-).

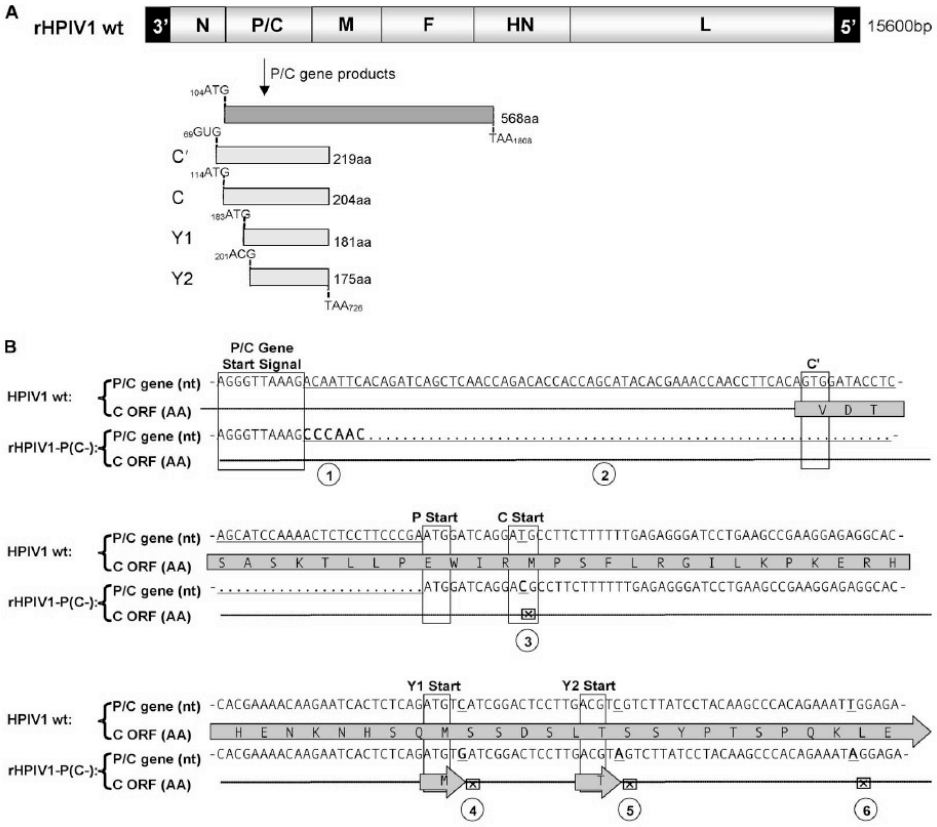

C

Changes introduced into the P/C gene to generate the P(C-) gene.

Mutations	Effect on C Proteins	Effect on P Protein
1 Insertion: 6 nt	No change - insertion is between the gene start sequence and the P start codon.	Improved Kozak sequence will result in a more efficient translational start site for the P start codon.
2 Deletion: 93 nt	Deletion of amino-terminal end of C ORF, between gene start sequence and P start codon, including C' start codon. Eliminates C' expression	No change - Deletion is between gene start sequence and P start codon.
3 ATG → ACG	M (C Start) → T	No change.
4 TCA → TGA	S → Stop	No change.
5 TCG → TAG	S → Stop	No change.
6 TTG → TAG	L → Stop	No change.

Recovery of infectious rHPIV1-P(C-)

rHPIV1-P(C-) was recovered using a reverse genetics system, similar to previously described methods (138), in BHK-T7 cells constitutively expressing T7 polymerase (20) that were grown to 90 to 95% confluence in six-well plates. Cells were transfected with 5 µg of the FLC, 0.8 µg each of the N and P, and 0.1 µg of the L support plasmids in a volume of 100 µl of Opti-MEM per well. Transfection was carried out with Lipofectamine 2000 (Invitrogen, Inc., Carlsbad, CA), according to the manufacturer's directions. The transfection mixture was removed after a 24 h incubation period at 37°C. Cells were then washed and maintained in GMEM supplemented with amino acids and 1.2% TrypLE Select and transferred to 32°C. On day 2 following transfection, the supernatant was harvested. Virus was amplified by passage on LLC-MK2 cells and cloned biologically by two successive rounds of terminal dilution using LLC–MK2 monolayers on 96–well plates (Corning Costar Inc., Acton, MA). To confirm that rHPIV1-P(C-) contained the appropriate mutations and lacked adventitious mutations, viral RNA (vRNA) was isolated from infected cell supernatants using the QIAamp viral RNA mini kit (Qiagen Inc., Valencia, CA), reverse transcribed using the SuperScript First–Strand Synthesis System (Invitrogen, Inc., Carlsbad, CA), and amplified using the Advantage HF cDNA PCR Kit (Clontech Laboratories). The viral genome was sequenced in its entirety, confirming its sequence.

Western Blot

LLC-MK2 monolayers grown in 6 well plates (Costar) were mock-infected or infected at an input multiplicity of infection (MOI) of 5 $TCID_{50}$/ml with sucrose-purified rHPIV1 wt or rHPIV1-P(C-). Cell lysates were harvested 48 h post infection (p.i.) with 200 µl of 1X Loading Dye Solution sample buffer (Qiagen, Inc) and purified on QIAshredder (Qiagen, Inc.) spin columns. Ten µl (for Skia-31 probing) or 6 µl (for Skia-2 probing) of each sample was reduced, denatured and loaded onto 10-well 10% Bis-Tris gels (Invitrogen, Inc.). Gels were run in MOPS buffer (Invitrogen, Inc.), and protein was transferred onto PVDF membranes (Invitrogen, Inc.) and blocked overnight at 4°C in PBS/Tween (0.1%) containing 3% BSA. PDVF membranes were incubated with 15 ml of a 1:1000 dilution of primary antibody in PBS/Tween with 1% BSA at room temperature (RT) for 2 h and then were washed 3 times for 10 min with PBS/Tween. Membranes were incubated for 1 h at RT with a 1:20,000 dilution of peroxidase labeled goat anti-rabbit IgG (KPL, Gaithersburg, MD) as the secondary antibody. After washing 3 times for 10 min with PBS/Tween, SuperSignal West Pico Chemiluminescent Substrate (Pierce, Rockford, IL) was added for 10 min at RT. Membranes were developed on Kodak MR films (Kodak, Rochester, NY).

Kinetics of replication of rHPIV1-P(C-)

The rHPIV1 wt and rHPIV1-P(C-) viruses were compared in multi-cycle growth curves. Confluent monolayer cultures of LLC-MK2 cells in 6-well plates were infected in triplicate at a MOI of 0.01 $TCID_{50}$/cell. Virus adsorption was performed for 1 h in media containing trypsin. The inoculum was then removed and cells were washed three times, after which fresh medium containing trypsin was added and then harvested as the day 0

sample and replaced with fresh media containing trypsin. On days 1-7 p.i., the entire supernatant was removed for virus quantitation and was replaced with fresh medium containing trypsin. Supernatants containing virus were frozen at -80°C, and virus titers (log_{10} $TCID_{50}$/ml) were determined with endpoints identified by hemadsorption. Cytopathic effect (cpe) was visually monitored. The amount of cpe observed under the microscope was given a score ranging from 1-5 based on the percentage of cells in the monolayer showing cpe. Cpe of less than 20% of cells was scored as 1; 21-40% as 2; 41%-60% as 3; 61-80% as 4; 81-100% as 5.

Immunostaining and confocal microscopy

LLC-MK2 cells were seeded onto 24 well plates containing 12 mm glass cover slips, were mock-infected or infected with rHPIV1-P(C-) or rHPIV1 wt at a MOI of 10 $TCID_{50}$/cell, and were incubated for 72 h. Media was removed and cover slips were washed twice with PBS. Cells were then fixed with 3% formaldehyde solution in PBS for 40 min at RT, washed once with PBS, permeabilized with 0.1% Triton X-100 in PBS for 4 min at RT, and washed twice with PBS prior to blocking with PBS containing 0.25% BSA and 0.25% gelatin for 1 h at RT. HPIV1 HN staining was performed using a 1:4000 dilution of a mixture of HPIV1-HN 8.2.2.A and HPIV1-HN 4.5, two murine antibodies directed against the HPIV1 HN protein**,** kindly provided by Yasuhiko Ito, Mie University School of Medicine, as primary antibody. After incubation at RT for 1 h, cells were washed twice with PBS and stained with a 1:1000 dilution of Texas Red conjugated donkey anti-mouse IgG (Jackson Immunochemicals, West Grove, PA), as secondary antibody, for 1 h at RT. Activated caspase 3 was detected using a 1:25 dilution of a

FITC-conjugated rabbit anti-human activated caspase 3 antibody (BD Pharmingen, San Jose, CA). Cells were washed twice with PBS and immediately mounted onto slides with the DAPI-containing antifade reagent, ProLong Gold (Invitrogen, Inc.). Slides were covered with foil and left to dry overnight at RT, then stored at -20°C until microscopy was performed on a Leica SP5 confocal microscope.

FACS analysis

LLC-MK2, Vero, or A549 cells in 6-well plates were mock-infected or infected with rHPIV1 wt or rHPIV1-P(C-) at a MOI of 5 $TCID_{50}$/cell. Cells were harvested at 24, 48, and 72 h p.i. by scraping cells into 2 ml of fresh FACS buffer (PBS; 1% FBS) and pelleting at 1200 rpm for 10 min at 4°C. Cells were resuspended in 1 ml of 3% paraformaldehyde (PFA) and fixed for 15 min on ice, then rinsed twice in 3 ml FACS buffer. Cells were permeabilized and stained with the following antibodies diluted in FACS buffer containing 0.1% Triton-X-100: i) rabbit anti-human activated caspase 3 FITC (1:100; BD Pharmingen); and ii) mouse anti-PIV1 HN (1:2000 of a 1:1 mix of HPIV1-HN 8.2.2.A and HPIV1-HN 4.5). Staining was performed for 45 min at RT in a dark environment then cells were rinsed twice with 2 ml FACS buffer and stained with APC-conjugated goat anti-mouse IgG (1:1000; Jackson ImmunoResearch Laboratories, West Grove, PA), diluted in FACS buffer containing 0.1% Triton-X-100. Staining was carried out for 30 min at RT. Finally, cells were rinsed twice in FACS buffer and resuspended in 250 μl FACS buffer for analysis. Sample analysis was carried out on a FACSCalibur (BD Biosciences, San Jose CA) using CellQuestPro software. Further analysis was performed using FlowJo software (TreeStar Inc., Ashland, OR).

Type I IFN bioassay

The amount of type I IFN produced by HPIV1-infected A549 cell cultures was determined by an IFN bioassay, as previously described (192). Type I IFN concentrations were determined by measuring the ability of samples to restrict replication of VSV-GFP on HEp-2 cell monolayers in the samples in comparison to a known concentration of a human IFN-β standard (AVONEX; Biogen, Inc., Cambridge, MA). Briefly, samples were treated at pH 2.0 to inactivate virus and acid-labile type II IFN prior to being serially diluted 10-fold in duplicate in 96-well plates of HEp-2 cells along with the IFN-β standard (5000 pg/ml). After 24 h, the cells were infected with VSV-GFP at $6.5x10^4$ PFU/well. After an additional 24 to 36 h, plates were read for GFP expression using a typhoon 8600 phosphorimager (Molecular Dynamics, Sunnyvale, CA). The dilution at which the level of GFP expression was approximately 50% of that in untreated cultures was determined as the end-point. The end-point of the AVONEX standard was compared to the end-point of the unknown samples, and IFN concentrations were determined and expressed as mean ± SE (pg/ml).

Viral inoculation of HAE

Apical surfaces of HAE were rinsed with PBS to remove apical surface secretions and fresh media was supplied to the basolateral compartments prior to inoculation. The apical surfaces of HAE were inoculated with HPIV1s at a low input MOI (0.01 $TCID_{50}$/cell) in a 100 µl inoculum, and the cultures were incubated at 37°C. The inoculum was removed 2 h p.i., and apical surfaces rinsed for 5 min with PBS and then

incubated at 37°C. At days 0-7 p.i., apical samples were collected by incubating the apical surface with 300 µl of media for 30 min at 37°C, after which the media was recovered. Samples were stored at -80°C prior to determination of virus titer.

Statistical analysis

The Prism 5 (GraphPad Software Inc., San Diego, CA) one-way ANOVA test (Student-Newman-Keuls multiple comparison test) was used to assess statistically significant differences between data groups ($P < 0.05$).

Results

Construction and recovery of a rHPIV1 mutant not expressing any of the four C proteins

The P/C gene of HPIV1 wt encodes the phosphoprotein, P, in one ORF and four carboxy co-terminal C proteins, C', C, Y1 and Y2, in a second, overlapping ORF (**Figure 1A**). We engineered rHPIV1 to silence expression of all four C proteins without affecting the P protein, creating the mutant virus rHPIV1-P(C-) (**Figure 1B and C**). The changes introduced to silence expression of the C proteins included the deletion of the 3' portion of the P/C gene containing the C' start, conversion of the C start to an ACG codon, and the introduction of three stop codons into the C ORF immediately downstream of the Y1 and Y2 start codons (**Figure 1B and C**). Importantly, all of the introduced changes were silent in the P protein (**Figure 1B and C**). The Y1 and Y2 start codons were not modified since any changes introduced at these sites would have altered P protein amino acid assignments. The AUG to ACG change at the start site of C would not necessarily silence its expression entirely, since ACG functions (inefficiently) as a start codon for the

C' protein of SeV, but other changes at this site could not be accommodated without affecting P coding, and in any event any residual expression of C would be ablated by the three stop codons that were introduced downstream. The recombinant virus was recovered from this mutant cDNA in cell culture and the virus replicated to 8.0 $\log_{10}$ $TCID_{50}$/ml. Sequence analysis of the entire virus genome revealed that rHPIV1-P(C-) contained all the intended mutations and no unintended changes (data not shown).

Western blot analysis of infected LLC-MK2 cell lysates using an antibody directed against the carboxy terminus of the C proteins demonstrated the expression of the C' and C proteins in cells infected with HPIV1 wt, but not rHPIV1-P(C-) (**Figure 2A**). C' was found to be the most abundant C protein, and Y1 and Y2 were not detected. An additional unidentified species, indicated with an asterisk in **Figure 2A**, was detected in cells infected with rHPIV1-P(C-), but not in cells infected with rHPIV1 wt (**Figure 2A**). This species was not detected using an antibody directed against the amino terminus of the C' and C proteins (data not shown). An ATG codon in the C ORF that is downstream of the last inserted stop codon in Y2 could potentially give rise to a truncated protein that would be carboxy-coterminal with the C proteins and would be 157 aa in length, compared to 204 aa for the C protein and 175 aa for Y2 (**Figure 1A**). This 47 aa difference in predicted size between C and the unknown protein in **Figure 2A** would correspond to an approximately 5 kDa difference in the proteins' apparent molecular weights, consistent with the mobility difference observed in our Western blot (**Figure 2A**). The P protein could be detected in both rHPIV1 wt- and rHPIV1-P(C-)-infected cells (**Figure 2B**). The ability to recover the rHPIV1-P(C-) mutant indicates that the four

wild type C proteins are not essential for replication *in vitro*, with the caveat that there was expression of a new species that may have been a truncated C protein.

Figure 2. Identification of HPIV1 C and P proteins in lysates from infected LLC-MK2 cells. Lysates were prepared 48 h p.i. from LLC-MK2 cells that were mock-infected or infected with sucrose-purified rHPIV1 wt or rHPIV1-P(C-) at an input MOI of 5 $TCID_{50}$/cell. Reduced, denatured cell lysates were resolved by SDS-PAGE electrophoresis and Western blots were prepared and analyzed using rabbit anti-peptide antisera against (A) the HPIV1 C proteins and (B) the HPIV1 P protein. The asterisk (*) in panel A indicates a new band of unknown identity, detected only in the rHPIV1-P(C-)-infected cell lysates.

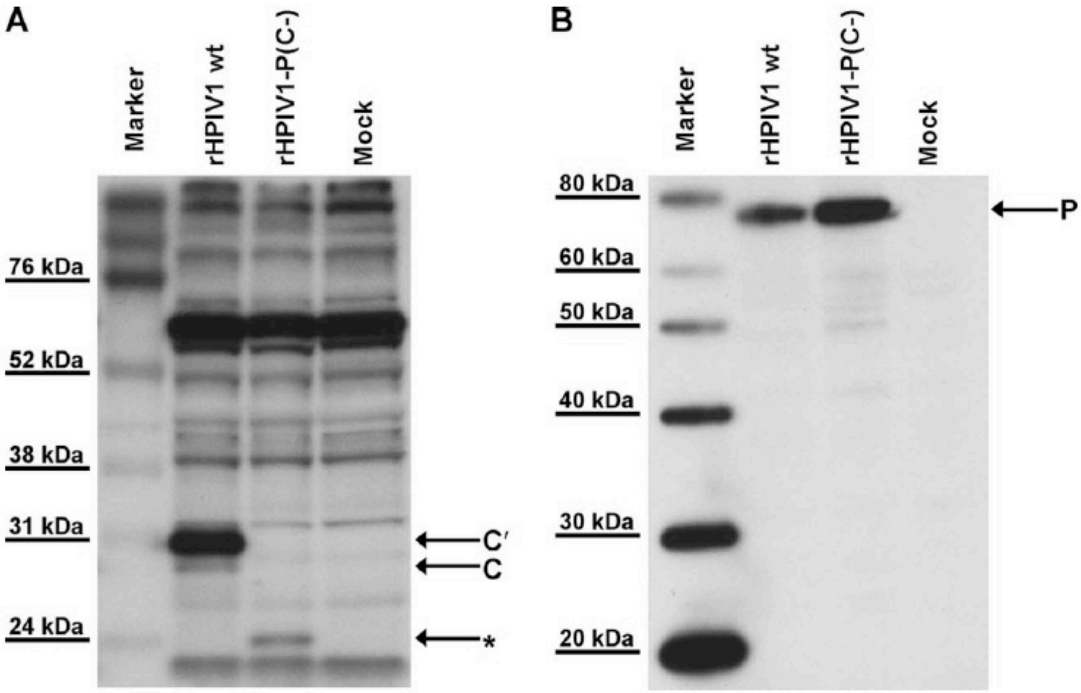

The rHPIV1-P(C-) mutant replicates efficiently in vitro but causes increased cpe compared to rHPIV wt

Multi-cycle replication of the rHPIV1-P(C-) mutant was assessed in LLC-MK2 cells infected at a MOI of 0.01 $TCID_{50}$/cell (**Figure 3A**). LLC-MK2 cells were chosen since HPIV1 wt replicates efficiently in this cell line. rHPIV1-P(C-) and rHPIV1 wt replicated to similar titers until day 3 p.i., when rHPIV1 wt continued to increase in titer whereas rHPIV1-P(C-) decreased in titer. Concomitantly, rHPIV1-P(C-)-infected LLC-MK2 cells developed extensive cpe while rHPIV1 wt-infected cells did not (**Figure 3B**). This also is evident in photomicrographs of LLC-MK2 cells taken 72 h following infection at MOIs of 0.01 or 5 $TCID_{50}$/cell (**Figure 3A**). In LLC-MK2 cells infected at a MOI of 5 $TCID_{50}$/cell, increased cpe associated with rHPIV1-P(C-) but not rHPIV1 wt became evident at approximately 48 h p.i. (data not shown). Similarly, enhanced cpe associated with infection by the rHPIV1-P(C-) mutant was observed in A549 cells (data not shown), which were evaluated since they are a human respiratory tract-derived continuous cell line and *in vivo* HPIV1 replicates preferentially, if not exclusively, in respiratory epithelial cells. In summary, rHPIV1-P(C-) and rHPIV1 wt replicated with equal efficiency early in infection, but there was a subsequent decrease in rHPIV1-P(C-) titers that was temporally associated with development of extensive cpe, a phenomenon not seen in rHPIV1 wt-infected cells.

Figure 3. Comparison of the replication of rHPIV1 wt and rHPIV1-P(C-) viruses *in vitro*. (A) Multi-cycle replication in LLC-MK2 cells infected at a MOI of 0.01 $TCID_{50}$/cell. On days 0-7 p.i., the overlying medium was harvested for virus titration, shown as the means of 3 replicate cultures. On days 1-7 p.i., the cell monolayers were monitored for cpe and assigned a score of 1-5 according to the extent of cpe (Materials and Methods), shown as the means of the 3 replicate cultures. (B) LLC-MK2 cells were mock-infected or infected with rHPIV1 wt or rHPIV1-P(C-) at a MOI of 0.01 or 5 $TCID_{50}$/cell, as indicated in parentheses below the virus names. Photomicrographs taken at 72 h p.i. show increased cytopathic effect (cpe) in the rHPIV1-P(C-)-infected cultures (magnification, x10).

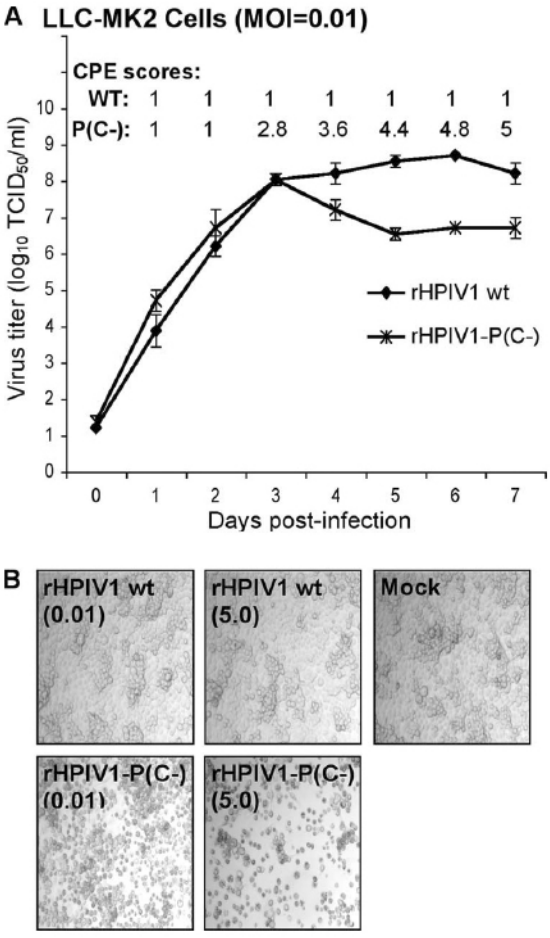

Infection with rHPIV1-P(C-) infection induces apoptosis

To further explore the basis of the enhanced cpe associated with the rHPIV1-P(C-) mutant, we assayed virus-infected LLC-MK2 cells for activation of caspase 3, the major effector caspase in the apoptotic pathway. Activated caspase 3 was visualized by immunofluorescence (**Figure 4A**) and by FACS analysis (**Figure 4B**) using an antibody that specifically recognizes the cleaved, activated form of the enzyme. Replicate LLC-MK2 monolayers were infected at a MOI of 10 $TCID_{50}$/cell, incubated for 24, 48 and 72 h, fixed, permeabilized, and stained with antibodies for HPIV1 HN (Texas-Red) and for activated caspase 3 (FITC). The HPIV1 HN antigen was detected in the vast majority of cells infected with either virus (**Figure 4A**). By 72 h p.i., activated caspase 3 was detected in the majority of the rHPIV1-P(C-)-infected cells but not rHPIV1 wt-infected cells (**Figure 4A**). In addition, cell rounding and nuclear condensation was seen in the majority of rHPIV1-P(C-)-infected cells but not in rHPIV1 wt-infected cells (**Figure 4A**, asterisk), consistent with the interpretation that the rHPIV1-P(C-)-induced cpe is the direct result of virus-induced apoptosis.

We next determined the frequency of apoptosis in infected cells using flow cytometry. The rHPIV1-C^{F170S} mutant, which encodes a F170S substitution in C, and which has previously been associated with type I IFN induction and effective type I IFN signaling, but not with cpe *in vitro*, was included here for comparison. Replicate cultures of LLC-MK2 cells were infected with rHPIV1 wt, rHPIV1-C^{F170S}, or rHPIV1-P(C-) at a MOI of 5 $TCID_{50}$/cell and, at 24, 48, and 72 h p.i., were fixed, permeabilized, and immunostained

for HPIV1 HN protein and activated caspase 3 (**Figure 4B**). More than 70% of cells in the rHPIV1-P(C-)-infected cultures were positive for activated caspase 3 by 72 h p.i., compared to approximately 5% and 7% in the rHPIV1 wt- and rHPIV1-C^{F170S}-infected cell cultures respectively (**Figure 4C**). Similar studies in Vero and A549 cells confirmed that rHPIV1-P(C-) was a potent activator of caspase 3 activation while rHPIV1 wt was not, although the level of caspase 3 activation in these cells was lower than in LLC-MK2 cells (data not shown). Vero cells were also evaluated here since vaccine viruses to be used in clinical trials are prepared in this cell line and therefore it is important to determine the growth characteristics of potential vaccine viruses in this cell line. By 72 h p.i., approximately 12% and 18% of rHPIV1-P(C-)-infected Vero and A549 cell cultures, respectively, were positive for activated caspase 3, compared to approximately 4% of rHPIV1 wt-infected cell cultures for both cell types.

Figure 4. Infection with rHPIV1-P(C-) induces activation of caspase 3, indicative of apoptosis. Caspase 3 activation was evaluated by immunostaining and FACS analysis. (A) Evaluation of caspase 3 activation by immunofluorescence. LLC-MK2 cells were mock-infected or infected with rHPIV1 wt or rHIV1-P(C-) at a MOI of 10 $TCID_{50}$/cell. At 72 h p.i., cells were fixed, permeabilized, and stained for HPIV1 HN protein (*red*) and activated caspase 3 (*green*), and nuclei were stained with DAPI (*blue*). Cells were visualized by confocal microscopy and scale bars represent 10 μm. (B) Evaluation of caspase 3 activation by FACS analysis. LLC-MK2 cells were mock-infected or infected with rHPIV1 wt, rHPIV1-C^{F170S}, or rHPIV1-P(C-) at a MOI of 5 $TCID_{50}$/cell in triplicate. Cells were harvested at 24, 48, and 72 h p.i., fixed, permeabilized and stained for HPIV1

HN and activated caspase 3 in FACS buffer prior to analysis. Sample analysis was carried out using a FACSCalibur flow cytometer and FlowJo software. Dot plots of representative data for samples from the 48 h time point are shown. (C) Percentage of cells positive for activated caspase 3 at 24, 48 and 72 h p.i., as determined by FACS analysis ± S.E.

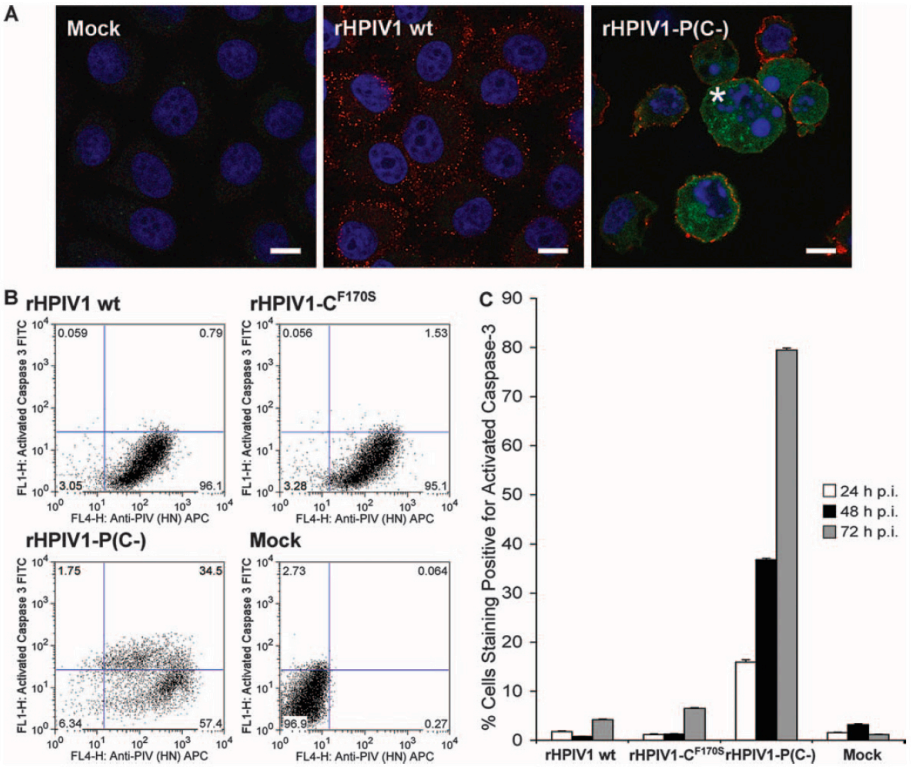

rHPIV1-P(C-), but not rHPIV1 wt, induces type I IFN production and signaling

HPIV1 C proteins have been shown to inhibit production of and signaling by type I IFN (18, 192). We have previously demonstrated that type I IFN was not detected during infection of A549 cells with HPIV1 wt but was efficiently produced in response to rHPIV1-C^{F170S} (192). To determine the relative effect of deleting all four C proteins on the ability of HPIV1 to inhibit the type I IFN response, we infected A549 cells at a MOI

of 5 $TCID_{50}$/cell with rHPIV1-P(C-), rHPIV1 wt or rHPIV1-C^{F170S} and subsequently quantified type I IFN in medium supernatants using a bioassay based on the inhibition of infection and GFP expression by VSV-GFP (**Figure 5A**). As shown previously, rHPIV1 wt inhibited the IFN response effectively (**Figure 5A**), with barely detectable levels of IFN-β appearing late in infection, at 72 h p.i. In contrast, both rHPIV1-P(C-) and rHPIV1-C^{F170S} induced a robust type I IFN response, with IFN detectable in the supernatant as early as 24 h p.i. and until 72 h p.i., achieving a peak concentration of approximately 300 pg/ml at 48 h p.i. These data suggest that C proteins play a critical role in antagonism of type I IFN production but that IFN generation is unrelated to the apoptotic response seen with the C mutants since the F170S mutant generates similar levels of IFN with no observable cpe beyond wt HPIV1.

We have previously demonstrated that type I IFN signaling leading to the establishment of an antiviral state is inhibited following infection with HPIV1 wt, but not with mutants that encode defective C proteins, e.g. rHPIV1-C^{F170S} (192). To determine the relative effect of deleting all four C proteins on the ability of HPIV1 to inhibit type I IFN signaling, Vero cells were mock-infected or infected with rHPIV1 wt, rHPIV1-C^{F170S}, or rHPIV1-P(C-) at a MOI of 5 $TCID_{50}$/cell for 24 h, treated with 0, 100 or 1000 IU of IFN-β for 24 h, and infected with 200 PFU/well of VSV-GFP. The number of VSV-GFP foci were counted 48 h later and the percent inhibition due to IFN-β treatment was calculated relative to cells that did not receive IFN-β (**Figure 5B**). In control cells that were not infected with rHPIV1, VSV-GFP replication was completely inhibited by IFN-β treatment. In contrast, infection with rHPIV1 wt ablated the ability of 100 IU/ml of IFN-

β to inhibit VSV-GFP replication and blunted the inhibitory effect of 1000 IU/ml of IFN-β, indicating that rHPIV1 wt can prevent IFN-β signaling and the induction of an antiviral state. Infection with rHPIV1-P(C-) did not inhibit the antiviral effect of IFN-β at either concentration, an effect similar to that for rHPIV1-C^{F170S} (**Figure 5B**). In summary, unlike rHPIV1 wt, rHPIV1-P(C-) is unable to inhibit both the production of type I IFN and the induction of an antiviral state by IFN-β.

Figure 5. rHPIV1 wt, but not rHPIV1-P(C-), inhibits type I IFN induction and signaling. (A) Induction of type I IFN. A549 cell monolayers were either mock-infected or infected with rHPIV1 wt, rHPIV1-C^{F170S}, or rHPIV1-P(C-) at a MOI of 5 $TCID_{50}$/cell. Aliquots of the overlying medium were taken at 0, 24, 48 and 72 h p.i. and assayed on fresh cells for the ability to inhibit infection and GFP expression by VSV-GFP as measured with a phosphorimager. IFN concentrations were determined by comparison with a standard curve prepared in parallel with an AVONEX® IFN-β standard and are expressed in pg/ml ± SE based on triplicate samples. The lower limit of detection was 39.1 pg/ml (dashed line). (B) Type I IFN signaling. Vero cells in 6-well plates were infected with the indicated rHPIV1s at a MOI of 5 $TCID_{50}$/cell and incubated for 24 h. Cells were then left untreated or were treated with 100 or 1000 IU/ml IFN-β (1 well per treatment per virus) for 24 h. The cells were then infected with VSV-GFP and incubated for 48 h. The VSV-GFP foci were visualized using a phosphorimager and counted. The graph represents the percent inhibition of VSV-GFP replication in IFN-β treated versus untreated cells based on two independent experiments.

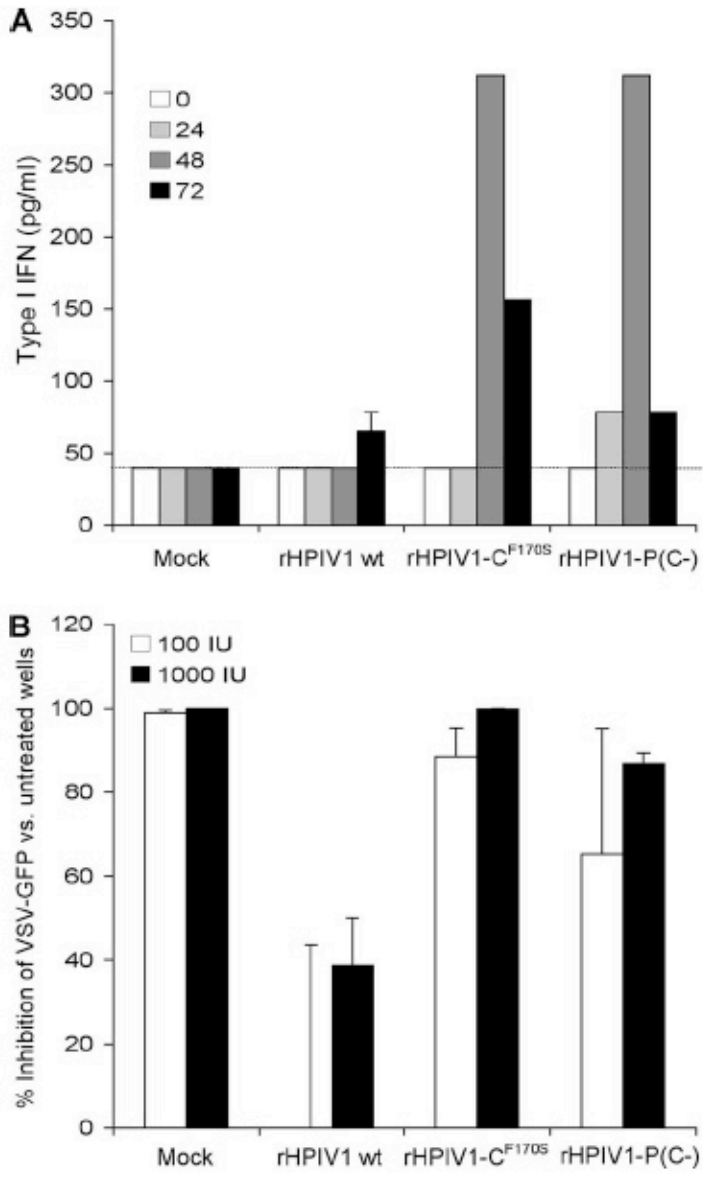

Replication of rHPIV1-P(C-) is restricted in human airway epithelial (HAE) cells in vitro

HPIV1 wt has previously been shown to infect ciliated apical cells in an *in vitro* model of the human airway epithelium (11). Here, we characterized the ability of the rHPIV1-P(C-) to infect HAE in a multiple cycle growth curve. Following apical inoculation at low input MOI (0.01 $TCID_{50}$/cell), rHPIV1 wt replicated efficiently in HAE, reaching a peak titer of 7.4 $\log_{10}$ $TCID_{50}$/ml in the apical wash fluid. However, replication of the

rHPIV1-P(C-) was severely restricted in human ciliated cells, reaching a barely detectable peak of 1.8 $\log_{10}$ $TCID_{50}$/ml (**Figure 6**).

Figure 6. rHPIV1-P(C-) replicates very poorly in primary human airway epithelial (HAE) cells compared to rHPIV1 wt. HAE cultures were inoculated on the apical surface with either virus at a MOI of 0.01 $TCID_{50}$/cell, and virus titers were determined in apical surface washes at days 0-7 p.i. These are shown as the means of triplicate cultures from two donors ± S.E., and the limit of detection is 1.2 $\log_{10}TCID_{50}$/ml.

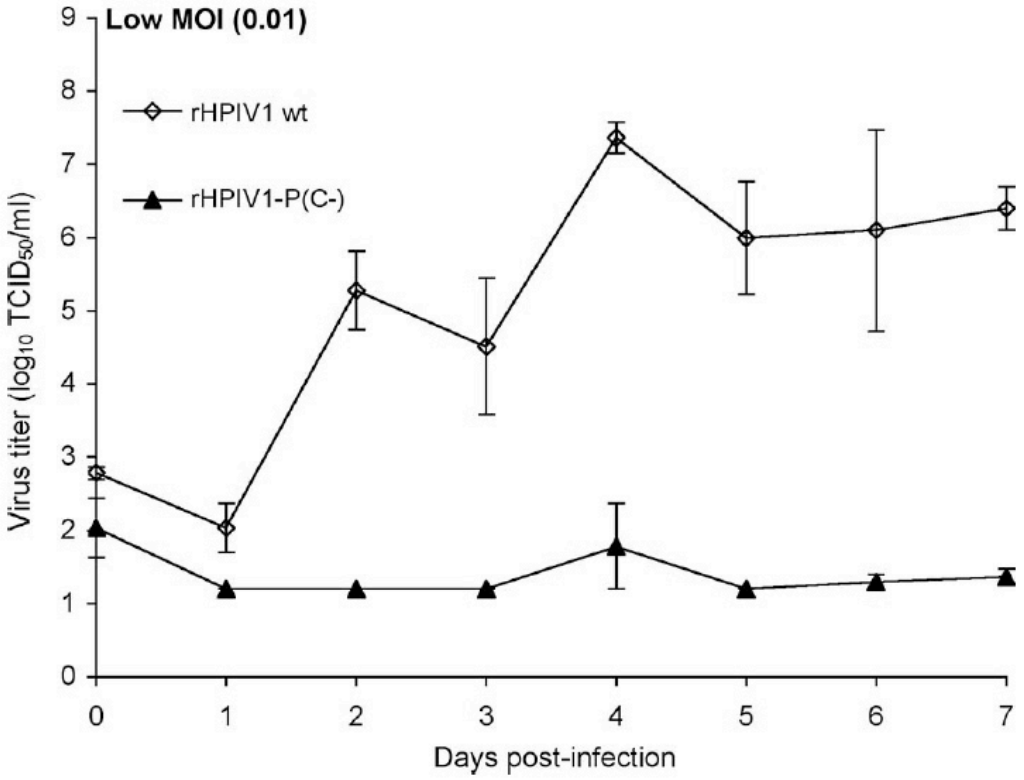

Discussion

A recombinant HPIV1 mutant, rHPIV1-P(C-), that does not express any of the four wild type C proteins but does express a wild type P protein was generated and characterized *in*

vitro and *in vivo*. rHPIV1-P(C-) was found to replicate efficiently *in vitro*, implying that the HPIV1 C proteins are non-essential accessory proteins. However, rHPIV1-P(C-) expressed a novel protein not seen with rHPIV1 that may have been a truncated form of C, and thus we cannot yet conclude that C-related proteins are completely dispensable. rHPIV1-P(C-) replicated with the same efficiency as HPIV1 wt early after infection of human- and monkey-derived cell lines, but its replication subsequently decreased coincident with the onset of extensive cpe that was not observed with rHPIV1 wt. The C proteins of SeV have been extensively characterized as non-essential gene products with multiple functions (105, 109, 110). However, SeV and HPIV1 differ with regard to the genetic organization of their accessory proteins and the phenotypes specified by accessory protein mutations. First, SeV encodes a V protein in addition to the C proteins, whereas HPIV1 does not (90). Second, deletion of all four C proteins in SeV significantly restricted its replication *in vitro* (66, 105, 109), whereas loss of the wild type forms of all four HPIV1 C proteins did not appear to reduce the replication efficiency of rHPIV1-P(C-) apart from the indirect effect of its enhanced cpe. Third, a six amino acid deletion in the N terminal region of the SeV C protein had a profound effect on replication in its natural host, i.e., rodents (47), whereas a similar mutation in HPIV1 C did not affect replication in non-human primates, the closest available animal model to its natural human host (5). Fourth, the F170S mutation in SeV C induced apoptosis in primary mouse pulmonary epithelial cells (83), whereas the same mutation in HPIV1 failed to specify this phenotype in the present study. Since the genetic organization of the accessory proteins of SeV and HPIV1 differ and since the phenotypes of C protein mutants differ significantly *in vitro* and *in vivo*, the functions of the HPIV1 C proteins

cannot be reliably inferred from findings obtained with SeV C protein mutants, and therefore they must be determined directly. An amino acid alignment of the HPIV1 and Sendai virus C proteins is provided in **Figure 7**. In the case of HPIV1, this information has added importance since live attenuated vaccine candidates that are presently being prepared for clinical trials include mutations in the C protein.

Figure 7. CLUSTAL W alignment of the C protein amino acid sequences of Sendai virus and HPIV1 (Genbank accession numbers NP_056874 and NP_604436, respectively). The alignment was generated using the MacVector software program (MacVector Inc., Cary, NC) using default parameters. Conserved amino acids are indicated with asterisks.

```
HPIV1 C:   1 MPSFLRGILKPKERHHENKNHSQMSSDSLTSSYPTSPQKLEKTEAGSMVS  50
Sendai C:  1 MPSFLKKILKLRGRRQEDESRSRMLSDSSTQSYQVNQLTSEGTEAGSTIP  50
             *****  ***   *  *    * * *** * **       * *****

HPIV1 C:  51 STTQKKTSHHAKPTITTKTEQSQRRPKIIDQVRGVESLGEQVSQKQRHML 100
Sendai C:  51 STPSKGQALPTESKVRAREKSRHRRPKIIDQVRRVESLGEQASQRQKHML 100
             **  *                    ********** ******* ** * ***

HPIV1 C: 101 ESLINKVYTGPLGEELVQTLYLRIWAMKETPESTKILQMREDIRDQYLRM 150
Sendai C: 101 ETLINKIYTGPLGEELVQTLYLRIWAMEETPESLKILQMREDIRDQVLKM 150
             * **** ******************** ***** ************ * *

HPIV1 C: 151 KTERWLRTLIRGKKTKLRDFQKRYEEVHPYLMMERVEQIIMEEAWKLAAH 200
Sendai C: 151 KTERWLRTLIRGEKTKLKDFQKRYEEVHPYLMKEKVEQIIMEEAWSLAAH 200
             ************ **** ************** * ********** ****

HPIV1 C: 201 IVQE 204
Sendai C: 201 IVQE 204
             ****
```

Replication of rHPIV1-P(C-) in cell culture peaked early and then decreased steadily coincident with the development of extensive cpe that was not observed with HPIV1 wt. This cpe was associated with caspase 3 activation, cell rounding, nuclear condensation and nuclear fragmentation, indicating that it was apoptotic in nature. In this report, we

identified a novel protein expressed by rHPIV1-P(C-), therefore there is also the alternative possibility - albeit unlikely - that the observed apoptosis during infection with rHPIV1-P(C-) was a gain-of-function due to the novel protein. However, in other work in progress, we have generated additional HPIV1 mutants that also express this novel protein but do not induce apoptosis and do not specify an attenuation phenotype (data not shown). This indicates that the absence of the four C proteins, and not the presence of the additional protein, is associated with the apoptosis-inducing (and also the attenuation) phenotypes of rHPIV1-P(C-). Taken together, our data indicate that one function of the HPIV1 C proteins is to delay or prevent the apoptotic response of the infected cell. Apoptosis has also previously been associated with Sendai virus C protein mutants. SeV C deletion mutants have been shown to induce apoptosis *in vitro*, whereas SeV wt did not (83, 105), suggesting that both SeV C proteins and HPIV1 C proteins act as inhibitors of apoptosis. In addition, the SeV mutant Ohita MVC11, containing the C^{F170S} substitution, was observed to induce cell death *in vitro* while SeV wt did not (83). Similar to our observations of rHPIV1-P(C-), Ohita MVC11 titers peaked early and decreased concomitant with the induction of apoptosis (83). However, data we have presented suggests that despite the relatively high degree of amino acid conservation (70% identity) between HPIV1 and Sendai virus C proteins (**Figure 7**), the induction of apoptosis and/or virus-mediated inhibition of apoptosis may be mediated by different mechanisms for HPIV1 and SeV C proteins. For example, although SeV Ohita MVC11 induces apoptosis, the HPIV1 mutant containing the homologous C^{F170S} substitution, rHPIV1-C^{F170S}, does not induce apoptosis. Furthermore, IRF-3 activation was recently shown to be required for apoptosis during SeV infection in human cell lines (145), but we have

previously shown that rHPIV1-C^{F170S}, which does not induce apoptosis, stimulates IRF-3 activation (192). Studies to define the mechanism of apoptosis inhibition by HPIV1 have been initiated.

The most extensively characterized function of paramyxovirus C proteins is their type I IFN antagonist activity. HPIV1 C proteins have been shown to disrupt the host type I IFN response by (i) inhibiting IRF-3 activation and thereby inhibiting the production of type I IFN, and (ii) inhibiting STAT nuclear translocation (18) and thereby inhibiting the JAK-STAT signaling pathway (192). Our results support these previous findings by demonstrating that, in the absence of C proteins, type I IFN is produced in response to HPIV1 infection and is able to successfully establish an antiviral state in respiratory epithelial cells. In contrast, infection with HPIV1 wt inhibits type I IFN production as well as the establishment of an antiviral state that results from the activation of the JAK/STAT pathway (54, 60, 114, 158, 183, 198). This pathway controls transcription of a group of more than 300 genes termed the IFN-stimulated genes, which have antiviral, antiproliferative, immunomodulatory, and apoptosis modulating functions (114). Therefore, it is not surprising that many viral proteins that have been characterized as IFN antagonists have also been identified to play a role in the regulation of apoptosis. Examples of such proteins include the Bunyamwera virus NSs proteins (101, 197), the RSV NS1 and NS2 proteins (14, 173) and the influenza A virus NS1 protein (166, 182, 196, 220). Our data demonstrate that the HPIV1 C proteins also act both as type I IFN antagonists and as apoptosis antagonists. Interestingly, however, the anti-IFN and anti-apoptosis activities of the HPIV1 C proteins were separable: while the rHPIV1-P(C-) and

rHPIV1-C^{F170S} mutants were indistinguishable with regard to the induction of IFN production and signaling in cell culture, only rHPIV1-P(C-) induced apoptosis.

Since the type I IFN response and apoptosis are both components of the host's innate antiviral response, viruses that have lost the ability to inhibit these responses are often attenuated. The attenuation phenotype of the rHPIV1-P(C-) virus was evaluated in an *in vitro* model of human ciliated airway epithelium (HAE). In order to obtain an assessment of attenuation prior to the initiation of clinical trials, replication of rHPIV1-P(C-) was characterized in a HAE model, which uses primary human airway epithelial cells grown at an air-liquid interface to generate a differentiated, pseudo-stratified, ciliated epithelium that bears close structural and functional similarity to human airway epithelium *in vivo* (149, 219). A similar model has been used previously to evaluate the attenuation of RSV vaccines (205). We have also recently characterized the replication of HPIV1 wt and several HPIV1 vaccine candidates in the *in vitro* HAE model and observed a strong correlation between attenuation in AGMs and attenuation in HAE cells, indicating the potential usefulness of the HAE model for evaluating potential respiratory virus vaccine candidates (11). In our current HPIV1 study, growth of rHPIV1-P(C-) in HAE cells was barely detectable, whereas rHPIV1 wt grew to high titer. This suggests that this virus might be over-attenuated in humans, potentially limiting its efficacy as a vaccine. Therefore, we are currently proceeding to clinical trials with a previously characterized virus, rHPIV1-$C^{R84G/\Delta 170}HN^{T553A}L^{Y942A}$ (8), that is less attenuated than rHPIV1-P(C-). Only if rHPIV1-$C^{R84G/\Delta 170}HN^{T553A}L^{Y942A}$ proves to be insufficiently attenuated will we advance rHPIV1-P(C-) into clinical trials.

Previous studies of rHPIV1 C mutants demonstrated that *in vivo* attenuation correlated with the ability to stimulate an effective type I IFN response, including IFN production and IFN signaling (5, 192). This was demonstrated in detail for rHPIV1-C^{F170S} (192). The rHPIV1-P(C-) virus was indistinguishable from rHPIV1-C^{F170S} with regard to the induction of type I IFN production and signaling to establish an antiviral state *in vitro*. However, rHPIV1-P(C-) was much more attenuated in AGMs than rHPIV1-C^{F170S}. This increased level of attenuation might be due to the induction of apoptosis by rHPIV1-P(C-), a property not shared by rHPIV1-C^{F170S}. We did not determine whether apoptosis was induced *in vivo* following rHPIV1-P(C-) infection, however, a SeV mutant containing the C^{F170S} mutation was shown to induce apoptosis both *in vitro* and *in vivo*, in the bronchial epithelium of mice, and this virus was also attenuated in its natural host (49, 83). It is possible that the *in vitro* apoptosis phenotype of rHPIV1-P(C-) can translate to *in vivo* effects. This would suggest that the greater level of attenuation of rHPIV1-P(C-) versus rHPIV1-C^{F170S} is based on two additive effects: i) the ability (of both viruses) to activate the type I IFN response; and ii) the ability of rHPIV1-P(C-) (but not PIV1-C^{F170S}) to induce apoptosis. However, it is also possible that a C protein function other than inhibition of the IFN response and apoptosis contributed to the high level of attenuation of rHPIV1-P(C-).

In summary, we have demonstrated that the HPIV1 C proteins are non-essential viral proteins that play an important role in viral replication *in vitro* and *in vivo* and act as antagonists of the type I IFN response and of apoptosis. Our HPIV1 C protein deletion

mutant is highly attenuated in primary human airway epithelium. It remains to be determined whether such a highly attenuated virus would be useful as a vaccine candidate against PIV1 in humans.

Chapter 3: The C proteins of human parainfluenza virus type I (HPIV1) control the transcription of a broad array of cellular genes that would otherwise respond to HPIV1 infection

From Journal of Virology 2009 Feb; 83(4): 1892-1910

Jim B. Boonyaratanakornkit, Emmalene J. Bartlett, Emerito Amaro-Carambot, Peter L. Collins, Brian R. Murphy and Alexander C. Schmidt

Laboratory of Infectious Diseases, RNA Viruses Section, National Institute of Allergy and Infectious Diseases, National Institutes of Health, Department of Health and Human Services, Bethesda, MD 20892-8007, USA.

Abstract

HPIV1 is an important respiratory pathogen in children and the most common cause of viral croup. We performed a microarray-based analysis of gene expression kinetics to examine how wild-type (wt) HPIV1 infection altered gene expression in human respiratory epithelial cells and what role IFNβ played in this response. We similarly evaluated HPIV1-P(C-), a highly attenuated and apoptosis-inducing virus that does not express any of the four C proteins, and HPIV1-C^{F170S}, a less attenuated mutant that contains a single point mutation in C and, like wt HPIV1, does not efficiently induce apoptosis, to examine the role of the C proteins in controlling host gene expression. We also used this data to investigate whether the phenotypic differences between the two C mutants could be explained at the transcriptional level. Mutation or deletion of the C proteins of HPIV1 permitted the activation of over 2000 cellular genes that otherwise would be repressed by HPIV1 infection. Thus, the C proteins profoundly suppress the response of human respiratory cells to HPIV1 infection. Cellular pathways targeted by the HPIV1 C proteins were identified and their transcriptional control was analyzed using bioinformatics. Transcription factor binding sites for IRF and NF-κB were over-represented in some of the C protein targeted pathways, but other pathways were dominated by less known factors such as forkhead transcription factor FOXD1. Surprisingly, the host response to the P(C-) and C^{F170S} mutants was very similar, and only subtle differences in the expression kinetics of caspase 3 and the TRAIL receptor 2 were observed. Thus, changes in host cell transcription did not reflect the striking phenotypic differences observed between these two viruses.

Introduction

Human parainfluenza virus type 1 (HPIV1) is the principal cause of laryngotracheobronchitis or croup, and HPIV1, 2, and 3 are collectively the second most common cause of pediatric respiratory hospitalizations, only surpassed by respiratory syncytial virus (42, 134). The clinical manifestations of HPIV1 range from mild disease, including rhinitis, pharyngitis, and otitis media, to severe disease, including croup, bronchiolitis, and pneumonia (30). Licensed vaccines are currently not available against any of the HPIVs but ongoing HPIV3 vaccine development efforts that employ cDNA derived live attenuated viruses have progressed to phase 1/2 clinical evaluation (89, 91, 93).

HPIV1 is an enveloped, negative sense, nonsegmented RNA virus. The viral genome, 15.6 kb in length, consists of 6 genes (3' – N-P/C-M-F-HN-L – 5') that encode the nucleoprotein (N), phosphoprotein (P), C proteins (C), matrix protein (M), fusion protein (F), hemagglutinin-neuraminidase protein (HN), and the large polymerase protein (L). The C proteins comprise a nested set of four carboxy-coterminal proteins, designated C', C, Y1, and Y2, that are expressed from individual start sites in a second open reading frame (ORF) within the P/C gene and are thought to play an important role in HPIV1 virulence (138). The C proteins of Sendai virus (SeV), or murine PIV1, are the best studied of the paramyxovirus C proteins, and there is considerable sequence conservation between the SeV and HPIV1 C proteins. However, the P/C gene organization of SeV differs from that of HPIV1 in that SeV expresses a second accessory protein, the V protein, in addition to the C proteins. There are also phenotypic differences between SeV

and HPIV1 C protein mutants. SeV mutants that do not express any of the C proteins (SeV C knockouts) could be recovered using reverse genetics which identified the C proteins as non-essential viral proteins (108). However, SeV C knockouts are restricted in replication *in vitro* and *in vivo*, which reflects the observation that the C proteins are multifunctional (48, 83, 123, 152). SeV C proteins have been shown to regulate viral replication (33), promote viral assembly (66), confer virulence in mice (85), suppress apoptosis in HEp-2 cells (105), and interfere with antiviral host defense through interferon (IFN) antagonism (57, 96). Recent studies evaluating the HPIV1 C proteins have also identified them as non-essential (9) and demonstrated an important role for the HPIV1 C proteins as IFN antagonists following infection of A549 and MRC-5 human respiratory epithelial cells (18, 192). Specifically, the HPIV1 C proteins inhibit the induction and signaling of IFN in the host cell.

The induction of IFN synthesis following virus infection depends on a number of pattern-recognition receptors that recognize conserved pathogen-associated molecular patterns and initiate downstream signaling cascades (87). The IFN antiviral pathway can be activated by double stranded RNA (dsRNA), 5'-triphosphate single stranded RNA or viral infection. The presence of dsRNA, an intermediate of viral replication, is recognized as a pathogen-associated molecular pattern by Toll-like receptor 3 (TLR3) and two caspase recruitment domain (CARD) containing RNA helicases, retinoic acid-inducible gene I (RIG-I) and melanoma associated-differentiation gene 5 (MDA-5), which are constitutively expressed and act as intracytoplasmic sensors of dsRNA (2, 180, 214). RIG-I also specifically binds single stranded RNA with 5’- triphosphate ends to

distinguish self from non-self RNA (76, 147, 180, 212). TLR3 uses the adaptor TIR domain-containing adaptor inducing IFNβ (TRIF) while RIG-I and MDA-5 recruit another CARD-containing adaptor mitochondrial antiviral signaling protein (MAVS, also referred to as IPS-1, Cardif or VISA) to relay the signal to the kinases TBK1 and IKK-i, which phosphorylate IRF3 (interferon regulatory factor 3), and to IKKβ, which activates the NF-κB pathway (41, 99, 140, 167, 207). Once activated, IRF3 translocates into the nucleus and binds the positive regulatory domain III (PRDIII) of the IFNβ promoter. RIG-I and MDA-5 can distinguish between different RNA viruses (98). IFN production in response to SeV infection is specifically dependent on RIG-I expression, whereas IFN production in response to picornavirus infection is dependent on MDA-5 expression (98). IRF-3 and NF-κB, together with ATF-2/c-Jun, form an enhanceosome that binds to the IFNβ promoter, inducing transcription of the IFNB gene. IFNβ, in turn, controls the expression of a broad array of antiviral genes (210). Transcriptional activation of type I IFN is biphasic. One gene encodes the prototypical IFNβ, while more than a dozen IFN species comprise the IFNα family (183). Recognition of viral infection results in phosphorylation of constitutively expressed IRF3 to induce IFNβ and IFNα1 expression in human cells as part of the early response to virus infection. Once early type I IFN is produced and secreted, it binds to the type 1 IFN receptor on the surface of the infected and neighboring cells, activates the JAK-STAT signal transduction cascade, and induces formation of IFN-stimulated gene factor 3 (ISGF3) which consists of a heterotrimeric complex of STAT1, STAT2, and IRF9. ISGF3 binds to the IFN-stimulated response elements (ISRE) within the promoter regions of several hundred IFN-inducible genes, including 2'-5'-oligoadenylate synthetase (OAS), dsRNA dependent protein kinase

(PKR), and IRF7. The *de novo* produced IRF7 is phosphorylated and can then activate production of additional type I IFNs, including IFNβ and the full set of IFNα's (163). Thus, immediate-early expression of IFNβ and IFNα1, induced by IRF3, NF-κB, and ATF-2, occurs soon after viral infection is detected, while delayed expression of the entire type I IFN family, induced by IRF7, occurs only after IFNβ and IFNα1 secretion, receptor binding, and signaling to amplify a robust feed-forward antiviral response (121, 183).

Our laboratory has established a reverse genetics system for HPIV1 that allows the generation of infectious virus from cDNA (85, 137). Using this system, a number HPIV1 mutants containing mutations in the C gene have been generated to investigate C protein function and to generate novel live attenuated experimental vaccines that are attenuated by disturbing the IFN antagonistic function of the C gene (192). Previously, a phenylalanine to serine substitution of amino acid 170 of SeV was shown to significantly attenuate a highly virulent SeV strain, increasing the lethal dose 50% (LD_{50}) 20,000-fold in mice (50). This C^{F170S} mutation, which affects all four C proteins without affecting the P protein, was introduced into the P/C gene of recombinant (r) HPIV1 by reverse genetics (85, 137). This mutant, designated as rHPIV1-C^{F170S} and also referred to here as C^{F170S}, was previously found to be defective in inhibiting IFNβ induction and signaling *in vitro* and to be attenuated for replication in the respiratory tract of hamsters and African green monkeys (AGMs) (5, 192). Whereas wild-type (wt) HPIV1 infection abrogated IRF3 dimerization and nuclear translocation, infection with rHPIV1- C^{F170S} resulted in IRF3 activation and IFNβ production (192). The wt HPIV1 C proteins were also shown to

inhibit IFN signaling by blocking STAT1 and STAT2 nuclear translocation, and wt HPIV1 could overcome a pre-existing IFNβ-induced antiviral state in MRC-5 cells (18). In contrast to wt HPIV1, rHPIV1- C^{F170S} did not inhibit the establishment of an antiviral state (192).

More recently, we constructed a mutant HPIV1 that does not express any of the four C proteins, which is designated rHPIV1-P(C-) and also is referred to here as P(C-) (9). In this virus, the C' start codon was deleted, the C start codon was mutated, and several stop codons were inserted to ensure that the C', C, Y1, and Y2 proteins could not be expressed. All of the above mutations were designed to be silent in the P ORF. Interestingly, the P(C-) and C^{F170S} mutant viruses differ in their *in vitro* and *in vivo* phenotypes. The P(C-) mutant is highly attenuated *in vivo* in AGMs whereas the C^{F170S} mutant is only moderately attenuated. In addition, infection with the P(C-) mutant leads to early and significant induction of apoptosis while C^{F170S} and wt HPIV1 are very weak inducers of apoptosis (9).

Microarray-based analyses are increasingly being used in virology and have helped to elucidate virus-host interactions for a number of viruses (reviewed in (88)). In the present study, we used a microarray-based analysis of the kinetics of gene expression to examine: 1) how wt HPIV1 infection altered human respiratory epithelial cell gene expression; 2) what role IFNβ played in this response; 3) how the response to infection with the C mutant viruses C^{F170S} and P(C-) compared to the response to wt HPIV1; and 4) whether the phenotypic differences between the two C mutant viruses (level of

attenuation and apoptosis phenotype) could be explained on a transcriptional level. We compared the mRNA levels in A549 cells treated with IFNβ or infected with wt HPIV1, C^{F170S}, or P(C-) using a microarray that represented the full complement of known human genes. To examine the function of the C proteins in the infected cell, the expression patterns of cells infected with HPIV1 C mutant viruses were compared to that of cells infected with wt HPIV1. We show that the C proteins of HPIV1 profoundly suppress the innate response of human respiratory cells to infection with this important pediatric respiratory virus.

Materials and Methods

Cell culture and viruses

A549 human respiratory epithelial cells (ATCC catalog number CCL-185, Manassas, VA) were maintained in F-12 medium supplemented with 0.1mg/mL gentamicin sulfate, 4 mM L-glutamine (Gibco-Invitrogen, Carlsbad, CA) and 5% fetal bovine serum (Hyclone, Logan, UT). LLC-MK2 cells (ATCC) were maintained in Opti-MEM I (Gibco-Invitrogen) supplemented with 0.1mg/mL gentamicin sulfate and 5% fetal bovine serum.

Recombinant wt HPIV1 and mutant C^{F170S} and P(C-) were each recovered from cDNA as previously described (9, 137, 138). All viral infections were carried out at 32°C in media containing 1.2% recombinant trypsin TrypLE Select (Gibco-Invitrogen) without fetal bovine serum. Virus stocks were generated by infecting LLC-MK2 cells at a multiplicity of infection (MOI) of 0.01 50% tissue culture infectious dose ($TCID_{50}$) per cell and by

harvesting supernatant on day 7 post infection (p.i.). Virus particles in the supernatant were purified by centrifugation in a discontinuous 30%/60% sucrose gradient in 0.05M HEPES and 0.1M $MgSO_4$ (Sigma-Aldrich, St. Louis, MO) at 120,000*g* for 90 minutes at 4°C. This purification was performed to minimize contamination of virus suspensions used to infect cells with cellular proteins, including IFN. Virus titers were determined by infecting LLC-MK2 cell monolayers with serial 10-fold dilutions of virus, and infected cultures were detected 7 days p.i. by hemadsorption with guinea pig erythrocytes (168). The titer of sucrose purified wt HPIV1, C^{F170S}, and P(C-) was determined at 8.9, 9.1, and 8.5 $\log_{10}TCID_{50}$ per mL, respectively.

Viral genomic RNA was isolated from the sucrose purified stocks for sequence analysis using the QIAamp viral RNA Mini Kit (Qiagen, Valencia, CA), then reverse transcribed using the Superscript II First Strand Synthesis System (Invitrogen), amplified using the Advantage HF-PCR Kit (Clontech, Mountain View, CA), and purified using the High Pure PCR Purification Kit (Roche, Indianapolis, IN) per the manufacturers' protocols and as previously described (138). The identity of each virus was confirmed by sequencing the entire viral genome using BigDye Terminator v1.1 on a DNA Analyzer 3730 (Applied Biosystems, Foster City, CA) and analysis with Sequencher 4.7 (Gene Codes Corporation, Ann Arbor, MI).

Microarray sample preparation and expression analysis

A549 cells were mock infected or infected in triplicate at a MOI of 5 $TCID_{50}$ per cell with wt HPIV1, C^{F170S}, or P(C-) for 6, 12, 24, and 48 h. In an independent experiment,

additional A549 cell cultures were treated in triplicate with 300 pg/mL (60 IU/mL) of IFNβ (Avonex, Biogen Inc, Cambridge, MA) for 6 or 24 h. We chose this concentration because we previously found that infection of A549 cells with C^{F170S} and P(C-) led to IFN secretion that resulted in an IFN concentration of approximately 300 pg/mL in the cell supernatant (9, 192). Thus, four treatment groups, i.e. IFNβ treatment, as well as infection with wt HPIV1, C^{F170S}, or P(C-) were separately analyzed; IFN treatment at two time points and each of the three virus infections at 4 time points.

Cellular RNA was extracted from infected/treated cells using the RNeasy Mini Kit and treated with the RNase-free DNase set (Qiagen). RNA from virus infected and IFNβ treated A549 cells was labeled with Cy5 while RNA from mock infected samples was labeled with Cy3 using the 2-Color Low RNA Input Linear Amp Kit PLUS (Agilent Technologies, Foster City, CA) as per the manufacturer's protocol. Labeled RNA was hybridized onto Whole Human Genome 44K Oligo Microarrays (catalog number G4112F) and was scanned with a DNA Microarray Scanner (Agilent Technologies) per the manufacturer's protocol. This microarray detects the expression of over 41,000 genes and expressed sequence tags, representing all known genes in the human genome. Spot detection, signal quantitation, dye normalization by Lowess regression, and quality control assessment of control RNA spike-ins was performed using Feature Extraction Software v9.5 (Agilent Technologies). Data was then loaded into GeneSpring GX 7.3.1 (Agilent Technologies) for signal normalization, statistical tests, and hierarchical clustering. Relative gene expression ratios in virus infected and IFNβ treated cells compared to mock were calculated by dividing the intensity of the Cy5 signal by the Cy3

signal intensity. Each array was normalized to the median signal ratio of all probes on the array. Genes were defined as being differentially expressed between two samples if they were flagged as present in at least one sample and exhibited at least a 4-fold difference that was statistically significant after multiple testing correction with a Benjamini-Hochberg false discovery rate of $P < 0.01$. The 4-fold cutoff was chosen to minimize false positives and increase confidence in our data interpretation. Wei, et al. give sample sizes required for detecting differential gene expression with 1.5-, 2-fold, and 4-fold change cutoffs. Lower fold-change cutoffs lead to a greater rate of false positives and a requirement for much larger sample sizes to detect significant changes by statistical tests (200). The phenotypic differences between the C mutant viruses were striking and were expected to be associated with large changes in expression that could be detected above 4-fold. 2,612 genes were identified as significantly differentially expressed compared to mock in at least one of the four infection/treatment groups. To identify differences in gene expression between wt HPIV1, C^{F170S}, and P(C-), we selected 1,314 of the 2,612 genes that demonstrated significant differential expression in at least one pair-wise comparison between virus infections at the same time point and/or between IFNβ treatment and mock. Hierarchical clustering was performed on individual samples based on the expression ratios at each time point using a Pearson correlation as a measure of similarity between expression profiles. These clusters are groups of genes that share similarities in the pattern with which their expression varies over all sampling time points (38). All of the microarray data was deposited according to the MIAME standards to the Gene Expression Omnibus with accession number GSE12664 at http://www.ncbi.nlm.nih.gov/geo/.

Functional genomic bioinformatics

The clusters identified above were further examined for commonalities in functional characteristics including over-representation of biological pathways and over-representation of transcription factor binding sites (TFBSs) within the respective cluster. Over-represented functional pathways within each cluster of genes were searched against the Agilent Whole Human Genome Reference Set using Ingenuity Pathway Analysis 5.5.1 (Ingenuity Systems, Redwood City, CA). Statistically over-represented functional pathways ($P < 0.05$ using a right-tailed Fisher's exact test) were retained for further analysis. A P value less than 0.05 in the Fisher exact test indicates that the proportion of probes in the cluster, compared to every other probe on the Agilent Whole Genome array, involved in a pathway is greater than would be expected by chance. TFBSs that were over-represented within each cluster were identified using oPOSSUM Single Site Analysis software to search the 2000 base pair (bp) upstream sequence of each gene in the cluster against the JASPAR database (72, 161, 193). JASPAR is an open-access, curated, non-redundant database of 123 sequence motif matrices of experimentally defined TFBSs. Genes with assigned Entrez Gene identifiers were loaded into oPOSSUM to examine upstream sequences in all of the genes within the respective cluster of genes. oPOSSUM retrieves upstream promoter sequences from Ensembl (www.ensembl.org), uses phylogenetic footprinting to identify conserved, functional, non-coding DNA, and aligns sequences to position specific scoring sequence matrices in JASPAR in order to identify high-quality, predicted, evolutionarily conserved TFBSs. We used an 85% matrix match threshold, a Z-score > 10, and a Fisher exact test $P < 0.05$ to select for

statistically over-represented TFBSs within each cluster compared to the background of all genes in oPOSSUM. These criteria have been shown by testing randomly generated gene lists to yield a specificity of 86% (72).

Real-time quantitative PCR (RT-qPCR) expression analysis

Total RNA was reverse transcribed using the High-Capacity cDNA Reverse Transcription Kit (Applied Biosystems, Foster City, CA) and amplified using the TaqMan Universal PCR Master Mix (Applied Biosystems). TaqMan Gene Expression Assays (Applied Biosystems) for IFNB1 (Hs01077958_s1), IRF7 (Hs00242190_g1), MX1 (Hs00182073_m1), NFKB1 (Hs00231653_m1), TRAF1 (Hs01090170_m1) and GAPDH (Hs99999905_m1) were chosen to validate microarray expression profiles, and samples were prepared for analysis as per the manufacturer's protocol. The microarray analysis verified that GAPDH was an appropriate endogenous control since GAPDH expression was constant throughout all conditions and time points. Samples were run on the 7900HT Fast Real-time PCR System (Applied Biosystems). Quantitative PCR analysis was performed using SDS 2.3 and RQ Manager 1.2 (Applied Biosystems). All expression values were normalized against the GAPDH endogenous control and then normalized against mock infected samples to obtain relative gene expression ratios using the Pfaffl method (146).

Results

Differential gene expression following wt HPIV1 infection goes beyond modulation of the type 1 IFN response

In order to better understand the host cell response to HPIV1 infection, A549 human respiratory epithelial cells were infected with wt HPIV1 at a MOI of 5 $TCID_{50}$ per cell or were mock infected, and total cellular RNA was extracted at 6, 12, 24, and 48 h p.i. RNA was reverse transcribed and changes in gene expression were compared to mock infected cells using a two-color 60-mer cDNA microarray platform representing more than 41,000 human genes and expressed sequence tags. To directly identify IFN-inducible genes in A549 cells for comparison to the wt HPIV1 induced genes, additional A549 cells were treated with 300 pg/mL (60 IU/mL) of IFNβ or left untreated, and analyzed in the same way as the wt HPIV1 infected cells. This dose of IFNβ was chosen because it approximates the concentration previously shown to be induced in this cell line by infection with the C^{F170S} and P(C-) viruses (9, 192). An overview of this data set is depicted in **Figure 1**, column I. Each treatment group (i.e. wt HPIV1 or IFNβ) at each time point consists of three replicates. A considerable number of known IFN-inducible genes, e.g. IRF7 and MX1, were up-regulated late in the course of wt HPIV1 infection, i.e., 48 h p.i., even though wt HPIV1 is known to inhibit type 1 IFN production and signaling in A549 cells (192). A total of 343 genes were differentially expressed (i.e. a four-fold or greater change compared to mock and $P < 0.01$) at one or more time points following infection with wt HPIV1 and/or IFNβ treatment; overall, 284 genes for HPIV1 and 191 genes for IFNβ (**Fig. 2**).

Figure 1. Comparison of A549 cellular genes responsive to infection with wt HPIV1 (referred to here as WT) or treatment with IFNβ. **Column I)** Hierarchical clustering of the 343 genes that were differentially expressed (4-fold or greater change relative to mock, $P < 0.01$ with multiple testing correction) following wt HPIV1 infection and/or IFNβ treatment, with the fold-change indicated in color. Each colored row represents an individual transcript, with representative genes identified immediately to the right. Each colored column consists of three replicates, side by side, with the treatment condition/time point identified at the bottom. The genes were clustered into five groups (A through E, demarcated to the right) according to similarity of expression kinetics and magnitude of expression versus mock at each time point using a Pearson correlation as a measure of similarity. The number of genes in each cluster is given in parentheses. Three of the clusters (A, B, and D) contain genes that were predominantly responsive to IFNβ and/or wt HPIV1; one cluster (C) contains genes that were predominantly responsive to IFNβ but not wt HPIV1, and one cluster (E) contains genes were predominantly responsive to wt HPIV1 but not IFNβ (see the text). **Column II)** The gene expression profiles for clusters A through E are shown in panels A through E, respectively, with the geometric mean gene expression (y-axis) plotted against each treatment condition at the indicated time-points in h p.i. (x-axis). **Column III)** Functional pathways that are over-represented in clusters A through E were determined using Ingenuity Pathway Analysis and are indicated on the left, next to the expression profile of the respective cluster. TFBSs that are over-represented among the genes within each cluster were identified using oPPOSUM to search the JASPAR core database, and are indicated to the right. The JASPAR database contains IRF1 and IRF2 but does not include an entry for other IRFs.

To identify potential binding sites for other IRFs and ISGF3, we also scanned all clusters for the shared core sequence motif for the IRFs and ISGF3, GAAANNGAAA.

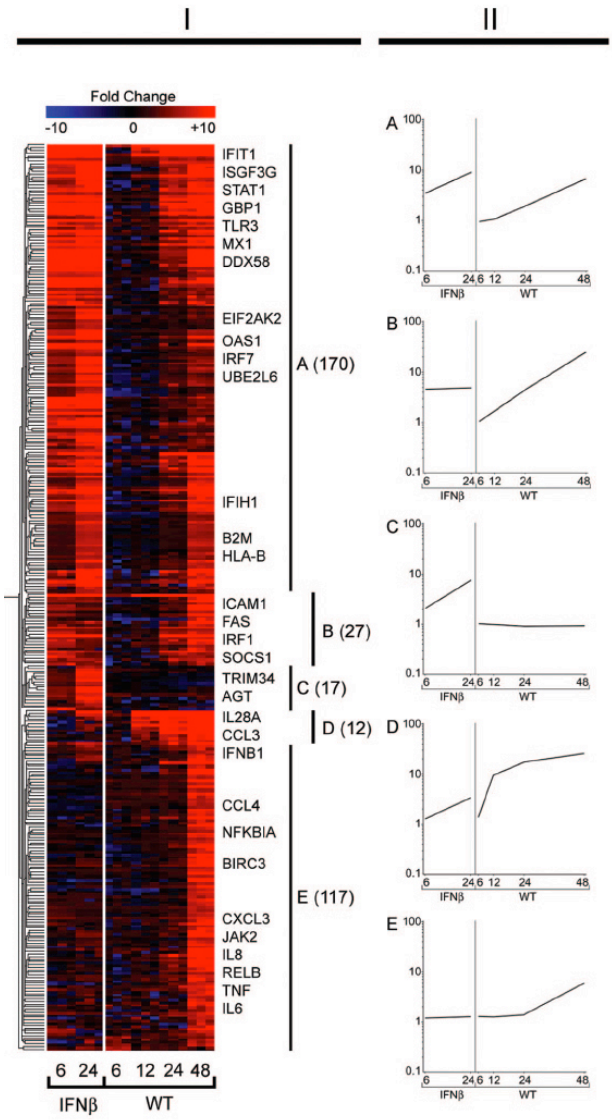

Overrepresentation of:

Functional Pathways		Transcription Factor Binding Sites	
Pathway	P-value	Promoter	P-value
IFN Signaling	1.5E-18		
Ag Presentation	1.8E-13		
Protein Ubiquitination	1.2E-08	IRF1	5.9E-03
Nucleotide Metabolism	1.6E-02	ISGF3/IRF*	4.0E-03
TLR Signaling	3.0E-02		
NF-κB Signaling	4.4E-02		
JAK/STAT Signaling	4.6E-02		
IFN Signaling	4.1E-04	NF-κB1	2.3E-03
IL6 Signaling	4.2E-03		
-	-	-	-
IFN Signaling	1.5E-02	IRF1	1.6E-02
Chemokine Signaling	4.0E-02	c-REL	2.6E-02
		FOXQ1	3.5E-02
Apoptosis Signaling	2.1E-05	c-REL	4.9E-06
IL6 Signaling	2.6E-05	RELA	1.4E-05
NF-κB Signaling	2.1E-04	NF-κB1	1.981E.5
Acute Phase Response	5.2E-04	HLF	2.2E-02
		SPIB	3.3E-02

*The JASPAR database contains IRF1 and IRF2 but does not include an entry for other IRFs. The shared core sequence motif for the IRFs and ISGF3, GAAANNGAAA, was searched in all clusters.

Figure 2. Total number of genes differentially expressed during HPIV1 infection and IFNβ treatment compared to mock over time in h p.i. Specifically, the number of genes that were significantly differentially expressed, in comparison to mock infected cells, in cells infected with WT, C^{F170S}, or P(C-) viruses at 6, 12, 24, and 48 h p.i., or in IFNβ treated A549 cells at 6 and 24 h is indicated. Total represents the cumulative number of genes differentially expressed taking all time points into consideration. Infection with C^{F170S} or P(C-) viruses led to a significant alteration of gene expression in many more genes than did infection with WT or treatment with IFNβ.

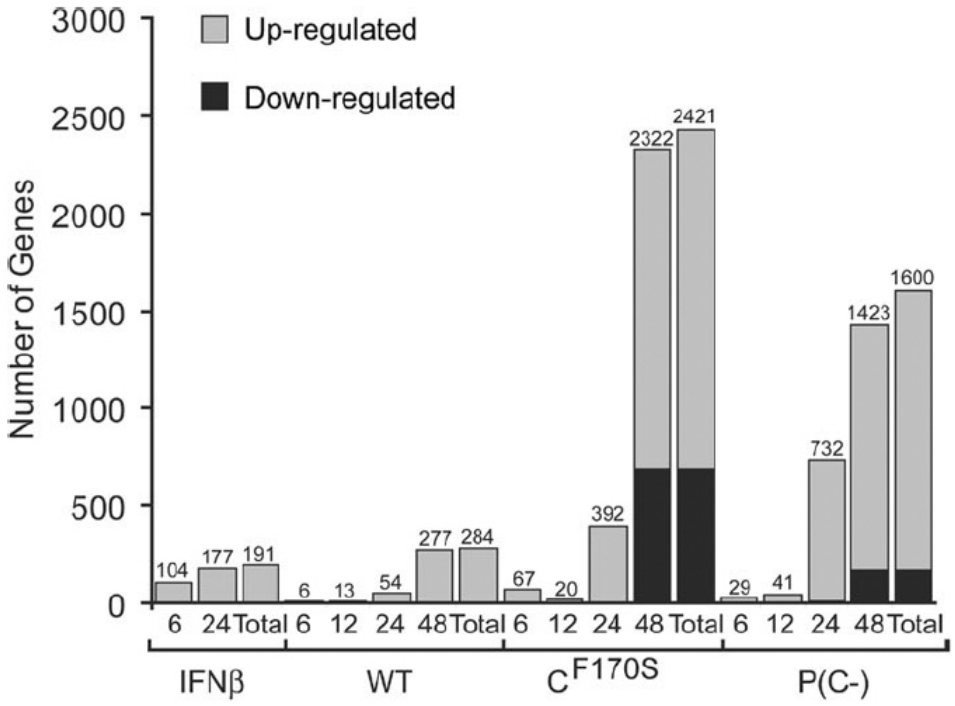

The 343 genes that were differentially expressed in response to wt HPIV1 and/or IFNβ treatment were grouped into clusters based on the kinetics and magnitude of gene expression. This was done using a hierarchical clustering analysis of the 343 genes across

both treatments and all of the time points (e.g. wt HPIV1 at 6, 12, 24 and 48 h p.i., and IFNβ at 6 and 24 h). Five different gene expression profile patterns were identified, including 3 clusters containing a combined total of 209 genes that were predominantly responsive to both IFN and wt HPIV1 (**Fig. 1**, clusters A, B and D), one cluster of 17 genes that was predominantly responsive to IFNβ but not wt HPIV1 (cluster C), and one cluster of 117 genes that was predominantly responsive to wt HPIV1 but not IFNβ (cluster E). Although, in total, the 226 genes from clusters A, B, C, and D can be grouped together based on the predominant kinetics of gene expression after IFNβ treatment, only 191 of the 226 genes satisfied the 4-fold change criteria for IFN-responsive genes (**Fig. 2**). The remaining 34 genes were up-regulated less than 4-fold with IFNβ treatment but greater than 4-fold with wt HPIV1 infection. Some representative members of each cluster are indicated in **Fig. 1**, column I; a complete list of the genes and their expression levels is provided in supplementary **Table S1** of the appendix. The graphs in **Fig. 1**, column II represent the geometric mean value for the fold change over time compared to mock for all genes within each cluster and indicate a signature profile for the genes in that cluster.

Nearly all of the 170 genes in cluster A were responsive to IFNβ treatment, and a majority also were responsive to wt HPIV1 infection, although the response to wt HPIV1 infection was delayed by approximately 24 h (**Fig. 1**, column II, cluster A). In both treatment groups, the fold change increased with time. We next analyzed cluster A (and each succeeding cluster) for over-representation of functional pathways within each

cluster of genes using a software tool that determines the likelihood of a given number of genes being represented within a defined pathway (Ingenuity Pathway Analysis). The *P* value (Fisher's exact test) for that likelihood is indicated next to the pathways in **Fig. 1**, column III. Genes involved in the Toll-like receptor and NF-κB pathways were over-represented in cluster A, which is not surprising given the observed up-regulation in response to IFNβ and wt HPIV1 (**Fig. 1**, column III and **Table S1**). Aiming to understand the regulation of gene expression within a given cluster, the JASPAR database of TFBSs was searched for over-representation of specific TFBSs within the genes contained in each cluster. In cluster A, IRF1 and IRF3/ISGF3 TFBSs, which all share the same conserved consensus sequence, were found to be significantly over-represented (**Fig. 1**, column III). Since ISGF3, a heterotrimeric complex of STAT1, STAT2, and IRF9, is induced by binding of IFNβ to the IFN receptor, this finding was not unexpected. Translocation of ISGF3 into the nucleus activates the transcription of genes with ISREs. IRF1 similarly binds to and activates upstream cis-acting elements of the IFNA and IFNB genes**.**

Cluster B contained 27 genes that were predominantly up-regulated by IFNβ and wt HPIV1. The mRNAs in cluster B were rapidly induced at 6 h post IFNβ treatment but, on average, failed to increase further at 24 h, whereas HPIV1 infection led to a steady increase in the expression of the cluster B genes (**Fig. 1** column II, cluster B). Genes within this cluster seem to be functionally involved in IFN signaling and IL6 signaling. Analysis of upstream cis-acting elements reveals that the family of NF−κB binding sites

was significantly over-represented amongst these genes. IFIT2 (IFN-induced protein with tetratricopeptide repeats-2/ISG-54) was one of the most strongly expressed genes in cluster B and was up-regulated 85-fold by IFNβ treatment and more than 500-fold following wt HPIV1 infection (**Table S1**).

The 17 genes in cluster C were up-regulated by IFNβ but not by wt HPIV1. Up-regulation was rapid, occurring by 6 h with continued increase at 24 h (**Fig. 1**, column II, cluster C). The genes in cluster C formed a relatively heterogeneous group that contained no significantly over-represented functional pathways or TFBSs, and contained only a few genes with known antiviral function such as the tripartite motif protein 34 (TRIM34) (115). It is significant that infection with wt HPIV1 did not induce or activate expression of the subset of IFNβ-responsive genes that are represented in cluster C, suggesting that HPIV1 might activate a selective negative feedback mechanism that inhibits transcription of a subset of IFNβ-responsive genes.

Cluster D is comprised of 12 genes that as a group were strongly induced by wt HPIV1 infection but weakly induced with IFNβ treatment. Only 2 genes were significantly induced by IFNβ beyond 4-fold. Genes involved in IFNβ and chemokine signaling, such as CCL3, CCL5, CXCL10 and IL28A/IFNλ, were over-represented in this cluster, and both IRF1 and c-REL binding sites dominated in the promoter regions of cluster D genes (**Fig. 1**, column III, Table S1).

Cluster E contained 117 genes that were predominantly induced by wt HPIV1 but not by IFNβ. Induction of the genes in cluster E was significantly delayed, i.e., it was not observed until 48 h p.i. This cluster notably included the cytokines IL6, IL8, TNF (tumor necrosis factor α), and CXCL3, and, as a result, pathways involved in apoptosis, NF-κB, and death receptor pathways as well as in IL6 signaling were significantly over-represented in cluster E. The family of NF-κB TFBSs, but not ISRE or IRF, were statistically over-represented in the promoters of these genes. The five species of NF-κB transcription factors, RELA (p65), RELB, c-REL, NF-κB1 (p105/p50), and NF-κB2 (p100/p52), are present in homo- and heterodimers that are bound by IκB proteins and localized in the cytoplasm until IκB is phosphorylated by the IκB kinase, leading to its ubiquitination and proteasome-mediated degradation. This releases the various NF-κB dimers for nuclear translocation and binding to NF-κB TFBS in target genes. RELA, RELB, and c-REL each contain a transactivator domain that strongly activates transcription whereas NF-κB1 and NF-κB2 lack this domain and, when binding as homodimers, can function as transcription repressors (188). Taken together, two key signaling pathways, the NF-κB and the IFN pathway, are central to regulating the cellular antiviral and inflammatory response to wt HPIV1 infection.

The HPIV1 C proteins inhibit the induction of gene expression in A549 cells

The HPIV1 C proteins play an important role in the inhibition of IFNβ production and signaling (18, 192). The recently generated rHPIV1 mutant that does not express any of the C proteins, designated P(C-), is similar to C^{F170S} with regard to its IFN phenotype in A549 cells but differs from C^{F170S} in that P(C-) is a strong inducer of apoptosis in LLC-

MK2 and A549 cells whereas C^{F170S} more closely resembles wt HPIV1 in that it is a weak inducer of apoptosis (9, 192). In addition, P(C-) is more attenuated than C^{F170S} in the respiratory tracts of hamsters and AGMs (9). We first sought to compare the number of genes that were differentially expressed by infection with wt HPIV1 or HPIV1 C mutant viruses to assess the role of the C proteins in controlling the host response to viral infection. Therefore, the number of significantly differentially regulated genes (4-fold cutoff, $P < 0.01$) in A549 cells infected with either the C^{F170S} or the P(C-) mutant was compared to that with wt HPIV1 infection or IFNβ treatment. Surprisingly, infection with C^{F170S} or P(C-) altered the expression of a substantially greater number of genes than wt HPIV1 infection or IFNβ treatment. Specifically, taking all of the time points into consideration, the C^{F170S} mutant significantly induced 1,734 genes and suppressed 690 genes, whereas P(C-) induced 1,430 genes and suppressed 170 genes by 48 h p.i. In contrast, wt HPIV1 significantly induced 281 genes and suppressed 3 genes (**Fig. 2**). This indicates the profound effect the C proteins have on suppression of the host cell response to HPIV1 infection.

Treatment with IFNβ differentially induced 190 genes and suppressed only 1 expressed sequence tag at 6 h and/or 24 h post-treatment, based on a four-fold or greater change compared to mock-treatment, for a total of 191 IFNβ-responsive genes (**Fig. 2**). For comparison, previous microarray-based studies that surveyed only a fraction of the human genome identified 14, 56, and 268 genes whose expression changed 10-fold, 4-fold, and 2-fold, respectively, in IFNβ treated HT1080 human fibrosarcoma cells by 6 h and 42 genes whose expression changed 5-fold in IFNα treated A549 cells by 24 h (36,

59, 160). Interestingly, to the best of our knowledge, 66 of the 190 induced genes whose expression changed 4-fold or greater in the present study have not been previously described as IFN-regulated (**Table S1**) (36, 59, 160).

Pair-wise comparisons of the fold change in the global gene expression (i.e., the entire microarray) was conducted for C^{F170S} versus wt HPIV1, P(C-) versus wt HPIV1, and C^{F170S} versus P(C-) at 6, 12, 24, and 48 h p.i. (**Fig. 3**). In this comparison, each gene is represented by a single dot, and the accumulation of dots along the center diagonal line in each plot in **Fig. 3** indicates a similar fold change between the viruses represented on the x- and y-axes, whereas the two outer lines indicate a four-fold difference. This comparison of the kinetics of the cellular response to infection showed that global gene expression in cells infected with C^{F170S} or P(C-) at 6 and 12 h p.i. did not differ significantly from that of wt HPIV1 infected cells (**Fig. 3**, 6 h and 12 h panels). Points deviate from the central diagonal only at 24 h and/or 48 h p.i., especially when either of the C mutant viruses are compared to WT due to the potent effects of infection with mutant viruses that are unable to suppress the cellular response to viral infection. By 24 h p.i., a significant proportion of genes were either up- or down-regulated more than four-fold in both the C^{F170S} and P(C-) groups, as indicated by the number of dots outside the two outer boundaries that run parallel to the diagonal, while wt HPIV1 virus did not have this effect (**Fig. 3**, 24 h). At 48 h p.i., this difference in gene expression between each of the C mutants versus wt HPIV1 was even more pronounced. It was also important to compare transcriptional patterns between the two C mutant viruses in order to investigate why complete deletion of the C gene conferred a greater level of attenuation and an

apoptotic phenotype, in contrast to C^{F170S}. Surprisingly, there was no apparent difference in global gene expression between the C^{F170S} and P(C-) infected cells with the exception of a slightly more pronounced gene induction in P(C-) infected cells at 24 h p.i. (**Fig. 3**, right column). However, none of the genes differed four-fold or more in expression between these two C mutant viruses. Because of the remarkable lack of obvious differential gene expression between C^{F170S} and P(C-) infected cells, the sequence identity of C^{F170S} and P(C-) was confirmed in the supernatant of the respective cell cultures used in the RNA extraction for gene expression analysis (data not shown).

Figure 3. Pair-wise comparisons of global gene expression in A549 cells indicates that the C^{F170S} and P(C-) viruses induce a highly similar host cell response that differs greatly from the wt HPIV1 (WT) -induced response. Each plot depicts the geometric mean difference for individual transcripts (represented by dots) from triplicate samples in pair-wise comparisons between cells infected with C^{F170S} versus WT (left panels), P(C-) versus WT (middle panels), and C^{F170S} versus P(C-) (right panels) at 6, 12, 24, and 48 h p.i. (rows 1, 2, 3, and 4, respectively). The central diagonal line indicates equal fold change between the virus pair under comparison; the outer boundaries indicate a four-fold change.

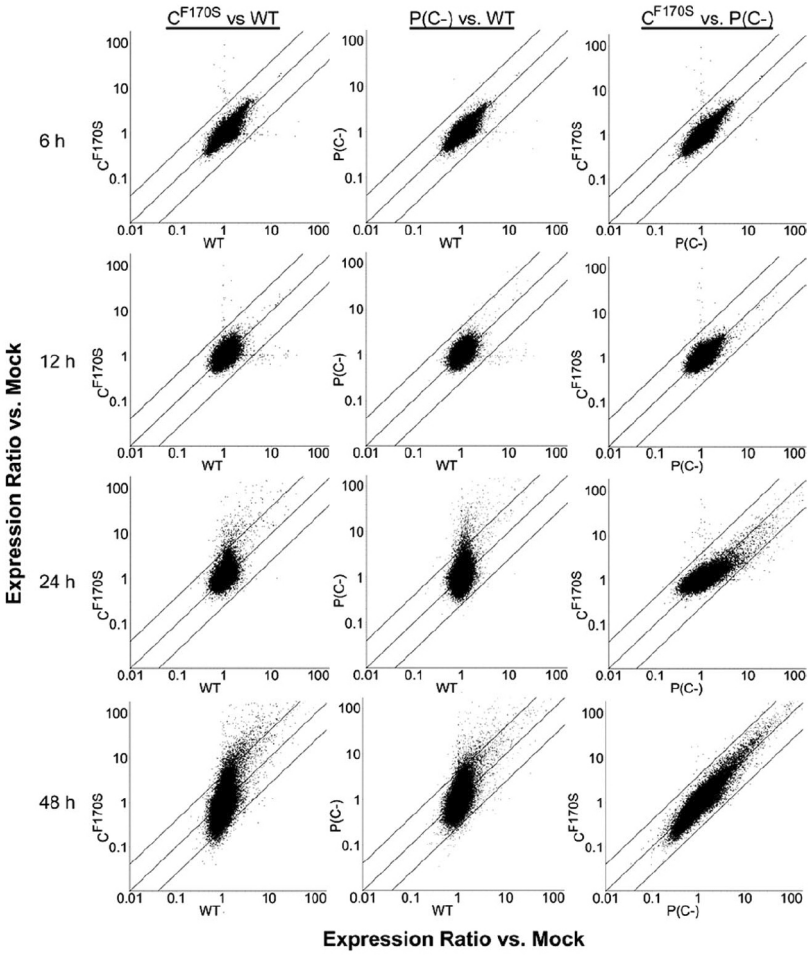

The observation that there was not a single gene that differed with statistical significance by four-fold or more between the two C mutant viruses at any time point might seem inconsistent with the data in **Fig. 2** where, for example, the overall number of genes that were differentially regulated for each C mutant virus versus the mock-treated control was 1,600 for the P(C-) virus and 2421 for the C^{F170S} mutant, an apparent difference of 821 genes. This apparent discrepancy can be reconciled by constructing a Venn diagram and inspecting the genes that are differentially expressed only by P(C-) infection compared to mock or only by C^{F170S} infection compared to mock (**Fig. S1**). The difference in the number of differentially regulated genes, i.e. 821, between the P(C-) and C^{F170S} groups compared to mock does not accurately represent the total number of genes that were differentially expressed between the two C mutant viruses because not every one of the 1600 genes that was differentially expressed by P(C-) infection was also differentially expressed by C^{F170S} infection. The number of genes that are differentially expressed compared to mock during P(C-) or C^{F170S} infection can be grouped into three sets: 169 genes that were altered by P(C-) infection only, 990 genes that were altered by C^{F170S} infection only, and 1,431 genes that were altered by both C mutant infections (**Fig. S1**). Thus, in total, there were 1159 genes that were identified as differentially expressed compared to mock during infection with one C mutant but not the other. Of these 1159 genes, none was significantly diffesrentially expressed by 4-fold or more between the two viruses, suggesting that the differences were small and generally in the same direction, as indicated in the examples given in **Table 1**. Thus, fold-change and statistical filters that compared the two mutant viruses directly were needed to identify genes that differed

significantly so that subsequent functional bioinformatics analyses could be performed (**Table 2** and **Fig. S3**).

TABLE 1. Ten representative genes identified as differentially expressed by P(C−) infection only or C^{F170S} infection only compared to mock infection[a]

Group	Agilent probe ID[b]	Fold change[c]											
		C^{F170S}				P(C−)				Ratio of C^{F170S} to P(C−)			
		6 h	12 h	24 h	48 h	6 h	12 h	24 h	48 h	6 h	12 h	24 h	48 h
C^{F170S} infection only vs mock infection	A_32_P63162	1.1	1.2	2.2	**4.9**	1.2	1.2	2.8	3.6	0.9	1.0	0.8	**1.4**
	A_32_P60632	0.8	0.8	1.8	**5.2**	1.0	1.0	2.8	3.2	0.8	0.8	0.7	**1.6**
	A_32_P40476	1.2	1.3	1.7	**4.1**	1.2	1.1	2.4	3.0	1.0	1.2	0.7	**1.3**
	A_32_P36582	1.1	1.1	1.7	**5.1**	1.4	1.3	3.7	3.1	0.8	0.9	0.5	**1.7**
	A_32_P225870	1.5	1.4	2.1	**4.7**	1.4	1.3	2.4	3.9	1.1	1.0	0.9	**1.2**
P(C−) infection only vs mock infection	A_32_P171043	0.6	0.7	1.3	3.7	0.8	0.8	1.2	**4.6**	0.8	0.9	1.1	**0.8**
	A_32_P192354	1.2	1.1	1.7	3.6	1.5	0.8	2.5	**4.9**	0.8	1.3	0.7	**0.7**
	A_24_P932706	0.9	0.9	1.3	3.9	1.0	0.9	1.6	**4.8**	0.9	1.0	0.8	**0.8**
	A_24_P820087	1.0	1.0	3.9	3.5	0.8	1.2	3.3	**5.9**	1.2	0.8	1.2	**0.6**
	A_23_P216071	0.8	0.9	1.2	3.8	0.9	1.0	1.4	**4.5**	0.9	0.9	0.9	**0.8**

[a] Five representative genes each were taken from the 990 genes and 169 genes in the groups subjected to C^{F170S} infection only versus mock infection and P(C−) infection only versus mock infection, respectively, shown as the nonoverlapping region in the Venn diagram from Fig. S1 in the supplemental material.
[b] ID, identification.
[c] Values in boldface type indicate >4-fold increases in gene induction and the ratio of gene expression between C^{F170S} and P(C−) at 48 h p.i.

Organization of genes that are differentially regulated in wt and mutant HPIV1and in IFNβ treatment groups into hierarchical clusters

We further analyzed those genes that were differentially regulated (four-fold or greater difference, $P < 0.01$ with multiple testing correction) in any of the four treatment groups (wt HPIV1, C^{F170S}, P(C-), and IFNβ) versus the mock-treated control at any time point. These genes, which numbered 2,612, were subjected to pair-wise comparisons among the three virus treatment groups, analyzing each time point separately, in order to identify virus-to-virus differences that might account for phenotypic differences. Of the 2,612 genes, 1,238 were differentially regulated in at least one pair-wise comparison between any two virus groups at the same time point. Consistent with the analysis in **Fig. 3**, we did not identify a single gene that was significantly differentially expressed between C^{F170S} and P(C-) infection when using a four-fold cutoff and multiple testing correction. The 1,238 genes included all but 76 of the 191 IFNβ-responsive genes detected in this study; therefore, these additional 76 genes were added to the comparison so that the full

complement of IFNβ-responsive genes could serve as a benchmark for analysis of a possible transcriptional basis for the phenotypic differences seen between wt HPIV1, C^{F170S} and P(C-) infection, and also to permit an analysis of the behavior of IFN-responsive genes during infection with the HPIV1 C protein mutants. The total of 1,314 genes were hierarchically clustered into groups A-H based on similarities in the gene expression kinetics and magnitude, as described for **Fig. 1** (**Fig. 4** columns I and II; **Table S2**).

Figure 4. Infection of A549 cells with C^{F170S} or P(C-) drastically alters the expression of a large number of genes involved in diverse cellular functions. A total of 1,238 genes that were differentially expressed at 6, 12, 24, and 48 h p.i. following infection with C^{F170S}, P(C-), or WT viruses were combined with 76 genes that were differentially regulated at 6 or 24 h after IFNβ treatment and subjected to hierarchical clustering based on similarity of expression kinetics and magnitude of expression as described in the legend to **Fig. 1**, yielding eight clusters (A through H). **Column I)** As in **Fig. 1**, the clusters are depicted by a hierarchical clustering matrix with the columns representing treatment and time point and the rows indicating individual transcripts, with representative transcripts identified to the right. The number of genes in each cluster is given in parentheses. **Column II)** The geometric mean gene expression profiles for clusters A through H are shown in panels A through H, respectively, with the geometric mean gene expression (y-axis) plotted against each treatment condition at the indicated time-points in h p.i. (x-axis). **Column III)** Functional pathways that are over-represented in clusters A through H were determined using Ingenuity Pathway Analysis and are indicated on the left, next

to the expression profile of the respective cluster. TFBSs that are over-represented among the genes within each cluster were identified using oPOSSUM to search the JASPAR core database.

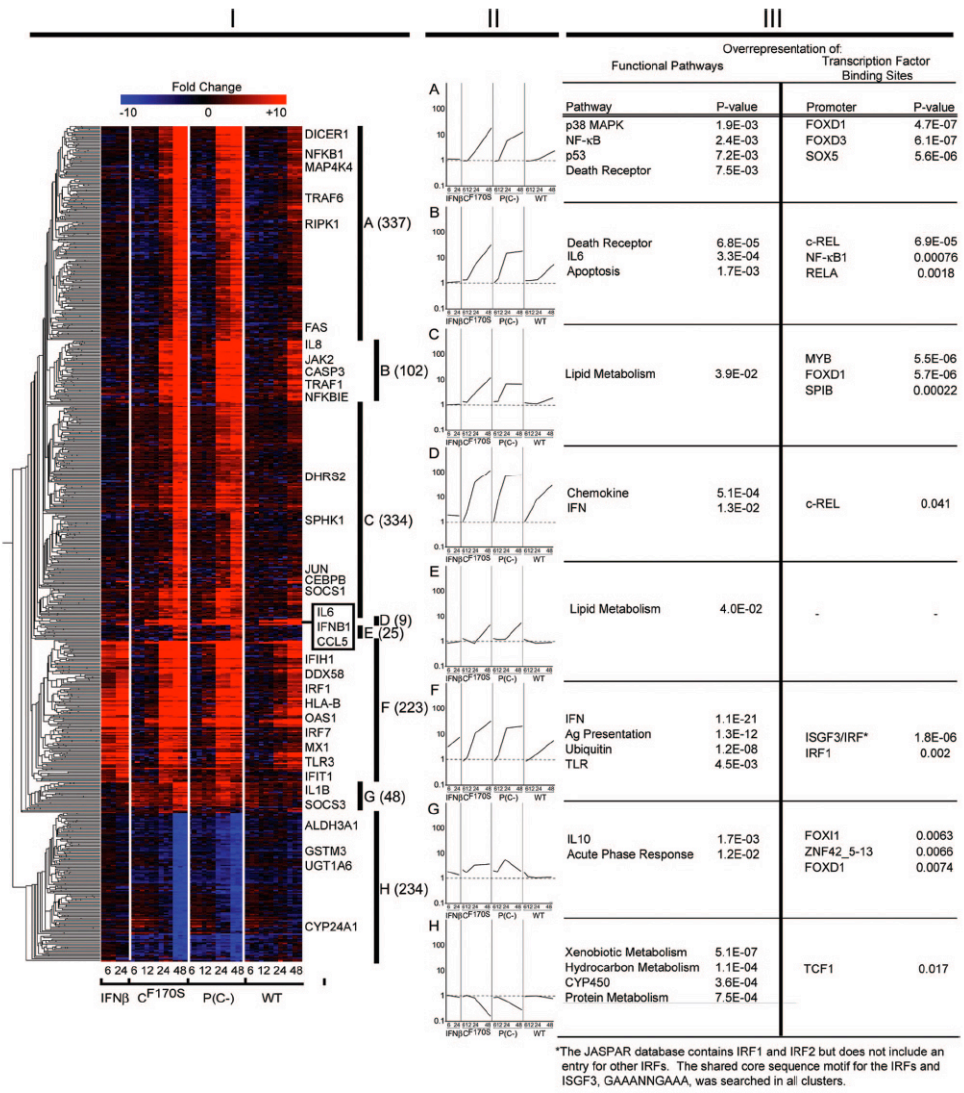

Cluster F represented a distinct group of 223 mRNAs that individually were responsive to most or all of the four treatments (IFNβ, C^{F170S}, P(C-), or wt HPIV1) (**Fig. 4**, column I; **Table S2**). Cluster F included most of the 191 IFNβ-responsive genes detected in this study. Cluster F is similar, but not identical, to cluster A in **Fig. 1**. In addition, the

majority of genes in cluster C of **Fig. 1**, which were up-regulated predominantly by IFNβ treatment and not at all by wt HPIV1 infection, are found in cluster F of **Fig. 4**. The expression of 16 of these 17 genes was significantly more highly induced by infection with the C mutant viruses beginning at 24 h p.i. (**Table S1** vs **Table S2**). Paradoxically, the remaining gene, namely angiotensinogen (AGT), in this group of 17 was down-regulated by the C mutant viruses even though it was induced by IFNβ. This is an indication that the effects of the C proteins are more complex than a general inhibition of IFN production and signaling. For the genes in cluster F as a whole, the mean fold change induced by IFNβ was approximately 3-fold at 6 h and approximately 8-fold at 24 h (**Fig. 4**, column II, cluster F). Infection with wt HPIV1 induced a delayed response that, at 48 h p.i., was similar in magnitude to the IFNβ induced response at 24 h, whereas C^{F170S} and P(C-) induced a far earlier and greater response than wt HPIV1 that equaled or exceeded that of IFNβ. By 24 h p.i., C^{F170S} and P(C-) induced on average a greater than 10-fold up-regulation of cluster F gene expression, exceeding the response induced by IFNβ treatment for 24 h **(Fig. 4** column II, cluster F). Amongst the genes within cluster F, genes involved in IFN signaling, antigen presentation, ubiquitination, and Toll-like receptor signaling were over-represented. As expected, ISGF3, IRF1, and IRF3 TFBSs were over-represented within the upstream promoter sequences of cluster F genes (**Fig. 4**, column III, cluster F). Virtually every member of cluster F was induced much earlier and to a greater extent by the C^{F170S} and P(C-) mutants compared to wt HPIV1, suggesting that functional C proteins are crucial in suppressing the transcription of antiviral genes within this cluster.

The remaining 7 gene clusters (**Fig. 4**, column II) contained only a few IFNβ–responsive genes and consisted mainly of genes that were differentially expressed between virus groups. Genes in clusters A, B, and C shared three features: 1) they were not significantly up-regulated by IFNβ; 2) they were up-regulated by all three viruses; and 3) the fold increase in up-regulation was much greater for the C mutant viruses than for wt HPIV1. Nonetheless, each cluster exhibited a clear difference in the kinetics or magnitude of the up-regulation of expression. The 337 genes in cluster A, on average, were induced strongly following infection with either C mutant within 12 h and to a much more limited and delayed degree following wt HPIV1 infection **(Fig. 4** columns I and II, cluster A). The 102 genes in cluster B shared a similar expression profile. However, infection with P(C-) up-regulated cluster B gene expression at 24 h p.i. to an even higher level than in cluster A, and expression was maintained at that level through 48 h p.i. In cluster B, wt HPIV1 infection led to a slightly more pronounced average gene induction at 48 h than in cluster A (**Fig. 4** column II, cluster B). Cluster A included genes involved in the p38 MAPK, NF-κB, p53, and death receptor pathways, while genes involved in death receptor, IL6, and apoptosis pathways were over-represented in cluster B (**Fig. 4** column III, clusters A and B). Over-representation of TFBSs suggested a role for forkhead transcription factors FOXD1 and FOXD3 in the regulation of cluster A genes and for c-REL, RELA, and NF-κB1 in the regulation of cluster B genes (**Fig. 4**, column III, panels A and B). The specific function FOXD1 and FOXD3 have not yet been well defined, but the family of forkhead transcription factors are best known for their role in regulating cellular development and differentiation (150). The 334 genes in cluster C behaved similarly to those in clusters A and B, but the magnitude of expression was less than that

in clusters A and B, and over-representation of only one functional pathway (lipid metabolism) was found in this large cluster of genes (**Fig. 4**, column III, cluster C). Clearly, functional C proteins partially suppress the activation of genes in clusters A, B, and C.

Cluster D stood out because of its small size (only 9 genes were assigned to this cluster) and because these genes were up-regulated rapidly and to a very high level following wt or mutant HPIV1 infection. These findings indicate that wt C proteins permit the activation of these 9 genes. However, since the level of expression of these genes is slightly lower in the wt versus mutant HPIV1 infected groups, this indicates that the C proteins can have a quantitative effect on modulating the overall level of gene induction in response to viral infection (**Fig. 4**, column II, cluster D). Cluster D included mRNAs encoding IL6, IFNβ and IL28A/ IFNλ2, and the chemokines CX3CL1, CCL2, and CCL5 (**Fig. 4**, columns I-III, cluster D). c-REL TFBSs were over-represented in this set of genes. Cluster D genes contrast with those in clusters E and G which fail to activate during wt HPIV1 infection.

The 25 genes in cluster E and the 48 genes in cluster G were induced at a relatively low level and only late following infection with C^{F170S} or P(C-) but not at all following either wt HPIV1 infection or IFNβ treatment (**Fig. 4**, column II, clusters E and G). The two clusters differed in the magnitude of expression between 24 h and 48 h p.i. since, after infection with the C mutant viruses, average gene expression increased substantially for cluster E but remained flat or decreased for cluster G. The genes in cluster E were only

marginally over-represented in the lipid metabolism pathway, and none of the TFBSs were over-represented in this cluster (**Fig. 4**, column II, cluster E). The 48 genes in cluster G, however, including pro-inflammatory genes (e.g. IL1B) as well as inhibitors of inflammation (e.g. SOCS3), were over-represented in the acute phase response and the IL10 pathway, with complex transcriptional regulation (**Fig. 4**, column III, cluster G). The transcription factors over-represented in this cluster included FOXI1, zinc finger protein 42 (ZNF42), and FOXD1. ZNF42 and both forkhead transcription factors FOXI1 and FOXD1 are best known for regulating cellular development and differentiation (78, 150).

Lastly, cluster H included all of the genes down-regulated by infection with C^{F170S} or P(C-) (**Fig. 4**, column II, cluster H). Infection with either C mutant virus significantly suppressed the expression of the 234 genes in this cluster. Genes involved in xenobiotic, hydrocarbon, and cellular stress / protein metabolism pathways were over-represented in this cluster, including members of the cytochrome P450 superfamily, glutathione transferases, and UDP-glucuronosyltransferase. Wt HPIV1 infection and IFNβ treatment had no effect on these genes. The only transcription factor statistically over-represented was TCF1, also known as IFN production regulator factor, a protein that initially became known to control important liver specific genes involved in metabolism but more recently was found to be expressed in lung tissue as well (164) (**Fig. 4**, column III, cluster H). The gene expression profile of cluster H suggests that the C proteins expressed by wt HPIV1 inhibit the suppression of cluster H gene expression.

Taken together, the analysis of global gene expression in A549 cells infected with wt HPIV1, C^{F170S}, or P(C-) suggests that wt HPIV1 is able to control a large and diverse array of host genes involved in the recognition of non-self and the initiation of an antiviral response. Ablation of HPIV1 C protein function, by mutation or deletion, allows for an innate response of epithelial cells that encompasses a multitude of biological processes, including IFN signaling, cell death, inflammation, and metabolic regulation. We have observed that infection with P(C-) rapidly induces apoptosis, which is not seen during infection with C^{F170S} or wt HPIV1. The similarity of the host transcriptional response to infection with C^{F170S} and P(C-) was unexpected (**Figs. 2, 3, and 4** column I) since the C proteins are multifunctional. We applied a principal component analysis, using all genes on the microarrays to examine the level of similarity between treatments, and found that overall gene expression during P(C-) and C^{F170S} infection was highly similar (**Fig. S2**). Furthermore, both C mutant viruses induced gene expression patterns that were significantly different from WT infection. This identifies a high degree of similarity between the global gene expression profiles of the two mutants, but it does not rule out the possibility that small, specific differences exist between the two mutants, as addressed below. One might have expected that the host cell response to infection with C^{F170S}, the virus containing only a single point mutation in each of the four C proteins, would not be as dramatic as the response to infection with P(C-), the virus not encoding any of the C proteins.

Real-time quantitative PCR confirms microarray-based observations regarding differential gene expression

In order to validate the kinetics of gene expression observed in the microarray study, five differentially expressed genes that encompassed a range of expression levels, kinetic patterns, and pathways representing all four treatment groups were selected for RT-qPCR analysis (**Fig. 5**). For all five mRNAs, the gene expression profiles determined by microarray analysis were generally confirmed by the RT-qPCR analysis, indicating that this microarray platform yielded reliable semiquantitative results when using triplicate samples. However, the microarray-generated data underestimated the magnitude of expression compared to RT-qPCR by a factor of 10 to 1000. This probably reflected the more limited dynamic range in microarray analyses and probe saturation with high mRNA levels, as reported previously in a comparison of expression levels determined by Northern blot versus microarray (52). However, the expression profiles derived from microarray data and RT-qPCR data, in general, followed the same trend over time. This confirmed that IRF7 and MX1 mRNAs were strongly induced by IFNβ treatment, whereas IFNB mRNA was only weakly induced, and NFKB1 (transcription factor NF-κB p100/p52) and TRAF1 (tumor necrosis factor receptor-associated factor 1, involved in signal transduction) mRNAs were not induced at all by this treatment (**Fig. 5**). In addition, IRF7, NFKB1, and TRAF1 mRNAs were barely induced by wt HPIV1 infection but strongly induced by infection with either C mutant (**Fig. 5**). IFNB and MX1 mRNAs were also induced by wt HPIV1 infection, but not as strongly as following C^{F170S} or P(C-) infection, confirming the previous expression pattern observed for cluster D genes (**Fig. 4**, column II, cluster D).

Figure 5. Comparison of the kinetics and magnitude of expression of representative genes quantified by microarrays versus RT-qPCR. An aliquot of the total RNA that was used for microarray analysis was reverse transcribed and amplified using TaqMan probes for **A)** IFNB, **B)** IRF7, **C)** MX1, **D)** NFKB1, and **E)** TRAF1. These include both IFN-responsive (A, B, and C) and IFN-independent (D, E) genes. Values were normalized to the endogenous control gene GAPDH and expressed as fold-increase relative to mock infection. Microarray expression values are indicated with a continuous line, while the dotted line represents qPCR expression values. Note, both axes are in logarithmic scale, and the qPCR data (left-sided axes) spans a much larger dynamic range than the microarray data (right-sided axes).

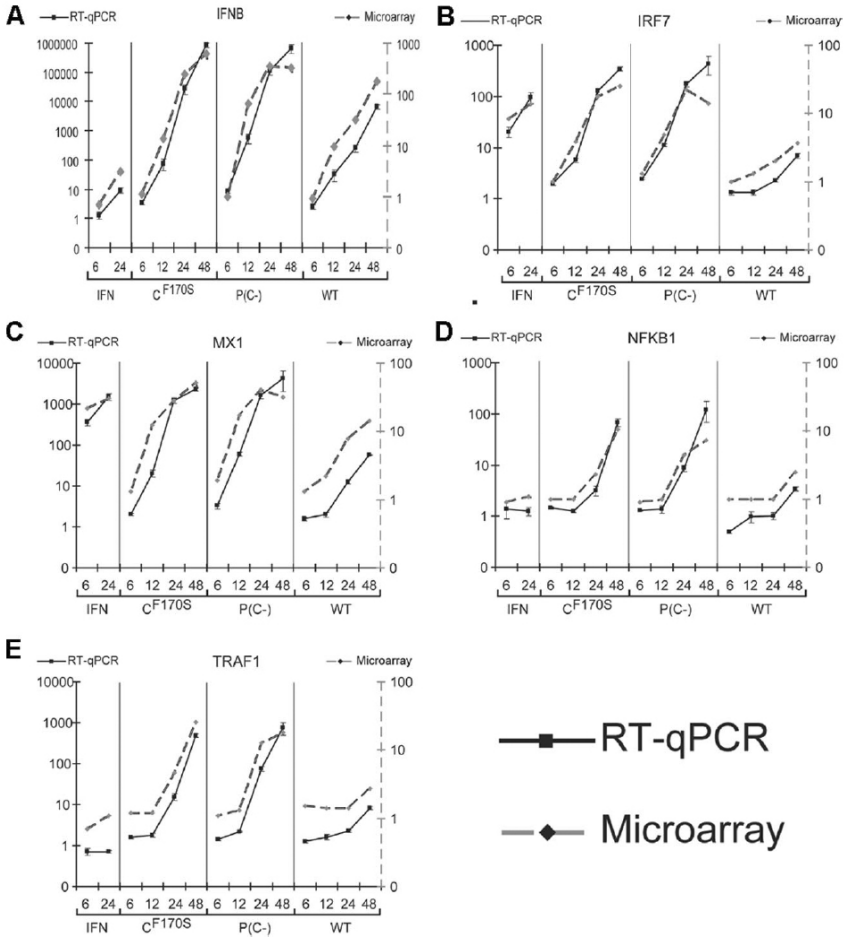

A more detailed examination of the IFN pathway

Since ablation of the function of IFN antagonist proteins results in restriction of replication of many viruses *in vivo* (46, 192, 216) and since C^{F170S} and P(C-) are attenuated *in vivo* but differ in their level of replication, we took a closer look at individual genes in the IFN pathway to examine whether subtle differences in their expression level in C^{F170S} and P(C-) infected cells could explain the greater level of attenuation of P(C-). We examined the kinetics and magnitude of expression of genes encoding type 1 IFNs and their receptors (**Fig. 6A**), as well as that of genes involved in IRF3 and IFN signaling (**Fig. 6B**). Since the number of genes in these pathways is large, only selected genes representative of most pathway members are presented. Interestingly, C^{F170S} and P(C-) infection, but not wt HPIV1 infection or IFNβ treatment, induced transcription of members of the family of IFNA genes such as IFNA4, 5, 8, 10, and 14, but the expression of the type 1 IFN receptors IFNAR1 and IFNAR2 was not affected by any of the treatments (**Fig. 6A**).

IRF3 can induce a subset of antiviral effector molecules in the absence of IFNβ, such as IFIT1 (IFN-induced protein with tetratricopeptide repeats-1/ISG60), ISG15, and IFI44. A hierarchical clustering matrix for these three genes is shown in **Fig. 6B**, top panel. These IRF3-regulated genes were more strongly induced in C mutant virus infected cells compared to wt HPIV1 infected or IFNβ treated cells (see expression profile in **Fig. 6B**). Since IRF3 dimerization and activation occurs upstream of IFNβ and ISGF3 signaling during viral infection, these genes would be induced more rapidly than genes that are

only ISGF3-stimulated, but, later in infection, IFN-stimulation would contribute to expression of both sets of genes. A selection of genes that are only ISGF3-stimulated is shown in the lower panel of **Fig. 6B**, and indeed appears to be induced less rapidly than the IRF3-stimulated genes. For all of these genes, the expression profiles were highly similar in C^{F170S} and P(C-) infected cells.

Throughout the time course, wt HPIV1 failed to induce ISGF3-responsive genes to a level comparable to that induced by C^{F170S} or P(C-), consistent with the reduced expression of IFN (**Fig. 6B**). MX2 expression was completely suppressed for 24 h in the presence of wt C protein whereas C^{F170S} or P(C-) induced high levels of MX2 mRNAs by 24 h p.i. (**Fig. 6B**). Importantly, wt HPIV1-induced expression of IFNβ- and IRF3-responsive genes, including IRF7, ADAR, and PKR, was delayed, diminished, or completely absent even at 48 h p.i. compared to C^{F170S} or P(C-) induced up-regulation (**Fig. 6B**). Interestingly, C^{F170S} or P(C-) infection up-regulated these IFNβ- or IRF3-responsive genes far more than IFNβ treatment (**Fig. 6B**).

Figure 6. The C^{F170S} and P(C-) mutant viruses are similar with regard to the expression of IFNs, IFN receptors, and IRF3-responsive genes. **A)** Hierarchical clustering matrix of genes encoding IFNs and IFN receptors and **B)** Hierarchical clustering matrix of genes encoding IRF3-responsive (first three entries) and ISGF3-responsive (all of the entries) genes. Treatment conditions and time points are indicated below the hierarchical clustering matrix. On the right, expression kinetics are shown for four representative genes of each group, with the geometric mean gene expression (y-axis) plotted against each treatment condition at the indicated time-points in h p.i. (x-axis), to illustrate the full range of differential gene expression.

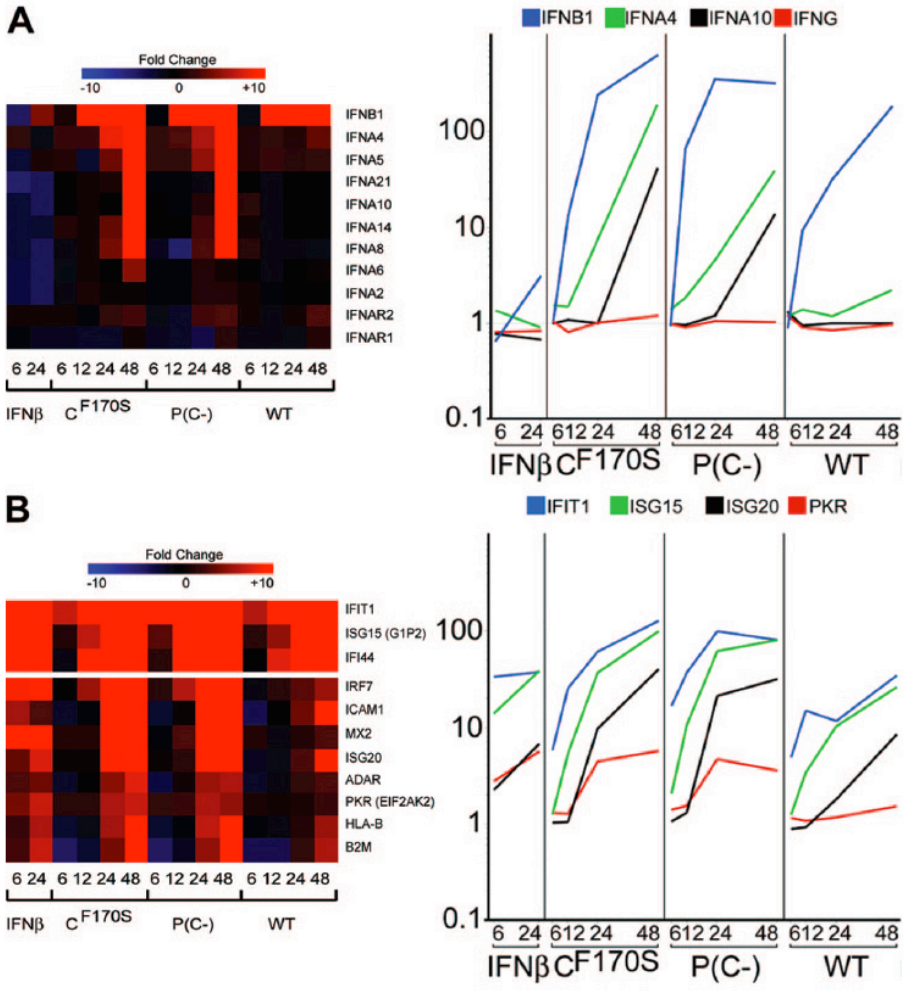

Changes in host cell transcription do not reflect the striking cytopathic effect induced by P(C-) infection

P(C-) is a potent inducer of apoptosis in A549 cells while C^{F170S} and wt HPIV1 are not (9). We sought to examine individual genes in the apoptosis pathway to see if subtle differences in their expression level in C^{F170S}, P(C-), and wt HPIV1 infected cells could be detected that might explain the apoptosis phenotype seen in cells infected with P(C-). To do this, we looked at the kinetics and magnitude of expression of individual genes in the extrinsic and intrinsic apoptosis pathways. Despite this prominent phenotypic difference, C^{F170S} and P(C-) induced remarkably similar transcriptional profiles (**Fig. 7**). Both C mutant viruses up-regulated the expression of the same death ligands and death receptors examined with highly similar kinetics and magnitude (**Fig. 7A and B**). In addition, no difference was found in the regulation of apoptosis inhibitors such as BIRC3 and BIRC5 (Baculoviral IAP Repeat-Containing Protein 3 and 5), BCL2A1 (BCL2-Related Protein A1) and MCL1 (Myeloid Cell Leukemia I) (**Fig. 7C**; **Table S4**). We also compared gene expression in the intrinsic apoptosis pathway, for instance CASP9, DIABLO, and BAX, and, again, found no difference in gene expression induced by the C mutant viruses (**Table S5**). As already noted, direct comparison between C^{F170S} and P(C-) at 6, 12, 24, or 48 h did not detect a single gene that differed by 4-fold or more between the two mutants with a $P < 0.01$ after multiple testing correction. We appreciate that the statistical criteria chosen are somewhat arbitrary and that we may have missed genes that differed between infection with the C mutant viruses due to the stringency of our original selection criteria. To detect subtle differences in gene expression profiles that could

explain the marked cytopathic effect seen during P(C-) infection but not during C^{F170S} infection, we tested several fold change cutoffs below the 4-fold level (**Table 2**). While we were unable to find any genes that were differentially expressed between C^{F170S} and P(C-) infection using a 4-fold cutoff, we found 28 genes that differed significantly ($P < 0.01$) between the two C mutants by 2-fold if multiple testing correction was performed sequentially and not simultaneously with the fold change cutoff (**Fig. S3** and **Table S6**). Functional analysis revealed that 2 of these 28 genes are known mediators of cell death. Notably, caspase 3 was up-regulated 6.5-fold with P(C-) infection at 24 hours post infection, 2.8-fold greater than with C^{F170S} infection. However, by 48 hours post-infection, caspase 3 expression during C^{F170S} infection increased to 6.3-fold above mock, whereas the up-regulation of caspase 3 induced by P(C-) diminished to 4.1-fold. The second apoptosis-related gene, TNFRSF10B or TRAIL receptor 2 (TRAIL-R2), is responsible for signaling through the extrinsic apoptosis pathway. Similar to caspase 3, TNFRSF10B was up-regulated 4.8-fold with P(C-) infection at 24 hours post-infection, 2.1-fold greater than that seen with C^{F170S} infection. However, at 48 hours post-infection, TNFRSF10B expression during C^{F170S} and P(C-) infection were comparable. At 24 h p.i., TNFSF10 (TRAIL) itself was upregulated 50.9-fold by C^{F170S} infection, 1.95-fold greater than that seen with P(C-) infection, although apoptosis was induced only during P(C-) infection (**Fig. 7A**). The earlier expression of TNFRSF10B and caspase 3 may contribute to the significant cytopathic effect observed during P(C-) infection at 48 hours post-infection although the induction of TNFSF10 (TRAIL) itself was more pronounced in cells infected with C^{F170S}, the C mutant virus that did not induce apoptosis.

Figure 7. The C^{F170S} and P(C-) mutant viruses share remarkably similar expression profiles for genes encoding death ligands, death receptors, and apoptosis inhibitors despite distinct cytopathic phenotypes. Hierarchical clustering matrices and gene expression profiles comparing the gene expression of **A)** death ligands, **B)** death receptors, and **C)** apoptosis inhibitors following infection with wt HPIV1 (WT) or the indicated mutant HPIV1 or following IFNβ treatment. A significant difference was not detected between C^{F170S} and P(C-) in any of the apoptosis-related genes depicted.

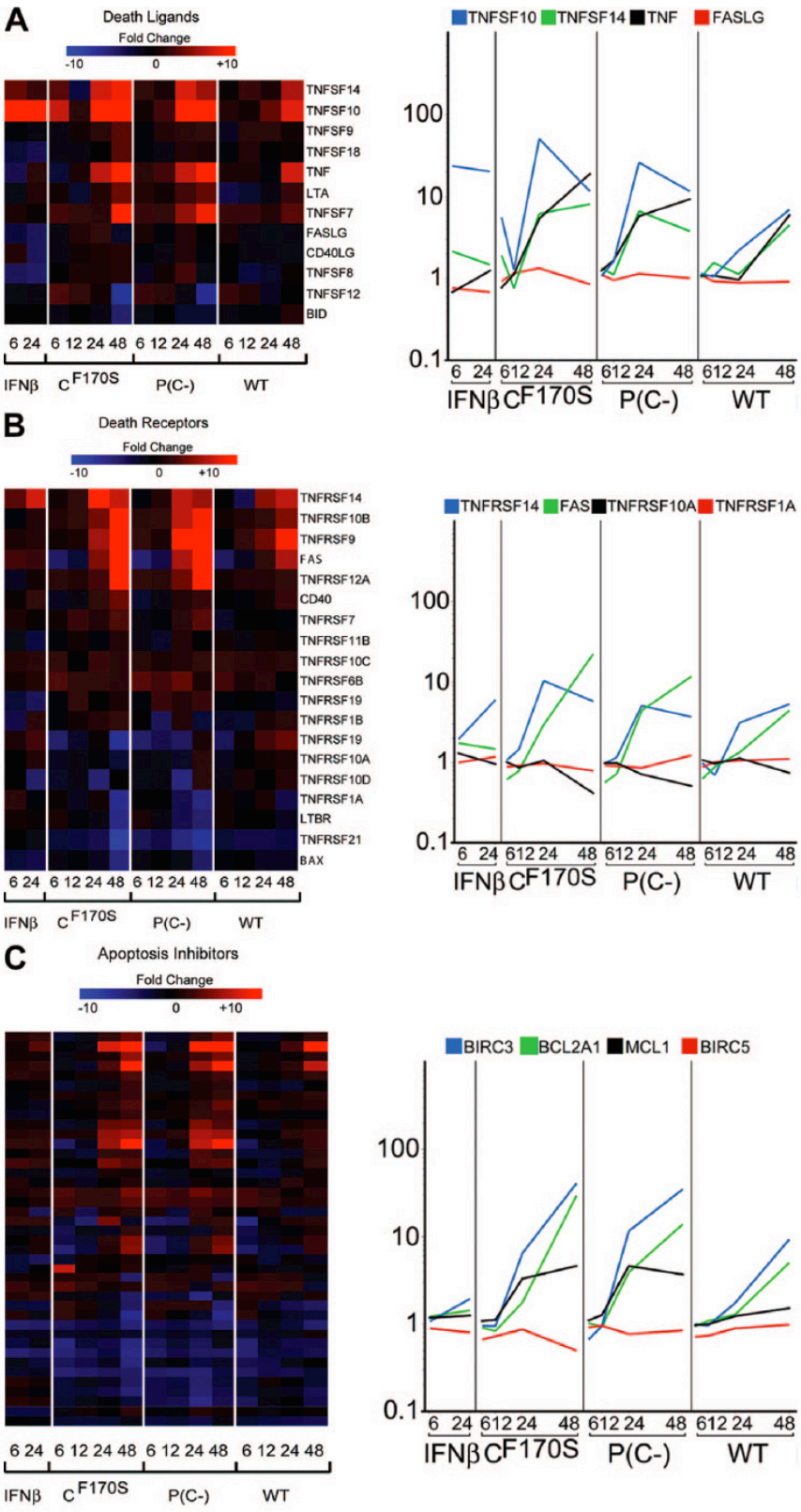
A
Death Ligands
Fold Change
-10
0
+10
TNFSF14
TNFSF10
TNFSF9
TNFSF18
TNF
LTA
TNFSF7
FASLG
CD40LG
TNFSF8
TNFSF12
BID
6 24 6 12 24 48 6 12 24 48 6 12 24 48
IFNβ C F170S P(C-) WT
TNFSF10 TNFSF14 TNF FASLG
100
10
1
0.1
6 24 612 24 48 612 24 48 612 24 48
IFNβ CF170S P(C-) WT
B
Death Receptors
Fold Change
-10
0
+10
TNFRSF14
TNFRSF10B
TNFRSF9
FAS
TNFRSF12A
CD40
TNFRSF7
TNFRSF11B
TNFRSF10C
TNFRSF6B
TNFRSF19
TNFRSF1B
TNFRSF19
TNFRSF10A
TNFRSF10D
TNFRSF1A
LTBR
TNFRSF21
BAX
6 24 6 12 24 48 6 12 24 48 6 12 24 48
IFNβ C F170S P(C-) WT
TNFRSF14 FAS TNFRSF10A TNFRSF1A
100
10
1
0.1
6 24 612 24 48 612 24 48 612 24 48
IFNβ CF170S P(C-) WT
C
Apoptosis Inhibitors
Fold Change
-10
0
+10
6 24 6 12 24 48 6 12 24 48 6 12 24 48
IFNβ C F170S P(C-) WT
BIRC3 BCL2A1 MCL1 BIRC5
100
10
1
0.1
6 24 612 24 48 612 24 48 612 24 48
IFNβ CF170S P(C-) WT

TABLE 2. Numbers of genes differentially expressed between C^{F170S} and P(C−), as determined by significance criteria[a]

Statistic[b]	Fold change	Time p.i. (h)	No. of genes differentially expressed
t test with MTC	4	6	0
		12	0
		24	0
		48	0
		Overall	0
ANOVA[c] with MTC	4	Overall	18
t test with MTC	2	6	0
		12	0
		24	2
		48	0
		Overall	2[d]
t test with MTC	2[e]	6	0
		12	1
		24	13
		48	14
		Overall	28
t test with MTC	1.5	6	0
		12	0
		24	2
		48	0
		Overall	2

[a] Statistical tests ($P < 0.01$) were performed on genes at various cutoffs (*n*-fold changes) between C^{F170S} and P(C−) infections.
[b] MTC, Benjamini-Hochberg multiple testing correction.
[c] Two-way analysis of variance (ANOVA) results are shown in Fig. S4 and Table S7 in the supplemental material.
[d] These two genes are included within the 28 genes identified when the change cutoff was applied prior to statistical testing.
[e] A twofold cutoff was applied prior to statistical testing with multiple testing correction.

Discussion

Microarray-based analyses are increasingly being used in virology and have helped to elucidate virus-host interactions for a number of viruses (reviewed in (88)). Here, we performed a comprehensive analysis of the response of a human respiratory epithelial cell line to HPIV1 infection and to IFNβ treatment. Microarray analyses have been previously applied to study infection by murine PIV1 (SeV) (39, 178). However, these studies had methodological issues that limited the ability to interpret the results, including: 1) human cells were infected with a murine virus; 2) non-respiratory cells were infected with a

respiratory virus; 3) mRNA levels were determined only at a single time point; 4) customized arrays were used that included fewer than 1000 genes that focused on the IFN and antiviral pathways; and 5) the response to viral infection was not compared with the response to IFN treatment (39, 178). In the present study, gene expression kinetics following infection with a human respiratory virus or administration of IFNβ were determined across multiple time points in human respiratory epithelial cells, the natural target of HPIV1, using a microarray representing the entire human genome. We chose to analyze only genes whose expression was at least four-fold up- or down-regulated, thereby excluding genes that were more modestly induced or suppressed by viral infection or IFN treatment. In order to avoid a subjective or biased analysis, functional bioinformatics tools were used to group thousands of differentially expressed genes into distinct hierarchical clusters and to identify functional pathways over-represented in each cluster. oPOSSUM Single Site Analysis software was used to examine upstream sequences for predicted transcription factor binding sites within each hierarchical cluster (72, 161, 193), resulting in the identification of several key transcriptional regulatory pathways that are likely involved in the cellular response to HPIV1 infection.

As a first step in our analysis, we sought to identify genes that were differentially expressed as a result of wt HPIV1 infection. This set of genes was subsequently compared to the set of genes whose expression was altered by treatment with a physiological concentration of IFNβ, allowing us to segregate and separately analyze IFN-responsive from IFN-independent genes in the wt HPIV1 microarray data set. IFNβ treatment was chosen for comparison because A549 cells and human airway epithelial

cells produce this IFN in response to HPIV1, whereas IFNα is not secreted at all or is barely detectable. In agreement with previous reports that established the central role of the type I IFN response in innate antiviral immunity (35, 159), our clustering analysis indicated that approximately 60% of all genes induced late in infection with wt HPIV1 were also induced by IFNβ treatment. Specifically, 209 of the 343 genes were up-regulated by both wt HPIV1 infection and IFNβ treatment (**Fig. 1**, clusters A, B, and D). These 209 genes were over-represented in the IFN signaling, antigen presentation and ubiquitination pathways, as well as in the Toll-like receptor and NF-κB pathways. However, wt HPIV1 up-regulated an additional 129 genes that were not up-regulated by IFNβ (**Fig. 1**, column I, cluster E). Many of these genes were also under the control of the family of IRF and NF-κB transcription factors and were involved in apoptosis signaling and inflammation. This data is in agreement with and expands on a previous report on the dominant role of IRF3 and NF-κB regulated genes in the response of human embryonic kidney cells to SeV infection at 6 h (39). It can be concluded by inspection of the kinetic data that wt HPIV1 is able to silence the innate antiviral response for at least 6 to 12 h p.i., but IFN dependent and IFN independent antiviral pathways are activated at later time points as part of the innate response to infection.

Next, we sought to determine the role of the HPIV1 C proteins in suppressing the antiviral response of respiratory epithelial cells by analyzing gene expression patterns following infection of A549 cells with two C mutant viruses. Previous studies had established a role for the HPIV1 C proteins and SeV C proteins as inhibitors of IFN induction and signaling, as well as inhibitors of apoptosis (57, 96, 105). Two mutant

viruses with a single point mutation in C or a deletion of all four C proteins, C^{F170S} and P(C-) respectively, were selected for this analysis. Wt HPIV1 inhibits the induction of IFN and signaling of IFN through its receptor, but C^{F170S} and P(C-) each fail to inhibit these two activities. In addition, P(C-) infection induces apoptosis, whereas C^{F170S} and wt HPIV1 do not, and P(C-) is much more restricted in replication in AGMs than C^{F170S} (5, 9, 192). Using the C^{F170S} and P(C-) viruses, we sought to compare the host response following infection with these mutants to that following wt HPIV1 infection. We found that, following infection with either C mutant virus, the number of differentially expressed genes expanded dramatically, implicating a critical role for the HPIV1 C proteins in blunting the host's antiviral response. Using whole genome microarrays, we found that with C^{F170S} infection, 392 and 2,322 genes were differentially regulated more than 4-fold at 24 and 48 h p.i., respectively, while with wt HPIV1 infection, only 54 and 277 genes were differentially expressed at the same time points. Thus, approximately 1% of the over 41,000 unique probes analyzed in our study were altered by HPIV1-C^{F170S} at 24 h p.i., and only 14% of that subset of genes were altered by wt HPIV1, indicating that the wt HPIV1 C proteins inhibited modulation of the majority of antiviral genes that would otherwise be up-regulated or down-regulated as a result of HPIV1 infection. Importantly, this striking suppression of gene expression was associated with mutation in the C proteins but not with differences in virus replication. C^{F170S} and wt HPIV1 exhibited identical kinetics of replication *in vitro*, and although P(C-) was approximately 100-fold restricted in replication at 24 and 48 h p.i. compared to wt HPIV1 and C^{F170S} (**Fig. S5**), P(C-) infection was capable of suppressing gene expression just as well as C^{F170S}. Strähle et al. examined gene expression in human fibrosarcoma cells 24 h p.i. in

response to SeV-wt or SeV-C^{F170S} infection using a customized array designed to probe approximately 150 genes with over-representation of the IFN pathway (178). In their study, infection with SeV-C^{F170S} at a MOI of 20 induced 15 of 150 genes (10%) more than 2-fold at 24 h p.i. while SeV-wt (Ohita M strain) failed to induce the expression of any gene. We also found that the expression of IFNβ-inducible genes was greater following infection with C^{F170S} or P(C-) than following treatment with 300 pg/mL of IFNβ, the concentration of IFN induced by C^{F170S} infection of A549 cells (192). The greater induction seen with C mutant infection is due in part to direct viral recognition by RIG-I-like receptors (RLR) and subsequent activation of IRFs and NF-κB. Activated IRF3 not only stimulates the IFNB promoter to produce IFNβ but also can independently activate IFN stimulated response elements to augment the production of IFN stimulated genes (ISGs). In contrast, the effect of exogenous IFN is limited to signaling through the IFN receptor and activation of the ISGF3 transcription factor complex to up-regulate the expression of antiviral effectors and other ISGs. The wt C proteins likely block the RLR and IFN signaling pathways as evidenced by the lack of IRF3 and STAT activation and IFN production during infection with wt HPIV1, and this antagonism is ablated as a result of mutation or deletion of the HPIV1 C proteins (18, 192). In another similarly designed microarray study, Hartman et al. compared the host response to wt Ebola virus with a highly attenuated Ebola virus containing a single amino acid change, namely, R312A in the IRF3-inhibitory domain of VP35 (65). Like wt HPIV1, wt Ebola was remarkably effective in suppressing the activation of cellular antiviral and IFN-responsive genes. The single $VP35^{R312A}$ mutation in Ebola, however, reversed the inhibition of only 39 genes, whereas the single C^{F170S} mutation in HPIV1 reversed the

inhibition of over 2000 genes (**Fig. 2**). The Ebola VP35 protein confers virulence during infection by inhibiting IRF3 activation and IFNβ production, whereas the VP24 protein inhibits STAT1 nuclear translocation and IFN signaling (64, 155). Unlike Ebola which utilizes two separate viral proteins to antagonize IFN production and signaling, HPIV1 encodes the C proteins from a single gene segment that blocks both arms of the viral recognition and IFN pathways and probably suppresses the expression of many more genes compared to VP35 alone.

Following comparison of gene expression between wt HPIV1 and the two C mutant viruses, we next compared the cellular response to C^{F170S} versus P(C-) infection to determine whether differences in gene expression profiles were associated with the observed differences in the mutants' apoptosis and attenuation phenotypes. Surprisingly, the cellular response to C^{F170S} infection was comparable to the response to P(C-) infection, both qualitatively and quantitatively (**Figure 4**). Although the microarray-based analysis may have missed differences between C^{F170S} and P(C-) due to decreased sensitivity compared to RT-qPCR, this limitation occurred only with very highly up-regulated genes where gene induction is already qualitatively clear. For example, IFNB, which was induced 853,062-fold as measured by RT-qPCR and 628-fold by microarray analysis, showed 1358-fold greater sensitivity by qPCR due to saturation of the IFNB probe on the microarray. However, less strongly up-regulated genes such as NFKB1, which was induced 68-fold as measured by RT-qPCR and 11-fold by microarray analysis, showed only 6-fold greater sensitivity in detecting differential expression. The difference is significantly less pronounced since genes that are up-regulated less do not

suffer as much from microarray probe saturation. Thus, although the microarray-based analysis may have missed small differences in gene expression between viruses, we have shown that both technologies have comparable sensitivity at lower expression levels. Based on the phenotypic differences between the two mutants, with P(C-) being the more attenuated *in vivo* and a strong inducer of apoptosis *in vitro*, we expected to find transcriptional differences in at least the apoptosis pathway. However, not a single mRNA was differentially expressed using our predefined criteria, i.e. 4-fold and $P < 0.01$. To detect any subtle differences between infection with the two C mutant viruses, we tested several fold-change cutoffs. After relaxing our fold-change cutoff to two-fold and subsequently performing a t-test with multiple testing correction, we identified two genes, caspase 3 and the TRAIL receptor 2 (TNFRSF10B), that could potentially contribute to P(C-)-induced apoptosis. P(C-) infection up-regulated both genes earlier, at 24 h p.i., compared to C^{F170S} infection. However, in both cases, the magnitude of up-regulation during C^{F170S} infection caught up by 48 h p.i., and the TRAIL ligand (TNFSF10) itself was comparably induced by both viruses at 24 h p.i.

It was surprising that the C^{F170S} mutant, that contains a single point mutation at amino acid 170 of the C protein, induced a transcriptional profile that was almost indistinguishable from that induced by the P(C-) mutant, a virus that does not express any of the C genes. Although P(C-) infection induces apoptosis much more rapidly and extensively than C^{F170S} (9), the expression kinetics of death ligands, death receptors, or antiapoptotic factors that could account for P(C-) induced cell death did not differ significantly by 4-fold from C^{F170S} at any time (**Fig. 7a, b, and c**). Since knockout of the

C gene causes cell death whereas expression of the wt C gene does not, we hypothesized that the wt HPIV1 and C^{F170S} C proteins prevented cell death through apoptosis inhibition, i.e., either through inhibition of proapoptotic pathways or activation of antiapoptotic pathways. Previous studies on SeV suggested that a delicate balance exists between proapoptotic and antiapoptotic pathways during viral infection. SeV infection activates the cellular phosphatidylinositol 3-kinase (PI3K) pathway and, through AKT activation, prevents apoptosis (145). Thus, the differences in the apoptosis phenotype between the two C mutants likely lies in the interaction of one or more of the C proteins of C^{F170S} and wt HPIV1 with one or more constitutively expressed factors, which results in the suppression of the apoptosis response. Both wt C proteins and point mutated C proteins could potentially activate apoptosis inhibitory proteins or antagonize proapoptotic proteins that would otherwise be triggered during HPIV1 infection. These two possibilities can be tested once the mechanism of interaction with the host apoptosis machinery has been defined. The greater level of attenuation of P(C-) versus C^{F170S} likely reflects a contribution of apoptosis to the decreased replication of P(C-), but the loss of a yet undefined function of C required for replication *in vivo* may contribute as well.

Although wt HPIV1 suppressed the up-regulation of a broad array of cellular genes that were induced by P(C-) and C^{F170S} infection, global shutoff of host transcription did not occur. In fact, only 234 of 2612 differentially expressed genes were down-regulated (**Fig. 4**, panel II, cluster H). Interestingly, both C mutant viruses down-regulated these genes to a greater extent than wt HPIV1 (**Table S2**). Thus, the wt C proteins blunted both induction and suppression of a specific set of host genes that would otherwise react to

viral infection. This is in stark contrast to what has been described for vesicular stomatitis virus which shuts down transcription globally through M protein-mediated inhibition of the three cellular RNA polymerases I, II, and III (1, 202), or for Rift Valley fever virus which, through inhibition of TFIIH transcription factor complex assembly via its NSs protein, leads to the rapid destabilization of host cellular RNA synthesis (111). However, other members of the order Mononegavirales, such as the Marburg and Ebola filoviruses, suppress the antiviral and type I IFN responses without shutting down host cell functions globally, and the degree of antiviral suppression by these viruses seems to correlate with virulence *in vivo* (95). Similarly, our data indicate that wt HPIV1 C protein function, i.e., suppression of antiviral pathways early in infection, is an important virulence factor and that the loss of this activity in both C^{F170S} and P(C-) leads to attenuation *in vivo*.

Following global analysis of virus modulated pathways, we attempted a more detailed analysis of the IFN and apoptotic pathways in order to understand the different *in vivo* and *in vitro* phenotypes of wt HPIV1, P(C-) and C^{F170S}. We found that by 48 h p.i., wt HPIV1 induced IFNB expression 180-fold, as measured by microarray, and 1200-fold, as measured by qPCR (**Fig. 5A**). Previously, we reported that IFNB mRNA was not detectable at any time point in response to HPIV1 infection (192). Re-examination of that data identified a 5600-fold induction of IFNB mRNA following C^{F170S} infection versus a 12-fold induction following wt HPIV1 infection at 48 h p.i., i.e., a 458-fold reduction in IFNB transcription following wt HPIV1 infection, as compared to C^{F170S} infection (192). In the present study, C^{F170S} induced 695 times more IFNB mRNA than wt HPIV1 at 48 h p.i., confirming that IFNB mRNA is strongly induced by C^{F170S} but not by wt HPIV1

(**Table S3**). At the protein level, we previously were unable to detect IFNβ in the supernatant of wt HPIV1 infected A549 cells by IFN bioassay, not even after 96 h p.i. (192). In contrast, Bousse et al. detected 380 IU/mL of IFNβ by ELISA in MRC-5 cells 48 h p.i. with wt HPIV1 strain C-35 (Genbank M74081) (18). This difference in IFNβ secretion could be due to the use of different cell lines (MRC-5 versus A549) and/or different virus strains. Protein sequence alignment of the C protein of the C-35 strain of HPIV1 used by Bousse et al. with our Washington 1964 wt HPIV1 strain revealed a C^{Q38P} substitution in the C gene that could potentially be responsible for a distinct IFN phenotype. The C^{F170S} virus serves as an example for the role a single amino acid substitution in the C protein can potentially have on the IFN phenotype. Importantly, the deficient IFNβ response of A549 cells to wt HPIV1 infection was also seen in primary human airway epithelial cell cultures, confirming the IFN production deficiency of respiratory epithelial cells infected with wt HPIV1 (11).

One aim of this project was to identify cellular pathways that are targeted by the HPIV1 C proteins and to define how the C proteins exert such impressive transcriptional control of the host's innate immune system. We analyzed the gene expression profiles for all 14 transcription factors identified by bioinformatics analysis (**Fig. S6**) and found that the expression of 4 genes IRF1, ISGF3G, NF-κB1, and c-Rel were significantly up-regulated increasingly over time, confirming the importance of the IRF3 and NF-κB signaling pathways during parainfluenza infection and furthermore providing a feed-forward mechanism to amplify the host transcriptional response to viral infection. We expected to identify IRF and NF-κB TFBSs over-represented in genes induced by IFN treatment and

HPIV1 infection, but other unexpected TFBSs were also identified. For example, FOXD1 and FOXD3 TFBS were identified in genes up-regulated by the HPIV1 C mutant viruses. Only recently has an important role for FoxD1 been identified in the regulation of immune activation through the NF-κB pathway (117). FoxD3 is well known for controlling cellular differentiation but no role has yet been defined for FoxD3 in the regulation of the immune response or the response to viral infection. In future work, it will be important to define how the HPIV1 C proteins modify the activity of FOXD1, FOXD3, and other transcription factors and how C', C, Y1, and Y2 differ in their ability to alter transcriptional activity.

In summary, the HPIV1 C proteins exert remarkable control over the cellular transcriptional response to viral infection, indicating that the C proteins are important virulence factors for HPIV1. Mutations within the C gene permit the activation of a broad array of cellular genes involved in the type I IFN, IRF3 and NF-κB pathways that would otherwise be repressed by HPIV1 infection, and these mutations specify an attenuation phenotype *in vivo*. However, the lack of a clear differential regulation of antiapoptotic and proapoptotic genes in P(C-) and C^{F170S} infected cells allows for two models of P(C-) induced apoptosis that could individually, or in combination, play a key role in determining the apoptosis phenotype of HPIV1 infection: 1) earlier expression of TNFRSF10B and caspase 3 or 2) alterations in post-translational events involving constitutively expressed cellular proapoptotic or antiapoptotic factors.

Chapter 4. The C proteins of human parainfluenza virus type 1 limit double stranded RNA accumulation that would otherwise trigger MDA5 and PKR activation

Submitted

Jim Boonyaratanakornkit[1], Emmalene Bartlett[1], Henrick Schomacker[1], Sonja Surman[1], Shizuo Akira[2], Yong-Soo Bae[3], Peter Collins[1], Brian Murphy[1], and Alexander Schmidt[1]

[1]Laboratory of Infectious Diseases, RNA Viruses Section, NIAID, NIH, Bethesda, MD 20892, USA. [2]Laboratory of Host Defense, WPI Immunology Frontier Research Center, Osaka University, Osaka 565-0871, Japan. [3]Department of Biological Sciences, Sungkyunkwan University, Choenchoen-Dong, Jangan-Gu, Suwon, Gyeonggi-Do 440-746, South Korea

Abstract

Human parainfluenza virus type I (HPIV1) is an important respiratory pathogen in young children, the immunocompromised, and the elderly. We found that infection with wild-type (WT) HPIV1 suppressed the innate immune response in human airway epithelial cells by preventing not only phosphorylation of IRF3 but also degradation of IκBβ, thereby inhibiting IRF3 and NF-κB activation, respectively. Both of these effects were ablated by a F170S substitution in the HPIV1 C proteins (F170S) or by silencing the C open reading frame (P(C-)), resulting in a potent IFNβ response. Using murine knockout cells, we found that IFNβ induction following infection with either mutant relied mainly on MDA5 rather than RIG-I. Infection with either mutant, but not WT HPIV1, induced a significant accumulation of intracellular dsRNA. These mutant viruses directed a marked increase in the accumulation of viral genome, antigenome, and mRNA that was coincident with the accumulation of dsRNA. In addition, the amount of viral proteins was reduced compared to WT HPIV1. Thus, the accumulation of dsRNA might be a result of an imbalance in the N protein-to-genomic RNA ratio leading to incomplete encapsidation. PKR activation and IFNβ induction followed the kinetics of dsRNA accumulation. Interestingly, the C proteins did not appear to directly inhibit intracellular signaling involved in IFNβ induction; instead, its role in preventing IFNβ induction appeared to be in suppressing the formation of dsRNA. PKR activation contributed to IFNβ induction and also was associated with the reduction in the amount of viral proteins. Thus, the HPIV1 C proteins normally limit the accumulation of dsRNA and thereby limit activation of IRF3, NF-κB, and PKR. If C protein function is compromised, as in the case of F170S HPIV1, the resulting PKR activation and reduction

in viral protein levels enables the host to further reduce C protein levels and to mount a potent antiviral type I IFN response.

Introduction

Human parainfluenza virus type 1 (HPIV1) is an important and uncontrolled respiratory pathogen that causes a significant burden of disease, mainly in young children, the immunocompromised, and the elderly (30, 42, 58, 79, 134, 154). HPIV1 is a single stranded, negative sense, nonsegmented RNA virus in the Paramyxoviridae family. The viral genome, 15.6 kb in length, consists of 6 genes (3' – N-P/C-M-F-HN-L – 5') that encode the nucleoprotein (N), phosphoprotein (P), C proteins (C), matrix protein (M), fusion protein (F), hemagglutinin-neuraminidase protein (HN), and the large polymerase protein (L). Each gene encodes a single major protein with the exception of the P/C gene, which encodes the P protein in one open reading frame and a nested set of four carboxy-coterminal C proteins (C', C, Y1, and Y2) expressed from individual start sites in a second open reading frame. The C proteins play a critical role in HPIV1 virulence by inhibiting apoptosis, regulating type I interferon (IFN) production and signaling, and controlling the transcription of a large number of host genes (9, 17, 18, 192). The C proteins of Sendai virus (SeV), or murine PIV1, have considerable sequence conservation with the HPIV1 C proteins. However, the P/C gene organization of SeV differs from that of HPIV1 in that SeV expresses, in addition to the C proteins, a second accessory protein, the V protein, that also exerts an inhibitory role on the host innate antiviral response (3). In addition, some of the immune evasion activities of SeV and HPIV1 are species-specific (18, 22), indicating that a careful examination of the innate immune response to

HPIV1 may yield important clues about the pathogenesis of this human respiratory virus that differ from the murine SeV.

Type I IFN is a central mediator of antiviral innate immunity. The induction of IFN synthesis following virus infection depends on a number of pattern-recognition receptors that recognize conserved pathogen-associated molecular patterns and initiate downstream signaling cascades (87). The presence of dsRNA, an intermediate of RNA viral replication, is recognized as a pathogen-associated molecular pattern by Toll-like receptor 3 (TLR3) and two caspase recruitment domain (CARD)-containing RNA helicases, retinoic acid-inducible gene I (RIG-I) and melanoma associated-differentiation gene 5 (MDA5), which act as intracytoplasmic sensors of dsRNA (2, 76, 147, 180, 212, 214). Whereas TLR3 mainly senses extracellular dsRNA on antigen-presenting cells, RIG-I and MDA5 are constitutively present and detect intracellular dsRNA (2, 214). TLR3 signals through an adaptor called TIR domain-containing adaptor inducing IFNβ (TRIF), while RIG-I and MDA5 recruit another CARD-containing adaptor called mitochondrial antiviral signaling protein (MAVS, also referred to as IPS-1, Cardif, or VISA) to relay the signal to the kinases TBK1 and IKKε, which phosphorylate IRF3 (interferon regulatory factor 3), and to IKKβ, which activates the NF-κB pathway (41, 99, 140, 167, 207). Once activated, IRF3 translocates into the nucleus and binds the positive regulatory domain III (PRDIII) of the IFNβ promoter. RIG-I and MDA5 can distinguish between different RNA viruses (98). It was originally reported that IFN production in response to infection with negative-sense RNA viruses, including SeV, was dependent on RIG-I expression whereas the response to infection with positive-sense

RNA viruses was dependent on MDA5 expression (98, 195). This model was in agreement with earlier reports that found a substantial accumulation of cytoplasmic dsRNA during infection with positive-sense RNA viruses but not with negative-sense RNA viruses (199). However, a more recent study suggested that MDA5 does contribute *in vivo* to sustaining the IFN response and restricting SeV infection (53). After the host cell recognizes and signals the presence of foreign RNA, IRF-3 and NF-κB, together with ATF-2/c-Jun (AP-1), form an enhanceosome that binds to the IFNβ promoter, inducing transcription of the IFNβ gene. Once type I IFN is produced and secreted, it binds to the type 1 IFN receptor on the surface of the infected and neighboring cells to amplify a robust antiviral response (121, 183). One IFN-inducible gene, PKR, is best known for its ability to bind dsRNA and subsequently phosphorylate EIF2A thereby inhibiting translation initiation during viral infection (70). PKR has also been implicated in contributing to NF-κB activation, IRF1 activation, and IFN induction by poly I:C, independent of its kinase activity, as another mechanism of innate antiviral host defense (4, 16, 25, 107, 209, 218).

We generated a number of HPIV1 mutants to investigate C protein function as well as to generate novel live vaccines that would be attenuated by disturbing the IFN antagonistic function of the C proteins, a strategy that has been shown to result in attenuation of replication *in vivo* (5, 6, 192). Previously, a phenylalanine to serine substitution of amino acid 170 of SeV was shown to significantly attenuate a highly virulent SeV strain, increasing the lethal dose 50% (LD_{50}) 20,000-fold in mice (50). This C^{F170S} mutation was introduced into the P/C gene of recombinant HPIV1 by reverse genetics (85, 137).

Whereas WT HPIV1 infection prevented IRF3 dimerization, its nuclear translocation, and IFNβ production, infection with HPIV1 containing the C^{F170S} mutation (F170S virus) led to IRF3 activation and IFNβ production (192). Not unexpectedly, the F170S mutant was attenuated for replication in the respiratory tract of hamsters and African green monkeys (AGMs) (5, 192). We also constructed a HPIV1 mutant, referred to as P(C-), that does not express any of the four C proteins due to point mutations that silence the C ORF, and which was even more attenuated than F170S *in vivo* (9).

In the present study, we found that the C proteins of HPIV1 profoundly suppress the innate immune response in epithelial cells by preventing the activation of both IRF3 and NF-κB. We found that mutation or silencing of the C gene ablated both of these inhibitory effects. In contrast to WT, infection with both F170S and P(C-) HPIV1 resulted in the accumulation of significant amounts of cytoplasmic dsRNA with kinetics that were more rapid for the P(C-) virus. The accumulation of dsRNA coincided with an increase in the accumulation of viral genomic/anti-genomic RNA or mRNA and a decrease in N protein levels, and thus appeared to result from incomplete encapsidation. The enhanced induction of IFNβ observed with these mutants relied mainly on MDA5 rather than on RIG-I. PKR activation coincided with dsRNA accumulation, contributed to IFNβ induction, and restricted viral C protein expression. Thus, PKR activation provides a mechanism that allows the host cell to eliminate the very protein responsible for evading virus detection.

Materials and Methods

Cells, viruses, and DNA transfection

A549 human respiratory epithelial cells were maintained in F-12 medium supplemented with 0.1 mg/mL gentamicin sulfate, 4 mM L-glutamine, and 10% fetal bovine serum (FBS). Human embryonic kidney 293T cells were maintained in DMEM medium supplemented with 10% FBS and gentamicin sulfate. Mouse embryonic fibroblasts were prepared from RIGI MDA5 +/- +/-, RIGI -/-, and MDA5 -/- mice and maintained in DMEM with 10% FBS and gentamicin sulfate as described (98). Stable shPKR knockdown and shCON control 293A cells were maintained in DMEM with 10% FBS and gentamicin sulfate supplemented with 1 μg/mL puromycin as described (215). Doxycycline-inducible, stable cells that express WT C′ protein tagged at the C-terminus with a c-Myc epitope were generated using Flp-In T-REx 293 cells grown in 100 μg/mL Hygromycin and 15 μg/mL Blasticidin (Invitrogen). C expression was induced by incubation for 24 h with 1 μg/mL Doxycycline (Sigma). Sucrose gradient-purified recombinant WT, F170S, and P(C-) HPIV1 were prepared and titered by limiting dilution assay as reported (17). All viral infections were carried out using a multiplicity of infection (MOI) of 5 $TCID_{50}$/mL at 32°C in medium containing 1.2% trypsin TrypLE Select (Invitrogen). For type I IFN neutralization, 5000 NU/mL anti-IFNα and 2000 NU/mL anti-IFNβ antibodies (PBL InterferonSource) were added at 12 h p.i. For transient transfections, 3 μL Lipofectamine 2000 (Invitrogen) per 1 μg total DNA was added for every 400,000 293T cells for 48 h at 37°C. For poly I:C-induced IFNβ expression, 3 μL Lipofectamine 2000 per 1 μg of poly I:C (Sigma) was added for every 400,000 293T cells for 6 h at 37 °C. For the preparation of cellular extracts, cells were

suspended in lysis buffer (1% Triton X-100, 50 mM Tris HCl pH 7.4, 150 mM NaCl, 1 mM EDTA) with protease inhibitor cocktail (Sigma) at a concentration of 2000 cells/μL for 30 min at 4°C and centrifuged at 15,000 g for 10 min. Halt protease and phosphatase inhibitor cocktail (Pierce) was added to the lysis buffer whenever phosphorylation states were examined. After centrifugation, the supernatant was used for Western blotting and immunoprecipitation.

Real-time RT-PCR

Intracellular RNA or virion-associated RNA was extracted and analyzed by real-time RT-PCR as described previously (17). The relative levels of expression of mRNA for human and murine IFNβ and GAPDH were determined using TaqMan Gene Expression Assays (Applied Biosystems) for human IFNβ (Hs01077958_s1), human GAPDH (Hs99999905_m1), mouse IFNβ (Mm00439546_s1), and mouse GAPDH (Mm99999915_g1), with the RT performed on intracellular RNA using random hexamers. Experiments were performed in triplicate. Combined genomic/anti-genomic RNA, genomic RNA, anti-genomic RNA, and IFNβ expression in shPKR 293 cells was measured in triplicate and confirmed in two independent experiments. Student's t-test was used to determine statistical significance. To measure the relative copy numbers of HPIV1 genome plus antigenome in sucrose-purified virus stocks, RT was performed on extracted virion RNA with random hexamers and PCR was performed to amplify genome nucleotides 15,502-15,600, corresponding to the downstream end of the L gene and the adjoining trailer region (forward primer ACCAGACAAGAGTTTAAGAAATATCGA, reverse primer AGAAATCCCTTTAACTGACTCATAAAAACATAGT, probe

CAACAGACAAGAGTATTAATAAT). To distinguish between genomic and antigenomic RNA in intracellular RNA, RT was performed with a positive-sense primer representing genome nucleotides 15502-15519 (AGAAATCCCTTTAACTGA) to measure genome or with a negative-sense primer representing genome nucleotides 15583-15600 (CTTAAACTCTTGTCTGGT) to measure antigenome. PCR was then performed to amplify nucleotides 15,502-15,600 of the genome or its complement, using the primer/probe set described above. To measure the relative copy numbers of the N and P mRNAs in intracellular RNA, RT was performed with oligo-dT primer and PCR was performed to amplify, in the case of N, genome nucleotides 917-1014 (forward primer AGCATCTTTCATGAACACCATCAAGT, reverse primer GGCTTCTCAATTTGTTTATATCTGGTCTCA, probe CCGCCCTGACACTAT) and, in the case of P, genome nucleotides 2624-2685 (forward GAAGACCACAACACCAAAACCA, reverse primer GCTGCTGACTCTTCGTTCTTTG, probe ACGGTGGAACTTTTG).

Western blotting and antibodies

Cells were lysed and clarified as described above for the preparation of cellular extracts, and the resulting extracts (15 µL) were denatured and reduced in sample loading buffer (0.3M Tris HCl, 5% SDS, 50% glycerol, 0.1M DTT) at 95 °C for 5 min, separated by SDS-PAGE on 4-20% Tris-Glycine gels (Invitrogen), and transferred to 0.45 µm PVDF membranes (Invitrogen). Membranes were blocked overnight with 5% milk powder and 1% BSA or, whenever probing with phospho-specific antibodies, with 5% BSA in 0.1% Tween-PBS. Rabbit polyclonal anti-serum was raised against a synthetic peptide

corresponding to an internal sequence (amino acids 78–92, TITTKTEQSQRRPK) in the HPIV1 C proteins shared by C', C Y1, and Y2 by ProSci (Poway, CA), against a synthetic peptide corresponding to an internal sequence (amino acid residues 485–499, RRLADRKQRLSQANN) in the HPIV1 N protein by ProSci, and against a synthetic peptide corresponding to a N-terminal sequence (amino acids 10-24, RDPEAEGEAPRKQES) in the HPIV1 P protein by Spring Valley Laboratories (Woodbine, MD). Membranes were probed with rabbit anti-serum at a 1:1000 dilution with 5% milk and 1% BSA in 0.1% Tween-PBS for 1 hour. Antibodies used included rabbit polyclonal antibodies to human pIRF3 (S396) (Millipore; #07-582), IRF3 (Santa Cruz Biotechnology; sc-9082), IκB-β (Santa Cruz; sc-945), ATF2 (Santa Cruz; sc-187), pP38 (T180/Y182) (Santa Cruz; sc-101759), P38 (Santa Cruz; sc-7149), PKR (Santa Cruz; sc-707), pEIF2α (S51) (Enzo Life Sciences; BML-SA405), EIF2α (Sigma; E0157), MDA5 (Alexis Biochemicals; ALX-210-935), Flag epitope tag (Sigma; F7425), HA epitope tag (Sigma; H6908), Myc epitope tag (Sigma; C3956), rabbit monoclonal antibody to human pPKR (T451) (Epitomics; #2283-1), or mouse monoclonal antibodies to human pATF2 (T71) (Santa Cruz; sc-8398), GAPDH (Sigma; G9295) and V5 epitope tag (Invitrogen; R960-25). Horseradish peroxidase-conjugated goat anti-rabbit secondary antibody (Santa Cruz) was used at a dilution of 1:5000 and horseradish peroxidase-conjugated goat anti-mouse secondary antibody (Kirkegaard & Perry Laboratories) was used at a dilution of 1:2400 for 1 hour. Membranes were washed 3 times for 5 minutes with 0.1% Tween-PBS after primary and secondary antibody incubations. Enhanced chemiluminescent substrate (Pierce) was used to visualize proteins on BIOMAX MR film (Kodak). Relative band intensity was determined by densitometry using ImageJ.

Immunoprecipitation

Cell lysates extracted from transfected 293T cells were mixed for 16 h at 4°C with anti-Myc agarose (Pierce), washed extensively with wash buffer (50 mM Tris HCl pH 7.4, 150 mM NaCl), eluted with 0.1 M glycine pH 2.8, and separated by SDS-PAGE.

Immunofluorescence

A549 cells were fixed with 2% paraformaldehyde, permeabilized with 0.2% Triton X-100, and blocked with 10% goat serum and 0.02% BSA for 2 h. Mouse monoclonal J2 anti-dsRNA antibody (English and Scientific Consulting) at a 1:200 dilution or rabbit polyclonal anti-HPIV1 P antibody at a dilution of 1:100 was added in 1% goat serum and 0.002% BSA for 1 h at 37°C. Texas Red-conjugated goat anti-rabbit and FITC-conjugated goat anti-mouse secondary antibodies (Jackson ImmunoResearch) were added at a dilution of 1:250 for 45 min at 37°C. Cells were mounted in ProLong Gold reagent with DAPI (Invitrogen) and visualized on a Leica SP5 confocal microscope.

Plasmid constructs

A cDNA for HPIV1 C was generated by PCR (forward primer CATCGGTACCGTGGATACCTCAGCATCCAAAACTCTCCTTCCC and reverse primer ATCACATGCGGCCGCTTACAGATCTTCTTCAGAAATAAGTTTTTGTTCTTCTTG TACTATGTGTGCTGCTAGTTTCC) of the full-length antigenomic cDNA for WT HPIV1 and constructed with the insertion of a C-terminal c-Myc tag and KpnI and EagI

restriction sequences to allow cloning into pcDNA3.1 (Invitrogen). The nucleotide sequence was confirmed using BigDye Terminator and a DNA Analyzer 3730 (Applied Biosystems). pEF-IRES V5-TRIM25 was kindly provided by Michaela Gack and Jae Jung (45). pEF-BOS HA-Riplet was kindly provided by Hiroyuki Oshiumi and Tsukasa Seya (141). pRK5 Flag-TRAF3 and Myc-TRADD3 were kindly provided by Jurg Tschopp (128). pCMV2 Flag-TRAF6 was kindly provided by Masashi Muroi and Ken-ichi Tanamoto (132). pEF-BOS Flag-RIGI and Flag-MDA5 were kindly provided by Takashi Fujita (213, 214). pcDNA3 Flag-TBK1 was kindly provided by Katherine Fitzgerald and Makoto Nakanishi (41, 190). pCMV2 Flag-IPS1 has been previously described (99). pcDNA3 Flag-BIRC2 and Flag-BIRC4 were kindly provided by Temesgen Samuel (162). pFlag-CMV2 Flag-FADD was kindly provided by Andrew Thorburn (189).

Results

HPIV1 activation of the interferon induction pathway

We found previously that, in stark contrast to WT HPIV1, HPIV1 with a F170S point mutation in the C proteins or in which the C gene was silenced by point mutations induced the transcription of a broad array of cellular genes, in particular genes involved in type I IFN production and the subsequent antiviral response (17, 192). To investigate the mechanism of C-mediated antagonism of the host innate immune response, we used three cell types. A549 cells were used to model infection in human respiratory epithelial cells, 293 human kidney cells were used for transfection and knockdown experiments, and mouse embryonic fibroblasts were used for knockout experiments. We found that

the HPIV1-induced IFN phenotype was comparable between the three cell types: specifically, in each cell type, F170S and P(C-) HPIV1 induced similar, abundant levels of IFNβ expression mRNA expression, whereas WT HPIV1 did not induce significant IFNβ (not shown).

IFNβ induction is transcriptionally controlled by the coordinate assembly of an enhanceosome consisting of IRF3, NF-κB, and AP-1 at the IFNβ promoter (120, 210). We examined the activation of the three components of the IFNβ enhanceosome during HPIV1 infection and found that both F170S and P(C-) HPIV1 induced IRF3 phosphorylation and IκBβ degradation, which would permit nuclear translocation of IRF3 and NF-κB, respectively, whereas WT HPIV1 effectively blocked IRF3 phosphorylation and IκBβ degradation (**Fig. 1**). On the other hand, WT, F170S, and P(C-) HPIV1 did not induce detectable phosphorylation of P38 or ATF2 **(Supplementary Fig. 1)**.

Figure 1. Activation of the IRF3 and NF-κB components of the IFNβ enhanceosome by infection with WT and mutant HPIV1. A549 cells were infected with WT, F170S, or P(C-) HPIV1 at a MOI of 5 for 6 or 48 h. Phosphorylated IRF3 (Ser 396), total IRF3, and total IκBβ were detected by Western blot.

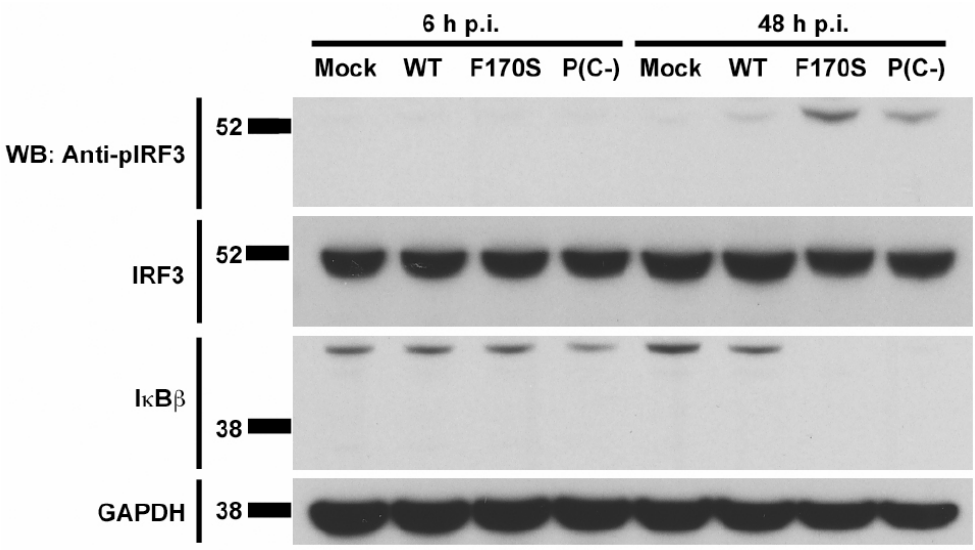

To investigate the basis for the observed antagonism of the host response by the WT HPIV1 C proteins, a selective search for cellular C-interacting proteins was performed among RIG-I/MDA5 pathway components. Cells transfected with expression plasmids expressing a tagged C' protein and various tagged proteins of the RIG-I/MDA5 pathway were lysed and analyzed in co-immunoprecipitation experiments using various conditions in an attempt to sensitively detect any interactions. However, we were unable to detect any cellular C-interacting proteins among those tested, including TRIM25, Riplet, RIGI, MDA5, IPS1, TBK1, TRAF3, TRAF6, BIRC2, BIRC4, TRADD, and FADD, even though, under these same conditions, TRAF3 was immunoprecipitated with TRADD, a known binding partner of TRAF3 (**Supplementary Fig. 2**). Since we could not identify

any cellular C-interacting proteins, we investigated whether supplying the HPIV1 C proteins in trans could block the IFNβ induction pathway triggered by infection with respiratory syncytial virus (RSV) or by transfection with poly I:C, which mainly involves activation of RIG-I and MDA5, respectively (118, 174). Infection with WT HPIV1, as a source of C proteins, strongly suppressed IFNβ induction in response to super-infection with P(C-) HPIV1, but failed to block IFNβ induction in response to super-infection with a RSV mutant that expresses GFP from an added gene and lacks the NS1 and NS2 RSV IFN antagonist genes (ΔNS1/NS2 RSV) (**Fig. 2a**). As a control, analysis of GFP expression showed that the efficiency of infection by ΔNS1/NS2 RSV was not affected by pre-infection with WT HPIV1 (not shown). To test whether the HPIV1 C proteins could interfere with IFN production triggered through MDA5, a doxycycline-inducible stable human cell line that expresses the HPIV1 C proteins was generated. In this system, expression of the HPIV1 C proteins in trans strongly suppressed IFNβ induction by infection with P(C-) HPIV1 (**Fig. 2b**), confirming the efficient expression of functional C protein. In contrast, expression of the HPIV1 C proteins had no effect on IFNβ induction in response to transfection with poly I:C (**Fig. 2c**). In this last experiment, the cells had also been transfected with a plasmid expressing human MDA5 to provide the homologous sensor for dsRNA prior to the transfection of poly I:C. Taken together, these results indicate that the HPIV1 C proteins supplied in trans can efficiently suppress IFN induction by HPIV1 mutants, but not by heterologous inducers.

Figure 2. IFNβ induction in A549 cells by heterologous RIG-I and MDA5 stimuli is not affected by expression of the HPIV1 C proteins in trans. (A) A549 cells were pre-infected with WT HPIV1 at a MOI of 5 for 24 h and then super-infected with either P(C-) HPIV1 or GFP-expressing ΔNS1/NS2 RSV at a MOI of 5 for another 24 h. IFNβ expression was measured by real-time PCR and was normalized to the mock pre-infected, mock super-infected sample. * denotes $P < 0.01$ compared to mock pre-infected samples. (B) C protein expression was induced in stable C-expressing 293 cells with 1 μg/mL doxycycline for 24 h. Cells were then mock-infected or infected with P(C-) HPIV1 at a MOI of 5 for another 24 h. IFNβ expression was measured by real-time PCR and was normalized to the control treated, mock infected sample. * denotes $P < 0.01$ compared to control treated cells. (C) C protein expression was induced in stable C-expressing 293 cells with 1 μg/mL doxycycline for 24 h, then transfected with 2.5 μg MDA5 expression plasmid for another 18 h, and then transfected with 10 μg poly I:C for 6 h. IFNβ expression was measured by real-time PCR and was normalized to the control treated, control transfected sample.

a.

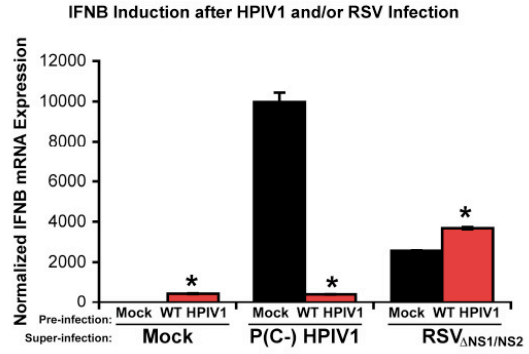

b.

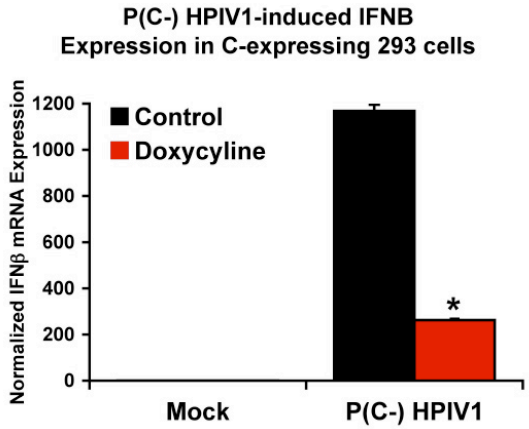

c.

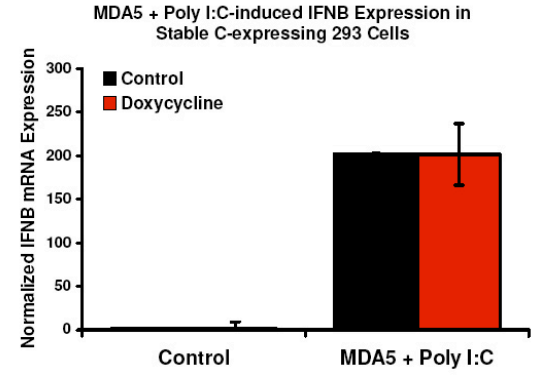

HPIV1-induced IFNβ expression is mediated mostly by MDA5

Since we were unable to obtain either direct or indirect evidence that the C proteins blocked IFN production by interacting with a host factor of the RIG-I/MDA5 pathway, we evaluated the involvement of this pathway in IFNβ induction by HPIV1 using

knockout MEFs. In contrast to WT HPIV1, F170S and P(C-) HPIV1 strongly induced IFNβ expression in control MEFs (**Fig. 3a**, black bars). RIG-I knockout led to a slight decrease (2.3-fold) in IFNβ expression in F170S-infected cells, but no effect was observed in P(C-)-infected cells (**Fig. 3a**). MDA5 knockout led to a greater reduction in IFNβ expression in both F170S- and P(C-)-infected cells (4.5-fold and 8.0-fold, respectively) (**Fig. 3a**). TBK1 and IKKε double knockout led to a dramatic reduction in IFNβ expression in both F170S- and P(C-)-infected cells, confirming the requirement for TBK1 and IKKε in IFN induction due to infection with F170S or P(C-) HPIV1 (**Fig. 3b**). The observation that knock-outs of TBK1 and IKKε led to almost complete inhibition of IFNβ mRNA synthesis, whereas knock-out of MDA5 led to only a partial inhibition, raised the possibility that factors in addition to MDA5 are contributing to the induction of IFNβ mRNA via TBK1 and IKKε.

Figure 3. IFNβ expression in RIG-I/MDA5 pathway knockout MEFs infected with WT or mutant HPIV1. (A) RIG-I and MDA5 knockout MEFs and (B) TBK1 and IKKε double knockout MEFs were infected with WT, F170S, or P(C-) HPIV1 at a MOI of 5 for 48 h. IFNβ expression was measured by real-time PCR and normalized to mock infected control MEFs. * denotes $P < 0.01$ compared to control MEFs infected with the same virus.

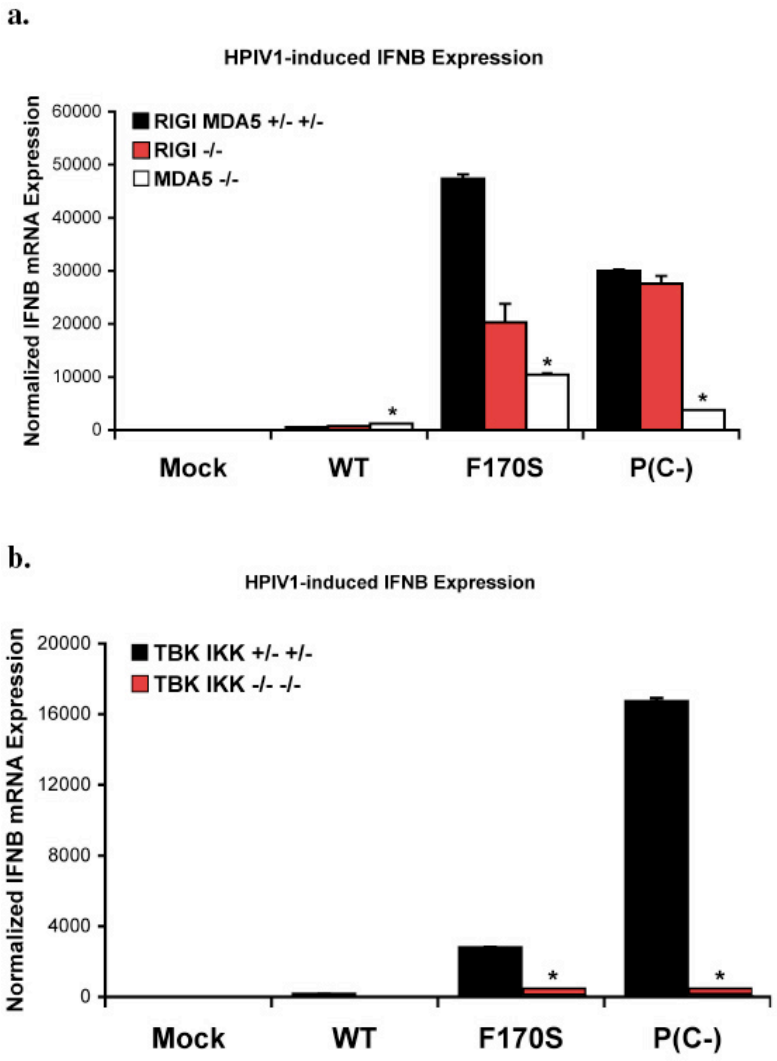

Intracellular dsRNA accumulates in cells infected with C mutant HPIV1 viruses

Since knockout of the dsRNA sensor MDA5 strongly reduced IFNβ expression during infection with F170S or P(C-) HPIV1, we looked for the presence of dsRNA in HPIV1-infected cells by immunofluorescence using a monoclonal antibody against dsRNA. Transfection of poly I:C was used as a positive control, demonstrating the ability of the dsRNA-specific monoclonal antibody to detect intracellular dsRNA (**Fig. 4a**). dsRNA was not detected in WT-infected cells at either 24 or 48 h (**Fig. 4b, e**), similar to observations previously reported for a number of negative sense RNA viruses, including influenza, La Crosse, Sendai, and Newcastle disease viruses (199). In contrast, dsRNA was readily detected in cells infected with either the F170S or P(C-) virus; however, the kinetics of accumulation differed. In the case of F170S HPIV1, less than 10% of infected cells were positive for dsRNA at 24 h, whereas over 60% of infected cells were positive at 48 h (**Fig. 4c, e, f**). In contrast to F170S HPIV1, the accumulation of dsRNA in response to P(C-) HPIV1 occurred more rapidly, with approximately 70% of infected cells containing detectable dsRNA at 24 h. However, the accumulation of dsRNA in response to the P(C-) virus was also transient: by 48 h, less than 10% of P(C-)-infected cells contained dsRNA (**Fig. 4d-f**). This difference did not appear to be due to differences in the kinetics or efficiencies of infection: the percent of cells infected with WT, F170S, and P(C-) HPIV1 was similar at 24 and 48 h, as assessed by immunofluorescence using polyclonal antibodies specific to the HPIV1 P protein (**Fig. 4g**).

Figure 4. Immunofluorescence of dsRNA in A549 cells infected with WT or mutant HPIV1. A549 cells were transfected with (A) poly I:C (0.02 μg/μL) or infected with (B) WT, (C) F170S, or (D) P(C-) HPIV1 at a MOI of 5 for 24 h. HPIV1 P protein (red) was detected using a rabbit polyclonal anti-P antibody and a Texas-Red conjugated secondary anti-rabbit antibody. dsRNA (green) was detected using a mouse monoclonal anti-dsRNA antibody and a FITC conjugated secondary anti-mouse antibody. (E) dsRNA and the HPIV1 P protein was examined as in A-D in A549 cells infected with WT, F170S, or P(C-) HPIV1 at a MOI of 5 for 24 and 48 h. (F, G) Quantitation of the number of cells in D with and without detectable dsRNA (F) or HPIV1 P protein (G) at 24 and 48 h. dsRNA levels are representative of two independent experiments.

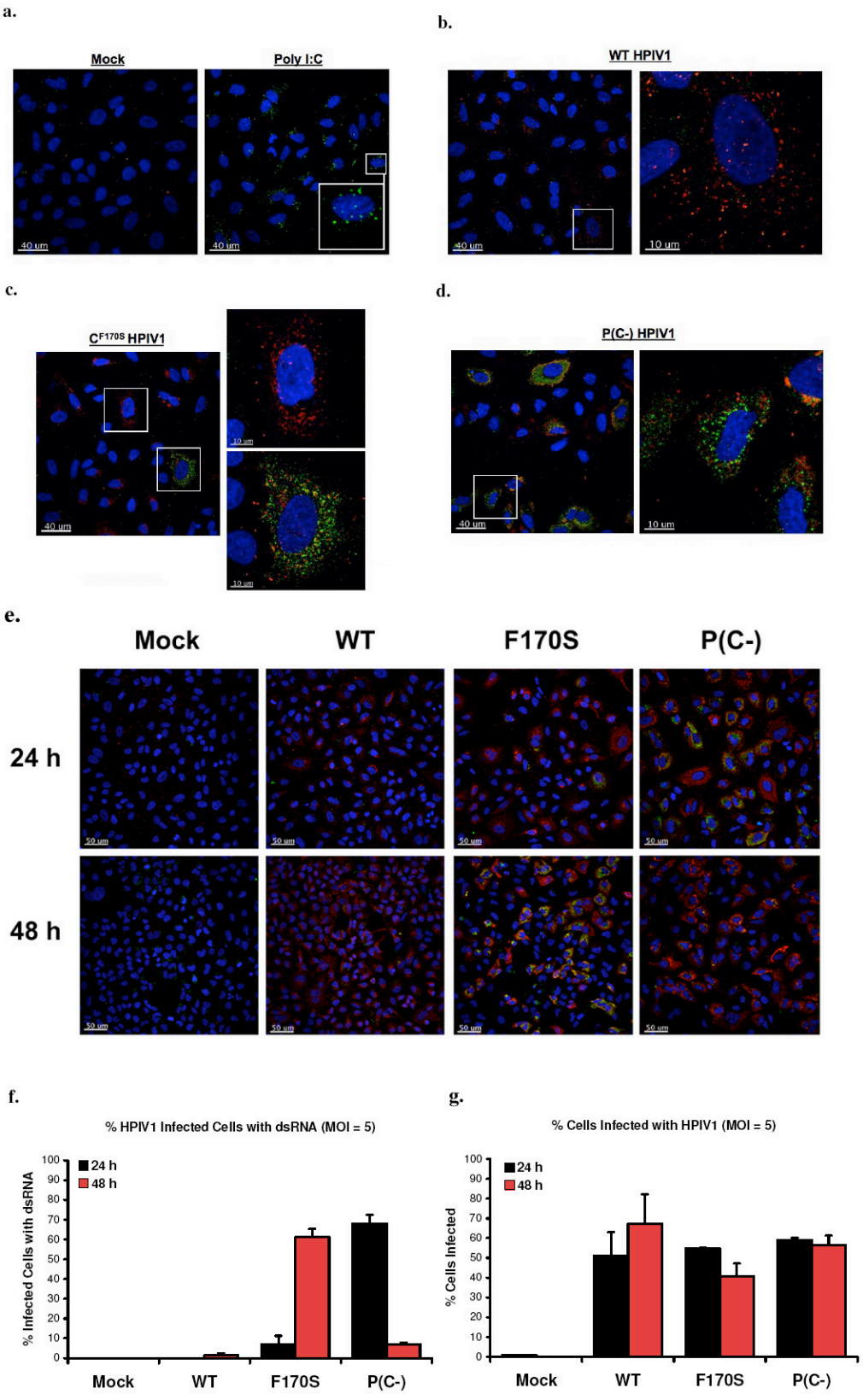
a.
Mock
Poly I:C
40 um
b.
WT HPIV1
10 um
c.
C^F170S HPIV1
d.
P(C-) HPIV1
e.
Mock
WT
F170S
P(C-)
24 h
48 h
50 um
f.
% HPIV1 Infected Cells with dsRNA (MOI = 5)
% Infected Cells with dsRNA
24 h
48 h
g.
% Cells Infected with HPIV1 (MOI = 5)
% Cells Infected

One possible explanation for the increased accumulation of intracellular dsRNA in cells infected with the F170S and P(C-) viruses was that these virus preparations contained disproportionately high levels of defective interfering particles, which, for nonsegmented negative strand RNA viruses, usually have copy-back genomes that can form base-paired panhandles. To investigate this possibility, we assayed a sucrose gradient-purified preparation of each virus for (i) the number of infectious particles, measured by limiting dilution assay, and (ii) the relative copy number of genomic plus antigenomic RNA, measured by real time RT-PCR with primers specific to the trailer region that would be present in both standard and defective genomes. We then calculated the ratio of infectious particles to genome/antigenome copies for each virus, and then normalized these ratios to that of the F170S virus, which was assigned the value of 1.0. The resulting values were: F170S, 1.0; WT, 0.28; and P(C-), 0.09. In other words, F170S HPIV1 had the highest ratio of infectious particles to genome copies, and P(C-) had the lowest, with WT HPIV1 being intermediate. This lack of a consistent trend, i.e. the F170S virus had a higher ratio of infectious particles to genome/antigenome copies than the WT virus and yet the F170S virus led to dsRNA accumulation whereas the WT virus did not, suggests that the dsRNA produced during infection with the F170S and P(C-) viruses probably cannot be attributed to the presence of a disproportionately high content of defective-interfering particles in the initial inoculum.

Mutation or deletion of the HPIV1 C proteins results in increased viral RNA synthesis and decreased accumulation of viral proteins

Another potential source for intracellular dsRNA could arise from annealing between incompletely encapsidated negative sense genomic RNA and either positive sense antigenomic RNA or mRNA, which might occur if mutation or deletion of the C proteins perturbed viral RNA production. We therefore used real-time RT-PCR to monitor viral RNA accumulation in A549 cells infected with the WT, F170S and P(C-) viruses. The combined amount of genomic plus antigenomic RNA was quantified using primer/probes specific for the trailer region (**Fig. 5a**), whereas the N and P mRNAs (**Fig. 5b and c**, respectively) were quantified using oligo-dT for reverse transcription followed by gene-specific primer/probes for PCR. In cells infected with WT HPIV1, the levels of genome/antigenome, N mRNA, and P mRNA rose gradually over the time-course of the experiment (**Fig. 5a-c**). For the F170S mutant, the levels of these RNAs were similar to those of WT HPIV1 at 24 h, but then increased substantially by 48 h. A very different pattern was observed during infection with P(C-) virus. The amount of genome/antigenome was higher than for the other two viruses at 24 h, and continued to increase to a very high level at 48 h (**Fig. 5a**). In contrast, the levels of N and P mRNAs were extremely high at 24 h, but thereafter dropped sharply (**Fig. 5b**). In addition, the relative levels of intracellular genomic versus antigenomic HPIV1 RNA were measured by reverse transcription with positive- or negative-sense primers, to prime genomic or antigenomic RNA, respectively, followed by real-time PCR (**Supplementary Fig. 3**). This showed that the ratio of genomic RNA to antigenomic RNA (average ratio 17:1)

was similar for each virus at each time point (**Supplementary Fig. 3**) and, thus, was not detectably perturbed by mutation/deletion of the C protein.

Figure 5. Viral RNA and protein expression over time during infection with WT and mutant HPIV1. A549 cells were infected with WT, F170S, or P(C-) HPIV1 at a MOI of 5 for 12, 24, or 48 h. Relative amounts of HPIV1 (A) combined genomic and anti-genomic RNA, (B) N mRNA, and (C) P mRNA were measured by real-time PCR. The values were normalized to the 12 h time point for WT HPIV1, which was assigned the value of 1.0. (D) HPIV1 N, C, and P proteins were detected by Western blot from samples collected in parallel to the samples in A-C. Shown is a representative of two independent experiments with similar results. (E) A549 cells were infected with F170S HPIV1 at a MOI of 5 for 24, 30, 36, 42, or 48 h. The C and P proteins were detected by Western blot. P denotes the position of the P protein, n.s. indicates a non-specific band, and * indicates a potential P cleavage or degradation product detected by the polyclonal anti-P antibody.

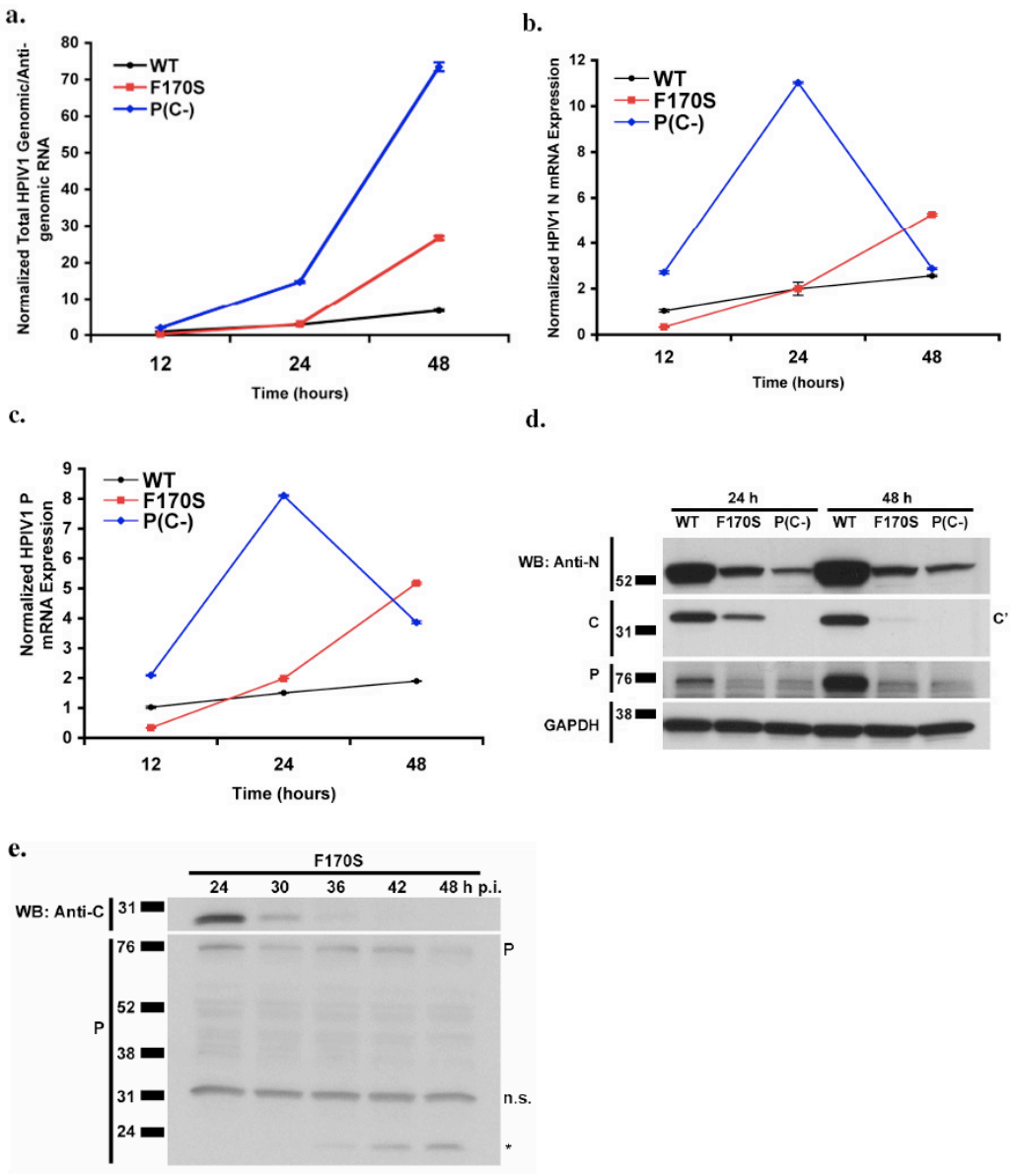

We also monitored the accumulation of cell-associated viral proteins in the time-course experiment described above by Western blot analysis (**Fig. 5d**). WT-infected cells contained higher levels of N and P protein at both 24 and 48 h compared to the mutant viruses, which was surprising since WT-infected cells contained the lowest levels of N and P mRNA (**Fig. 5d**). In contrast, although P(C-)-infected cells contained the highest levels of genomic/anti-genomic RNA at both time points and very high levels of N and P

mRNAs at 24 h, they contained the lowest levels of N and P protein at both time points (**Fig. 5a-d**). Similarly, F170S-infected cells contained much less N and P protein than WT-infected cells despite higher levels of N and P mRNA. Lysates from WT-infected A549 cells also contained a major band of C′ protein, which is the most abundant of the HPIV1 C proteins. As expected, no C proteins were detected with P(C-) HPIV1 infection. The C′ protein also was detected in lysates from F170S-infected cells at 24 h but, as with the N and P proteins, in lower abundance compared to WT HPIV1. Interestingly, however, the C'^{F170S} protein was not detected at 48 h. We further investigated the kinetics of accumulation of the C'^{F170S} protein in additional time course experiments. This showed that the C'^{F170S} protein was present at 12 and 24 h post-infection (not shown). However, beginning at 30 h post-infection, the level of C'^{F170S} protein began to decline until it was no longer detectable by 42 h (**Fig. 5e**). In this experiment, the level of the P protein expressed by F170S HPIV1 also decreased with time coincident with the appearance of a smaller P-specific band that might be a degradation product (**Fig. 5e**).

These observations indicated that HPIV1 RNA synthesis indeed was perturbed by mutation and, in particular, deletion of the C protein. These observations also indicate that viral protein synthesis was inhibited in cells infected with F170S and P(C-) HPIV1. The increased production of viral RNA by F170S and P(C-) HPIV1, in the context of reduced levels of N and P protein necessary for encapsidation, could provide for the accumulation of incompletely encapsidated genome capable of annealing with positive sense RNA to form the observed dsRNA.

HPIV1 infection and dsRNA accumulation induce PKR activation

Since dsRNA was highly abundant during infection with P(C-) and F170S HPIV1 at 24 and 48 h respectively, we examined PKR activation at these same time points. When bound to dsRNA, PKR is activated by autophosphorylation. Activated PKR can phosphorylate EIF2A, resulting in an inhibition of translational initiation (70) that potentially could contribute to the reduced accumulation of viral proteins in cells infected with F170S and P(C-) HPIV1. Consistent with this idea, we found that both F170S and P(C-) HPIV1 induced PKR autophosphorylation and EIF2A phosphorylation, with kinetics mirroring those of dsRNA accumulation (**Fig. 4e, f** and **Fig. 6**). Specifically, P(C-) HPIV1 infection induced activation of PKR by 24 h, and F170S HPIV1 infection induced activation of PKR by 48 h. In addition, infection with either mutant strongly induced the expression of MDA5, a highly IRF and IFN-inducible gene (**Fig. 6**). The expression of the C′ and C proteins was observed at 24 and 48 h in cells infected with WT HPIV1, and were not expressed by P(C-) HPIV1, as expected. Consistent with the results in **Fig. 5d**, both species were present in F170S-infected cells at 24h, and their accumulation greatly decreased by 48 h (**Fig. 6**). Thus, infection with F170S and P(C-) HPIV1 activated PKR and phosphorylated EIF2A, which might contribute to the reduced accumulation of viral proteins. However, this may not be a complete explanation for the reduced accumulation of viral proteins in the case of F170S HPIV1, since there was little activation of PKR and EIF2A at 24 h (**Fig. 6**), a time when the reduction in protein accumulation was already evident (**Fig. 5d and 6**).

Figure 6. PKR activation during infection with WT and mutant HPIV1. A549 cells were infected with WT, F170S, or P(C-) HPIV1 at a MOI of 5 for 24 or 48 h. PKR phosphorylation, total PKR, EIF2A phosphorylation, total EIF2A, total MDA5, and C proteins were detected by Western blot.

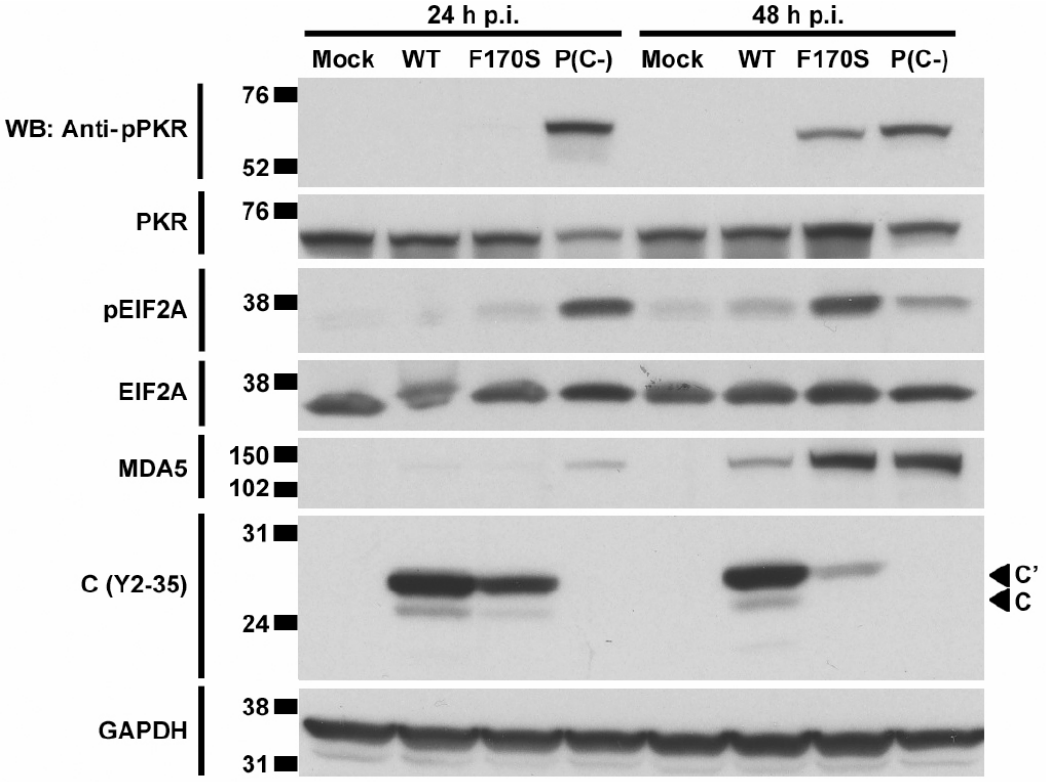

PKR contributes to HPIV1-induced IFN induction as well as the reduced accumulation of viral proteins

We examined the effects of PKR activation using stable PKR knockdown 293 cells, in which expression of PKR expression was strongly reduced, although not completely blocked, due to the constitutive expression of a shRNA specific to PKR. PKR knockdown significantly reduced IFNβ expression in F170S- and P(C-)-infected cells by 6.2 and 10.1-fold, respectively (**Fig. 7**). This reduction in IFNβ expression corresponded

with a reduction in IRF3 phosphorylation (3.1 and 3.4-fold, respectively) (**Fig. 8a**; see **Supplementary Fig. 4a** for quantitation). IκBβ degradation was only slightly reduced (1.3 and 1.6-fold, respectively) in PKR knockdown cells (**Fig. 8a**; see **Supplementary Fig. 4b** for quantitation). P38 phosphorylation was similar in control and PKR knockdown cells (**Fig. 8a**; see **Supplementary Fig. 4c** for quantitation). In the mock-infected cells, the expression of PKR in the knockdown cells was 25% that of the control knockdown cells (**Fig. 8a**; see **Supplementary Fig. 4d** for quantitation). Interestingly, PKR knockdown also reversed the decrease in the accumulation of C'^{F170S} between 24 and 48 h, an effect that was not observed with the wild-type C' protein (**Fig. 8a**; see **Supplementary Fig. 4e** for quantitation). These findings indicated that the reduction in viral protein synthesis in normal cells infected with the C mutant viruses (e.g., **Fig 5d, e, and Fig. 6**) indeed is linked to PKR activity. Since PKR is an IFN-inducible gene product, the induction of additional PKR due to IFN-mediated signaling could contribute to the loss of viral protein expression during infection with the mutant HPIV1 viruses. Indeed, we found that the decrease in C'^{F170S} protein expression could be partially blocked by IFN neutralizing antibodies (**Fig. 8b**).

Figure 7. IFNβ expression induced by infection with WT and mutant HPIV1 during PKR knockdown. Stable 293 cells expressing small hairpin RNAs shPKR and control shCON were infected with WT, F170S, or P(C-) HPIV1 at a MOI of 5 for 48 h. IFNβ expression was measured by real-time PCR and normalized to mock infected shCON cells. * denotes $P < 0.01$ compared to control 293A cells infected with the same virus.

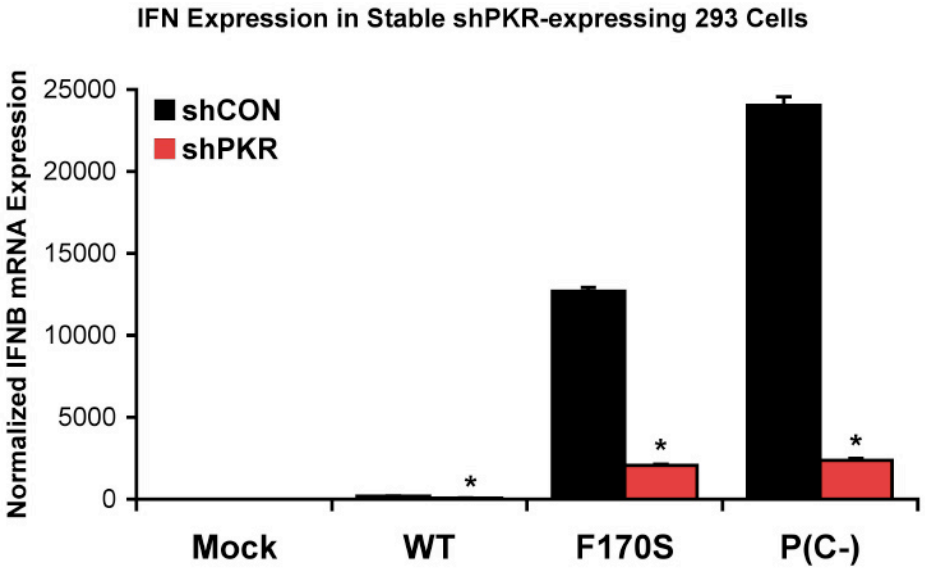

Figure 8. Effect of PKR on activation of the components of the IFNβ enhanceosome and accumulation of the C protein in HPIV1 WT and mutant virus-infected cells. (A) Stable shPKR-expressing and control shCON 293A cells were infected with WT, F170S, or P(C-) HPIV1 at a MOI of 5 for 48 h. Phosphorylated IRF3, total IRF3, total IκBβ, phosphorylated P38, total P38, total PKR, and C proteins were detected by Western blot. (B) Type I IFN affects C' protein expression during HPIV1 infection. A549 cells were infected with F170S HPIV1 at a MOI of 5. At 12 h post-infection, neutralizing antibodies against IFNα (5000 NU/mL) and IFNβ (2000 NU/mL) were added. C protein was detected by Western blot at 30 h.

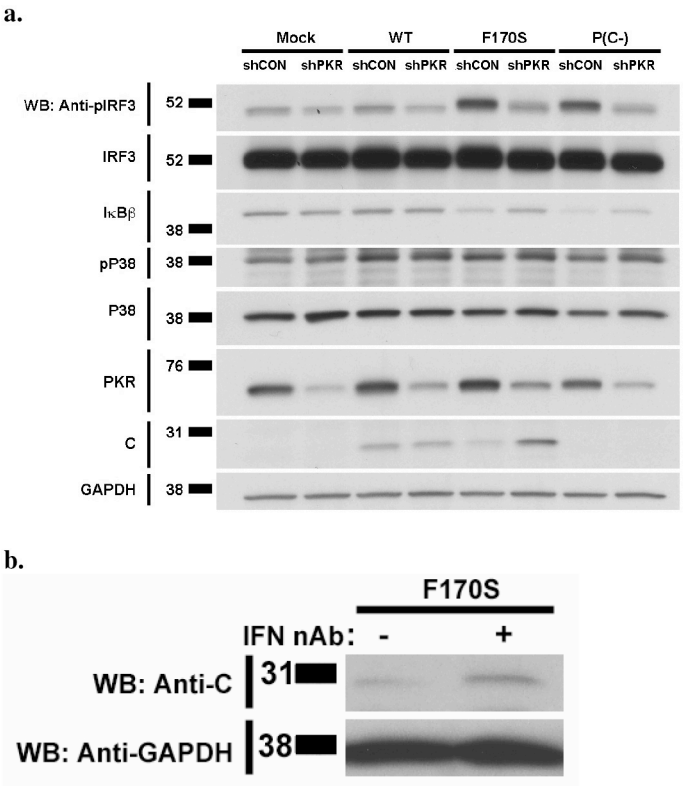

Discussion

We had previously demonstrated that infection with C mutant HPIV1s (F170S and P(C-)), but not WT HPIV1, effectively stimulated IFNβ production in epithelial cells (192). F170S, but not WT, HPIV1 triggered IRF3 dimerization and nuclear translocation, indicating that the wild-type C proteins block the activation of IRF3 (192). In the present study, the mechanisms by which the C proteins prevent IFNβ induction were explored in more detail. Since IFNβ production is induced optimally by the assembly of an enhanceosome comprised of IRF3, NF-κB, and AP-1 at the IFNβ promoter, the activation of these transcription factors during HPIV1 infection was examined first. Infection with HPIV1 containing a single point mutation in C (F170S) or lacking expression of the C proteins (P(C-)) triggered IRF3 and NF-κB activation, whereas WT HPIV1 inhibited activation of these two critical components of the IFNβ enhanceosome. Although crystal structures of ATF-2 and c-Jun bound to PRD IV of the IFNβ promoter are known, their contribution to the induction of a type I IFN response is less well understood (142). ATF-2 and c-Jun can be phosphorylated and activated by P38 and JNK; however, we found that WT, F170S, and P(C-) HPIV1 did not induce P38 phosphorylation or ATF-2 phosphorylation.

Numerous examples of viral proteins that antagonize IFNβ production by interacting with various proteins in the RIG-I/MDA5 pathway have been described (19). For instance, the influenza NS1 protein inhibits RIG-I activation by binding to TRIM25 and the hepatitis C NS3/4A protease cleaves and inactivates MAVS (44, 116). In this context, we initially hypothesized that the HPIV1 C proteins acted to inhibit IFNβ production by binding or

otherwise interfering with one or more components of the RIG-I/MDA5 pathway. Surprisingly, however, several observations made during the present study speak against this hypothesis. First, we were unable to immunoprecipitate the HPIV1 C proteins with any of the known members of the RIG-I/MDA5 pathway that we examined. In addition, we did not observe a significant decrease in abundance or a shift in the gel mobility of any of these host proteins, suggesting that the C proteins do not promote their modification or degradation. Finally, the HPIV1 C proteins, supplied in trans, failed to block IFNβ induction by two heterologous inducers, RSV and poly I:C, which are known to signal through RIG-I and MDA5, respectively. Specifically, while infection with WT HPIV1 was able to efficiently block IFNβ induction in response to a super-infection with P(C-) HPIV1, it was unable to do so against super-infection with a RSV mutant that does not express the RSV NS1 and NS2 IFN antagonist proteins (**Fig. 2a**). Similarly, expression of the C proteins in an inducible cell line was able to efficiently block IFNβ induction in response to super-infection with P(C-) HPIV1, but failed to prevent poly I:C-induced MDA5-mediated IFNβ expression (**Fig. 2b, c**). The inability of the HPIV1 C proteins to prevent induction in response to these heterologous inducers suggested that they do not antagonize the components of the IFN production pathway at or downstream of RIG-I and MDA5. On the other hand, the ability of the C proteins to inhibit IFNβ induction in the context of an HPIV1 infection suggested that their effect is specific to HPIV1.

Because the C proteins appeared to disrupt type I IFN production without interacting with key members of the RIG-I/MDA5 pathway, we wanted to confirm that IFNβ induction by

C mutant HPIV1 viruses did indeed depend on this pathway. Using murine knockout cells, we found that knockout of TBK1 and IKKε completely ablated the IFNβ response to F170S and P(C-) HPIV1 infection, confirming that the RIG-I/MDA5 pathway mediates IFNβ production for these two viruses. In addition, it was found that IFNβ induction relied more strongly on MDA5 than on RIG-I. This is in contrast to the original suggestion that recognition of paramyxovirus infection depends mainly on RIG-I whereas MDA5 is dispensable (67, 98, 119, 179). Several more recent studies with SeV indicated that both RIG-I and MDA5 can contribute to IFNβ production *in vitro* or to resistance *in vivo* (53, 217). However, these previous findings cannot be readily extrapolated to HPIV1, because SeV, but not HPIV1, also expresses a V protein, a known inhibitor of MDA5 (3, 22, 53, 179, 217). Since MDA5 primarily recognizes long dsRNA molecules (or, more specifically, webs of dsRNA and ssRNA (148)), its involvement in IFNβ expression during infection with F170S and P(C-) HPIV1 implied that dsRNA was involved.

A striking abundance of cytoplasmic dsRNA was observed in both F170S- and P(C-)-, but not WT-, infected cells. Earlier studies had reported large amounts of dsRNA after infection with positive-strand RNA viruses, double-strand RNA viruses, and DNA viruses but not with negative-strand RNA viruses (113, 177, 199, 201). However, more recently, dsRNA accumulation was detected in cells infected with a C deletion mutant of SeV (181). We did not detect appreciable amounts of dsRNA after infection with WT HPIV1, consistent with expectations (62). In contrast, infection with the P(C-) mutant that completely lacks C expression led to a relatively rapid accumulation of cytoplasmic

dsRNA that was readily detected by 24 h but subsequently decreased, and infection with the F170S virus that makes a mutated C protein led to a relatively slower accumulation of dsRNA that was detected in only a few cells at 24 h but increased substantially by 48 h. Thus, HPIV1, a negative-strand RNA virus, does indeed have the capacity to produce dsRNA, and functional C proteins are required during infection to prevent the accumulation of dsRNA that would otherwise trigger a potent host innate antiviral response.

The appearance of dsRNA was temporally associated with the activation of PKR, which in turn was associated with a reduction in viral protein accumulation. Infection by P(C-) and F170S HPIV1 was accompanied by autophosphorylation of PKR, phosphorylation of EIF2A, and decreased accumulation of the N, P, and C (in F170S-infected cells) proteins. C protein expression in F170S-infected cells was robust at 24 h but diminished at 30 h and was difficult to detect from 36 h onwards. PKR knockdown studies indicated that PKR is a major contributor to the loss of C^{F170S} from 24 h post-infection onwards. The decrease in C protein synthesis late during infection would render the F170S HPIV1 infection functionally similar to a P(C-) HPIV1 infection, i.e. yield a virus unable to accumulate needed amounts of C protein, and this gradual loss of C proteins in F170S HPIV1 infection accounts for the difference in the kinetics of dsRNA formation between these two mutants. In addition to its role in inhibiting translation during viral infection, PKR has also been implicated in NF-κB activation, IRF1 activation, and IFN induction by poly I:C via MAVS, effects that are independent of its kinase activity and that provide another mechanism of innate antiviral host defense mediated by PKR (4, 16, 25, 107,

124, 209, 218). Infection with SeV lacking the entire C gene led to the generation of a large amount of dsRNA with subsequent PKR activation and inhibition of translation (181). In addition, infection with a measles virus mutant lacking the C gene required PKR for maximal IFNβ induction (125). Our data indicated that PKR contributed significantly to the induction of IFNβ and, more specifically, IRF3 phosphorylation following infection with HPIV1 mutants that generated dsRNA. Thus, MDA5 and PKR each contribute to the generation of IFNβ during infection with C mutant HPIV1s, and the generation of dsRNA in F170S- and P(C-)-infected cells is the likely trigger for these two RNA sensors.

To investigate the mechanisms underlying the generation of dsRNA during infection with the HPIV1 mutants, we monitored viral RNA levels in infected A549 cells. Compared with WT-infected cells at 24 h post-infection, cells infected with the P(C-) mutant had greatly increased accumulation of genomic and anti-genomic RNA and viral mRNA. Similar findings were made for the F170S mutant, although the increases in viral RNA accumulation were delayed, consistent with the observed delay in dsRNA accumulation compared to the P(C-) mutant. These results indicate that deletion or mutation of the HPIV1 C proteins resulted in a substantial perturbation of viral RNA synthesis. We suggest that the increased accumulation of genomic and anti-genomic RNA in the context of reduced availability of N and P protein led to unencapsidated RNAs that could anneal with each other or with excess viral mRNA to form dsRNA. The C proteins of SeV have been previously implicated in inhibiting viral RNA synthesis and regulating the balance between genome and anti-genome levels (33, 80, 81). Interestingly, one study reported

that infection of primate LLC-MK2 and Vero cells with a C deletion SeV led to a predominance of anti-genomic RNA compared to genomic RNA and to an increase in viral protein synthesis (81). In contrast, our results differ in two ways: first, the accumulation of viral proteins was decreased rather than increased, and, second, deletion of the HPIV1 C proteins did not alter the ratio of viral genomic RNA to anti-genomic RNA. These findings suggest that the HPIV1 C proteins prevent the host innate response by modulating the production of viral RNA rather than directly inhibiting the RIG-I/MDA5 pathway. These results also may provide an alternative explanation for the observation that a recombinant SeV expressing HPIV1 C in place of SeV C failed to block IRF3 activation in murine cells (22). This originally was interpreted to indicate that the respirovirus C proteins, like the rubulavirus V protein, is a determinant of host range (22). However, it may be that the HPIV1 C proteins do not function efficiently in the context of the heterologous SeV N, P, and L proteins to prevent the accumulation of dsRNA and subsequent IRF3 activation.

It is not clear whether PKR- and IFNβ-induced inhibition of protein synthesis can fully account for the reduced accumulation of viral proteins during infection with the HPIV1 mutants. For example, in cells infected with the F170S mutant, the levels of N and P protein were reduced compared to WT-infected cells even at 24 h, a time point before the activation of PKR was detected. Also, while the extremely high accumulation of genomic and anti-genomic RNA with the P(C-) mutant could be imagined to outpace the synthesis of N and P protein and thus initiate the dsRNA formation resulting in PKR activation and IFNβ induction, this seemed less likely for the F170S mutant, since the

increase in RNA accumulation was more gradual. Thus, there may be an additional host inhibitory effect on viral protein accumulation that is unleashed by deletion/mutation of the C proteins or, alternatively, the C proteins may have a positive effect on viral protein synthesis. Further studies to explore these two alternative mechanisms of regulating viral protein synthesis are clearly needed.

Our results indicate that the wild-type C proteins regulate viral RNA synthesis to prevent the production of dsRNA that would otherwise activate MDA5 and PKR which, in turn, would activate IRF3 and NF-κB, result in the induction of IFNβ, and inhibit protein synthesis. We propose that the following series of events occur during infection with P(C-) HPIV1 (summarized in **Table 1**). dsRNA is generated early, within the first 24 h of infection, due to the combined rapid increase of mRNA, genomic RNA, and anti-genomic RNA. The dsRNA activates PKR and also induces IFNβ. PKR activation and IFNβ induction decrease viral protein synthesis, thereby maintaining low levels of N protein. IFNβ might also inhibit protein synthesis by the induction of inhibitors such as IFIT1 and IFIT2 (187). In addition, apoptosis is activated early in P(C-)-infected cells, but the mechanism underlying this induction remains undefined (9). The combined effects of PKR activation, IFNβ induction, and the initiation of apoptosis are likely responsible for the peak and subsequent decline in viral macromolecular synthesis observed between 24 and 48 h after infection with P(C-) HPIV1. The events occurring during infection with the F170S mutant represent a delayed version of what is observed following infection with P(C-) HPIV1. The more gradual increase in transcription and replication of viral RNA in F170S-infected cells delays the formation of dsRNA until

between 24 and 48 h, at which time PKR is activated and IFNβ is induced. The PKR-mediated loss of C protein accumulation in F170S-infected cells likely contributes to the increase of transcription seen at 48 h since C is an inhibitor of viral transcription. A more detailed analysis of the kinetics of viral and host cell RNA and protein synthesis in WT and C mutant HPIV1-infected cells is clearly needed to test the above hypotheses.

Table 1. Summary of C' protein expression, PKR activation, dsRNA accumulation, and IFNβ induction in WT- and C mutant-infected A549 cells

	WT				F170S				P(C-)			
Time (h)	C' Protein	PKR Activation	dsRNA	IFNβ mRNA	C' Protein	PKR Activation	dsRNA	IFNβ mRNA	C' Protein	PKR Activation	dsRNA	IFNβ mRNA
6	-	-	-	-	-	-	-	-	-	-	-	-
12	+	-	-	-	+	-	-	-	-	-	-	-
24	+	-	-	-	+	+	+	++	-	+++	+++	+++
48	+	-	-	+	-	+++	+++	+++	-	+++	+	+++

In summary, our initial working hypothesis that the HPIV1 C proteins inhibit IFNβ induction via a direct inhibition of the RIG-I/MDA5 pathway was not confirmed. Instead, we found that the HPIV1 C proteins regulate viral RNA synthesis to prevent the formation of dsRNA that otherwise triggers host antiviral responses, such as PKR activation and IFNβ induction. MDA5 was found to be a more important sensor than RIG-I for infection with these dsRNA-generating HPIV1 mutants. The kinetics of dsRNA accumulation and decreased expression of mutant C proteins suggest that a race between the evasion of host antiviral responses and the elimination of viral antagonists of dsRNA accumulation is key in determining the outcome of HPIV1 infections.

General Conclusion

HPIV1 was first discovered by Robert Chanock in 1959, but, after over 50 years, it remains an uncontrolled respiratory pathogen that continues to plague infants, children and even adults, in particular the elderly, nursing home residents, and the immunocompromised (23, 29). There are currently no antiviral agents with proven efficacy against HPIV1. Instead, the management of croup and other more severe manifestations of lower respiratory disease caused by HPIV1 is merely supportive. Furthermore, although vaccine development began in the 1960s, there is currently no licensed vaccine against HPIV1 (24, 133). To date, non-living inactivated and subunit vaccines have failed to confer protection against upper and lower respiratory disease in humans and none are currently in clinical trials (24, 43, 133). However, two live-attenuated vaccine candidates against HPIV1 are currently being tested in phase 1 clinical trials. One candidate is an unmodified Sendai virus that is administered intrasnasally as a HPIV1 vaccine (171). The only other vaccine candidate against HPIV1 (rHPIV1-$C^{R84G/\Delta 170}$ HN^{T553A} L^{Y942A}) was developed by this lab using reverse genetics (7). The polymerase mutation L^{Y942A} was first identified in HPIV3*cp*45 and confers a temperature-sensitive phenotype so that virus replication is permissive in the cooler upper respiratory tract but restricted in the warmer lower respiratory tract (126). This HPIV1 mutant virus was restricted in replication by ≥ 100-fold compared to WT HPIV1 when the temperature was increased from 32°C to 39°C, the viral shut-off temperature (7). The other attenuating mutations, C^{R84G} and $C^{\Delta 170}$, each interfere with the virus' ability to antagonize the host antiviral response (192). Although the HPIV1 C proteins are non-essential for viral replication *in vitro*, complete ablation of C protein expression results in a virus that

barely replicates in non-human primates and is over-attenuated as a vaccine candidate (9). However, the C proteins can be mutated by reverse genetics to incrementally attenuate HPIV1 in order to develop vaccine candidates that possess an acceptable balance between attenuation and immunogenicity (9). The C proteins are important virulence factors that play a key role in modulating the host response to HPIV1 infection. In the studies described here, we sought to examine the mechanisms by which the wild-type HPIV1 C proteins prevent a potent innate antiviral immune response and to investigate the mechanisms by which mutating or deleting the C proteins leads to attenuation.

To address these questions, we first created by reverse genetics a virus named P(C-) HPIV1 in which expression of the C proteins was silenced. We found that the complete lack of C protein expression significantly restricted viral replication and induced type I IFN production during infection. Using microarray-based transcriptional profiling, we found that the C proteins controlled the transcription of a broad array of genes in human respiratory epithelial cells. Additionally, we found that the global gene expression profile induced during infection with F170S HPIV1 was surprisingly similar to P(C-) HPIV1. We applied a bioinformatics analysis and identified a significant over-representation of IRF and NF-κB binding sites among many of the C protein-responsive genes. We also determined that the main components of the type I interferon (IFN) response activated upon infection with the C mutant HPIV1 viruses indeed consisted of IRF3 and NF-κB. We initially hypothesized that the C proteins might interact with a host factor in the RIG-I/MDA5 pathway to prevent IRF3 and NF-κB activation and IFNβ induction during

infection with WT HPIV1. Numerous examples of viral proteins that antagonize IFNβ production by this very mechanism had previously been described. For instance, the influenza NS1 protein inhibits RIG-I activation by binding to TRIM25 and the hepatitis C NS3/4A protease cleaves and inactivates MAVS (44, 116). Thus, we attempted to search for a host factor in the RIG-I/MDA5 pathway that might also interact with the C proteins. However, we made two key observations that contradicted this initial hypothesis. First, we were unable to immunoprecipitate the HPIV1 C proteins with any of the known members of the RIG-I/MDA5 pathway that we examined. Additionally, the HPIV1 C proteins, supplied in trans, failed to block IFNβ induction by two heterologous inducers, RSV and poly I:C, which are known to signal through RIG-I and MDA5, respectively. The inability of the HPIV1 C proteins to prevent IFNβ induction in response to these heterologous inducers suggested that they do not antagonize the components of the IFN production pathway at or downstream of RIG-I and MDA5. On the other hand, the ability of the C proteins to inhibit IFNβ induction in the context of an HPIV1 infection suggested that their effect was specific to HPIV1.

Even though the C proteins did not appear to interfere with the signaling pathway leading from RIG-I/MDA5 activation to IFNβ induction, we sought to determine whether the IFNβ induced during infection with the HPIV1 C mutant viruses occurred through the RIG-I/MDA5 pathway. With the use of knockout MEFs, we discovered that IFNβ induction by infection with the HPIV1 C mutant viruses relied mainly on MDA5. As a result, we began to suspect that HPIV1-induced IFNβ expression might also involve dsRNA, the substrate for MDA5 activation. We decided to test for the presence of

dsRNA in cells infected with the HPIV1 C mutants, even though previous reports suggested that dsRNA was absent in cells infected with other negative sense RNA viruses, including influenza, La Crosse, Sendai, and Newcastle disease (199). To our surprise, we discovered a striking accumulation of dsRNA in response to infection with the HPIV1 C mutants. We then began to explore the mechanisms by which the C proteins of WT HPIV1 suppress the accumulation of dsRNA by examining viral RNA and protein synthesis. We were surprised to find that infection with viruses in which C protein function was compromised led to increased levels of viral RNA species and decreased N protein levels, creating an imbalance between the N protein-to-genomic RNA ratio and thereby potentially permitting dsRNA accumulation. The formation of dsRNA would then trigger MDA5 activation and IFNβ production and also PKR activation and an inhibition of further protein synthesis (**Figure 1**).

Figure 1. Diagrammatic representation of the steps leading to dsRNA accumulation and activation of the MDA5 and PKR pathways during infection with P(C-) HPIV1 but not with WT HPIV1. The red lines represent the negative sense viral genome and the blue lines represent the positive sense viral antigenome or viral mRNA. On the left panel, WT HPIV1 attaches, enters, and introduces its negative sense genome into the cytoplasm of the infected cell. The antigenome serves as a template for the production of more genome and mRNA. The mRNAs are translated by the ribosome to produce viral proteins, including the C proteins and the N proteins. Encapsidation by the N protein shields genomic and antigenomic RNAs from recognition by intracellular sensors of dsRNA. As a result, the dsRNA binding proteins MDA5 and PKR which are present

constitutively at low levels in the cytoplasm remain latent, the transcription factors IRF3 and NF-κB remain in the cytoplasm and do not induce IFNβ expression, and EIF2A does not inhibit translation. On the right panel, the absence of C proteins during P(C-) HPIV1 infection leads to dysregulated viral RNA synthesis, i.e. increased production of negative sense genome and positive sense antigenome and mRNA. The formation of dsRNA webs (symbolized by a spider web) triggers MDA5 and PKR activation. MDA5 activates the transcription factors IRF3 and NF-κB and induces IFNβ expression. PKR activates EIF2A which inhibits the translation of viral mRNAs and may limit the amount of N protein available to encapsidate the genome and antigenome. The increase in viral RNA levels in the context of decreased N protein levels would further amplify the formation of dsRNA and the activation of the IFNβ enhanceosome.

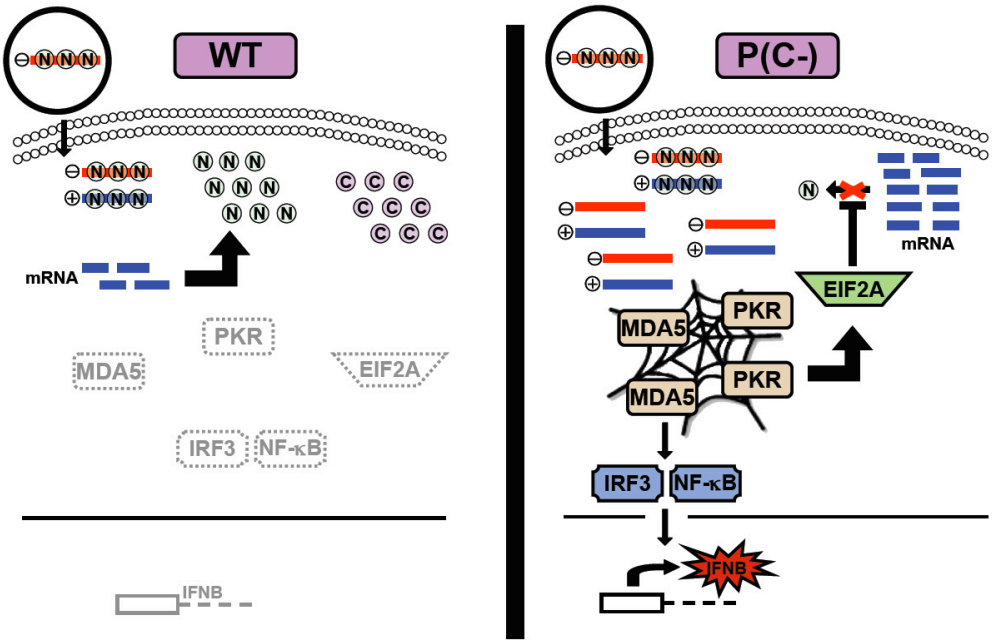

The N protein has long been thought to function as a highly stable and ribonuclease resistant nucleocapsid coat that protects the viral genome and antigenome from nuclease digestion (100). In the present study, we also found an association between the amount of N protein present and the accumulation of dsRNA. HPIV1 genome replication and mRNA transcription are normally tightly coupled to the amount of available N protein to allow sufficient encapsidation of the genome and antigenome, and this process may become dysregulated in the absence of the C proteins. The exact molecular mechanisms by which the HPIV1 C proteins maintain a balance between N protein levels and viral RNA synthesis to prevent the formation of immunostimulatory dsRNA remain to be determined. The C proteins of murine PIV1 (SeV) were found to inhibit viral mRNA transcription in an *in vitro* transcripton system in which the P and L proteins are combined with RNA templates (33, 97, 110). Furthermore, the SeV C proteins suppressed viral RNA synthesis from defective-interfering genomes in a promoter-specific manner (21). In particular, ablation of C protein expression during SeV infection led to a disproportionate increase in positive sense antigenomic RNA compared to negative sense genomic RNA (81). Thus, it was postulated that a ratio of genomic to antigenomic RNA skewed towards greater levels of positive sense antigenomic RNA was a potential catalyst for dsRNA formation (81). However, we found that, for HPIV1, deletion of the C proteins increased viral RNA synthesis but did not alter the ratio of viral genomic to antigenomic RNA. We also observed decreased levels of viral protein, including N protein, during infection with P(C-) HPIV1. Importantly, an infection with HPIV1 that does not express the C proteins induces the formation of dsRNA which triggers PKR and EIF2A activation and inhibits protein synthesis. This suggests that the

extremely rapid and high accumulation of viral RNA might outpace the synthesis of N protein thereby triggering and further amplifying dsRNA formation. Notably, one report has suggested that the SeV C proteins suppress viral RNA synthesis via an interaction with the L polymerase (75). We have found preliminary evidence that the C proteins co-localize with the N protein but not the P protein in cells infected with WT HPIV1 (not shown). Whether the HPIV1 C proteins interact with and alter the function of the viral replication complex or with an as yet unidentified host factor remains to be seen. The proximity of the C proteins to the N and L proteins may serve an important role in coupling viral RNA synthesis with encapsidation.

The study of the HPIV1 C proteins has yielded unexpected insights into how HPIV1 can cause disease in children. A better understanding of the mechanisms by which the C proteins control the balance between RNA and protein synthesis and interfere with innate immunity will require further study. In summary, the HPIV1 C proteins are clearly multifunctional and much work to define their functions remains to be done. However, significant progress has been made in the understanding of HPIV1 pathogenesis and in the development of a safe and efficacious vaccine against HPIV1.

Appendices

Supplementary Information for Chapter 3

Figure S1. Venn diagram comparison of the 2421 genes and the 1600 genes significantly differentially expressed compared to mock during C^{F170S} infection or P(C-) infection, respectively. Table 1 shows the expression of 10 representative genes from this Venn diagram that were not shared between the two C mutant infections. The expression of the majority of genes did not differ.

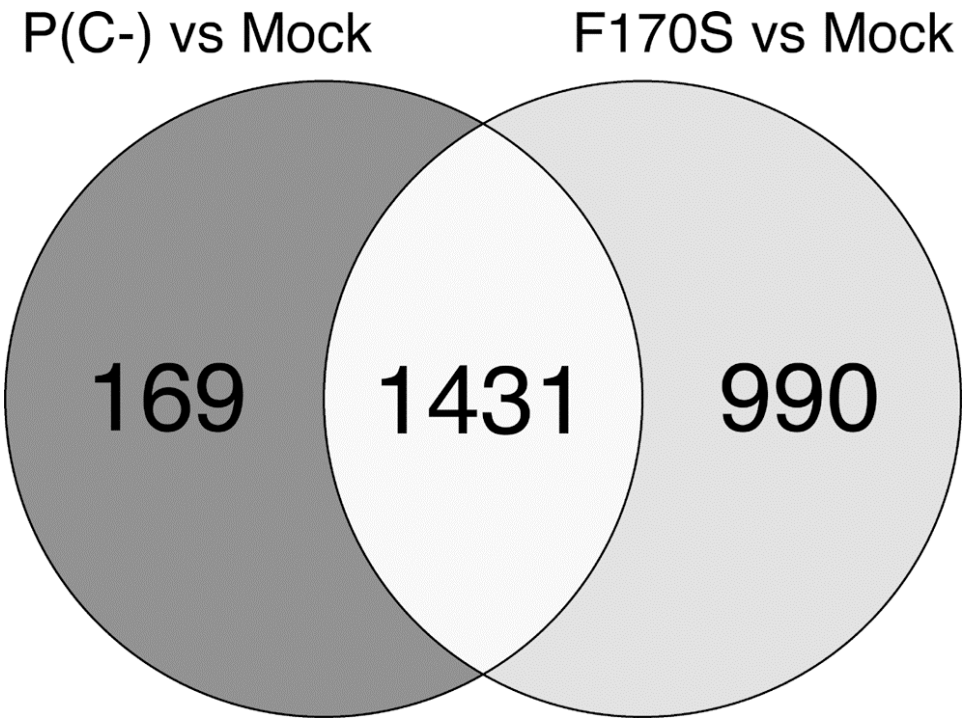

Figure S2. Principal component analysis of experimental conditions using all genes on the microarrays and mean centering to examine the level of similarity between each condition. Each point represents a specific condition (virus and time point post-infection). The distance between points indicates the level of similarity between the conditions based on the expression of all genes on the array. All genes were included in this analysis so that this analysis is not biased by any specific fold change or statistical selection criteria. The axes are eigenvectors, and the first eigenvector (x-axis) passes through the mean, minimizes the sum squared error for each point, and describes the direction of maximum variance. The eigenvalues represent the level of variance for each eigenvector. Overall gene expression during P(C-) and C^{F170S} infection was highly similar. Both C mutant viruses induced gene expression patterns that were significantly different compared to WT infection.

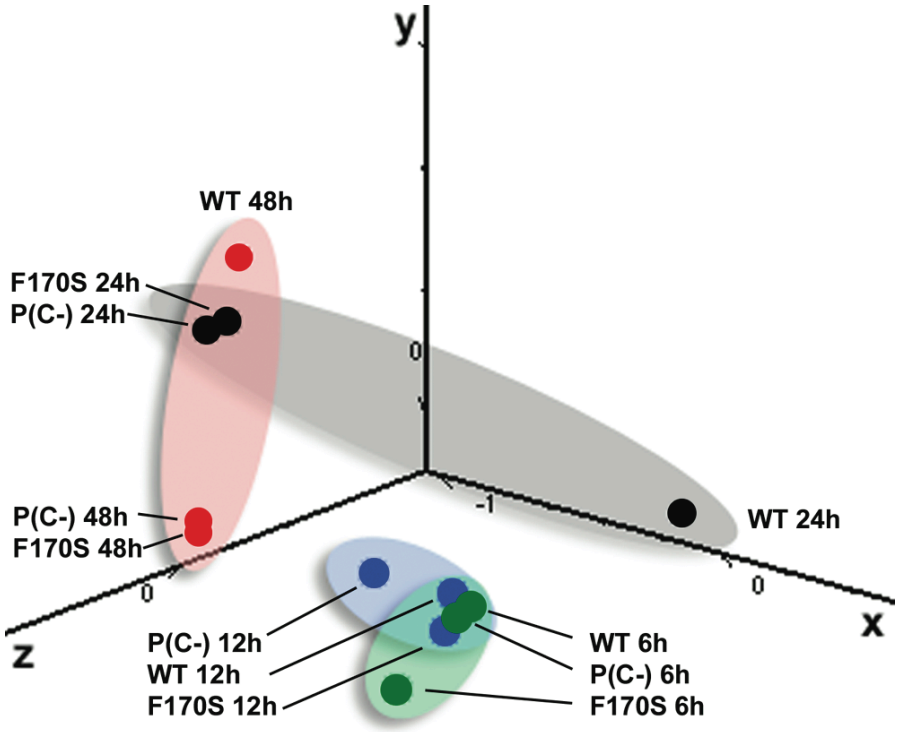

Figure S3. Hierarchical clustering and functional analysis of 28 genes that differed between the two C mutants by 2-fold followed by $P < 0.01$ with multiple testing correction.

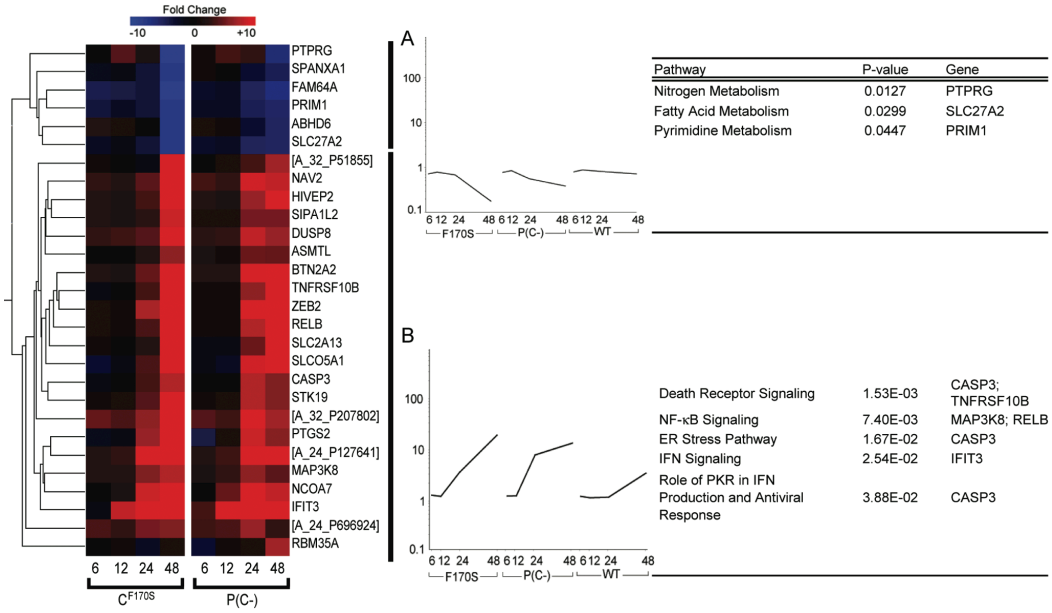

Pathway	P-value	Gene
Nitrogen Metabolism	0.0127	PTPRG
Fatty Acid Metabolism	0.0299	SLC27A2
Pyrimidine Metabolism	0.0447	PRIM1

Death Receptor Signaling	1.53E-03	CASP3; TNFRSF10B
NF-κB Signaling	7.40E-03	MAP3K8; RELB
ER Stress Pathway	1.67E-02	CASP3
IFN Signaling	2.54E-02	IFIT3
Role of PKR in IFN Production and Antiviral Response	3.88E-02	CASP3

Figure S4. Differential gene expression between C^{F170S} and P(C-) infection of A549 cells. An alternative analysis identified 18 genes by a two-way ANOVA with multiple testing correction (see **Table S7**) that were significantly different between the two C mutant viruses. Expression ratios between C^{F170S} and P(C-) for these 18 genes were plotted on a $\log_2$ scale to give a visual representation of the kinetics and magnitude of any differences in the transcriptional response between the two C mutant viruses. A ratio of 0 indicates that there is no difference, negative values indicate that the expression with C^{F170S} is lower compared to P(C-), and positive values indicate that the expression with C^{F170S} is higher compared to P(C-). The dotted lines denote a 4-fold difference. The majority of genes were only different by slightly greater than 4-fold. However, a kinetic shift in the transcriptional profile can be observed after 24 h p.i. Up to 24 h p.i., gene expression during C^{F170S} infection is, in general, lower than that during P(C-) infection. These differences do not persist at 48 h p.i., and both viruses approach equivalent expression for this set of genes. However, a small but distinct set of genes appears at 48 h p.i. in which gene expression during C^{F170S} infection is, in general, now greater than that during P(C-) infection.

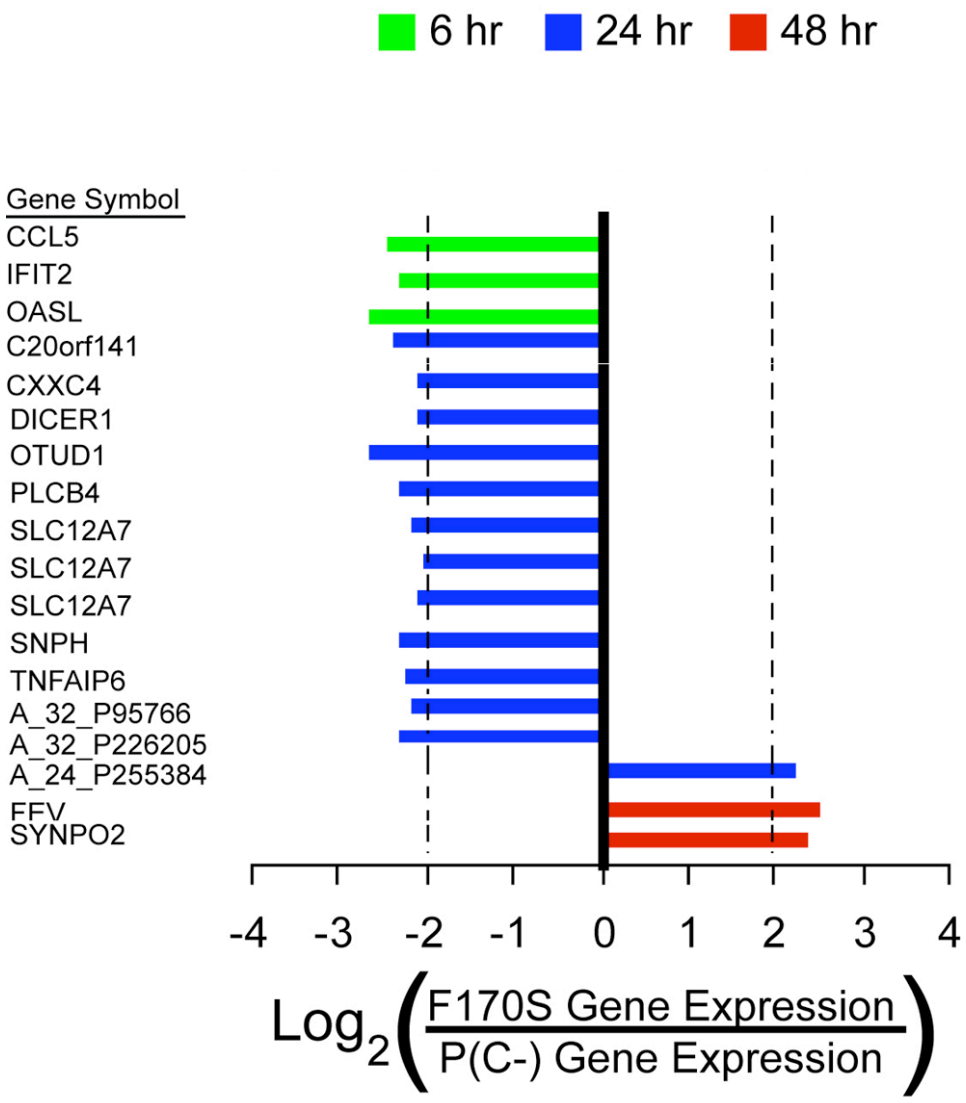
6 hr
24 hr
48 hr
Gene Symbol
CCL5
IFIT2
OASL
C20orf141
CXXC4
DICER1
OTUD1
PLCB4
SLC12A7
SLC12A7
SLC12A7
SNPH
TNFAIP6
A_32_P95766
A_32_P226205
A_24_P255384
FFV
SYNPO2
-4
-3
-2
-1
0
1
2
3
4
Log2(F170S Gene Expression / P(C-) Gene Expression)

Figure S5. Replication of wt HPIV1, C^{F170S}, and P(C-) in A549 cells. A549 cells were inoculated with sucrose purified viruses at a MOI of 5 $TCID_{50}$/cell and supernatant was harvested for virus quantitation at 0, 6, 12, 24, and 48 h p.i. Photomicrographs taken at 48 h p.i. show more extensive cytopathic effect in P(C-) infected A549 cells than in wt HPIV1 or C^{F170S} infected cells.

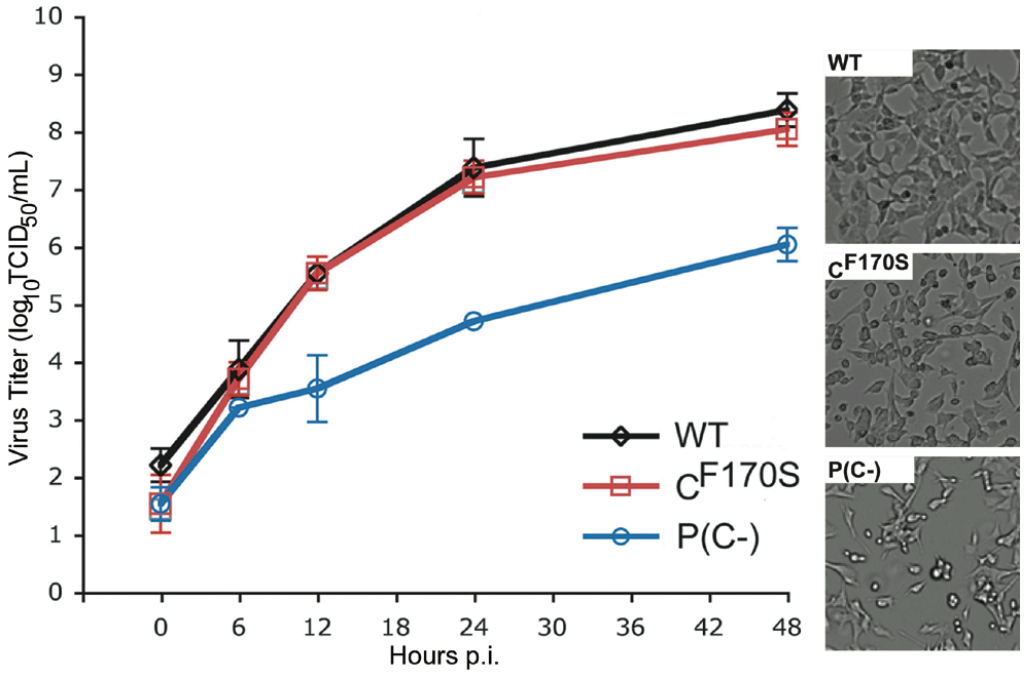

Figure S6. Gene expression profiles for all 14 transcription factors identified by bioinformatics analysis. The expression of 4 genes IRF1, ISGF3G, NF-κB1, and c-Rel highlighted in yellow was significantly up-regulated increasingly over time.

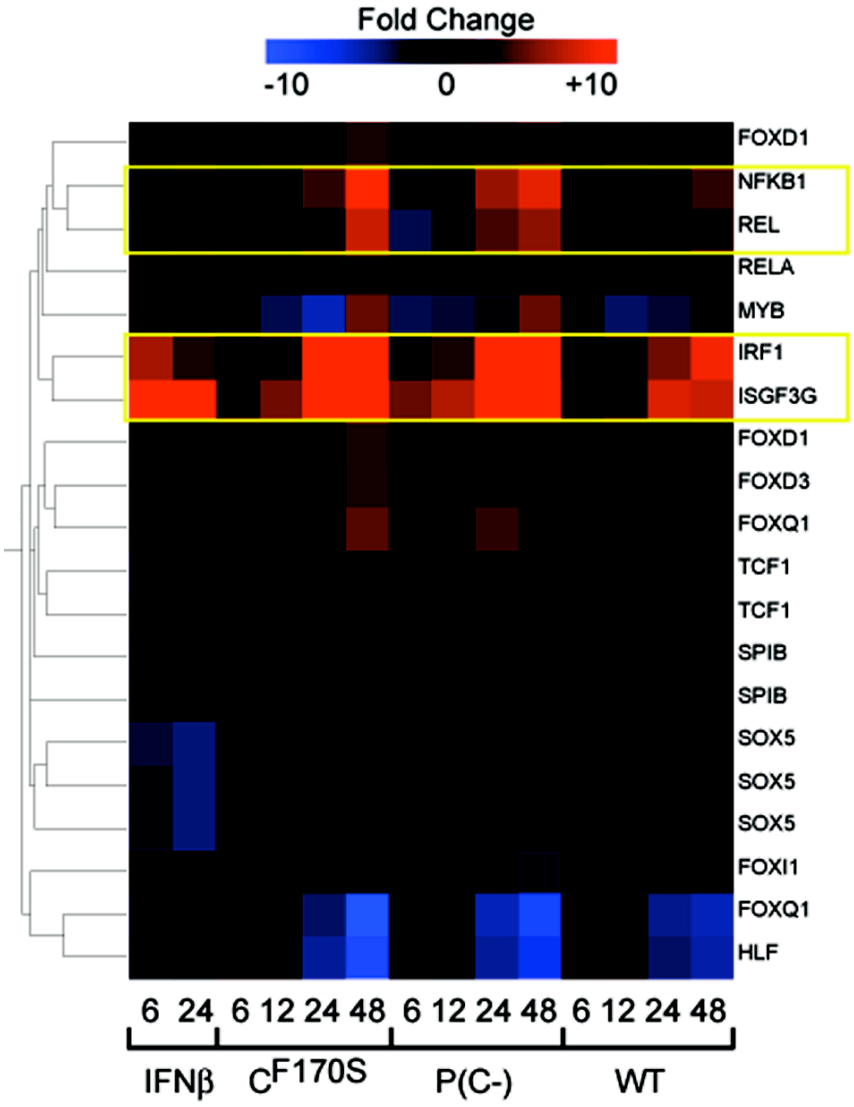

Table S1.

Table S1. Genes differentially expressed by wt HPIV1 or IFNβ compared to mock infection*†

Cluster‡	Symbol	Product	Agilent	IFN 6 hr	IFN 24 hr	WT 6 hr	WT 12 hr	WT 24 hr	WT 48 hr
A	APOL1	apolipoprotein L1 isoform b precursor	A_24_P87931	6.7	7.6	1.6	1.7	4.2	8.1
	APOL4	apolipoprotein L4 isoform 1	A_23_P380857	6.2	7.9	1.4	1.7	5.1	7.2
	APOL6	apolipoprotein L, 6	A_24_P941167	8.6	8.3	1.5	1.7	6.3	9
	APOL6	apolipoprotein L6	A_23_P155052	13.5	7.2	0.9	1	2.2	6
	APOL6	apolipoprotein L6	A_23_P155049	8.1	6.8	1.1	0.9	4.3	8.5
	APOL6		A_24_P7594	7.3	10.3	0.9	1.5	6.8	11.3
	B2M	beta-2-microglobulin precursor	A_23_P37441	1.7	5.5	0.7	0.7	1.4	4.6
	BATF2	basic leucine zipper transcription factor, ATF-like 2	A_23_P370682	8.8	14.8	0.9	1.1	3.3	8.3
	BST2	bone marrow stromal cell antigen 2	A_23_P39465	8.2	21.5	1.3	2.6	3.5	10.6
	BTC	betacellulin	A_23_P135722	2.3	5	1.5	1.4	1.4	2.7
	C15orf48	hypothetical protein LOC84419	A_23_P26024	1.6	3.6	0.9	1.1	1.4	4.8
	C1orf38	basement membrane-induced gene isoform 1	A_23_P873	14.2	16.6	1.2	1.5	2.1	3.6
	CASP1	caspase 1 isoform alpha precursor	A_23_P202978	6.2	46.2	0.8	0.9	6.3	17.1
	CD38	CD38 antigen	A_23_P167328	1.4	6	0.8	1.1	1.3	5.4
	CEACAM1	carcinoembryonic antigen-related cell adhesion molecule 1 isoform 1 precursor	A_24_P382319	20.4	15.5	1.3	1.7	6.4	13.6
	CEACAM1	carcinoembryonic antigen-related cell adhesion molecule 1 isoform 2 precursor	A_23_P434118	2.8	4.6	0.9	1	3	7.9
	CFB	complement factor B preproprotein	A_23_P156687	3	7.9	0.6	0.8	1.7	6.2
	CTSS	cathepsin S preproprotein	A_23_P46141	2.1	4.4	0.9	1.1	1.4	3.3
	DDX58	DEAD/H (Asp-Glu-Ala-Asp/His) box polypeptide RIG-I	A_23_P20814	28.7	32	1.3	1.6	4.1	27.3
	DTX3L	deltex 3-like	A_24_P941912	6.1	7.1	0.8	1	2.7	4
	DTX3L	deltex 3-like	A_23_P347040	9.8	8.6	0.9	1	2.1	4.1
	EIF2AK2	eukaryotic translation initiation factor 2-alpha kinase 2	A_23_P142750	2.7	5.5	1.1	1.1	1.1	1.5
	EMR1	egf-like module containing, mucin-like, hormone receptor-like sequence 1	A_23_P27556	1.3	5.2	0.7	1.1	1.4	2.9
	EXOC3L	exocyst complex component 3-like	A_23_P424734	1.3	4.5	0.9	1.3	1.8	4.9
	GBP1	guanylate binding protein 1, interferon-inducible, 67kD	A_23_P62890	57.4	82.6	1.1	1	14.3	64.2
	GBP1	guanylate binding protein 1, interferon-inducible, 67kD	A_32_P107372	48	41.4	1	1.3	18.1	70.7
	GBP3	guanylate binding protein 3	A_24_P370702	8.4	11.1	1.2	1.1	6.2	14.4
	GBP3	guanylate binding protein 3	A_23_P51487	10.8	17.2	0.6	0.7	8.4	17.6
	GBP4	guanylate binding protein 4	A_24_P45446	7.2	20.1	0.7	1.3	3.4	32.7
	HCP5		A_23_P111126	1	8.2	0.6	1.1	1.4	14.7
	HERC5	hect domain and RLD 5	A_23_P110196	4.3	21.4	0.7	1.5	4.1	40
	HLA-B	major histocompatibility complex, class I, B	A_23_P125107	1.5	5.2	0.8	0.9	1.2	4.2
	HLA-B	major histocompatibility complex, class I, B	A_24_P113674	1.6	4.3	1	0.9	1.2	3.9
	HLA-C	major histocompatibility complex, class I, C precursor	A_24_P298409	1.6	4.6	1.1	1.1	1.3	3.6
	HLA-C	MHC class I antigen	A_23_P95917	1.5	4.6	0.9	0.9	1.3	3.5
	HLA-C		A_23_P113716	1.5	4.3	1.1	1.1	1.3	3.5
	HLA-E	major histocompatibility complex, class I, E precursor	A_32_P460973	2.5	4.3	1	1	1.4	2.5
	HLA-E	major histocompatibility complex, class I, E precursor	A_24_P326082	2.2	4.2	0.8	0.8	1.1	2.8
	HLA-F	major histocompatibility complex, class I, F precursor	A_23_P314024	1.6	5.2	0.9	1	1.3	5.7

HRASLS2	HRAS-like suppressor 2	A_24_P364263	2	6.2	1.1	1.1	1.4	4.2
HRASLS2	HRAS-like suppressor 2	A_23_P105012	2.1	9.8	0.8	1.2	1.9	7.3
HSH2D	hematopoietic SH2 domain containing	A_23_P153372	6	10.6	1	1.2	1.5	3.7
IFI16	interferon, gamma-inducible protein 16	A_23_P160025	11.9	19.3	1	1	1.8	2.9
IFI16		A_23_P217866	11.3	16.7	1.2	1.1	1.6	2.6
IFI27	interferon, alpha-inducible protein 27	A_23_P48513	12.4	20.8	1.1	1.1	2.9	12.3
IFI27	interferon, alpha-inducible protein 27	A_24_P270460	9.8	12.5	1	1.3	2.4	11.3
IFI35	interferon-induced protein 35	A_23_P152782	2.4	7.8	0.8	0.8	1.5	2.1
IFI44	interferon-induced, hepatitis C-associated microtubular aggregate protein	A_23_P23074	50.7	65.1	1	7	16.1	55.2
IFI44L	histocompatibility 28	A_23_P45871	24.6	78.5	1	0.9	2.2	24.5
IFI6	interferon, alpha-inducible protein 6 isoform c	A_23_P201459	14.3	45.5	1	1.4	2.7	10.4
IFIH1	interferon induced with helicase C domain 1	A_23_P68155	16.7	30	1.2	3.3	8	53.8
IFIT1	interferon-induced protein with tetratricopeptide repeats 1 isoform 2	A_23_P52266	32.1	35.9	4.8	14.5	11.2	33.2
IFIT3	interferon-induced protein with tetratricopeptide repeats 3	A_23_P35412	81.5	108.1	0.8	4.1	15.8	73.4
IFIT5	interferon-induced protein with tetratricopeptide repeats 5	A_24_P30194	6.1	6.4	1.1	1.1	1.5	4.3
IFIT5	interferon-induced protein with tetratricopeptide repeats 5	A_23_P63668	5.4	5.5	1.3	1.3	1.5	3.8
IFITM1	interferon induced transmembrane protein 1 (9-27)	A_23_P72737	6.7	8	0.9	1.1	2.3	2.2
IL4I1	interleukin 4 induced 1 isoform 2	A_23_P502520	2.5	7.9	1.3	1	1.3	6.2
INDO	indoleamine-pyrrole 2,3 dioxygenase	A_23_P112026	10.6	39.4	1.1	1	21.3	71
IRF7	interferon regulatory factor 7 isoform d	A_24_P378019	8.4	13.6	1	1.3	2	3.7
ISG15	interferon, alpha-inducible protein (clone IFI-15K)	A_23_P819	13.5	36.9	1.2	3.3	9.9	25.2
ISG20	interferon stimulated gene 20kDa	A_23_P32404	2.2	6.5	0.9	0.9	1.8	8.2
ISGF3G	interferon-stimulated transcription factor 3, gamma 48kDa	A_23_P65442	14.1	11	1.4	1.9	6.9	6.2
LAMP3	lysosomal-associated membrane protein 3	A_23_P29773	7.8	114.5	1.3	1.4	1.8	7.6
LAP3	leucine aminopeptidase 3	A_23_P18604	2.2	5.4	0.5	0.8	1	1.5
LGALS9	galectin 9 long isoform	A_32_P452655	3.2	8.8	1.3	1.2	1.4	2.5
LMO2	LIM domain only 2	A_23_P53126	12.1	9.7	1	0.9	1.1	2.7
MX1	myxovirus resistance protein 1	A_23_P17663	22	30.4	1.3	2.2	7.8	14.4
MX2	myxovirus resistance protein 2	A_23_P6263	18.5	74.3	1.6	1.2	3	5.5
NMI	N-myc and STAT interactor	A_23_P154235	2.7	6.2	0.9	0.8	1.6	3.1
NT5C3	5'-nucleotidase, cytosolic III isoform 2	A_23_P59547	1.7	4.3	0.9	0.9	1.2	1.5
OAS1	2',5'-oligoadenylate synthetase 1 isoform 2	A_23_P64828	5.1	8.8	1	0.9	1.5	4.1
OAS2	2'-5'-oligoadenylate synthetase 2 isoform 1	A_23_P204087	10.5	30	0.7	0.8	1	3.7
OAS3	2'-5'oligoadenylate synthetase 3	A_23_P47955	3.9	17.6	1	1.1	1.7	5.1
OAS3	2'-5'oligoadenylate synthetase 3	A_24_P335305	2.9	10.3	0.8	0.9	1.4	3.5
OASL	2'-5'-oligoadenylate synthetase-like isoform a	A_23_P139786	40.8	49.6	2.4	24.5	33.3	58.9
PARP12	zinc finger CCCH-type domain containing 1	A_23_P111804	4	9.4	1.1	1.1	2	3
PARP14	poly (ADP-ribose) polymerase family, member 14	A_32_P56759	5.2	8	0.7	1.3	3.6	8
PARP14	poly (ADP-ribose) polymerase family, member 14	A_24_P161018	6.5	12.5	1.5	1.3	2.7	7
PARP9	poly (ADP-ribose) polymerase family, member 9	A_23_P69383	10.2	11.3	1.2	1.1	3.8	5.2
PLA1A	phospholipase A1 member A	A_24_P294408	1.9	8.7	0.9	1.2	2.2	5.7
PLA1A	phospholipase A1 member A	A_23_P29816	1.4	5.4	1.2	1.3	1.5	5.3

PLEKHA4	pleckstrin homology domain containing, family A (phosphoinositide binding specific) member 4	A_23_P67360	4.7	8.6	1	1.4	3.6	11.7
PLEKHA4	pleckstrin homology domain containing, family A (phosphoinositide binding specific) member 4	A_24_P408047	3.9	8.9	1.3	1.7	3.9	16.7
PLSCR1	phospholipid scramblase 1	A_23_P69109	3.7	12.6	0.9	0.8	1.1	3.2
PML	promyelocytic leukemia protein isoform 1	A_24_P207139	4.5	5.7	1.3	1	2	1.5
PML	promyelocytic leukemia protein isoform 6	A_23_P306148	2.7	4.1	1	1.2	1.6	1.7
PML	promyelocytic leukemia protein isoform 6	A_24_P198598	2.7	4.5	1	1.2	1.7	1.6
PNPT1	hypothetical protein	A_32_P76035	2.2	5.1	0.8	1.1	1.2	1.2
PNPT1	polyribonucleotide nucleotidyltransferase 1	A_23_P154488	2.4	4.8	0.9	1.1	1.2	1.2
PPM1K	protein phosphatase 1K (PP2C domain containing)	A_24_P214598	2.5	5.7	0.7	0.9	1.4	6.7
PSMB10	proteasome beta 10 subunit proprotein	A_23_P140807	1.5	4.6	1.2	1.2	2.1	4.9
PSMB8	proteasome beta 8 subunit isoform E1 proprotein	A_23_P250629	2.4	6.9	0.8	1	2.1	3.5
PSMB9	proteasome beta 9 subunit isoform 1 proprotein	A_23_P111000	3.1	12	0.6	0.9	3.8	8.8
RARRES3	retinoic acid receptor responder (tazarotene induced) 3	A_23_P1962	2.1	6	1	1.3	4.4	6.9
RASGRP3	RAS guanyl releasing protein 3 (calcium and DAG-regulated)	A_24_P54390	9.8	15.2	0.9	0.8	3.7	3.8
REC8	REC8 homolog	A_24_P344087	5.5	4.9	1.6	2.4	3.9	3.9
RGS22	regulator of G-protein signalling 22	A_32_P125771	2	12.6	1	0.9	1.3	3
SAMD9	sterile alpha motif domain containing 9	A_23_P355244	23	26.9	1	1.1	3.7	14.6
SAMD9	sterile alpha motif domain containing 9	A_24_P175187	42.2	25.2	0.9	1.1	3.5	13.4
SAMD9	sterile alpha motif domain containing 9	A_24_P175188	36.7	37	0.9	1.1	5	12.4
SAMD9L	sterile alpha motif domain containing 9-like	A_23_P145874	35.7	31.7	1.5	1.6	14.5	22.3
SIDT1	SID1 transmembrane family, member 1	A_23_P132515	4.5	9	0.9	1.9	2.7	2.6
SLC15A3	solute carrier family 15, member 3	A_23_P75786	4.9	14.9	0.9	0.8	1.7	7.1
SP100	nuclear antigen Sp100 isoform 2	A_24_P385611	2.9	5	0.8	0.9	1.2	1.9
SP100	nuclear autoantigen	A_24_P916816	5.8	7.1	1.8	1.2	1.9	3.4
SP110	SP110 nuclear body protein isoform b	A_23_P120002	8.8	14.5	1	0.9	1.8	2.2
SP140	SP140 nuclear body protein isoform 1	A_24_P328504	3.7	6.8	1.6	1.1	2	3.4
STAT1	signal transducer and activator of transcription 1 isoform alpha	A_23_P56630	3	8.3	0.6	1	3.7	4.9
STAT1	signal transducer and activator of transcription 1 isoform beta	A_24_P274270	4.6	10.1	0.9	1.5	4.7	5.7
STAT2	signal transducer and activator of transcription 2	A_23_P76090	4.9	3.8	0.9	1.1	2.1	2.5
TAP1	transporter 1, ATP-binding cassette, sub-family B	A_23_P59005	4.8	9.2	1	1.4	3.8	9.3
TGM2	transglutaminase 2 isoform a	A_32_P86763	1.7	4.2	0.6	0.7	1.2	1.5
TLR3	toll-like receptor 3	A_23_P29922	11.9	16.1	0.9	1	5.7	12.7
TMEM140	hypothetical protein LOC55281	A_23_P31177	12.1	8.5	1.2	0.9	3.4	4.4
TMEM140	hypothetical protein LOC55281	A_24_P372134	4.1	3.4	1.2	1	1.2	1.7
TNFRSF14	tumor necrosis factor receptor superfamily, member 14 precursor	A_23_P126908	1.9	6.1	1	0.7	3.1	5.3
TNFSF10	tumor necrosis factor (ligand) superfamily, member 10	A_23_P121253	23.5	20.1	1.2	1.1	2.2	6.9
TNFSF13B	tumor necrosis factor (ligand) superfamily, member 13b	A_23_P14174	6.2	13.1	1	1.2	2.8	4.3
TRIM14	tripartite motif protein TRIM14 isoform alpha	A_23_P425752	1.7	4.6	1	1.2	1.2	1.6
TRIM14	tripartite motif protein TRIM14 isoform alpha	A_23_P216655	2.1	7.3	0.7	1	1.5	2.6
TRIM14	tripartite motif protein TRIM14 isoform alpha	A_24_P197964	2.3	8.7	0.6	1	1.3	2.5
TRIM14	tripartite motif protein TRIM14 isoform alpha	A_23_P334083	1.7	4.6	0.6	0.7	1.2	1.9

	TRIM22	tripartite motif-containing 22	A_23_P203498	16.1	42	0.8	0.9	6.6	19.6
	TRIM34	tripartite motif protein 34 isoform 1	A_24_P398323	2.1	4.1	0.8	0.8	1.5	1.4
	TRIM69		A_24_P50543	4.1	3.8	1	0.7	1.6	2.9
	UBD	diubiquitin	A_23_P81898	6	12.9	1	0.8	3	41.6
	UBE1L	ubiquitin-activating enzyme E1-like	A_23_P21207	3.5	21.8	0.9	0.8	2.7	7.5
	UBE2L6	ubiquitin-conjugating enzyme E2L 6 isoform 2	A_23_P75741	2.8	9.2	0.7	1.1	1.8	2.9
	USP18	ubiquitin specific protease 18	A_32_P132206	5.3	9.2	1.2	1.3	1.7	4.2
	USP18	ubiquitin specific protease 18	A_23_P132159	4.9	9.6	0.9	1	1.5	3.5
	ZNFX1	zinc finger, NFX1-type containing 1	A_24_P23034	5.7	3.2	1	1.2	1.7	3.7
		hypothetical protein	A_32_P161292	2.9	5.4	1.1	1.1	2.8	4.2
		hypothetical protein LOC55337	A_24_P236949	2.3	7.6	0.8	0.8	1.1	1.7
		hypothetical protein LOC55337	A_23_P38894	3.8	9.8	1.4	1.2	1.6	2
		hypothetical protein LOC55601	A_23_P41470	5.1	13.7	0.4	0.8	3	10.7
		hypothetical protein LOC55601	A_24_P334361	5.8	18.1	0.4	0.8	3.9	16.4
		hypothetical protein LOC79132	A_23_P38346	11.8	50.6	1.2	2	6	48.6
		hypothetical protein LOC93349	A_23_P337753	2.8	4.3	0.9	1.1	2.6	3.2
		leukocyte-derived arginine aminopeptidase	A_23_P30243	4.3	4.6	1.1	1.3	3.1	5.8
		promyelocytic leukemia protein isoform 2	A_23_P358944	5.1	4.5	1.4	1.2	1.4	2.3
		Unknown (protein for MGC:105145)	A_24_P418044	1.7	5.4	1	1.1	1.4	4.2
		XIAP associated factor-1 isoform 1	A_23_P4286	65.7	270	1.6	1.4	7.9	77.7
		XIAP associated factor-1 isoform 1	A_23_P4283	52.8	95.9	1.4	0.9	5	38.6
			A_23_P354547	11.5	8.7	1.5	3.1	5.1	5
			A_32_P171793	6.2	12.8	0.9	1.3	4.2	10.5
			A_24_P829156	5.5	4.7	1.5	1.2	3.1	5.1
			A_24_P740662	11.5	8.7	1.6	1.9	7.2	10
			A_24_P127641	5.6	8.3	1.4	1.3	2.9	7.9
			A_23_P384355	63.7	88.6	0.8	1	2.8	24.8
			A_32_P156746	8.1	6.2	1.3	1	2.5	3.5
			A_24_P868905	4.2	12.9	0.9	1.1	1.4	2.3
			A_32_P54553	3.4	5.9	0.6	1	1.3	2.4
			A_23_P65174	2.3	4	1	1	1.5	1.8
			A_23_P30069	4	17.2	0.9	1.2	2.5	4.6
			A_24_P15702	2	4.3	0.5	0.9	1.1	1.4
			A_24_P118892	6.3	11.9	0.7	1.5	1.1	1.9
			A_32_P99533	5.5	10	1.8	2	6.1	21.4
			A_32_P56249	10	18.8	0.9	1	6.2	32
			A_32_P154726	2.6	3.4	0.9	0.9	1.5	4.3
			A_23_P370707	1.7	5.3	0.8	0.9	1.5	6.3
			A_24_P586264	3.3	6.3	0.9	1.2	1.6	8.3
			A_23_P250353	4	11.1	0.9	1.1	2	8.5
			A_24_P68079	4.6	9.3	1	1.1	2.9	7.7
			A_32_P92415	4.1	10	1.3	1.2	2.9	7.9
			A_23_P125109	1.5	5	0.9	1	1.2	4.7
			A_23_P373126	1.8	6.6	0.8	0.9	1.3	6.2
			A_24_P860781	1.5	4.6	0.9	1	1	3.2
			A_32_P143980	2	4.3	1.3	1.1	1.4	3.7
			A_23_P17837	5.3	10.7	1.1	1.8	3.4	7.9
			A_23_P203629	1.5	4.8	1.4	1.1	1.3	2.9
B	APOL2	apolipoprotein L2	A_23_P211488	5.6	2.5	1	1.3	3.6	6

	APOL2	apolipoprotein L2	A_24_P48898	3.7	3.1	1.8	1.8	3.5	5.2
	BTN3A3	butyrophilin, subfamily 3, member A3 isoform a	A_24_P311917	3.7	4.2	1.1	1.2	4.4	5.4
	C20orf141		A_32_P133182	6.2	2.4	1.1	1.1	4.1	13.9
	CA13	**carbonic anhydrase XIII**	**A_23_P381714**	**5.4**	**2.3**	**1.1**	**1.3**	**4.5**	**3.7**
	CCL2	small inducible cytokine A2 precursor	A_23_P89431	1.9	1.2	1	1	1.1	5
	CD274	CD274 antigen	A_23_P338479	3.6	2.7	0.8	1	2	8.2
	CXorf43	hypothetical protein LOC139324	A_23_P386364	2.8	3.7	0.6	0.8	1.8	4.7
	FAS	tumor necrosis factor receptor superfamily, member 6 isoform 1 precursor	A_23_P63896	1.7	1.5	0.6	0.9	1.3	4.4
	GBP5	guanylate-binding protein 5	A_23_P74290	25.7	20.1	1	1.3	16.5	88.5
	HOXB4	homeobox B4	A_24_P416370	2.9	2	1.2	0.9	2.1	5.8
	ICAM1	**intercellular adhesion molecule 1 precursor**	**A_23_P153320**	**4**	**1.8**	**0.7**	**1**	**2.5**	**23.3**
	IFIT2	**interferon-induced protein with tetratricopeptide repeats 2**	**A_23_P24004**	**72.6**	**85.4**	**2.9**	**14.5**	**42.9**	**531**
	IL15RA	interleukin 15 receptor, alpha isoform 2	A_23_P138680	3.5	2.7	1	1.2	2.8	4.1
	IRF1	**interferon regulatory factor 1**	**A_23_P41765**	**4.8**	**2.2**	**0.9**	**2**	**3.6**	**8.5**
	KLK10	**kallikrein-related peptidase 10 preproprotein**	**A_23_P107911**	**2.3**	**4.3**	**1**	**1.2**	**2.8**	**16.1**
	NLRC5	**nucleotide-binding oligomerization domains 27**	**A_23_P402892**	**8.9**	**4.9**	**0.9**	**1.1**	**10.3**	**7.6**
	NLRC5		**A_23_P26583**	**15.7**	**6.8**	**1**	**1**	**10.8**	**11.9**
	PMAIP1	phorbol-12-myristate-13-acetate-induced protein 1	A_23_P207999	2	1.4	0.7	1.1	1.8	5.3
	SOCS1	**suppressor of cytokine signaling 1**	**A_23_P420196**	**4.1**	**2.1**	**0.9**	**1.5**	**1.5**	**4.2**
	TNFAIP6	tumor necrosis factor, alpha-induced protein 6 precursor	A_23_P165624	1.5	1.2	0.5	0.6	0.7	7
	ZC3HAV1	**zinc finger antiviral protein isoform 2**	**A_24_P341938**	**4.1**	**1.7**	**1**	**1.1**	**1.9**	**10.5**
	ZC3HAV1	**zinc finger antiviral protein isoform 2**	**A_23_P20122**	**4.3**	**2.9**	**1.1**	**1.1**	**2.1**	**15.8**
	ZNFX1	**zinc finger, NFX1-type containing 1**	**A_23_P68462**	**5.8**	**2.9**	**0.7**	**1.2**	**1.4**	**3.8**
			A_23_P256487	3.3	3.6	0.8	0.9	2.1	12.9
			A_32_P224888	1.8	1.5	1	0.9	2.5	6.3
			A_24_P36898	**7.2**	**2.5**	**0.9**	**0.7**	**2.4**	**3.6**
C	**AGT**	**angiotensinogen preproprotein**	**A_23_P115261**	**7.5**	**2.7**	**0.9**	**1**	**1**	**0.7**
	GLI3	**GLI-Kruppel family member GLI3**	**A_23_P111531**	**1.3**	**4.2**	**1**	**0.9**	**1.2**	**1**
	GMPR	**guanosine monophosphate reductase**	**A_24_P277657**	**1.4**	**6.6**	**0.9**	**1**	**1**	**0.8**
	IFITM2	**interferon induced transmembrane protein 2 (1-8D)**	**A_24_P287043**	**1.8**	**5.4**	**1**	**1**	**0.8**	**0.7**
	IFITM3	**interferon-induced transmembrane protein 3 (1-8U)**	**A_23_P87545**	**2.6**	**9.7**	**1**	**1**	**1**	**1.2**
	IFITM4P		**A_24_P16124**	**2.2**	**11.5**	**1**	**0.9**	**0.8**	**0.9**
	LGALS9	**galectin 9 long isoform**	**A_23_P116557**	**1.7**	**9.3**	**1**	**1**	**1.4**	**1**
	RET	ret proto-oncogene isoform c	A_24_P343695	0.9	4.6	1	1	1	1
	SP100	**hypothetical protein**	**A_23_P209712**	**2.5**	**6.4**	**2**	**1.4**	**1.6**	**1.7**
	TRIM34	**tripartite motif protein 34 isoform 3**	**A_23_P124190**	**3.4**	**7**	**2.2**	**1.3**	**1.6**	**2**
		similar to galectin 9 short isoform	**A_23_P101025**	**1.4**	**7**	**1.6**	**1.4**	**1.1**	**1.2**
			A_24_P254933	**2**	**8.1**	**1**	**1**	**0.9**	**0.9**
			A_32_P167592	**2.2**	**7.4**	**1**	**1**	**0.9**	**0.9**
			A_24_P15502	**1.6**	**4.4**	**1**	**1**	**0.9**	**0.8**
			A_24_P7040	**2.8**	**10.4**	**1**	**0.9**	**0.9**	**1.2**
			A_23_P202245	2.2	13.4	1	0.6	0.7	1.4
			A_32_P154321	**1.9**	**4.4**	**1.3**	**1**	**1.8**	**1.7**
D	ATP4A	ATPase, H+/K+ exchanging, alpha polypeptide	A_23_P430728	0.8	0.9	1	2.7	13.5	45.9
	CCL3	chemokine (C-C motif) ligand 3	A_23_P373017	0.7	1.5	1.6	5.2	8.7	14.6

CCL3L3	chemokine (C-C motif) ligand 3-like 3 precursor	A_23_P321920	1	1.3	0.8	2	5.8	10.2
CCL3L3	chemokine (C-C motif) ligand 3-like 3 precursor	A_24_P228130	0.8	0.7	0.9	2.6	4.8	6.3
CCL5	small inducible cytokine A5 precursor	A_23_P152838	1.6	12	1.8	17.5	23	29.9
CXCL10	small inducible cytokine B10 precursor	A_24_P303091	0.8	2.2	0.9	3.9	9.3	12.4
GPR109B	G protein-coupled receptor 109B	A_23_P64721	1.6	2.3	1.5	4.1	10.2	42.3
IFNB1	interferon, beta 1, fibroblast	A_23_P71774	0.7	3	0.9	9.3	31.7	180.6
IL28A	**interleukin 28A**	**A_23_P409438**	**1.3**	**6.3**	**2.1**	**14.8**	**21**	**32.2**
IL28B	interleukin 28B	A_23_P373619	1	3.7	1	18	19.9	21.5
IL29	interleukin 29	A_23_P337800	0.8	3	1.1	6.2	8.7	11.3
TAC3	tachykinin 3 isoform 1	A_23_P2283	1.3	1.2	1.3	2.8	4.5	9.3
E ACAN	aggrecan isoform 2 precursor	A_23_P307310	1	1.3	1.2	0.9	2.1	14.2
ATF3	activating transcription factor 3 isoform 2	A_23_P34915	1.6	1.1	1.1	1.3	1.7	5.7
BCL2A1	BCL2-related protein A1	A_23_P152002	1.2	1.4	0.9	1.1	1.3	5
BIRC3	baculoviral IAP repeat-containing protein 3	A_23_P98350	1.1	1.9	1	1	1.7	9.2
BTN3A1	butyrophilin, subfamily 3, member A1	A_24_P329065	1.7	3.7	1	1.4	2.7	6.4
C19orf30	hypothetical protein LOC284424	A_23_P353667	1.5	1.4	1	1.5	0.7	6.3
CCL17	small inducible cytokine A17 precursor	A_23_P26325	1.1	1.3	1	1.3	2.5	9.3
CCL20	chemokine (C-C motif) ligand 20	A_23_P17065	0.7	0.7	0.8	0.9	0.9	27.4
CCL4	chemokine C-C motif ligand 4 isoform 1 precursor	A_23_P207564	0.7	1.4	0.9	2.2	3.3	30.7
CCRN4L	CCR4 carbon catabolite repression 4-like	A_24_P213794	1.2	1.1	1.3	1.4	1.4	5.2
CENTD1	centaurin delta 1 isoform a	A_32_P83784	1.4	1.9	1.3	1	1.3	4.5
CHEK2	protein kinase CHK2 isoform c	A_23_P109452	1.1	0.9	1.1	1.1	1.2	4.1
CREB5	cAMP responsive element binding protein 5 isoform alpha	A_23_P157117	0.8	1	0.8	1.2	1.4	14.5
CREB5	cAMP responsive element binding protein 5 isoform alpha	A_24_P532232	0.7	1.6	0.9	1.4	1.7	12.3
CSAG1	chondrosarcoma associated gene 1 isoform b	A_24_P11061	1.8	2.1	1	1.2	1.4	8
CSAG2	CSAG family, member 2	A_24_P567298	1.3	2.1	1.3	1.3	1.6	8.2
CSAG3A	CSAG family, member 3A	A_24_P79529	1.3	2.8	1.1	1.1	1.7	15.7
CX3CL1	chemokine (C-X3-C motif) ligand 1	A_23_P37727	1.7	2.4	1.4	1.6	2.2	19.7
CXCL1	chemokine (C-X-C motif) ligand 1	A_23_P7144	1	1.1	1.1	0.9	0.9	4.6
CXCL2	chemokine (C-X-C motif) ligand 2	A_23_P315364	1.8	1.5	1.4	1.4	1.8	5.2
CXCL3	chemokine (C-X-C motif) ligand 3	A_24_P251764	1.6	1.2	1.2	1.2	1.4	4.3
CXCL3	chemokine (C-X-C motif) ligand 3	A_24_P183150	1.7	1.3	1.1	1	1.3	6.1
CXCR4	chemokine (C-X-C motif) receptor 4 isoform a	A_23_P102000	0.8	1	1.3	1.4	1.7	27.2
DNAJC15	DNAJ domain-containing	A_23_P117190	2.2	1.8	1.2	2.3	2.2	6.3
EGR4	early growth response 4	A_23_P380318	0.9	1.1	1.2	1.2	2.5	23.8
EPHA4	ephrin receptor EphA4	A_23_P108501	0.8	0.9	1.4	1.1	1.1	4.1
EPHA4	ephrin receptor EphA4	A_24_P274219	1.1	1.1	0.9	1.2	1.8	7.5
FUT1	fucosyltransferase 1	A_23_P107963	0.6	1.2	1.1	1.6	1.4	5.1
FZD4	frizzled 4	A_23_P64617	0.9	1.3	1.1	0.9	1.4	14.3
GALNTL4		A_24_P924301	1.4	3	4.6	1.7	2	1.9
GP1BA		A_23_P152926	1	1.9	2.5	2.1	1.5	5.1
GPBAR1	G protein-coupled bile acid receptor 1	A_23_P400378	0.8	1	1	1	1.3	4.6
HCP5	HLA complex P5	A_32_P85500	0.9	2.3	1.3	0.7	1.3	5.1
HCP5	HLA complex P5	A_24_P17870	1.4	3.4	1.2	1.1	1.3	8.8
HIP1R	huntingtin interacting protein-1-related	A_24_P229164	0.9	0.9	1.1	1.2	1.4	4.8
HIP1R	huntingtin interacting protein-1-related	A_23_P398294	1.1	1.2	1.8	1.4	1.8	11
HTR3E	5-hydroxytryptamine receptor 3 subunit E	A_24_P32139	0.8	1.6	1	1.1	1.1	5.7

IGF2AS	insulin-like growth factor 2 antisense	A_23_P116435	1.2	0.9	1.3	1.3	1.2	5.3
IL3RA	interleukin 3 receptor, alpha precursor	A_32_P217750	1.2	1.9	1.4	1	1.3	6.2
IL6	interleukin 6 (interferon, beta 2)	A_23_P71037	1.6	1.5	1	1.8	3.6	34
IL8	interleukin 8 precursor	A_32_P87013	2.1	1.2	1.1	1.4	2.8	17.7
JAK2	Janus kinase 2	A_23_P123608	1.8	1.2	0.9	1	1.6	5.1
KCNV1	potassium channel, subfamily V, member 1	A_23_P146125	1.3	0.7	1.2	1.2	1.4	11.7
KLF4	Kruppel-like factor 4 (gut)	A_23_P32233	1	0.8	0.8	1	2.3	9.2
KLHDC7B	kelch domain containing 7B	A_24_P117410	1.2	2.6	1.1	1.3	1.9	11.1
LRRN3	leucine rich repeat neuronal 3	A_23_P31376	1	1.7	0.9	1.5	7.3	81.3
LTB	lymphotoxin-beta isoform a	A_23_P93348	0.8	1.1	0.8	1	1.1	18.7
MBOAT4	FKSG89	A_24_P306824	1.1	1.3	1	0.9	1.8	7.8
MXD1	MAX dimerization protein 1	A_24_P379750	1.2	1.1	1	1.1	1.4	4.1
MXD1	MAX dimerization protein 1	A_23_P408094	1.1	1.2	1.2	1.2	1.3	4.6
NCF2	neutrophil cytosolic factor 2	A_23_P138194	1.1	1	1	1	1.5	5.9
NFKBIA	nuclear factor of kappa light polypeptide gene enhancer in B-cells inhibitor, alpha	A_23_P106002	1.1	1.3	1	1.1	1.6	7.1
NOV	nov precursor	A_23_P82929	1	0.7	1.1	1.2	1.6	4.6
NPHS1	nephrin	A_23_P5200	0.8	1	1	0.7	1.2	5.2
OTUD1		A_24_P374834	0.8	0.8	0.7	0.5	1	5.3
OTUD1		A_32_P60459	1.1	1	0.9	0.6	1.1	7.1
PLA2G4C	phospholipase A2, group IVC	A_23_P50508	1	1.1	0.9	1	1.3	8.3
PLCG2	phospholipase C, gamma 2	A_23_P106675	1.4	1.4	1.7	1.2	1.4	6.2
PPP1R15A	protein phosphatase 1, regulatory subunit 15A	A_23_P90172	0.9	1	1	1.1	1.4	5.7
PRR15	proline rich 15	A_32_P154911	2.4	1.6	1.8	1.5	2.3	6.8
PTGER4	prostaglandin E receptor 4, subtype EP4	A_23_P148047	1.1	0.9	0.7	1.1	2.3	14.4
PTX3	pentraxin-related gene, rapidly induced by IL-1 beta	A_23_P121064	0.8	1.2	0.7	0.8	1.4	20.1
RELB	reticuloendotheliosis viral oncogene homolog B	A_23_P55706	0.9	1.5	1.1	1	0.9	4.4
RGS9	regulator of G-protein signalling 9 isoform 1	A_23_P66881	0.7	0.7	1.2	1	2	5.5
RHCG	Rhesus blood group, C glycoprotein	A_23_P151975	1	0.9	1.4	1.3	1.5	4.4
SLAMF7	SLAM family member 7	A_24_P353638	0.9	1.4	0.7	1.3	2.2	6.9
SLC12A7	solute carrier family 12 (potassium/chloride transporters), member 7	A_23_P61688	1.6	1.6	1.5	1.3	1.5	5.1
SMPD3	sphingomyelin phosphodiesterase 3, neutral membrane	A_23_P163567	1.2	1.5	0.9	0.8	1.1	5.6
SNPH	syntaphilin	A_23_P102706	0.9	0.9	1.5	1.2	1.2	4.7
SOD2	**SOD2 protein**	**A_24_P935819**	**4**	**1.3**	**2**	**1.5**	**2.4**	**10.8**
TMC8	FLJ00400 protein	A_23_P346093	0.7	1.5	0.8	1.4	1.8	5.3
TNF	tumor necrosis factor alpha	A_23_P376488	0.7	1.2	1.1	1.1	1	5.9
TNFAIP2	tumor necrosis factor, alpha-induced protein 2	A_23_P421423	0.9	1.1	1.8	1.4	1.3	5.3
TNFAIP3	tumor necrosis factor, alpha-induced protein 3	A_24_P166527	1	0.7	0.9	1	1.5	6.6
TNFAIP3	tumor necrosis factor, alpha-induced protein 3	A_24_P157926	1.4	1.5	1.2	1.2	1.9	13.8
TNFRSF9	tumor necrosis factor receptor superfamily, member 9 precursor	A_23_P51936	1.1	1.2	1	1.4	2.3	8.2
TTC9B		A_23_P332392	1	1	1	1.2	1.4	7.2
ULBP2	UL16 binding protein 2	A_23_P168259	1.1	1	0.7	1	1.4	4.1
UNC5B	unc-5 homolog B	A_23_P52336	1	1	0.7	1.2	1.2	6.3
WARS	tryptophanyl-tRNA synthetase isoform a	A_23_P65651	1.4	2.1	1	1.6	2.4	6.7
ZBTB32	testis zinc finger protein	A_23_P131024	0.8	1.6	1.3	1.2	8.2	61
ZC3HAV1	zinc finger antiviral protein isoform 1	A_23_P425224	3.7	0.7	1.2	1.1	1.6	5.7
ZEB2	zinc finger homeobox 1b	A_23_P142560	1.5	1.5	1.3	0.9	1	5.9
		A_32_P75867	**3.3**	**5.8**	**1.8**	**2**	**7.2**	**20.1**

	A_24_P126282	1.5	2.9	1.3	1	2.6	5
	A_23_P6535	0.9	3.9	1.1	1.4	2	12.6
	A_32_P219135	1	1	1.6	1.8	1.8	8.6
	A_24_P933828	0.8	0.7	1.2	1.4	1.4	6.2
	A_32_P222684	1	1.2	1.2	1.5	1.5	6.3
	A_32_P170664	1.1	1	0.8	1.2	1.3	4.3
	A_23_P328740	1	1.7	0.9	1.1	1.5	8.6
	A_32_P703	1	1.1	1.1	1	1.2	4.8
	A_32_P147395	1.2	1.1	1	0.9	1.1	7.8
	A_32_P158181	1.4	1.6	1.2	0.9	1.2	5.7
	A_32_P68504	1.3	1.4	1.2	1.3	1.4	7
	A_32_P217261	1.4	1.2	1	0.9	1.3	4.7
	A_32_P45844	1.4	2.5	1.4	1.8	2.1	18.9
	A_23_P11980	0.9	1.3	1.8	0.9	1.3	11.2
	A_24_P652537	1.6	1.6	0.9	1.1	2.8	15.2
	A_24_P101651	1.3	2	1.2	1.8	2.1	7.8
	A_32_P104841	1.4	1.5	1.3	1.4	3.3	9.4
	A_32_P52632	1	1.6	1.2	0.9	1.3	7.7
	A_24_P255384	0.9	2.1	0.9	0.9	0.9	7.3
	A_32_P168375	1.1	1.3	1.4	1.3	1.2	4.5
	A_24_P174353	0.9	2.1	1.5	1.9	1.1	8.3
	A_32_P91773	2.2	1.1	2.3	1.9	2	10.6
	A_32_P210038	1.2	1.2	1.3	1.1	1.4	5.1
	A_24_P937817	1.5	1.1	0.7	1.1	1.6	4
	A_24_P47329	2.7	2	1.4	2.3	2.9	6.3
	A_32_P3317	1	0.8	0.6	0.8	3.8	5.2
	A_32_P42989	1.5	1.3	1.4	1.7	1.3	4
	A_32_P117322	1.2	1.1	1.1	1.3	0.6	4.8
	A_32_P118010	2.4	0.7	1.3	1.5	2.4	4.1
	A_32_P55987	1.2	1.6	4.1	1.8	1.7	2.9
	A_23_P320407	0.6	2.1	2.1	1.3	1.3	4.7
	A_32_P184039	0.9	1.5	3.1	1.4	1.6	5.7
	A_24_P930337	2.3	1.9	4.9	1.3	1.4	1.2

[‡]Genes listed in each cluster correspond to the same genes hierarchically clustered in Figure 1.
***Rows in bold correspond to the 190 IFN-induced genes. 1 expressed sequence tag A_23_P416305 was down-regulated by IFNβ treatment.**
[†]Rows in blue correspond to 66 of the 190 genes that have not been previously described as IFN-responsive.

Table S2.

Table S2. Genes differentially expressed by wt, C^{F170S}, and P(C-) HPIV1 compared to mock infection and to each other*†

Cluster‡	Symbol	Product	Agilent	Avonex 6 hr	Avonex 24 hr	F170S 6 hr	F170S 12 hr	F170S 24 hr	F170S 48 hr	P(C-) 6 hr	P(C-) 12 hr	P(C-) 24 hr	P(C-) 48 hr	WT 6 hr	WT 12 hr	WT 24 hr	WT 48 hr
A	ACTR3B	actin-related protein 3-beta isoform 1	A_24_P303594	0.9	0.7	0.5	0.7	0.8	5	0.5	0.8	1.6	3.2	0.6	0.8	0.9	1
	ACVR1	activin A type I receptor precursor	A_23_P79221	1.1	1.1	0.6	0.7	2.2	11.8	0.5	0.7	4.4	7.6	0.7	0.7	1.1	2.2
	ADAM23	ADAM metallopeptidase domain 23 preproprotein	A_23_P351667	1	1	1.1	1.1	1.3	6.5	1	1.1	3	5.7	1.1	1.1	1.2	1.5
	ADAR	adenosine deaminase, RNA-specific isoform a	A_23_P200439	1.8	2.5	0.9	1.3	3.8	12.3	0.9	1.3	5	7.6	0.9	1	1.6	2.2
	AFF1	myeloid/lymphoid or mixed-lineage leukemia trithorax homolog 2	A_23_P29897	1.2	1.3	1.2	1.1	3.3	21.6	1.3	1.3	5.7	9.1	1.1	0.7	1.4	3.2
	AFF1	myeloid/lymphoid or mixed-lineage leukemia trithorax homolog 2	A_23_P169619	1.3	1.8	0.9	1.1	3.5	16.5	1.1	1.1	5.9	8.2	1.1	0.8	1.4	3
	AFF4	ALL1 fused gene from 5q31	A_23_P218977	1.1	1.3	0.9	0.9	2.1	14.6	0.8	1	3.2	11.5	0.8	0.9	1.3	1.9
	AFF4	ALL1 fused gene from 5q31	A_24_P942636	1.3	1.2	0.7	0.6	2.3	36.4	0.7	0.8	4	29.7	0.7	0.8	1.4	3.3
	AGL	amylo-1, 6-glucosidase, 4-alpha-glucanotransferase isoform 1	A_23_P200298	1.2	1	0.9	1	1.4	7.4	0.8	0.9	2.7	4.2	0.9	1	1.3	1.7
	ALOX5AP	arachidonate 5-lipoxygenase-activating protein	A_23_P2793	0.9	0.9	0.6	0.7	1.2	8.6	0.6	0.7	1.7	5.9	0.6	0.8	0.9	1.8
	ANKS1A	ankyrin repeat and sterile alpha motif domain containing 1	A_23_P156748	1.1	1	1.2	1.1	2.4	17.6	1	1.1	8.8	9.8	1.1	1.1	1.3	2.1
	ARFGEF2	ADP-ribosylation factor guanine nucleotide-exchange factor 2	A_23_P5995	0.8	0.9	0.9	0.9	1.1	7	0.8	0.9	1.8	5.1	0.9	0.9	1.1	1.3
	ARHGAP24	Rho GTPase activating protein 24 isoform 2	A_23_P110151	1.1	0.9	0.8	0.7	1.6	8.7	0.7	0.9	2.5	7.8	0.9	0.7	1	1.4
	ARHGAP24	Rho GTPase activating protein 24 isoform 2	A_24_P380061	1.2	1	0.8	0.9	1.7	8.9	1.2	1	2.8	6.8	1.3	0.7	1	1.5
	ARHGAP26	GTPase regulator associated with the focal adhesion kinase pp125	A_24_P28165	1.1	1.5	1.7	1.3	2.3	11.8	1.6	1.4	6.9	6.6	1.3	1.2	1.3	2.6
	ARL14	ADP-ribosylation factor 7	A_23_P92161	0.9	1.4	0.9	0.8	2.4	19.8	0.7	0.9	7.6	17.9	0.7	0.6	1.1	1
	ARL4A	ADP-ribosylation factor-like 4A	A_32_P806841	1.1	1.1	0.9	0.8	2.6	10.5	0.8	0.8	5.1	6.6	1	1	1.2	2.4
	ARL4A	ADP-ribosylation factor-like 4A	A_23_P145761	1.1	1.1	1	0.8	2.3	9.3	0.9	0.9	5.3	6.1	1	1	1.1	2.1
	ARL5B	ADP-ribosylation factor-like 8	A_24_P943997	1.4	1.3	0.7	0.7	6.2	94.9	0.7	0.8	12.4	79.3	0.7	0.9	1.3	4.4
	ARL5B	ADP-ribosylation factor-like 8	A_23_P378588	1.3	1	0.7	0.8	6	50.1	0.6	1	16.3	38.9	0.7	0.8	1.3	2.7
	ARNTL2	aryl hydrocarbon receptor nuclear translocator-like 2	A_23_P53345	1.1	1.3	0.7	0.8	1.7	14.8	0.7	0.8	2.2	8.9	0.7	0.8	1.1	2.3
	ATF3	activating transcription factor 3 isoform 2	A_23_P34915	1.6	1.1	1.2	1.3	11.6	64.7	1.1	1.9	19.5	58.4	1.1	1.3	1.7	5.7
	BANK1	B-cell scaffold protein with ankyrin repeats 1 isoform 1	A_23_P10232	1.2	1.5	0.9	0.9	1.2	11.9	0.8	0.7	2.1	5.2	0.9	1	1	1.5
	BCL2A1	BCL2-related protein A1	A_23_P152002	1.2	1.4	0.9	0.8	1.8	29.3	1	0.9	3.9	13.9	0.9	1.1	1.3	5
	BIK	BCL2-interacting killer	A_23_P404667	0.9	1.1	1.1	1	1.2	12.2	1.1	1	3.1	14.2	1.2	0.9	0.9	2.9
	BNIP3	BCL2/adenovirus E1B 19kD-interacting protein 3	A_23_P138635	1.1	1.3	0.9	0.8	1.1	7.4	0.8	0.8	1.6	6.4	0.8	0.8	1.3	1.7
	BSN	bassoon protein	A_23_P29735	1.4	1.2	1.1	1.3	1.6	7.2	1.1	1.3	2.8	7.5	0.8	0.9	1.1	1.4
	BTG1	B-cell translocation protein 1	A_23_P87560	1.2	1	0.9	0.9	1.8	5.4	0.8	1	2	4.9	0.9	0.8	1	1.3
	BTN2A2	butyrophilin, subfamily 2, member A2 isoform b	A_24_P346210	1	1.4	1.4	1.4	2.4	8	1.4	1.5	5.2	5.9	1.4	1.2	1.2	1.9
	BTN2A2	butyrophilin, subfamily 2, member A2 isoform b	A_24_P337592	0.9	1.4	1.4	1.3	3.3	27.3	1.4	1.4	9	19	1.4	1.1	1.3	2.6
	BTN2A2	butyrophilin, subfamily 2, member A2 isoform b	A_24_P249072	1.1	1.4	1.2	1.1	2.8	14.3	1.1	1.2	5.7	10.5	1.1	1	1.2	2
	BTN2A2	butyrophilin, subfamily 2, member A2 isoform b	A_23_P122439	0.8	1.4	1.2	1.1	3.1	20.8	1	1.1	7.4	15.2	1.2	1	1.1	2.3
	C10orf118	CTCL tumor antigen L14-2	A_24_P942694	0.9	0.8	0.7	0.8	1.4	7.4	0.7	0.8	1.9	6.9	0.8	0.6	1.2	1.6
	C18orf19	hypothetical protein LOC125228	A_23_P380978	1.1	1.1	0.6	0.7	1.4	11.9	0.6	0.8	4.7	16.9	0.6	0.8	1.2	1.6
	C19orf12	hypothetical protein LOC83636 isoform 2	A_23_P209195	1.6	1.2	0.9	0.9	1.6	7	0.8	0.9	2.4	5.2	0.9	1	1.2	1.6
	C19orf12	hypothetical protein LOC83636 isoform 2	A_24_P113341	1.3	1	1	0.9	1.4	8.4	0.9	0.9	2.7	5.6	0.9	0.9	1	1.5
	C2orf13	chromosome 2 open reading frame 13	A_32_P16339	1.1	1.1	0.7	0.9	1.2	8	0.8	0.9	3	7.8	0.9	0.7	0.7	2

	C3orf19	hypothetical protein LOC51244	A_23_P354277	0.9	1	1	1	1.6	6.3	1	0.9	2.2	5.1	1	1	1	1.4
	C3orf33	hypothetical protein LOC285315	A_23_P301476	1.2	1	0.9	1	1.5	7.6	0.8	0.9	2.9	4.7	1	1.1	1.2	1.4
	C3orf52	TPA-induced transmembrane protein	A_23_P58009	1.1	1.1	0.7	0.9	1.6	6.1	0.8	0.9	1.5	3.7	0.7	1.1	1.3	1.5
	C3orf59	hypothetical protein LOC151963	A_32_P117464	1.5	1.4	0.7	0.7	3.9	17.3	0.6	0.9	5.8	13.4	0.8	1	1	2.4
	C8orf46	hypothetical protein LOC254778	A_23_P353614	0.7	1.4	1	0.8	3.2	16.1	0.8	1.1	4.7	12.2	0.7	1	0.7	1.8
	CA8	carbonic anhydrase VIII	A_23_P83838	0.9	1	0.7	1	1.7	10	0.9	0.9	3.3	8.7	0.8	1	0.9	2.1
	CCDC117	coiled-coil domain containing 117	A_23_P432034	1	1	0.9	0.8	1.2	5.6	0.9	0.8	2.2	4.1	0.9	0.8	0.9	1.3
	CCDC6		A_23_P127117	1.3	1.3	0.9	0.9	1.4	13	1	1	3.4	12.7	0.8	0.9	0.9	2.1
	CCRN4L	CCR4 carbon catabolite repression 4-like	A_24_P213794	1.2	1.1	1.4	1.2	9	68.2	1.4	1.6	20.5	49.6	1.3	1.4	1.4	5.2
	CDKN2C	cyclin-dependent kinase inhibitor 2C	A_23_P85460	0.9	0.7	1.1	0.8	1.9	12.4	1	0.9	5.2	8.5	1.1	0.8	0.9	2
	CEBPG	CCAAT/enhancer binding protein gamma	A_23_P356755	1	1.1	1	1	1.8	9.7	0.9	0.9	2.4	10.8	1	1	1.1	2
	CENTD1	centaurin delta 1 isoform a	A_32_P83784	1.4	1.9	1.3	0.9	5.1	45.9	1	1	14.6	28.2	1.3	1	1.3	4.5
	CHEK2	protein kinase CHK2 isoform c	A_23_P109452	1.1	0.9	1.5	1.2	4.4	35.2	1.1	1.2	14.5	15.8	1.1	1.1	1.2	4.1
	CITED2	Cbp/p300-interacting transactivator, with Glu/Asp-rich carboxy-terminal domain, 2	A_23_P214969	0.9	1	0.9	0.8	2.6	14.8	0.7	0.9	5.7	9.2	0.9	0.7	1	2.8
	CLMN	calponin like transmembrane domain protein	A_23_P25706	1.2	0.9	0.8	0.8	2	9.6	0.7	0.8	3.2	7.5	0.8	1.1	1.1	1.7
	CPEB3	cytoplasmic polyadenylation element binding protein 3	A_23_P46813	1.3	1.1	1.2	1	7.2	21.1	1	1.3	17.2	22.7	0.9	1.1	1.4	3
	CPEB3	cytoplasmic polyadenylation element binding protein 3	A_23_P46812	3.2	2.6	1.9	1	5.3	22.1	1.9	1.9	10.1	16.3	2.4	1.5	1.4	3.3
	CREB5	cAMP responsive element binding protein 5 isoform alpha	A_24_P532232	0.7	1.6	0.8	1.3	5	153.1	0.9	0.7	21.8	176.7	0.9	1.4	1.7	12.3
	CREB5	cAMP responsive element binding protein 5 isoform alpha	A_23_P157117	0.8	1	0.9	1	9	347.7	0.9	1.1	42.4	280.9	0.8	1.2	1.4	14.5
	CRYM	crystallin, mu isoform 1	A_23_P77731	1.1	0.8	0.9	1	2	7.3	1	1.1	6	6.4	1	1	1.3	1.1
	CSRP2	cysteine and glycine-rich protein 2	A_23_P44724	1.1	1	0.7	0.8	0.9	5	0.9	0.9	1.4	4.1	0.8	0.9	1	0.9
	CYLD	ubiquitin carboxyl-terminal hydrolase CYLD isoform 1	A_24_P48078	1.2	1.2	0.8	0.9	2.6	23.4	0.9	0.9	5.5	18.2	1	0.9	1.1	2.8
	CYLD	ubiquitin carboxyl-terminal hydrolase CYLD isoform 1	A_23_P65996	1.1	1	0.5	0.8	2.1	15.8	0.5	0.6	4	11.2	0.6	0.7	1.2	2.6
	DAB2IP	DAB2 interacting protein isoform 2	A_24_P149704	1	1.1	1	0.8	2.1	8.2	1.1	1	3.5	6.3	1.3	0.8	0.8	1.6
	DDEF1	development and differentiation enhancing factor 1	A_23_P44831	1.2	1.2	1.1	1	1.9	11.9	1.1	1.1	4.2	8.2	1	1	1.3	1.9
	DDEF1	development and differentiation enhancing factor 1	A_23_P216278	1.1	1.2	1	1	1.7	20.5	1.1	1	5.2	14.8	1	0.9	1	2.1
	DDEF2	development- and differentiation-enhancing factor 2	A_23_P40088	1.1	1	0.6	0.7	0.9	14	0.7	0.8	2.7	9.4	0.6	0.8	0.8	2
	DDIT3	DNA-damage-inducible transcript 3	A_23_P21134	0.9	1.2	0.8	1.3	3.3	8.6	0.9	2.1	6.3	8.7	0.8	1.3	1.3	1.8
	DENND4A	c-myc promoter binding protein	A_24_P409265	2	1	0.9	1	1.9	15.1	0.9	0.9	3.3	9.9	1.1	0.8	1.2	1.8
	DENND4A		A_23_P384329	1.2	1.2	0.7	0.7	1.9	11.2	0.7	1	3.8	5.8	0.8	0.6	1.1	1.7
	DENND4C		A_24_P93633	1.2	1.4	1.1	0.7	1.5	11.3	0.8	0.8	2.3	9.3	0.9	0.9	1.4	1.8
	DICER1	dicer1	A_24_P22163	1.1	1.1	1.5	1.1	2.2	25.7	1.4	1.2	9.5	13.4	1.4	1	1.1	2.7
	DNAJB4	DnaJ (Hsp40) homolog, subfamily B, member 4	A_24_P393958	1	1	0.4	0.6	2.4	9	0.4	0.6	3.9	4.6	0.5	0.6	0.9	1.3
	DNAJB4	DnaJ (Hsp40) homolog, subfamily B, member 4	A_23_P51339	1	0.9	0.5	0.6	2.2	8.2	0.4	0.6	3.9	4.6	0.5	0.7	1	1.2
	DNAJB5	DnaJ (Hsp40) homolog, subfamily B, member 5	A_23_P112241	0.7	0.8	1.4	1.2	4.1	23.3	1.4	1.6	10.5	18.5	1.3	1.2	1.3	2.9
	DOCK11	dedicator of cytokinesis 11	A_23_P148584	1.1	0.9	0.6	0.7	1.1	8.2	0.5	0.7	2.1	3.4	0.7	0.7	1	1.6
	DSCR1	calcipressin 1 isoform a	A_23_P166248	1.4	1	0.7	0.8	2.2	9.1	0.6	0.8	3.2	4.9	0.8	0.8	1	1.6
	DUSP10	dual specificity phosphatase 10 isoform a	A_23_P51856	1.3	1.3	1	1	1.4	9.9	1	0.9	3.5	4.6	1.1	0.8	0.9	1.5
	DUSP10	dual specificity phosphatase 10 isoform a	A_24_P182494	1.1	1.1	1.1	1	1.3	5.5	1	1.1	2.7	3.2	0.9	0.9	1	1
	DUSP16	dual specificity phosphatase 16	A_24_P189739	1	1.1	0.8	0.9	1.9	5.6	0.6	0.9	2.2	3.2	0.8	1.2	1.1	1.2
	DUSP8	dual specificity phosphatase 8	A_32_P98298	1	1.1	1	1.1	2.7	12.5	1.1	1	4	4.8	1	1	1	2.3
	EBF4	KIAA1442 protein	A_23_P109122	1.1	1.1	1.4	1.3	3.7	20.3	1.4	1.4	10.7	11.7	1.3	1.3	1.2	2.7
	ECM2	extracellular matrix protein 2 precursor	A_23_P303671	1	1.1	0.7	0.7	2.6	28	0.7	1.2	6	48.3	0.7	1.6	1.7	4

	EFNB2	ephrin B2	A_24_P355944	1.2	0.8	0.8	0.9	3	29.5	0.8	0.9	6.8	19.3	1	1.3	1.2	2.4
	EIF5	eukaryotic translation initiation factor 5	A_23_P205265	1.1	1.1	0.6	0.8	1.2	7.2	0.8	0.9	1.2	7.7	0.7	0.8	1.1	1.6
	ELOVL7	ELOVL family member 7, elongation of long chain fatty acids	A_24_P32473	1	1.7	0.6	0.7	3.2	41.4	0.5	0.7	8.3	18.9	0.5	0.9	1.4	4.5
	EPHA4	ephrin receptor EphA4	A_24_P274219	1.1	1.1	0.8	0.9	3.9	98.4	1	0.8	12.1	52.1	0.9	1.2	1.8	7.5
	EPHA4	ephrin receptor EphA4	A_23_P119899	1.1	1	0.7	1.5	3.3	48.4	1.3	1.2	10.5	50.1	0.6	2.2	1.2	3.8
	EPRS	glutamyl-prolyl tRNA synthetase	A_23_P97632	0.9	0.7	0.6	0.8	1.1	10.1	0.6	0.7	1.4	5.6	0.7	1	1.1	1.3
	ETS1	v-ets erythroblastosis virus E26 oncogene homolog 1	A_23_P127525	1.1	1	1.2	1.2	2.2	15.4	1.5	1.3	3.4	14.9	1.1	1	1	2.1
	EXT1	exostosin 1	A_23_P43273	1.2	1.8	0.9	0.9	2	12.6	0.9	1	2.1	4.6	1	0.9	1.1	1.7
	FAM126A	down-regulated by Ctnnb1, a	A_23_P8582	1.1	0.8	0.7	0.8	1.4	9.3	0.7	0.8	2.1	9.7	0.7	0.9	1.4	1.9
	FAM62B	family with sequence similarity 62 (C2 domain containing) member B	A_23_P8744	1.1	1.2	1	1	1.5	13.4	0.9	1.1	2.5	8.8	1	1	1.2	2.4
	FAS	tumor necrosis factor receptor superfamily, member 6 isoform 1 precursor	A_23_P63896	1.7	1.5	0.6	0.8	2.9	22.7	0.6	0.7	4.4	11.8	0.6	0.9	1.3	4.4
	FGF2	fibroblast growth factor 2	A_23_P218918	1.1	1.1	1.1	1.1	2.4	13.4	1.2	1.2	5.3	12.3	1.1	1	1.2	3.5
	FNDC3A	fibronectin type III domain containing 3A isoform 2	A_23_P25503	1.1	1.2	1	0.8	2.6	24.8	0.9	0.8	8	14.2	0.9	0.9	1.4	3.3
	FNDC3A		A_24_P409126	1.1	1.8	1.2	1.1	2.5	47	0.9	1	7.4	60.8	1.2	1.3	1.3	3.9
	FOLR2	folate receptor 2 precursor	A_23_P47709	1.1	0.9	1	0.8	1.3	6.1	0.7	1	2.5	3	0.8	0.9	0.9	1.3
	FRMD6	FERM domain containing 6	A_24_P330303	0.9	1	0.6	0.7	1.9	5.4	0.6	0.8	2.1	6.2	0.6	0.8	1.1	1.2
	FYN	protein-tyrosine kinase fyn isoform a	A_23_P502142	1	0.9	1.1	1.1	3.2	17.4	1.1	1.1	9.4	11	1	1.1	1	2.8
	FZD4	frizzled 4	A_24_P278621	1.4	1.4	1.3	1.3	3.3	50.4	1.1	0.9	10.6	31.1	1.7	0.9	0.7	6.4
	GABARAPL1	GABA(A) receptor-associated protein like 1	A_24_P4816	0.8	0.8	0.6	0.8	1.5	6.1	0.6	0.7	2	3.9	0.7	0.6	0.8	1.3
	GABARAPL1	GABA(A) receptor-associated protein like 1	A_23_P162640	0.9	1	0.8	0.9	1.8	9	0.8	0.9	2.6	5.7	0.8	0.8	0.9	1.7
	GADD45A	growth arrest and DNA-damage-inducible, alpha	A_23_P23221	0.9	1.1	0.9	0.9	2.4	8.6	0.9	1	2.9	9.9	0.9	1.2	1.1	1.7
	GATA6	GATA binding protein 6	A_23_P304450	1.8	1.6	1.6	1.2	5.7	17.3	1.1	1.3	6.6	14.8	1.7	1.3	1.4	2.6
	GCA	grancalcin, EF-hand calcium binding protein	A_23_P28485	1.4	1.2	1.1	1	2.1	18.4	0.9	1	4.9	8.1	1.2	1	1	1.7
	GLCCI1		A_23_P336198	1.1	0.9	0.7	0.9	2.3	14.4	0.8	0.9	7.2	7.6	0.8	0.8	1.2	2.6
	GMFG	glia maturation factor, gamma	A_23_P208866	1.1	1	0.8	0.8	1	6.4	0.9	0.8	2.1	5.8	0.8	0.9	0.8	1.3
	GPBP1	vasculin	A_23_P364465	1	1	0.9	0.9	1.8	7.1	0.8	0.9	3.4	4.6	0.9	0.8	0.9	1.6
	GRAMD1B	PTSS3032	A_24_P58620	1.1	1	0.9	1.1	2.3	12.8	1	1	4	7.5	0.8	1.1	1.4	2.3
	GRB10	growth factor receptor-bound protein 10 isoform c	A_23_P122863	2.5	0.9	1.2	0.9	2.5	19.1	1.1	1	7.6	15.3	1	0.9	1.4	3.1
	HIAT1	hippocampus abundant transcript 1	A_23_P45851	1.1	1.1	0.7	0.9	3	20.1	0.7	1	6.2	13.3	0.7	1	1.6	3.4
	HOXB3	homeobox B3	A_23_P316511	1	1.2	1.4	1.2	2.1	7.6	1.1	1.3	3.5	4.7	1.1	1.1	1.2	1.7
	HOXB9	homeobox B9	A_23_P27013	0.9	1	1.1	1.2	2.4	10.9	1.2	1.2	4.8	8.1	1	1.1	1.1	1.9
	HSCB	J-type co-chaperone HSC20	A_23_P40588	1.2	1.2	0.7	0.9	2	11.4	0.8	0.9	4.3	9.8	0.7	0.9	0.9	1.6
	HSD17B7	hydroxysteroid (17-beta) dehydrogenase 7	A_32_P52282	0.9	0.8	0.6	0.8	1.4	4.9	0.8	1.1	2	4.7	0.7	0.9	1.1	0.9
	HSPB8	heat shock 27kDa protein 8	A_23_P162579	1.1	0.8	0.6	0.8	1.5	10.5	0.4	0.8	3.5	7.5	0.7	0.9	1.4	1.3
	IGF2	insulin-like growth factor 2	A_23_P150609	1.1	0.8	1.5	1.3	4.5	37.5	1.2	1.4	21.1	25.9	1.3	1.1	0.8	3.9
	IGF2AS	insulin-like growth factor 2 antisense	A_23_P116435	1.2	0.9	1.1	1.2	6.4	42.9	1.3	1.3	20.4	25.9	1.3	1.3	1.2	5.3
	ING3	inhibitor of growth family, member 3 isoform 1	A_23_P111811	1.3	1.3	1.2	1.2	1.7	9	1.2	1.2	3.2	7.9	1.2	1.1	1.1	1.7
	INHBA	inhibin beta A precursor	A_23_P122924	1	1.7	1.3	1.3	2.6	18.2	1.1	1.5	5.6	9.1	1.2	1.2	1.2	3
	INTS6	integrator complex subunit 6 isoform a	A_24_P167614	1.2	1.3	0.9	0.9	1.8	5.5	1	0.9	2.2	4.2	0.9	1.1	0.9	1.4
	ITGA5	integrin alpha 5 precursor	A_23_P36562	0.9	0.8	0.7	0.8	1.9	5.8	0.8	0.8	2.6	4.4	0.7	1	1.3	1.3
	JAZF1	JAZF zinc finger 1	A_32_P36694	1.3	1.2	0.9	0.9	3	33.3	0.9	0.9	8.3	29	1	1.1	1.5	3.4
	KCNG3	potassium voltage-gated channel, subfamily G, member 3 isoform 1	A_32_P800799	1.1	1.1	1	0.9	2	52.8	0.9	0.9	6.2	30	0.9	1	1.1	4.5
	KCNV1	potassium channel, subfamily V, member 1	A_23_P146125	1.3	0.7	1	1.1	9.7	101.6	1	1.3	25.3	120.8	1.2	1.2	1.4	11.7
	KLF6	Kruppel-like factor 6	A_24_P69654	1.4	1	0.9	1	2.9	7.2	1	1.6	3.8	3.9	0.8	0.8	0.8	1.3

	KLF6	Kruppel-like factor 6	A_23_P63798	1.5	1.1	1	1.1	3.5	9.7	1.1	1.7	5.3	5	0.9	0.9	0.8	1.4
	KLF7	Kruppel-like factor 7 (ubiquitous)	A_23_P67980	1	1	0.9	0.9	1.9	7.4	0.9	1.1	3.8	7	1	0.9	1	1.4
	KTN1	kinectin 1 isoform a	A_23_P106131	1	0.9	0.6	0.8	1.1	5.2	0.7	0.8	2.1	3.7	0.7	0.7	1	1.3
	LRIG3	leucine-rich repeats and immunoglobulin-like domains 3	A_23_P47885	1.1	1	0.9	0.9	1.9	10.6	0.7	0.9	2.2	3.2	0.9	0.8	1	1.3
	LST1	leukocyte specific transcript 1 isoform 1	A_24_P94916	1.2	1.3	1	1.2	2.3	17.3	1.2	1.2	9.5	14.4	1.1	1.2	1.5	2.8
	MAFB	transcription factor MAFB	A_23_P17345	1.1	1.1	0.9	1.1	5	17.8	1.2	1.2	7.3	9.2	1	1.5	1.1	3.2
	MAFF	transcription factor MAFF	A_23_P103110	1	1.1	0.9	0.9	2.3	8.2	0.9	0.9	3.7	6.5	0.9	0.7	0.9	1.6
	MAL2	MAL2 proteolipid protein	A_23_P60130	1.1	1.3	1	1.7	2.3	80.1	0.8	0.7	7.3	79.1	1.2	1.4	1.6	6.2
	MAOA	monoamine oxidase A	A_23_P83857	0.9	0.7	0.8	0.8	1.1	6.5	0.8	0.9	1.9	5.8	0.8	0.8	0.9	1
	MAP4K4	mitogen-activated protein kinase kinase kinase kinase 4 isoform 2	A_23_P108604	1	0.9	0.9	0.9	1.8	13.2	0.9	0.9	4	8.8	0.9	0.9	1.1	2.2
	MAP4K4	mitogen-activated protein kinase kinase kinase kinase 4 isoform 2	A_23_P102192	0.8	0.7	0.7	0.7	1.6	9.2	0.7	0.8	3.6	5.9	0.6	0.7	0.9	1.7
	MCL1	myeloid cell leukemia sequence 1 isoform 1	A_24_P319635	1.4	1.4	0.6	0.9	3.8	9.2	0.7	1	5.1	8.4	0.7	0.9	1.1	1.6
	MLL3	hypothetical protein	A_23_P168419	0.9	0.9	1	0.9	1.5	6.6	0.9	0.9	3.4	4	1	0.9	1	1.4
	NAV2	neuron navigator 2 isoform 1	A_23_P52727	0.8	0.9	1	0.8	1.6	12	0.9	0.9	4.7	7.4	0.9	0.7	1	2.2
	NAV2	neuron navigator 2 isoform 1	A_23_P354791	0.7	0.7	0.7	0.4	1.3	8.8	0.8	0.4	3.8	8.5	0.6	0.5	0.9	1.5
	NAV3	neuron navigator 3	A_24_P318160	0.9	1.1	0.7	0.9	2.3	40.1	0.8	0.8	7.8	31.2	0.6	0.9	1.9	3.2
	NAV3	neuron navigator 3	A_23_P13740	0.9	1	0.9	1	1.7	12.9	0.9	0.8	3.8	8.4	0.8	0.9	1.7	2.2
	NCALD	neurocalcin delta	A_23_P215883	0.8	0.6	0.9	1	3.8	16.8	0.9	0.7	5.8	14.7	1.3	1.2	1.1	2.3
	NCF2	neutrophil cytosolic factor 2	A_23_P138194	1.1	1	1	1.1	3.1	31.8	1	1	5.3	25.4	1	1	1.5	5.9
	NEFH	neurofilament, heavy polypeptide 200kDa	A_23_P300600	0.9	0.8	0.9	0.9	2.5	8.5	1.6	1.1	1.9	9.6	0.8	0.9	1	1.9
	NFIL3	nuclear factor, interleukin 3 regulated	A_23_P32253	1.5	1.2	1	1	3.1	6.2	0.9	1	3.1	6.3	1	1.1	1.2	1.5
	NFKB1	nuclear factor kappa-B, subunit 1	A_23_P30024	0.9	1.1	1	1	2.3	10.6	0.9	1	4.4	7.2	1	1	1	2.5
	NFKB2	nuclear factor of kappa light polypeptide gene enhancer in B-cells 2 isoform b	A_23_P202156	0.8	1.4	1.2	1.1	1.9	9.1	1.2	1.1	3.7	7.3	1.1	1.3	0.9	2.9
	NLRP3	NLR family, pyrin domain containing 3 isoform a	A_23_P9883	1.5	1	0.7	1.1	6.8	74.6	1.4	1	18.6	33.2	1.1	1	0.9	7.4
	NPPB	natriuretic peptide precursor B preproprotein	A_23_P62752	1	1.1	1.3	1.3	2.8	17.6	1.2	1.3	5.3	14.5	1.1	1.3	1.2	1.4
	NTN4	netrin 4	A_23_P204630	1	1	0.8	0.8	1.4	14	0.6	0.7	3.4	4.6	0.8	0.7	0.7	2.1
	OR1F1	olfactory receptor, family 1, subfamily F, member 1	A_23_P318890	1.2	1.3	1.6	1.4	2.7	13.3	1.4	1.3	7.1	6.7	1.1	1.1	1.1	3
	OTUD1		A_32_P60459	1.1	1	0.8	0.9	7.2	150.9	0.7	1.1	29.3	102.4	0.9	0.6	1.1	7.1
	OTUD1		A_24_P374834	0.8	0.8	0.6	0.6	6.8	85	0.5	0.7	24.1	55.8	0.7	0.5	1	5.3
	PAG1	phosphoprotein associated with glycosphingolipid microdomains 1	A_23_P347070	0.8	0.7	0.7	0.9	2.3	20.9	0.6	0.7	6.7	16	0.7	1.3	1.8	3
	PAM	peptidylglycine alpha-amidating monooxygenase isoform a, preproprotein	A_23_P213678	1.1	1.1	1.2	1.1	1.3	5.9	1.1	1	1.9	3.2	1.1	1.1	1.2	1.4
	PAPD4	PAP associated domain containing 4	A_23_P314202	1	1.2	1	0.9	1.8	5.6	0.8	1	3.1	4.5	0.9	1.1	1.2	1.4
	PELI1	pellino protein	A_23_P120345	1.4	1.1	1.1	1.3	2.5	13.8	1.2	1	5.3	8.6	1.1	1.1	1.2	3.5
	PHLDB2	pleckstrin homology-like domain, family B, member 2	A_24_P240166	1.5	1.4	0.9	0.9	2.7	9.6	0.7	0.9	5	5.1	0.9	0.8	1.3	1.7
	PLAG1	pleiomorphic adenoma gene 1	A_23_P411723	0.9	1	1	1.1	1.2	5.4	0.9	1	2.2	6	1	0.8	0.9	1.3
	PLCB4	phospholipase C beta 4 isoform a	A_23_P28898	0.9	1.2	1.3	1.7	3.6	22.5	1.5	1.7	16	23.9	1.1	1.2	1.2	1.9
	PLCG2	phospholipase C, gamma 2	A_23_P106675	1.4	1.4	1.6	1.4	3.5	50.2	1.4	1.4	11.7	32.6	1.7	1.2	1.4	6.2
	PLXNA1	plexin A1	A_23_P69068	0.9	0.7	0.6	0.7	1.4	6.5	0.9	0.9	3.2	4.2	0.8	1.3	1.3	1.6
	PPID	peptidylprolyl isomerase D	A_23_P386411	1	0.9	0.8	0.8	1.1	4.4	0.8	0.9	1.5	4	0.7	0.9	1.1	1.1
	PPM1K	hypothetical protein	A_24_P162532	1.9	0.7	1	1.1	4.7	8.9	1	1	3.5	7.3	1.1	1	0.9	2.7
	PRKD1	protein kinase D1	A_23_P106016	1.2	1	0.9	0.9	1.3	5.3	0.9	0.9	2	3.5	1.1	0.9	1	1.2
	PRRG4	proline rich Gla (G-carboxyglutamic acid) 4 (transmembrane)	A_23_P127663	1.8	1.6	1.3	1.4	3.3	16.5	1.5	1.2	4.9	6.8	1.4	1.1	1.7	3.3
	PTEN	phosphatase and tensin homolog	A_23_P98085	1	1	1.1	1	1.2	7.5	1.1	1	2.3	6	1	0.9	1	1.5
	RAB8B	RAB8B, member RAS oncogene family	A_23_P37535	1.4	1.4	1	1	1.9	10.1	0.9	1	2.6	5.6	1.2	1	1.1	2.2

	RAB9A	RAB9A, member RAS oncogene family	A_23_P45389	1	1	0.8	0.8	1.3	5.6	0.7	0.8	1.8	4.7	0.9	0.8	0.9	1.3
	RAPH1	Ras association and pleckstrin homology domains 1 isoform 1	A_24_P929570	0.9	0.9	0.5	0.7	2.9	22.2	0.6	0.7	6.6	19.3	0.7	0.9	1.3	2
	RASGRP1	RAS guanyl releasing protein 1	A_23_P124642	1.1	1.2	1.2	0.9	1.3	21.5	0.7	0.8	2.7	11.7	1.2	1.1	1.1	2.4
	RASSF5	Ras association (RalGDS/AF-6) domain family 5 isoform C	A_24_P171268	1.1	1	0.7	0.8	1.6	19.8	0.6	0.6	1.6	7.8	1.4	1.3	1.3	2.1
	RCOR1		A_23_P205247	1.2	0.8	0.8	0.8	2.5	12	0.7	0.8	4.1	9.4	0.6	0.5	0.7	1.5
	RELB	reticuloendotheliosis viral oncogene homolog B	A_23_P55706	0.9	1.5	1.2	1.1	2.4	25.7	1.1	1	6.2	22.2	1.1	1	0.9	4.4
	REV3L	REV3-like, catalytic subunit of DNA polymerase zeta	A_23_P214139	1	1.1	1	1.1	1.9	10.7	1.2	1.1	4.6	5.4	1	1	1.1	1.9
	RGAG1	retrotransposon gag domain containing 1	A_23_P306352	1	0.8	0.6	0.8	5	200.9	0.9	0.9	57.8	105.4	1	0.6	1.1	15.4
	RGMB	RGM domain family, member B isoform 2 precursor	A_24_P363100	1.1	1.2	1.2	1.2	1.9	7.3	1.1	1.3	3.2	5.8	1.1	1.3	1.2	1.7
	RGS20	regulator of G-protein signalling 20 isoform a	A_23_P73097	1	1.2	0.8	0.9	1.4	9.4	0.8	1	2.7	7.6	0.8	1	1.2	1.2
	RIPK1	receptor (TNFRSF)-interacting serine-threonine kinase 1	A_23_P370005	1.4	1.2	1.1	1	3	8.1	1.1	1.1	5.3	5.6	1	1	1	1.7
	RNF144	ring finger protein 144	A_23_P131566	1.3	1.3	1.2	0.9	2	12.3	1	1.2	2.2	9.7	1	1	1.1	2.1
	RNMT	RNA (guanine-7-) methyltransferase	A_23_P55515	0.9	1	0.6	0.7	1.2	6.6	0.6	0.7	2.1	7.7	0.7	0.8	0.9	1.1
	RP2	XRP2 protein	A_23_P22433	1.2	1.2	1.1	1	2.3	7.3	1.1	1	4	4.3	1	0.8	1	1.7
	RPS6KA6	ribosomal protein S6 kinase, 90kDa, polypeptide 6	A_23_P125596	0.8	0.8	0.7	0.9	1.3	5.9	0.7	0.8	2.4	5.7	0.7	0.8	1	1.4
	RPS6KC1	ribosomal protein S6 kinase, 52kDa, polypeptide 1	A_23_P104109	1.3	1.4	1.1	1	2.4	28.6	1.1	1	7	18.4	1.2	1	1.1	2.6
	RSRC2	arginine/serine-rich coiled-coil 2 isoform b	A_24_P350160	1.1	1.2	0.9	1	1.8	8.2	1	1.1	3.7	8.2	1.2	1.1	1.1	1.4
	SALL1	sal-like 1	A_23_P328074	0.8	0.8	1	1.1	1.5	35.3	1	1	4.5	15.4	1.6	0.8	0.9	3.2
	SAMD4A	KIAA1053 protein	A_23_P335661	1.1	1.2	1.1	1.1	2.7	14.2	1.1	1.2	7.4	9.1	1	1	1.2	2.2
	SAMD4A	sterile alpha motif domain containing 4	A_24_P383523	1.1	1.2	0.8	1.1	4.5	31.1	1.1	1.2	11	23.3	0.9	1.1	1.2	3.2
	SAMD8	sterile alpha motif domain containing 8	A_23_P63870	1.2	1.2	0.7	0.9	1.6	7.4	0.7	0.9	1.6	6.9	0.9	0.9	1.3	1.4
	SAR1A	SAR1a gene homolog 1	A_24_P158421	1.1	1.1	0.9	0.9	2.1	15.2	0.9	0.9	3.8	9	0.9	1	1.2	3.2
	SAR1A	SAR1a gene homolog 1	A_23_P127175	1	1.2	1.1	1	1.7	29.3	1.1	1.1	4.5	28.2	1	1	1.1	2.9
	SATB2	SATB family member 2	A_32_P174365	1.2	1.2	1	1	1.2	6.1	1	0.9	2.4	3.1	1	0.9	0.9	1.3
	SCN3A	sodium channel, voltage-gated, type III, alpha isoform 1	A_23_P67896	1.8	1.5	1.1	1.3	2.9	130.8	1.6	1.3	11.4	45.4	1.4	1.1	1.3	1.7
	SCYL1BP1	NTKL-binding protein 1	A_23_P368145	1.1	1.3	1	1	1.6	7.3	1	1.1	3.3	8.1	1	0.9	1.1	1.7
	SDK1	FLJ00148 protein	A_23_P93722	1	1	1.1	1	2.2	14.3	1.3	1.3	4.9	11.1	1	1.3	1.3	1.6
	SEPSECS	Sep (O-phosphoserine) tRNA:Sec (selenocysteine) tRNA synthase isoform 1	A_23_P167201	1.1	1.1	0.8	0.8	1.9	7.5	0.7	0.8	2.2	7.9	0.8	0.6	0.7	1.5
	SERTAD1	SERTA domain containing 1	A_23_P218463	1.2	1.1	1.2	1.1	2.1	6.6	1	1.1	3.6	5.4	1.1	1.3	0.9	1.1
	SLA	Src-like-adaptor	A_23_P216340	1.3	1.3	1.5	0.7	2.1	25	0.6	0.9	5.4	9.3	1.2	1.3	1	2
	SLC12A7	solute carrier family 12 (potassium/chloride transporters), member 7	A_24_P60634	1	1	1	0.8	2.4	20.4	0.8	1.1	11.8	17.7	0.9	1.2	1.3	3.1
	SLC12A7	solute carrier family 12 (potassium/chloride transporters), member 7	A_23_P251855	1	0.8	0.7	0.9	2.4	23.8	0.7	0.9	14.6	16	0.7	0.8	1	3.4
	SLC12A7	solute carrier family 12 (potassium/chloride transporters), member 7	A_23_P61688	1.6	1.6	1.7	1.3	3.6	50.1	1.5	1.5	26.5	45.1	1.5	1.3	1.5	5.1
	SLC25A25	solute carrier family 25, member 25 isoform b	A_24_P355267	1.1	1.1	1	1	2.4	6.7	0.9	1.1	3	5.8	1	1.1	1	1.4
	SLC2A13	solute carrier family 2 (facilitated glucose transporter), member 13	A_32_P199801	1	1	0.9	1	2.5	31.3	1	1.2	7.8	21.8	0.9	0.9	1.1	3.2
	SLC2A13	solute carrier family 2 (facilitated glucose transporter), member 13	A_23_P10211	1.2	0.9	1.1	1	1.5	14	0.9	0.9	3.5	11.3	1.2	0.9	1.4	2.8
	SLC30A7	zinc transporter like 2	A_23_P22915	1.1	1.1	0.8	0.9	1.3	5.3	0.9	1	2.2	4.6	0.8	0.9	1.7	1.3
	SLC31A2	solute carrier family 31 (copper transporters), member 2	A_23_P217109	1	0.8	0.7	0.8	1	9.4	0.6	0.7	2	8.1	0.7	0.7	0.9	1.1
	SLC33A1	acetyl-coenzyme A transporter	A_23_P144188	1.3	1.2	0.9	0.9	2.6	12.1	0.8	1	4.8	8.3	1	1	1.7	2.5
	SLC41A2	solute carrier family 41, member 2	A_23_P204801	1	1.1	0.9	0.9	2.5	19.2	0.7	0.8	4.7	15	1	0.9	1.1	2.8

	SLC6A12	solute carrier family 6 (neurotransmitter transporter, betaine/GABA), member 12	A_23_P76386	1.2	1.3	1.1	1.2	3.2	40.5	0.7	0.7	8.8	11.1	1.1	1.1	0.6	4.4
	SLCO5A1	organic anion transporter polypeptide-related protein 4	A_23_P135669	0.7	1.4	0.7	0.9	2.3	38.3	0.9	0.8	8.4	17	0.9	1.2	1	2.6
	SMPD3	sphingomyelin phosphodiesterase 3, neutral membrane	A_23_P163567	1.2	1.5	0.8	1.1	3.4	50.6	1	1.2	4.3	20.6	0.9	0.8	1.1	5.6
	SNAPC1	small nuclear RNA activating complex, polypeptide 1, 43kDa	A_23_P37244	1.4	1.3	1.1	1	2	6.3	0.9	0.9	2.8	8.9	1	1.1	1	1.7
	SNPH	syntaphilin	A_23_P102706	0.9	0.9	1.4	1.2	5.2	34.9	1.3	1.5	24.9	24.5	1.5	1.2	1.2	4.7
	SOD2	manganese superoxide dismutase isoform A precursor	A_23_P134176	2.1	1.9	1	1.1	1.9	11.4	0.8	0.9	3.1	9.1	1.1	1.1	1.2	2.5
	SPAG9	SPAG9 protein	A_23_P207476	1	1.2	0.9	1	2.4	15.4	1	1.3	6.2	8.2	0.9	1.1	1.2	2.3
	SPAG9	sperm associated antigen 9	A_24_P365025	1	1	0.8	0.9	1.4	8.8	0.8	0.9	3.2	6.5	0.8	0.9	1.2	1.8
	SPRY2	sprouty 2	A_23_P128698	0.8	1.1	0.7	0.8	2.8	20.1	0.8	1	7.3	14	0.7	0.8	0.7	1.8
	SRPK2	SFRS protein kinase 2 isoform b	A_23_P406438	1	1	0.8	0.8	1.5	11.4	0.7	0.7	2.7	7.8	0.8	0.9	1.1	2.1
	SRPK2	SFRS protein kinase 2 isoform b	A_23_P215599	1	0.9	0.9	0.9	1.7	10.8	0.8	0.9	3.1	7.7	0.9	0.9	1.2	1.9
	STARD13	START domain containing 13 isoform alpha	A_23_P342727	1.1	1.1	0.6	0.8	2.9	9.3	0.8	1	4.3	7.8	0.7	0.6	0.9	1.3
	STARD13	START domain containing 13 isoform alpha	A_24_P210420	1	0.7	0.7	0.7	2.3	6.5	0.8	0.8	4.1	5.9	0.8	0.6	1	0.8
	STK38L	serine/threonine kinase 38 like	A_23_P64743	1.3	1.2	1	1.1	2.5	15.3	1	1.1	4.1	13.4	1.1	1.1	1.3	2.5
	STX11	syntaxin 11	A_23_P156788	0.9	0.8	0.7	0.8	2.4	11	0.7	0.8	3.4	9.5	0.8	1	1.1	2.3
	SYDE1	synapse defective 1, Rho GTPase, homolog 1	A_23_P101796	0.9	0.9	0.6	0.8	1.4	8.8	0.9	0.9	2.5	5.5	0.8	0.9	0.8	1.3
	TAL2	T-cell acute lymphocytic leukemia 2	A_23_P409449	1	0.8	0.9	1.3	2	23.9	1	1.3	6.4	13.2	0.9	1.5	1.8	2.2
	TEP1	telomerase-associated protein 1	A_23_P65481	1.2	1.4	1.3	1.4	3.9	16.5	1.2	1.2	8.8	10.9	1.2	1.1	1.2	2.1
	TESK2	testis-specific protein kinase 2	A_23_P9875	1	0.9	1.1	1.3	3	16.2	1.5	1	5.3	8.3	1.3	1	1	3
	THRAP1	mediator of RNA polymerase II transcription, subunit 13 homolog	A_23_P27247	1.2	1	0.9	0.9	2.1	7	0.8	0.9	4.1	5.4	0.9	1	1.2	1.7
	TMEM38B	transmembrane protein 38B	A_23_P60259	1.1	1	0.7	0.8	1.1	10	0.7	0.8	1.6	7.1	0.7	0.9	1.2	1.7
	TMEM38B	transmembrane protein 38B	A_24_P278156	1	1	0.6	0.8	1	6.4	0.6	0.7	1.2	5.6	0.7	0.9	1.2	1.2
	TMEM47	transmembrane 4 superfamily member 10	A_24_P143171	1.1	1.1	0.3	0.8	2.2	65.6	0.3	0.5	3.3	44	0.6	1	1.9	3.6
	TNFAIP6	tumor necrosis factor, alpha-induced protein 6 precursor	A_23_P165624	1.5	1.2	0.5	0.5	1	50.9	0.9	1	4.3	26.5	0.5	0.6	0.7	7
	TNFRSF10B	tumor necrosis factor receptor superfamily, member 10b isoform 1 precursor	A_23_P169030	1	1.2	0.9	1	2.3	11.5	1.1	1	4.8	8.9	0.9	1	1.2	2.5
	TRAF1	TNF receptor-associated factor 1	A_23_P216970	0.7	1.1	1.2	1.2	4.6	25.8	1.1	1.3	12.8	18.2	1.5	1.4	1.4	2.7
	TRAF6	TNF receptor-associated factor 6	A_23_P75921	1	1.1	0.8	0.8	1.6	6.1	0.7	0.9	1.9	5.4	0.9	0.9	1	1.4
	TRAPPC6B		A_24_P304581	1.1	1.1	0.6	0.9	1.3	5.6	0.7	1	2.6	6.8	0.6	0.9	1	1.6
	TRIM26	tripartite motif-containing 26	A_24_P898583	1.6	1.4	1.2	1.2	3.8	12.1	1.2	1.3	6.2	8.4	1.2	1.3	1.3	2.3
	TRIM26	tripartite motif-containing 26	A_23_P214587	1.3	1.2	0.8	0.8	2.4	6.9	0.7	0.9	4	5	0.8	0.9	1	1.5
	TRIM69	tripartite motif-containing 69 isoform a	A_23_P48826	1.3	1.4	1.3	1.1	1.8	7.9	1.3	1.2	2.3	3.5	1.2	1.2	1.2	1.6
	TRPC4	transient receptor potential 4	A_23_P105873	0.6	0.4	0.7	0.8	3	107.7	0.7	0.7	30.2	98.8	0.5	0.5	0.7	4.5
	TTC26	tetratricopeptide repeat domain 26	A_24_P89718	1	0.8	0.6	0.9	1.1	5.4	0.6	1	1.8	3.3	0.7	0.8	0.9	1
	TTC28	KIAA1043 protein	A_23_P29185	1.2	1.2	1.2	0.9	1.3	6	1	1	2.5	4.5	1.2	0.9	1	1.4
	UBE2Z	ubiquitin-conjugating enzyme E2Z (putative)	A_24_P378506	1	1.1	1	1	1.8	10.4	1	1.1	3.1	7.8	1	1	1	1.7
	UBE2Z	ubiquitin-conjugating enzyme E2Z (putative)	A_23_P83438	1	1	0.9	0.9	1.7	10.5	0.9	0.9	2.6	9	0.9	0.9	1	1.7
	UTX	ubiquitously transcribed tetratricopeptide repeat, X chromosome	A_23_P217304	1	1.1	0.8	0.8	2.4	26.3	0.8	0.9	6	15.1	0.8	0.7	1	2.3
	WDR48	WD repeat domain 48	A_23_P80409	1.1	1.2	1	1	1.3	5.4	0.9	1	2.1	5.5	0.9	0.9	1	1.2
	WHDC1		A_24_P307827	1.5	1.4	1.3	1.2	4.1	15.3	1.2	1.3	5.8	10	1.2	1	1.2	1.9
	WNK1	WNK1 protein	A_24_P51127	1	1	0.6	0.8	1.4	10.3	0.5	0.7	1.7	6.3	0.7	0.7	0.8	1.3
	WTAP	Wilms' tumour 1-associating protein isoform 1	A_23_P371155	1.5	1.3	1.5	1.3	1.8	11.1	1.5	1.4	4	9.2	1.4	1.2	1.1	2
	WTAP	Wilms' tumour 1-associating protein isoform 2	A_23_P215037	1	0.8	0.4	0.6	0.9	6.4	0.4	0.6	1.1	4.3	0.5	0.7	0.9	1.4

	XPA	xeroderma pigmentosum, complementation group A	A_23_P60283	1.1	1.1	0.8	0.8	1.2	7.2	0.7	0.8	2.2	8	0.8	0.8	0.8	1.2
	ZBTB10	zinc finger and BTB domain containing 10	A_23_P385114	1.1	0.9	0.6	0.7	1.8	19.3	0.6	0.7	3.4	15.9	0.6	0.8	1	1.8
	ZBTB43		A_24_P149713	1	1	0.8	0.8	1.6	4.7	0.9	1.1	2.2	4.3	0.8	1	1	1.1
	ZC3HAV1	zinc finger antiviral protein isoform 1	A_23_P425224	3.7	0.7	1.2	1.2	7.1	88.4	1	1.5	24.1	40	1.2	1.1	1.6	5.7
	ZEB2	zinc finger homeobox 1b	A_23_P142560	1.5	1.5	1.1	1.1	6.1	90.6	1	1.1	19.2	62.2	1.3	0.9	1	5.9
	ZFY	zinc finger protein, Y-linked	A_24_P942743	1	0.9	0.8	0.7	1.5	10.1	0.6	0.7	2.4	8.5	0.8	0.8	0.9	2.1
	ZFY	zinc finger protein, Y-linked	A_23_P62465	1.2	1.1	0.8	0.9	1.4	5.4	1	1	2	4.7	0.9	1	1.1	1.2
	ZHX2	zinc fingers and homeoboxes 2	A_23_P168951	1	0.9	0.8	0.9	1.3	11	0.8	0.9	2.1	8.5	0.9	1.2	1.1	2
	ZNF134	zinc finger protein 134	A_23_P141866	1	1.1	0.7	0.9	1.5	4.8	0.8	1	2	5.7	0.7	0.9	1	1.3
	ZNF134	zinc finger protein 134	A_23_P325661	1	1.1	0.8	0.9	1.6	6.2	0.8	1	2.2	6.2	0.9	1	0.9	1.3
	ZNF14	zinc finger protein 14	A_23_P101811	1	1.1	1	1	1.7	6.2	0.9	1	3.9	5.7	0.9	0.9	0.9	1.4
	ZNF200	zinc finger protein 200 isoform 1	A_23_P152356	1.1	1	0.7	0.8	1.5	9.7	0.6	0.7	3.1	7.3	0.8	0.8	0.9	1.4
	ZNF24	zinc finger protein 24 (KOX 17)	A_24_P339450	1.2	1	0.8	0.7	1.9	9.1	0.6	0.8	1.9	10.1	0.8	0.9	1.2	1.7
	ZNF323	zinc finger protein 323 isoform 1	A_24_P137713	1	1	0.8	0.9	1.8	5	0.7	0.9	2.5	6	0.8	0.9	0.9	1.4
	ZNF416	zinc finger protein 416	A_23_P55688	0.9	1	0.8	0.9	1.6	3.6	0.9	1.1	2	4.9	0.9	0.9	0.9	1.2
	ZNF529	zinc finger protein 529	A_23_P433676	1.1	1.3	1.2	1.1	1.5	8.2	1	1.2	2.4	8.2	1.1	1	1.1	1.6
	ZNF567	zinc finger protein 567	A_23_P354894	1.1	1.2	1.1	1.1	1.2	9	1	1.1	3	6.2	1.1	1	1	1.3
	ZNF597	zinc finger protein 597	A_23_P3753	1.4	1.2	0.9	1	2.4	7.9	1.2	1.5	3.5	6.5	1	1.2	1.1	1.4
	ZNF638	zinc finger protein 638	A_24_P419177	0.9	1.1	1	1	2	4.7	1	1	2.8	4.6	0.9	1.1	1	1.1
	ZNF670	zinc finger protein 670	A_23_P74981	1.1	1.1	0.8	1	1.7	7.1	0.7	0.9	2.8	6.5	0.8	1	1.1	1.5
	ZNF671	zinc finger protein 671	A_23_P50217	0.7	1	0.8	0.6	1.2	5.1	0.7	0.8	2.7	6.2	0.8	0.7	0.8	1
	ZNF697		A_32_P19716	1	0.9	0.8	0.7	2.8	21.1	0.5	0.9	5.9	21.4	0.9	0.9	1	2.6
	ZNF711	zinc finger protein 711	A_23_P217297	1	1.1	0.8	0.9	1.8	7.5	0.6	0.8	2	11.3	0.9	1	1	1.8
	ZNF79	zinc finger protein 79 (pT7)	A_24_P128312	1.1	1.2	0.9	1	2	5.7	1	1.2	2.5	6.3	1	1.2	1	1.4
	ZNF79	zinc finger protein 79 (pT7)	A_23_P303763	1.2	1.3	1	1	2.1	6.3	1.1	1.2	2.1	7.2	1	1.3	1	1.5
	ZSWIM3	zinc finger, SWIM domain containing 3	A_23_P165984	0.9	1.1	0.6	0.7	1.4	4	0.8	0.9	2	4.1	0.7	0.8	0.9	1
		adenosylhomocysteinase 3	A_24_P72518	1.1	1	0.9	0.9	1	7.7	0.7	0.8	1.2	3.8	0.9	1	1	1.5
		adenosylhomocysteinase 3	A_23_P252075	1.2	1.3	1	1.2	2.1	20.9	1.1	1.3	3.8	13.3	0.9	1	1.1	2.5
		hypothetical protein	A_23_P389250	1.4	1.7	1	1.6	3	15.5	1.2	1.3	6	10.5	1	1.2	1.6	2.4
		hypothetical protein	A_32_P82863	1.2	1.2	0.7	0.9	1.7	7.5	0.8	0.8	1.8	13	0.7	1.1	0.9	1.9
		hypothetical protein LOC152641	A_24_P354496	0.9	1.2	0.7	1	1.6	6.8	0.9	1.1	2.8	6.7	0.9	0.8	0.8	1
		hypothetical protein LOC79912	A_23_P204187	1	0.9	0.7	0.8	1.4	5.9	0.6	0.8	1.7	6.6	0.7	0.9	1	1.4
		hypothetical protein LOC79912	A_24_P221407	0.9	0.9	0.7	0.7	2.8	8.1	0.7	0.8	1.6	5.9	0.5	0.8	0.9	1.6
		hypothetical protein LOC90634 isoform 1	A_23_P76658	2	1.4	1.1	1.4	1.9	6.1	1	1.2	6.4	6	1.2	1.3	1	1.3
		junction-mediating and regulatory protein	A_32_P176550	1	1.1	1	0.9	2.2	12.5	1	1	4.2	7.5	1	0.6	0.8	2.1
		KIAA2002 protein	A_23_P65851	1	1.1	0.7	1	1.4	5.3	0.9	1	2.6	8.1	0.9	1	1.1	1.5
		niban protein isoform 2	A_23_P217832	1	0.8	0.8	0.9	2.1	18.6	0.8	0.7	2.2	19.9	0.8	1	1.2	2.7
		PALM2-AKAP2 protein isoform 1	A_23_P359043	1.2	0.8	0.5	0.6	1.5	7.6	0.5	0.6	1.8	4.5	0.6	0.7	1.1	1.6
		TRAF-interacting protein with a forkhead-associated domain	A_24_P350686	1.1	1.1	1	1	1.4	9	0.8	1	2.6	10.4	1.1	1	1	2.3
			A_32_P99804	1.7	1.5	1.3	1.3	4.6	29.7	1.5	1.7	14.2	22.6	1.3	1	1.2	3.6
			A_32_P88905	1.2	1.1	1.2	1.2	2.6	14.9	1.2	1.3	8.4	8.7	1.2	1	1	2.4
			A_24_P68222	1.1	1.1	1.4	1.2	4.2	32.6	1.3	1.5	13.5	22	1.3	1.1	1.1	3.6
			A_32_P165407	0.7	1	1.1	1	2.9	19.9	0.9	1	8.3	8.4	0.9	0.9	1	1.9
			A_32_P192389	1.1	1.3	1.3	1	3.5	31.8	1	1.1	8.4	23.6	1.1	0.9	1	2.7
			A_32_P117322	1.2	1.1	1	0.9	6.7	171.2	1	1.2	24	98.1	1.1	1.3	0.6	4.8
			A_32_P137604	0.7	1.1	1.2	1.1	2.5	17.7	1.2	1.1	6.8	9.4	1.1	0.8	0.9	2.7
			A_32_P68504	1.3	1.4	1.3	1.5	5.4	86.3	1.3	1.4	26.8	46.3	1.2	1.3	1.4	7

			A_24_P823011	1	1	0.7	0.8	1.8	7.6	0.6	0.9	4.5	4.9	0.9	0.9	1	1.9
			A_32_P73143	1	0.7	1.3	1	11.9	69.5	0.8	0.9	18.3	58.8	1	1.9	1.8	5.3
			A_24_P67574	1.6	1.4	1.8	1.3	3.8	12.9	1.7	1.1	7.9	9.9	1.1	1.5	1.9	2.7
			A_24_P915784	1.3	1.2	0.9	0.9	2.2	40.2	0.8	0.9	5.2	27.6	0.8	1.1	1.3	2.9
			A_24_P20139	1.2	1.3	0.7	0.8	2.7	22.5	0.7	1	5.7	19.1	0.8	0.9	1.1	2.5
			A_23_P368909	1.2	1.1	0.9	1.1	2	27.6	0.8	0.8	4.4	17.2	0.7	0.9	1	1.7
			A_23_P356041	0.8	0.7	0.5	0.6	1.4	6.7	0.5	0.7	2.3	4.6	0.5	0.7	1.1	1.4
			A_32_P62196	1	1.3	1.2	1	2.1	16.9	1.2	1.1	5	12.2	1	1.5	2	2.2
			A_32_P104841	1.4	1.5	1.4	0.9	3.4	64.6	0.8	1.2	14.4	45.3	1.3	1.4	3.3	9.4
			A_32_P53183	0.8	0.9	0.9	0.9	2.1	11.2	0.8	1.2	4.4	9.7	0.8	1	1.1	1.4
			A_23_P64962	1.1	0.7	0.9	1	3.6	39.5	1.5	1.2	7.1	19.9	1.1	1.5	1.2	2.5
			A_24_P8454	0.8	0.8	0.8	0.9	1.8	8.2	0.9	1.2	3.8	5.5	0.8	1	1.2	1.8
			A_32_P88349	1.1	1.8	1.3	1.2	2.7	10.8	1.4	1.3	5.4	11.2	1.3	1.1	1.1	2.7
			A_24_P255384	0.9	2.1	0.9	1	1.8	52.3	0.8	1.3	13.5	31	0.9	0.9	0.9	7.3
			A_23_P49725	0.8	2	1.2	1.1	2.4	35.6	1.6	1.2	8.3	17.4	1.4	0.5	0.7	3.7
			A_32_P66908	1.3	1	0.8	0.8	16.3	65.5	0.9	0.9	17	44.2	1.1	0.9	1.2	2.8
			A_24_P389612	1.2	1.2	0.8	0.8	3.6	18.2	0.7	0.9	8.2	14	0.8	0.8	1.2	2.1
			A_32_P118847	1.2	1.1	0.9	1	2.6	11.3	0.9	0.9	6	7.5	0.9	0.9	1.1	1.5
			A_24_P535256	1	2.1	0.8	0.6	3.6	14.8	0.6	1	6.7	7.1	0.6	1.2	1.7	2.5
			A_32_P36280	1.1	1.3	0.9	0.8	2.4	9.5	1.3	1.2	4	8.5	0.8	0.6	0.9	1.6
			A_23_P435029	1.1	1.3	1	0.8	1.8	5.8	1.4	1.2	4.3	4.4	1.2	0.7	0.9	1.4
			A_24_P364066	1.3	0.9	1	1	2	7.7	0.9	1	4	3.6	1	1	1.2	1.8
			A_32_P6172	1	0.9	0.8	0.8	1.5	15.2	0.9	1	5.4	10.1	0.8	0.9	1	1.7
			A_24_P814096	1	1	0.8	0.9	1.5	5.2	0.8	0.9	2.2	3.8	0.8	0.7	0.8	1.2
			A_24_P523061	1	1	1	1	1.5	5.5	1	1.1	2.6	4	1	0.8	0.9	1.3
			A_32_P39384	1.2	1	0.9	0.9	1.4	7.7	0.8	0.8	2.7	7.6	1	0.8	0.7	1.5
			A_32_P148407	0.9	0.9	1.3	1	1.3	15.9	1	0.9	3.1	10	1	1.1	1.4	2.5
			A_24_P929835	1	1.5	0.8	1	2	5.9	1.1	1.3	4.2	5.9	0.9	0.9	1.1	1.4
			A_24_P222591	1	1.1	0.7	0.9	1.7	5.5	0.8	1	2.1	6.4	0.8	0.9	1.2	1.3
			A_32_P174110	1.2	1.1	0.9	1.8	1.8	7.9	0.8	1.2	2.8	6	1.2	1	1.3	1.4
			A_23_P317654	1.2	1	0.7	0.9	1.6	5.5	0.8	0.9	2.3	3.2	0.7	0.9	1.1	1.1
			A_24_P887092	2	0.9	0.9	1	1.9	18.2	0.9	1.1	2.6	12.2	0.9	1	0.7	4.5
			A_24_P47329	2.7	2	1.7	1.4	4.2	39.6	0.9	1.1	7.5	12	1.4	2.3	2.9	6.3
			A_24_P307395	0.9	0.8	0.5	0.5	1	7.3	0.5	0.6	1.7	3.4	0.5	0.8	0.9	1.5
			A_23_P14302	1.1	1	1.2	1.1	1.9	10.6	1.3	1.3	2.2	4.8	1.2	1.1	1.5	2.6
			A_32_P222571	1.9	1.5	1.7	1.6	3.7	9.3	1.7	1.9	5.6	7.1	1.4	1.3	1.3	2
			A_32_P207767	1.1	1.2	1	0.8	2	8.2	0.8	0.9	2.9	6.9	0.6	0.8	1	1
			A_23_P418031	1.4	1.5	1.5	1.3	2.5	6.1	1.5	1.4	3.9	4.8	1.5	1.6	1.3	1.4
			A_23_P143016	1.3	1.2	1.1	1.1	2.8	6.5	1.3	1.2	3.6	4.4	1	1.3	0.9	1.2
			A_32_P108567	0.7	0.8	1.2	1	3.9	11.1	1.2	0.8	3.8	7.3	1.1	0.5	1.1	1.9
B	ACAN	aggrecan isoform 2 precursor	A_23_P307310	1	1.3	1.4	1.4	12.4	30.8	1.4	1.2	19.6	20.3	1.2	0.9	2.1	14.2
	ACTN2	actinin, alpha 2	A_23_P115021	0.8	1.6	0.9	1.1	16.3	475.3	1	1	185.3	235.8	1.1	0.9	1.4	40.8
	ATF3	activating transcription factor 3 isoform 2	A_24_P33895	1.4	0.8	0.5	0.6	7.1	21.1	0.4	1.4	11.1	19.3	0.5	0.8	1.5	3.4
	BAMBI	BMP and activin membrane-bound inhibitor precursor	A_23_P52207	0.9	0.7	1.2	1	4.6	18.9	0.8	1	11.6	9.8	1.3	1.1	1.3	3
	BIRC3	baculoviral IAP repeat-containing protein 3	A_23_P98350	1.1	1.9	1	0.9	6.5	40.8	0.7	0.9	11.6	34.9	1	1	1.7	9.2
	C17orf66	hypothetical protein LOC256957	A_23_P430792	0.8	0.6	0.9	1.1	34.5	123.5	1	1.7	100.1	79.3	0.9	1.3	3.3	40.4
	C17orf76	hypothetical protein LOC388341	A_23_P368484	0.8	1.2	1.2	1.1	2.9	12	1.1	1.2	5.8	7.5	1.2	1.1	0.9	2.6
	C19orf30	hypothetical protein LOC284424	A_23_P353667	1.5	1.4	1.1	1.3	3.7	19.6	1.9	1.1	10.3	12.8	1	1.5	0.7	6.3

	C20orf141		A_32_P133182	6.2	2.4	0.8	1.5	48.5	166.7	0.8	3.4	237.7	99.4	1.1	1.1	4.1	13.9
	C3orf59	hypothetical protein LOC151963	A_23_P326963	1.3	1.5	0.9	0.5	4.5	9	0.8	0.8	4	12.9	0.6	1	1.4	1.4
	CASP3	caspase 3 preproprotein	A_23_P92410	1.1	1.1	0.9	1	2.3	6.3	1	1	6.5	4.1	1	1	1.1	2.5
	CCL20	chemokine (C-C motif) ligand 20	A_23_P17065	0.7	0.7	1	1.1	4.2	115.8	0.6	1.8	36.2	69.1	0.8	0.9	0.9	27.4
	CCL4	chemokine C-C motif ligand 4 isoform 1 precursor	A_23_P207564	0.7	1.4	1.1	1.8	40.2	142.2	1.1	4.3	69.3	81.1	0.9	2.2	3.3	30.7
	CSAG1	chondrosarcoma associated gene 1 isoform b	A_24_P11061	1.8	2.1	1.2	1.2	6.7	33.9	1	1	18.6	21.3	1	1.2	1.4	8
	CSAG2	CSAG family, member 2	A_24_P567298	1.3	2.1	1.1	1.2	7.4	43.6	1.1	1.5	23.5	30.2	1.3	1.3	1.6	8.2
	CSAG3A	CSAG family, member 3A	A_24_P79529	1.3	2.8	1.2	1	12.7	70.9	1	1.2	40.8	45.9	1.1	1.1	1.7	15.7
	CXCL1	chemokine (C-X-C motif) ligand 1	A_23_P7144	1	1.1	1.1	1	1.9	10.4	0.7	1.3	4.1	7.2	1.1	0.9	0.9	4.6
	CXCL2	chemokine (C-X-C motif) ligand 2	A_24_P257416	1.5	1.2	1.3	1.2	3.5	7.5	1.1	1.8	5.5	5.3	1.2	1.2	1.3	3.9
	CXCL3	chemokine (C-X-C motif) ligand 3	A_24_P251764	1.6	1.2	1.3	1.2	3.6	8.4	1.1	1.8	5.7	6.1	1.2	1.2	1.4	4.3
	CXCL3	chemokine (C-X-C motif) ligand 3	A_24_P183150	1.7	1.3	1.2	1	4.4	16.3	0.9	1.9	10.1	11.5	1.1	1	1.3	6.1
	CXCR4	chemokine (C-X-C motif) receptor 4 isoform a	A_23_P102000	0.8	1	1.2	1.3	25.1	273.6	1	1.3	81.9	72.2	1.3	1.4	1.7	27.2
	DCHS1	dachsous 1 precursor	A_23_P98645	0.8	1.4	1.4	1.1	7.4	14.9	1	1	13.3	10.4	1.5	1.5	1.8	6.9
	DENND4A		A_23_P420092	2.1	0.9	0.7	1.3	1.6	8.7	0.5	0.5	3.6	6	0.6	1.1	1	1.3
	DNAJC15	DNAJ domain-containing	A_23_P117190	2.2	1.8	1.8	1.4	10.2	48.1	0.8	1.8	22.7	17	1.2	2.3	2.2	6.3
	EGR4	early growth response 4	A_23_P380318	0.9	1.1	1.5	1.3	33.3	84	1.4	4.4	56.3	46.2	1.2	1.2	2.5	23.8
	FUT1	fucosyltransferase 1	A_23_P107963	0.6	1.2	1.3	1.3	5	25.6	1.4	0.9	8.8	17.7	1.1	1.6	1.4	5.1
	FZD4	frizzled 4	A_23_P64617	0.9	1.3	1.1	1.1	7.5	75.2	1.2	1.4	22.8	49.5	1.1	0.9	1.4	14.3
	GATA3	GATA binding protein 3 isoform 1	A_23_P75056	1.2	2.1	1	0.9	3.6	6.9	0.7	1	3.2	7.9	1.2	1	0.8	1.8
	HES4	hairy and enhancer of split 4	A_23_P149448	1.3	2.5	1.4	1.3	4.2	10.9	1.4	1.5	7.7	7.6	1.3	1.4	1.3	3
	HIP1R	huntingtin interacting protein-1-related	A_24_P229164	0.9	0.9	1.1	1.2	5.9	14.7	1.2	1.5	11.1	9.6	1.1	1.2	1.4	4.8
	HIP1R	huntingtin interacting protein-1-related	A_23_P398294	1.1	1.2	2	1.7	14.5	103.1	1.8	2.2	43.5	48.3	1.8	1.4	1.8	11
	HOXB4	homeobox B4	A_24_P416370	2.9	2	1.2	1.6	14.3	48.8	1.2	1.7	44	32.1	1.2	0.9	2.1	5.8
	HTR3E	5-hydroxytryptamine receptor 3 subunit E	A_24_P32139	0.8	1.6	1.1	1.1	3.8	39.6	0.8	1	21.8	23.4	1	1.1	1.1	5.7
	ICAM1	intercellular adhesion molecule 1 precursor	A_23_P153320	4	1.8	0.9	1	14.2	75	0.8	1	39.2	57.2	0.7	1	2.5	23.3
	IL3RA	interleukin 3 receptor, alpha precursor	A_32_P217750	1.2	1.9	1.9	1.1	3.9	15.2	1.9	1.5	6.9	10	1.4	1	1.3	6.2
	IL8	interleukin 8 precursor	A_32_P87013	2.1	1.2	1	1.1	18.9	112.8	0.7	2.2	42.3	43.2	1.1	1.4	2.8	17.7
	JAK2	Janus kinase 2	A_23_P123608	1.8	1.2	1	1	9.1	22.5	0.9	1.1	14.8	13.2	0.9	1	1.6	5.1
	KCNN1	potassium intermediate/small conductance calcium-activated channel, subfamily N, member 1	A_23_P119573	0.9	0.7	1	1.3	11.7	48.8	1	1.3	32.6	27.4	1	1	1.7	9.3
	KLF2	Kruppel-like factor	A_23_P119196	0.8	0.8	1.1	1.1	5.6	25.4	1.2	1.4	16.4	11.8	1	0.9	1	3.1
	KLF4	Kruppel-like factor 4 (gut)	A_23_P32233	1	0.8	0.7	0.9	11.2	51.6	0.6	1.1	24.8	34.7	0.8	1	2.3	9.2
	KLHDC7B	kelch domain containing 7B	A_24_P117410	1.2	2.6	1.4	1.1	10.2	56.3	1.3	1.3	17	27.1	1.1	1.3	1.9	11.1
	LRRN3	leucine rich repeat neuronal 3	A_23_P31376	1	1.7	0.7	1.1	109.1	386.8	0.9	1.8	192.9	193.2	0.9	1.5	7.3	81.3
	LTB	lymphotoxin-beta isoform a	A_23_P93348	0.8	1.1	0.9	1.3	3.3	34.4	1.6	1.5	9.8	28.6	0.8	1	1.1	18.7
	MED12L	mediator of RNA polymerase II transcription, subunit 12 homolog (S. cerevisiae)-like	A_32_P701268	0.8	0.7	1.9	1.2	4.1	46.7	1.6	1.2	18.3	23.7	1.4	2.4	1.3	6.6
	MXD1	MAX dimerization protein 1	A_23_P408094	1.1	1.2	1.3	1.2	5	21.7	1.5	1.5	9.8	10.4	1.2	1.2	1.3	4.6
	NFKBIA	nuclear factor of kappa light polypeptide gene enhancer in B-cells inhibitor, alpha	A_23_P106002	1.1	1.3	1	1.1	9.7	59	0.8	2	34.7	24.5	1	1.1	1.6	7.1
	NFKBIE	nuclear factor of kappa light polypeptide gene enhancer in B-cells inhibitor, epsilon	A_23_P30655	0.8	1.2	1.2	1.2	3.9	20.3	1.1	1.1	7.5	12.4	1.2	1.3	1.1	3.7
	PIWIL4	piwi-like 4	A_23_P427760	1	1.5	1.5	1.6	3.4	8.8	1.3	1.3	7.7	6	1.1	1.3	1.4	3.3
	PLA2G4C	phospholipase A2, group IVC	A_23_P50508	1	1.1	0.7	1	7.5	60.9	0.7	1.2	21.1	28.1	0.9	1	1.3	8.3
	PMAIP1	phorbol-12-myristate-13-acetate-induced protein 1	A_23_P207999	2	1.4	0.6	1.1	12.6	34.2	0.7	2	24.5	21.1	0.7	1.1	1.8	5.3
	PPP1R15A	protein phosphatase 1, regulatory subunit 15A	A_23_P90172	0.9	1	1.1	1.2	10.5	34.8	1.2	2.4	20.4	19.2	1	1.1	1.4	5.7

	PRDM1	PR domain containing 1, with ZNF domain isoform 1	A_23_P350451	1	1.5	1	1	6.9	7.9	0.9	1.1	5.3	6.2	1	0.9	1	2.9
	PRR15	proline rich 15	A_32_P154911	2.4	1.6	1.6	1.6	9	12.4	1	1.5	12.2	9.1	1.8	1.5	2.3	6.8
	PTGER4	prostaglandin E receptor 4, subtype EP4	A_23_P148047	1.1	0.9	0.6	0.9	20.5	146	0.5	2	41.7	72.9	0.7	1.1	2.3	14.4
	PTX3	pentraxin-related gene, rapidly induced by IL-1 beta	A_23_P121064	0.8	1.2	0.6	0.7	24.5	127.4	0.6	1	67.2	89.1	0.7	0.8	1.4	20.1
	RHEBL1	Ras homolog enriched in brain like 1	A_23_P2307	1.1	1.1	0.7	1	4.2	15.9	1	1.4	7.8	12.4	0.8	0.8	1.1	3.9
	SEMA3D	semaphorin 3D	A_32_P29118	0.9	0.8	0.9	1	19.8	258.3	1	1.3	73.8	127.7	1	1	2.2	21
	SLC1A3	solute carrier family 1 (glial high affinity glutamate transporter), member 3	A_24_P286114	0.8	0.8	1	1.1	33.5	195.1	1.5	1.4	125.4	105.4	1.4	0.9	1.8	17.1
	TMC8	FLJ00400 protein	A_23_P346093	0.7	1.5	1	1.6	5	21.8	1.7	1.9	11.7	15.4	0.8	1.4	1.8	5.3
	TNFAIP2	tumor necrosis factor, alpha-induced protein 2	A_23_P421423	0.9	1.1	2	1.6	2.9	19.5	1.5	1.5	9.6	13.4	1.8	1.4	1.3	5.3
	TNFAIP3	tumor necrosis factor, alpha-induced protein 3	A_24_P166527	1	0.7	0.9	1.2	11.1	36.7	1	2.5	29	23	0.9	1	1.5	6.6
	TNFAIP3	tumor necrosis factor, alpha-induced protein 3	A_24_P157926	1.4	1.5	1.1	1.5	17.1	78	0.8	2.7	34.1	37.5	1.2	1.2	1.9	13.8
	TNFRSF9	tumor necrosis factor receptor superfamily, member 9 precursor	A_23_P51936	1.1	1.2	1.1	1.1	4.2	28	1.4	1.1	12.4	19.1	1	1.4	2.3	8.2
	TRAF1	TNF receptor-associated factor 1	A_24_P89891	0.7	1.7	1.4	1.3	5.6	21.8	1.1	1.4	14.8	14.5	1.1	1.4	1.4	3.6
	TTC9B		A_23_P332392	1	1	1	1	8	25.1	1.2	1.3	15.3	16	1	1.2	1.4	7.2
	ULBP2	UL16 binding protein 2	A_23_P168259	1.1	1	0.7	1	8	26.5	0.6	1.4	16.2	16.8	0.7	1	1.4	4.1
	ULBP2	UL16 binding protein 2	A_24_P149314	1.2	1	0.6	0.7	6.5	13.7	0.7	1.1	13.1	8.9	0.9	1.1	1.5	2.8
	ULBP2	UL16 binding protein 2	A_23_P145485	1.1	0.9	0.6	0.8	6.4	16.6	0.8	1.3	13.4	10.7	0.8	1.1	1.3	3
	WISP1	WNT1 inducible signaling pathway protein 1 isoform 1 precursor	A_23_P354694	1.4	2	1.2	1	11.9	59.1	1.1	1.4	38.8	18.7	1.2	0.9	1.1	9.1
	XBP1	X-box binding protein 1 isoform XBP1(U)	A_23_P120845	1	1	0.8	0.9	5.1	12.9	0.7	1	7.4	12.7	0.8	1	1.7	2.3
	ZC3HAV1	zinc finger antiviral protein isoform 2	A_24_P341938	4.1	1.7	0.7	1	11.5	86.1	0.6	1.6	26	74	1	1.1	1.9	10.5
	ZC3HAV1	zinc finger antiviral protein isoform 2	A_23_P20122	4.3	2.9	1	1.3	14.7	109.8	1.1	2	33.6	77.2	1.1	1.1	2.1	15.8
		hypothetical protein	A_24_P119678	1.2	0.9	0.9	1.1	11.7	26.6	1.4	1.2	21.4	18.9	1.6	0.9	1.4	9.9
			A_32_P95766	0.8	0.7	0.9	1.1	16	125.9	1	1	84.6	88.1	1	1	1	25.5
			A_24_P931804	0.8	0.7	0.9	1.1	16.9	91	1	1.5	54	42.6	1	0.8	1.1	10
			A_32_P219135	1	1	1.7	1.6	9.7	26.6	1.5	1.8	19.2	18.8	1.6	1.8	1.8	8.6
			A_24_P933828	0.8	0.7	1.3	1.1	5.9	27.4	1.1	1.5	16.4	19.1	1.2	1.4	1.4	6.2
			A_23_P50646	1.3	1.3	1.6	1	11.4	38.3	1.2	2	23.2	25.3	1.6	1.4	2	9.1
			A_23_P11980	0.9	1.3	1.3	1.1	10.8	59.1	1	1.9	34.3	40.5	1.8	0.9	1.3	11.2
			A_32_P703	1	1.1	1.4	1.4	12.4	64.7	1.4	2.4	33.9	32.2	1.1	1	1.2	4.8
			A_32_P221437	1.1	1.1	1.2	1.2	4	13.3	1.4	1.3	8.8	7.2	1.2	1	1.2	2.9
			A_32_P30898	1.1	1.2	1.1	1.4	4.1	18.8	1.3	1.5	8.2	9	1	1.1	1.6	3.9
			A_32_P222684	1	1.2	1.3	1.4	9.1	46	1.1	1.4	40.7	26.8	1.2	1.5	1.5	6.3
			A_24_P401830	0.9	1.2	1.4	1.5	6.7	18.2	1.4	1.7	17.8	10.4	1.1	1.2	1.2	3.8
			A_32_P170664	1.1	1	0.9	1.2	5.4	19.7	1.1	1.4	16.8	8.8	0.8	1.2	1.3	4.3
			A_24_P652537	1.6	1.6	1.4	1.2	30.8	95	1.4	1.3	55.5	52.1	0.9	1.1	2.8	15.2
			A_23_P328740	1	1.7	0.9	1.3	8.9	36.8	1.1	1.9	17.7	35.7	0.9	1.1	1.5	8.6
			A_32_P224888	1.8	1.5	2.2	2	15.2	75.1	1.1	1.5	44.9	36.2	1	0.9	2.5	6.3
			A_32_P122494	1.2	1	1.6	1.3	4.6	14.9	1.2	1.3	9.9	8.8	1.7	1.2	2.1	3.3
			A_32_P217261	1.4	1.2	1	1.1	4.5	32.4	0.9	1	8	17.7	1	0.9	1.3	4.7
			A_24_P849245	1.2	1.1	0.8	1	3.1	10.2	0.8	0.9	4.5	7	0.8	1	1.1	3.4
			A_24_P101651	1.3	2	1.3	1	8.1	32.3	1.1	1.3	18.9	21.2	1.2	1.8	2.1	7.8
			A_23_P28582	0.7	1	0.7	0.7	2.2	14	0.9	0.8	5.8	7.7	0.8	0.7	0.8	3.9
			A_32_P45844	1.4	2.5	1.2	1.3	29	77.3	0.9	1.8	32.1	23.6	1.4	1.8	2.1	18.9
			A_24_P734406	1.3	3.1	0.9	1.9	14.8	23.5	1	1.6	14.2	16.4	1.2	1.1	1.8	7.5
			A_32_P169550	0.9	1.3	1.2	0.9	6.2	9.2	0.9	1.4	5.6	6.4	1.1	0.9	0.9	2.9

			A_23_P157766	1	1.2	1.3	1	4.9	8	0.8	0.9	5.7	5.1	1.4	1.1	0.9	3.1
			A_23_P320407	0.6	2.1	2.1	2.1	4.1	25.6	2.8	1.7	10.8	11.4	2.1	1.3	1.3	4.7
			A_24_P174353	0.9	2.1	1.6	1.1	3.9	14.9	1.5	1.4	9	15	1.5	1.9	1.1	8.3
			A_24_P231483	1.6	3.8	1.3	1.1	8.9	26.5	0.8	1.3	18.7	17.9	1	1.2	1.2	2.1
			A_32_P53524	1	0.9	0.7	1.3	1.7	9.7	0.9	0.5	4	4	0.9	1.3	1.1	1.9
			A_23_P207774	1	0.9	1.2	1.2	2.7	9.7	0.6	0.6	4.6	4.6	0.8	1	0.7	2.1
C	ABCA5	ATP-binding cassette, sub-family A , member 5	A_24_P67096	1	1	1.8	1.5	1.8	9.1	1.6	1.5	4.4	4.3	1.5	1.1	1.2	1.4
	ABCA5	ATP-binding cassette, sub-family A , member 5	A_23_P78018	1.1	1	1.5	1.4	1.7	7.7	1.5	1.5	3.8	3.5	1.3	1	1.1	1.4
	ABL2	v-abl Abelson murine leukemia viral oncogene homolog 2 isoform b	A_23_P138099	1.1	1	1.8	1	3.2	10.6	1.1	1.2	5.6	7.6	1.6	1.1	1.3	1.6
	ACTR3B	actin-related protein 3-beta isoform 1	A_23_P123193	1.1	0.8	1.1	1.1	1.1	7	1	1.1	2.7	3.7	1.1	1.1	1.1	1.2
	ALDH1L2	hypothetical protein	A_23_P87941	2.2	1.2	0.9	1.1	2.1	8.8	1.1	0.8	1.6	13.8	0.9	1.1	1.8	1.8
	ALOX12P2		A_32_P440768	0.9	1.1	1.9	1.3	1.6	3.9	1.3	1.5	2.6	4.3	1.4	1.1	1.3	1.1
	AMDHD1	amidohydrolase domain containing 1	A_32_P122226	1.1	1	1	1.1	2	7.6	0.9	1.1	5.4	4.2	1.1	1	1.1	1.6
	ANKRD1	cardiac ankyrin repeat protein	A_23_P161218	0.9	0.9	1.1	1.2	1.3	5.6	0.9	1.1	1.3	4.4	0.8	0.7	0.5	0.9
	AP3B2	adaptor-related protein complex 3, beta 2 subunit	A_23_P77304	1.7	1.4	1.4	1.4	1.2	10.5	1.2	1.2	1.7	6.5	0.9	1.2	1.4	1.1
	AQP9	aquaporin 9	A_23_P106362	0.8	0.8	0.9	1	0.7	22.8	1	0.9	1.8	26	0.9	0.9	1	1
	ARHGAP9	Rho GTPase activating protein 9 isoform 1	A_23_P64661	1.6	1.6	1.1	1.1	2.2	12.8	1	2.8	5.6	14	1.3	1.6	1.1	2.8
	ASMTL	acetylserotonin O-methyltransferase-like	A_23_P159539	1	0.9	1	1	1.4	4.9	1.3	1.1	3.4	3.2	1	1	0.9	1.1
	AVIL		A_23_P53257	1	1.3	1.6	1.4	2.6	6.8	1.9	1.6	7.8	2.8	1	0.8	0.6	1
	AXUD1	AXIN1 up-regulated 1	A_23_P121011	1.1	0.8	0.7	0.9	4.3	3.8	0.7	1.1	4.6	2.9	0.7	1.2	0.9	1.1
	BAGE4	B melanoma antigen family, member 4	A_24_P126262	0.8	0.9	1.5	0.9	2.2	13.8	1.6	1	4.2	8.7	1.1	1.5	0.8	1.4
	BBC3	BCL2 binding component 3	A_24_P305312	0.8	0.7	0.6	0.8	3.1	6	0.8	1.3	5.6	2.5	0.7	0.9	0.8	1.6
	BBC3	BCL2 binding component 3	A_23_P382775	1.4	1.2	1.5	2	9.8	35.1	1.9	3.5	28.5	10.3	1.2	1.4	1.2	3.9
	BCL6	B-cell lymphoma 6 protein	A_23_P57856	1.7	1	1.3	1.2	4.1	9.3	1.1	1.2	7.8	5.2	1.1	0.8	1.2	1.8
	BEXL1		A_24_P40551	1	0.9	0.9	1	1.1	5.4	0.8	0.9	1.3	5.1	0.9	1	0.8	1.1
	BMP7	bone morphogenetic protein 7 precursor	A_23_P68487	1.1	0.9	1.1	1	1.1	7.4	0.9	0.9	1.1	3.3	1	1.1	1	1.1
	BOC	brother of CDO	A_23_P257763	0.8	0.7	1.3	0.9	1.2	5	1.3	1.3	2.4	2.8	1	0.8	0.8	0.9
	C10orf10	fasting induced gene	A_23_P35597	0.8	1.3	0.9	0.8	1.4	8.9	0.9	1.2	2.7	4.5	0.7	0.5	0.3	1
	C10orf10	fasting induced gene	A_24_P329795	2.4	1.9	1	1.1	1.3	12.2	0.9	1.2	2.7	6.1	0.9	0.6	0.3	1.2
	C11orf17	chromosome 11 open reading frame 17	A_23_P52161	1	0.9	1.2	1.1	4	6.3	1.1	1.6	7.5	3.9	1.2	1	0.9	1.7
	C12orf28	hypothetical protein LOC196446	A_32_P424761	0.9	0.6	0.9	1.1	1	10	1	1.1	4.7	7.4	1.3	1	1	1.4
	C12orf34	hypothetical protein LOC84915	A_23_P128375	1	1	1.2	1.2	1.4	8	1.1	1.2	2	6	1.1	1.3	1.2	1.6
	C14orf81		A_24_P153558	0.8	1	1.5	1.3	1.2	8.6	1.4	1.1	3.9	4.1	1.3	1.1	0.8	1.2
	C17orf55	hypothetical protein LOC284185	A_23_P426565	1.1	1	1.4	1.2	2.7	4.9	1.1	1.2	7.7	2.9	1.3	0.9	1.1	2
	C19orf28	hypothetical protein LOC126321 isoform c	A_23_P345139	0.8	1.7	0.8	0.9	1.9	11.1	1	1.1	2.2	9	0.8	0.9	1.1	2.7
	C19orf47	hypothetical protein LOC126526	A_32_P505133	0.9	0.9	1	0.8	1.1	3.6	1	0.9	1.6	5	0.8	0.8	0.8	1.1
	C1orf102	oxidored-nitro domain-containing protein isoform 1	A_23_P103433	1.1	0.9	1.2	1.1	1.3	4.3	1.3	1.2	2.1	4.5	1.1	1	0.9	1.1
	C1orf79		A_23_P74581	1.1	1.3	1.5	1.4	2	6.5	1.3	1.3	2.4	6.2	1.3	1.3	1.1	1.6
	C2orf49	hypothetical protein LOC79074	A_23_P165698	1.1	1.1	0.9	0.9	1.3	5.8	0.9	1	1.6	6.1	0.9	1	0.9	1.4
	C3orf19	hypothetical protein LOC51244	A_24_P144481	1.1	1.3	1.3	1.2	2	8.5	1.4	1.2	4	8	1.2	1.1	1	1.6
	C5orf5	chromosome 5 open reading frame 5	A_24_P20700	1.1	1.3	1.3	1.2	2.7	6.6	1.6	1.6	2.9	5.6	1.3	1.2	1.4	1.4
	CAMK1G	calcium/calmodulin-dependent protein kinase IG	A_23_P97402	1.2	0.6	1	1.1	3.1	22.7	0.8	0.8	7.3	23	1	1.1	0.5	3.1
	CCDC65	coiled-coil domain containing 65	A_23_P47904	1.4	0.7	0.7	1.2	1	9.3	0.7	1.4	1.8	11.3	0.7	1.4	0.6	1.3
	CCL23	small inducible cytokine A23 isoform CKbeta8-1 precursor	A_24_P319088	0.3	0.9	1	1.2	1.2	9.6	1.1	1.1	2.9	2.9	1.1	1	0.9	1
	CD163L1	scavenger receptor cysteine-rich type 1 protein M160 precursor	A_23_P61466	1.2	1.3	0.7	1.1	1.6	5.7	1.3	0.6	2.3	5.2	1	0.8	1.2	1

	CD70	tumor necrosis factor ligand superfamily, member 7	A_23_P119202	1.1	1	1.7	1.4	1.3	10.4	1.6	1.4	3.3	7.8	1.5	1.5	1.2	2
	CD83	CD83 antigen isoform a	A_23_P70670	0.8	0.9	0.9	0.9	1.7	10.9	0.8	0.8	4	7.5	1.1	1	0.8	2
	CEBPB	CCAAT/enhancer binding protein beta	A_23_P411296	1.5	0.9	1.2	1.3	4.6	7.7	1.3	1.5	9.6	5.9	1.1	1.2	1.2	2.1
	CEBPB	CCAAT/enhancer binding protein beta	A_23_P143242	1.3	0.9	0.9	1	2.6	3.3	1	1.2	4.4	2.6	0.9	1	1	1.5
	CEBPE	CCAAT/enhancer binding protein epsilon	A_23_P2990	1.5	0.8	1	1.1	3.3	4.3	1.1	1.2	5.8	3.2	1	1	1	1.7
	CHGA	chromogranin A precursor	A_32_P27046	1	1	1.3	1.1	1.2	5.2	1.3	1.2	1.7	3.9	1.2	1.1	1.1	1.2
	CLEC4M	C-type lectin domain family 4, member M isoform 3	A_23_P208482	1	1.1	1.6	1	1.1	7.1	1.5	1.3	2.7	6.4	1	1.1	0.9	1.2
	CLK4	CDC-like kinase 4	A_23_P61674	0.9	1.1	1.4	1.2	1.6	6.3	1.3	1.4	3.9	4.3	1.2	1.1	1	1.4
	CLK4	CDC-like kinase 4	A_24_P123521	1	1	1.2	1.2	1.4	4.7	1.2	1.3	2.8	2.7	1	1.2	1	0.9
	COLEC11	collectin sub-family member 11 isoform b	A_23_P120125	1	1.2	1.6	1.3	2.4	40.4	1.2	1.3	9	14.8	1.4	1	0.8	2.7
	COLEC11	collectin sub-family member 11 isoform b	A_24_P388322	0.9	1.1	1.1	0.9	2	24.9	1.5	1.2	6.3	12.9	1	1.4	0.8	2.3
	CXXC4	CXXC finger 4	A_23_P121676	1.1	1	1.2	0.7	2.2	35.4	1.1	1	11.2	30.5	1.8	1.1	1.1	2.8
	DENND4A	c-myc promoter binding protein	A_24_P136497	1.5	1	1.7	1.4	2.9	11.9	1.5	1.3	6.6	4.9	1.3	1	1.1	1.6
	DHRS2	dehydrogenase/reductase (SDR family) member 2 isoform 1	A_23_P48570	1	0.9	1.5	1.5	1.6	8.6	1.1	1.1	2.5	7.5	1.4	1.3	1	2.2
	DICER1	dicer1	A_23_P37111	1.1	1.1	1.8	1.4	2.5	21.8	1.8	1.5	11.3	7.7	1.6	1.2	1.2	2.6
	DIP2B	DIP2 disco-interacting protein 2 homolog B	A_24_P68162	1	1.1	1.3	1.2	1.5	5.9	1	1.1	2.4	4.4	1.1	1.1	1.1	1.4
	DND1	dead end homolog 1	A_32_P42054	0.9	1.1	1.6	1.3	2	57.1	1.7	1.4	8.1	19.2	1.4	1	1	1.3
	DPYSL4	dihydropyrimidinase-like 4	A_23_P331049	1.1	1.1	1.2	1	1.5	6.1	1.3	1	3.9	3.8	1.1	1.1	1.2	1.3
	DUSP8	dual specificity phosphatase 8	A_24_P322867	1.1	1.4	1.8	2	2.7	10	1.7	1.8	7.4	5.2	1.8	1.8	1.1	1.9
	DUSP8	dual specificity phosphatase 8	A_23_P390528	1.1	1.4	2.3	2.1	2.7	10.6	2.1	2.1	7.9	5.1	2	1.7	1.2	1.8
	EBI3	Epstein-Barr virus induced gene 3 precursor	A_23_P119478	1.1	1.1	1.1	1.2	1.1	11.9	1.3	1.1	1.9	10.4	1	1.1	1.1	2.1
	EFNA1	ephrin A1 isoform a precursor	A_23_P254512	1.2	1.3	1.5	1.5	4.9	6	1.1	2.1	10	3.6	1.4	1.2	1	3.3
	EFNA1	ephrin A1 isoform a precursor	A_23_P113005	1.1	1.1	1.1	1.2	3.3	3.2	1	1.6	5.5	2.4	1.1	1	0.9	2.4
	EGR1	early growth response 1	A_23_P214080	0.7	1	1.4	1.4	4.4	9.1	1.2	2.4	13.7	4.4	1.4	1.3	1.1	1.3
	EGR3	early growth response 3	A_23_P216225	1	0.9	0.9	1.8	25.2	15.4	1.2	1.9	39.9	7.3	1	0.9	1	5.6
	ELL	elongation factor RNA polymerase II	A_23_P27936	1	1.1	1.1	1	1.4	4.7	1	1	1.7	5	1	0.9	0.9	1.1
	EPHA4	ephrin receptor EphA4	A_23_P108501	0.8	0.9	1.3	1.2	2.6	40.2	0.9	1	8.5	29.4	1.4	1.1	1.1	4.1
	ETV3	ets variant gene 3	A_23_P400945	1.1	1.1	1.6	1.7	5.1	3.9	1.7	2.5	6.6	2.1	1.5	1.4	1.5	3.1
	EZH2	enhancer of zeste 2 isoform a	A_23_P259641	1.1	1	1.2	1.1	1.2	8.2	1.2	1.3	3.5	4.2	1.2	0.9	1	1.1
	FAM110A	hypothetical protein LOC83541	A_23_P386241	0.9	0.8	1.1	0.9	1.1	5.3	1.2	1.1	2.3	6	1	0.9	0.8	1.4
	FAM90A1	hypothetical protein LOC55138	A_24_P643028	1.1	0.8	1	1.2	1.2	5.1	1.1	0.8	1.5	4.8	1	1.2	1	1.3
	FAM90A10	hypothetical protein	A_24_P903680	1	0.9	1.2	1.3	1.2	5.7	1.3	1.2	1.8	4.9	1.1	1.2	1	1.3
	FGF9	fibroblast growth factor 9 precursor	A_23_P105803	1	1	0.8	1	1.7	3.2	0.9	0.6	1.6	6.2	1.3	0.9	1.3	1.6
	GABPB2	GA binding protein transcription factor, beta subunit 2 isoform gamma 1	A_23_P205789	1.2	1.3	1.3	1.2	1.4	8.2	1.2	1.1	2	8.5	1.3	1.2	1.9	1.8
	GBA3	cytosolic beta-glucosidase	A_23_P18672	1	0.7	1	1.2	1	118.2	1	1.1	5	113.2	1	1.4	0.8	2.7
	GLCCI1	glucocorticoid induced transcript 1	A_23_P82402	1.2	1.1	1.3	1.4	3	15.3	1.5	1.3	9.3	8.1	1.2	1.1	1.3	2.7
	GLI3	GLI-Kruppel family member GLI3	A_23_P111531	1.3	4.2	0.9	1.4	5.5	9.7	1	1.5	5.9	5.1	1	0.9	1.2	1
	GOT1	aspartate aminotransferase 1	A_23_P63825	1.1	1	1.1	1.1	1.4	4.1	1.2	1.2	1.4	6.3	1	1.2	1.3	1.5
	GP1BA		A_23_P152926	1	1.9	1.9	1.7	3.7	85.4	1.5	1.4	17.2	112.9	2.5	2.1	1.5	5.1
	GRIP2	FLJ00218 protein	A_24_P930868	2.5	2.2	1.7	2.4	9.2	19.9	2.2	1.6	12.3	6.1	1.5	1.8	1.2	4.8
	HARS	histidyl-tRNA synthetase	A_24_P89284	0.8	0.8	1.2	0.9	0.9	20.1	1	0.9	1.3	8.2	0.9	1	0.9	0.9
	HARS	histidyl-tRNA synthetase	A_23_P133227	1	1	1.1	1	1.1	33.5	1.2	1	1.8	13	1	1.1	1	1
	HBG1	A-gamma globin	A_23_P53137	1	0.8	1	0.9	1.2	6.8	1	1	3.3	9.5	1	0.9	1.2	1.4
	HCFC2	host cell factor C2	A_23_P25403	1.3	1.3	1.3	1.1	1.5	5.4	1.1	1.1	2	5	1.3	1.1	1	1.2
	HCLS1	hematopoietic cell-specific Lyn substrate 1	A_23_P73429	1	1.1	1.7	1.3	3.3	18.8	1.7	1.6	9.8	15.1	1.4	1	0.9	2.2

	HCP5	HLA complex P5	A_24_P17870	1.4	3.4	1.4	1.6	1.5	40	1.5	1.6	4.1	18.1	1.2	1.1	1.3	8.8
	HCP5		A_23_P111126	1	8.2	0.8	0.8	3	72.6	0.8	1.6	3.7	40.2	0.6	1.1	1.4	14.7
	HIVEP2	human immunodeficiency virus type I enhancer binding protein 2	A_23_P214766	1.2	1	1.5	1.3	2.1	14.2	1.5	1.2	5.1	9.1	1.4	1	0.9	1.9
	HOXA4	homeobox A4	A_23_P253982	0.9	0.9	1.1	0.9	1.3	4.3	1.1	1	2.1	6.2	1	1	1	1
	HOXD10	homeobox D10	A_23_P381368	0.9	0.9	1.3	1.1	2.8	4.6	1.3	1.2	5	2.9	1.2	1.1	1.1	2.2
	HRK	harakiri	A_23_P25194	1	1.4	1.7	1.5	2.1	7.1	1.6	1.4	2.6	7.9	1.4	1.4	1.1	1.2
	HTATIP2	alternatively spliced product of metastasis-suppressor gene CC3	A_24_P307580	1.4	1.3	1.6	1.4	2.2	8.3	1.3	1.4	5.2	3.8	1.6	1.3	1.2	1.9
	IFNA4	interferon, alpha 4	A_24_P403459	1.4	0.9	1.5	1.5	7.5	191.3	1.4	1.8	4.5	38.8	1.2	1.4	1.2	2.2
	IFNA8	interferon, alpha 8	A_23_P146539	0.8	0.7	0.9	1	2.7	67	0.9	0.6	1.8	15.7	1.2	0.9	0.9	0.9
	IGF2	insulin-like growth factor 2	A_23_P421379	1	1.2	1.5	0.7	1.6	23.7	1.5	1.2	9.1	14	0.8	0.9	1	1.3
	IGF2		A_32_P56661	1.3	0.9	1.2	1.8	2.7	26.7	1.1	0.9	7.6	15.4	1.8	1.4	1.2	1.8
	IL23A	interleukin 23, alpha subunit p19 precursor	A_23_P76078	0.7	1	1.1	1.2	1.7	11.4	1.1	1.3	4.9	12.8	0.9	0.9	1	1.7
	INTU	PDZ domain containing 6	A_32_P118372	1	0.9	1.9	1.3	2.6	17.4	1.5	1.3	7.9	9.9	1.6	1.3	1	2.1
	ITGAM	integrin alpha M precursor	A_23_P124108	1.3	1.4	1.2	1.8	2	15	1.3	1.6	5.9	13.5	1.4	1.3	1.2	2.7
	JPH2	junctophilin 2 isoform 1	A_23_P394395	1	1.1	1	1	1.4	7.2	1.2	1	1.9	6.9	1	1	0.9	0.8
	JUN	jun oncogene	A_23_P201538	1	1.1	1.8	1.7	7.7	18.8	1.5	2.5	22.9	8.5	1.7	1.8	1.2	2.9
	JUNB	jun B proto-oncogene	A_23_P4821	1.2	1.4	1.3	1.5	3.5	6.3	1.2	1.7	6.3	3	1.2	1.3	1.2	1.7
	KIAA1267	hypothetical protein LOC284058	A_23_P55376	1	1.2	1.5	1.2	1.3	5.1	1.5	1.2	2.5	3.4	1.4	0.9	0.9	1.1
	KRT17	keratin 17	A_23_P96158	0.9	1.4	0.9	1.1	2.2	29.4	0.7	1.2	3.8	25.4	1.3	1.1	1.2	5
	KRT34	keratin 34	A_23_P101054	1	1	0.7	1.3	1.4	14.1	1	1	1.8	13.8	0.8	1.3	1.4	1.5
	LATS2	LATS, large tumor suppressor, homolog 2	A_23_P204958	1	1.1	1.4	1.1	1.8	4.1	1.3	1.1	2.8	3.3	1.2	1	0.9	0.9
	LCE1F	late cornified envelope 1F	A_23_P411321	1	1.1	1.4	1.6	1.5	6.5	1.5	1.4	2.3	3	1.3	1.4	1.3	1.6
	LPA	lipoprotein Lp(a) precursor	A_23_P95221	0.8	1.1	0.8	1	1.1	23	0.9	1	1.5	15.5	1.1	0.8	1.1	2.2
	LPXN	leupaxin	A_23_P87150	1	1.1	1.2	1.3	1.9	10	1.2	1.3	4.3	9.2	1.1	1	1	1.7
	LRRC46	leucine rich repeat containing 46	A_23_P152949	0.9	1	1	0.9	1.1	3.7	1.2	1.2	1.9	4.2	1	1	0.8	0.9
	LRRC48	leucine rich repeat containing 48	A_24_P270971	1.1	0.9	1.2	1.2	1.5	3.5	1.4	1.3	2.9	4.1	1.3	0.9	0.8	0.9
	LRRC49	leucine rich repeat containing 49	A_23_P129174	1.1	0.8	1.1	1	1.2	7.6	1.1	1.1	2.2	7.3	1.1	1	1	1.5
	LST1	leukocyte specific transcript 1 isoform 1	A_24_P103469	1	0.8	1.3	1	1.8	22.5	1.1	1.3	7.8	15.5	1.1	1	0.8	2
	LYPD1	LY6/PLAUR domain containing 1 isoform a	A_32_P101031	1.3	1.2	1.3	1	1.4	5.3	1.4	1.2	2	4	1.2	1.1	0.9	0.9
	MAP3K10	mitogen-activated protein kinase kinase kinase 10	A_24_P284523	1	1	1.9	1.6	2	10.2	1.9	1.4	4.3	7.3	1.5	1.2	1.1	1.5
	MAP3K7IP3	mitogen-activated protein kinase kinase kinase 7 interacting protein 3	A_23_P305033	1.2	1.4	1.2	1.2	1.4	8.1	1.5	1.2	1.9	7	1.2	1.1	1.1	1.5
	4-Mar	membrane-associated ring finger (C3HC4) 4	A_23_P333228	0.9	1.1	0.9	0.9	1.1	11.3	1.3	1.1	1.8	14.7	0.7	0.9	0.9	1.6
	MARK1	MAP/microtubule affinity-regulating kinase 1	A_23_P424	0.8	0.8	0.7	1.3	1.6	4.2	0.8	0.7	1	7.9	0.9	0.9	1	0.8
	MDM4	mouse double minute 4 homolog	A_23_P103503	1	1.4	1.5	1.3	1.9	10.7	1.5	1.6	3.6	7.6	1.3	1.1	1.1	1.9
	MEG3		A_24_P272993	0.9	1.1	2.2	1.7	1.6	7.7	1.9	1.6	2.6	3.8	1.9	1.3	1.3	1.7
	MLL3	myeloid/lymphoid or mixed-lineage leukemia 3 isoform 2	A_24_P840688	1.2	1.3	1.4	1.3	1.6	10.4	1.6	1.4	5.1	6.6	1.2	1.3	1.2	1.9
	NAV2	steerin2 protein	A_24_P933458	0.9	1	1.9	1.5	2.9	14.3	2.1	1.8	8.3	7.3	1.4	0.9	1	2
	NFKBIZ	nuclear factor of kappa light polypeptide gene enhancer in B-cells inhibitor, zeta isoform a	A_23_P212089	1.1	1.2	1.9	1.3	2.4	8.3	1.7	1.9	4.2	3.5	1.5	0.8	0.9	2.2
	NLGN3	neuroligin 3	A_23_P62298	1.1	1.8	1.3	1.3	2.1	5.5	1.9	1.3	2.6	3.5	1.7	0.9	1.1	0.9
	NR2F1	nuclear receptor subfamily 2, group F, member 1	A_23_P348737	1	1.1	2.1	1.3	6.8	37.5	1.9	1.6	29	17.7	1.7	1.1	1.2	2.8
	NSUN6	NOL1/NOP2/Sun domain family, member 6	A_23_P61580	1.2	1.2	1.8	1.2	2.4	27.9	2	1.5	8.7	31.6	1.5	1	1	1.9
	OGFRL1	opioid growth factor receptor-like 1	A_23_P7791	1.2	1.1	1.4	1.4	2.1	11.3	1.6	1.2	2.9	6.5	1.2	1.3	1.1	1.7
	OLFM3	olfactomedin 3	A_24_P402444	0.8	0.6	1	1.5	1	18.5	1	1	2	19.1	1.7	0.9	1	1
	PCDH7	protocadherin 7 isoform c precursor	A_23_P378364	0.7	0.7	1.1	1.3	1.2	15.9	0.9	0.9	2.4	13.4	0.8	1	0.8	1.1

	PEA15	phosphoprotein enriched in astrocytes 15	A_24_P250964	1	1	1.2	1.2	1.5	3.8	1.6	1.4	2	4.9	1.1	1.2	1.1	1.1
	PHLDB2	PHLDB2 protein	A_24_P178065	1.4	1	1.3	1.1	3	8	1	1.6	6.5	3.1	1.1	1	1.3	1.3
	PHLDB2	pleckstrin homology-like domain, family B, member 2	A_24_P260122	1.4	1.4	1.3	1.3	3.8	6.4	1.1	1.1	6.1	3.4	1.2	1.1	1.3	1.3
	PLA2G4C	phospholipase A2, group IVC	A_24_P316439	0.5	0.6	0.7	38.1	3.9	48.9	0.7	0.8	19	16.5	0.6	1	0.6	5.6
	PLXDC2	plexin domain containing 2 precursor	A_23_P161424	0.7	0.6	1	1	1	7.5	1	1	1.2	17.5	1.1	1.1	1	1
	PPP1R10	protein phosphatase 1, regulatory subunit 10	A_23_P156667	1	1.1	1	1.3	1.3	4.9	1.3	1.2	2.6	2.7	0.9	1.1	0.9	1.2
	PRICKLE1	prickle-like 1	A_23_P408285	1.1	0.9	1.2	1	2.1	8.6	0.8	1.1	2.8	5.9	1.2	1.2	0.9	1.4
	PRR8	PRR8 protein	A_23_P417113	1.3	1.5	1.3	1.2	1.3	6.3	1.4	1.3	1.5	5	1.2	1.1	1	1.5
	PSCD3	pleckstrin homology, Sec7 and coiled/coil domains 3	A_23_P111593	0.9	1.1	2.6	1.1	1.4	3.9	1.4	1.4	2.1	4.8	0.8	0.9	0.9	1
	PSORS1C1	SEEK1 protein	A_23_P133902	1.1	1.5	1.6	1.4	2.5	5.1	1.4	1.4	5	2.9	1.4	1.1	0.9	1.1
	PSORS1C1	SEEK1 protein	A_24_P24848	1.3	1.6	1.1	1.2	2.1	5.2	1.4	1.4	3.9	3	1.1	1.1	2.1	1.2
	PTPN14	protein tyrosine phosphatase, non-receptor type 14	A_23_P149111	0.9	1	1.2	1	1.8	6.9	1.2	1.2	2.7	6.3	1.1	1	0.9	1.3
	PTPN21	protein tyrosine phosphatase, non-receptor type 21	A_23_P77031	1	1.1	1.4	1.2	1.7	7.2	1.2	1.2	2.8	5.9	1.2	1	1	1.2
	RAI2	retinoic acid induced 2	A_23_P254165	1.2	1.2	1.1	1.2	1.3	7.1	1.3	0.9	1.9	6.2	1.5	1.2	1.1	1.1
	RANBP3L	RAN binding protein 3-like	A_23_P391207	0.8	0.7	0.8	1.1	1.9	21.5	1	0.9	3	10.4	1	0.9	0.6	1.5
	RAPH1	Ras association and pleckstrin homology domains 1 isoform 1	A_24_P924862	1	1	1.3	1.1	1.8	8	1.2	1.1	4.4	8.4	1.2	1.1	1.1	1.4
	RAPH1	Ras association and pleckstrin homology domains 1 isoform 2	A_23_P409966	1.6	1.2	1.8	1.4	3.9	19.4	1.6	1.4	14.5	9.1	2.3	1.9	1.3	1.7
	RASL10A	RAS-related on chromosome 22 isoform b	A_23_P166400	1	1	1.2	1.1	1.4	6.1	1.1	1.2	4.4	3.6	1.1	1.2	1	1.2
	RBMS3	RNA binding motif, single stranded interacting protein 3 isoform 2	A_24_P359942	0.9	1	1.6	1.4	2.9	5.6	1.6	1	5.4	2.9	1.3	0.8	0.9	1.4
	RND1	GTP-binding protein RHO6	A_23_P53370	0.9	0.9	0.7	1	3.2	3.7	0.8	1.8	5.4	2.5	0.8	0.8	1	1.8
	RNF180	ring finger protein 180	A_23_P377996	1	1.2	1.2	1.5	1.3	6.5	1.1	1.1	2.2	5.4	1.2	1.4	1.3	1.4
	RSRC2	arginine/serine-rich coiled-coil 2 isoform b	A_23_P53267	1.1	1.1	1.4	1.3	1.9	12.5	1.3	1.3	4.5	10.5	1.2	1.1	1.2	1.6
	RUNX1	AML1a protein	A_24_P34155	1.2	1	1.5	1.6	2.5	12.6	1.2	1.2	6.3	5.8	1.5	1.4	1.1	1.7
	SIPA1L2	signal-induced proliferation-associated 1 like 2	A_23_P137470	1	0.8	1.4	1.2	1.7	7.7	1.1	1.2	3.8	3.7	1.3	1.1	0.9	1.8
	SLC2A6	solute carrier family 2 (facilitated glucose transporter), member 6	A_23_P169249	0.9	1	1.2	1.2	1.6	8.2	1.2	1.2	3.5	4.5	1.2	1.2	1.5	1.9
	SLC39A9	solute carrier family 39 (zinc transporter), member 9	A_23_P380326	1	0.9	0.8	0.9	0.9	3.7	0.8	0.8	1	5.4	0.8	0.8	0.9	1.1
	SLC6A13	SLC6A13 protein	A_24_P923483	1.3	1.3	2	2.4	2.3	11.7	2	1.6	9.7	3.9	1.7	1.7	1.6	1.7
	SNX19	sorting nexin 19	A_24_P81691	0.9	1.1	1.2	1.1	1.5	4.5	1	1.1	2.6	3.9	1	1	0.9	1.1
	SOCS1	suppressor of cytokine signaling 1	A_24_P48014	2.1	1.2	1.4	1.2	5.6	3.2	1.4	1.3	4.3	2.4	1.3	1.5	1.2	1.3
	SOD2	SOD2 protein	A_24_P935819	4	1.3	5	2.7	21.3	53.4	2.3	6.7	45.3	20.5	2	1.5	2.4	10.8
	SPACA3	sperm acrosome associated 3	A_23_P317244	1.1	1.2	1.3	0.9	1	15.3	1.5	1.4	1.8	12.1	1.3	1.8	1.1	1.9
	SPHK1	sphingosine kinase 1 isoform 1	A_23_P38106	1.1	1.2	1.1	1.1	1.5	5.5	1	1.1	2	5.3	1	1.2	1	1.2
	SPINK1	serine protease inhibitor, Kazal type 1	A_23_P214079	1.5	1.1	1.3	1.4	1.6	12	0.9	0.9	1.5	5.7	0.8	0.8	0.7	1.2
	SPRR2C	small proline-rich protein	A_23_P126089	0.6	1.4	1.1	1	0.9	18.3	1.3	1.1	1.5	26.2	1.1	1.2	1	1.3
	SPRR2D	small proline-rich protein 2D	A_23_P11644	1.4	1.1	0.8	1.4	1.3	16.7	1.2	1.2	1.8	24.3	0.8	1.5	0.9	1.7
	STK19	serine/threonine kinase 19 isoform 2	A_23_P19479	0.9	0.9	1.1	1.1	2.8	10.6	1.1	1.2	6.4	4.2	1	1	1	1.8
	STMN4	stathmin-like-protein RB3	A_23_P31739	1.6	1.1	1.3	1.1	1.6	12.7	0.9	1.1	1.2	14.7	1.2	1	0.7	2.1
	TDGF1	teratocarcinoma-derived growth factor 1	A_23_P366376	1.8	1	0.9	1.3	1.5	9.7	0.7	0.8	1	11.1	1.1	0.8	1.1	1.1
	THAP2	THAP domain containing, apoptosis associated protein 2	A_23_P105382	1.1	1	0.9	0.8	0.8	4.8	0.6	0.7	1.1	3.9	1.1	0.8	0.8	0.9
	THRAP1	mediator of RNA polymerase II transcription, subunit 13 homolog	A_24_P17077	1.2	1.3	1.5	1.3	2	8	1.5	1.4	3.8	5.7	1.3	1.3	1.3	1.7
	TKTL1	transketolase-like 1	A_23_P259901	0.9	0.9	0.8	1	1.1	3.6	1.4	0.9	1.7	7.3	0.9	1	0.9	1.7
	TMEM135	hypothetical protein LOC65084	A_24_P127075	0.8	0.9	0.8	0.8	1	5.1	0.7	0.6	1.8	4.8	0.6	0.6	1.5	1
	TMEM27	transmembrane protein 27	A_23_P33984	1.4	2.2	0.9	0.9	1.6	8.9	0.8	0.8	3.1	7.8	0.9	0.8	0.7	1.6
	TNC	tenascin C (hexabrachion)	A_23_P157865	1.3	1.1	0.9	0.6	1.4	7.8	0.8	0.9	2.3	7.1	0.9	1.4	1.3	1.5

	TNFRSF12A	type I transmembrane protein Fn14	A_23_P49338	0.9	1.1	1.2	1.2	1.6	11.1	1.4	1.3	2.5	11.3	1.1	1.2	1.2	1.4
	TSC22D2	TSC22 domain family 2	A_23_P92230	1.1	1	1	0.8	1	4.8	0.8	0.8	1.7	3.5	1	1	0.8	1.1
	TSPAN10	tetraspanin 10	A_24_P213643	1.1	1	1.2	1.1	2.5	7.1	1.3	1.3	3.7	3.6	1.2	1.1	1.1	1.5
	TTC26	tetratricopeptide repeat domain 26	A_23_P257668	1	0.8	0.7	0.9	0.9	5.7	0.9	0.7	1.5	6.1	0.8	0.8	0.8	0.8
	TUFT1	tuftelin 1	A_23_P371824	0.8	0.9	1.2	1.1	2	4.5	0.9	1	2.3	5	1.2	1	0.9	1.1
	UCP3	uncoupling protein 3 isoform UCP3S	A_24_P292470	1	1.2	1.8	1.4	1.7	9	1.6	1.7	5	4.2	1.5	1.3	1.1	1.4
	VIP	vasoactive intestinal peptide isoform 1 preproprotein	A_23_P19650	0.8	0.7	0.9	1.4	1.8	19.7	0.9	1.2	1.6	27.2	1	0.9	1	1.6
	VNN1	vanin 1 precursor	A_23_P255345	1.2	1.1	1	1.3	0.9	14.1	0.7	1.2	2.4	12.1	1.4	0.7	0.5	3.7
	VPS16	vacuolar protein sorting 16 isoform 2	A_23_P143303	1	0.9	1	1.1	1.5	5.4	1.1	1.2	3.9	3.3	1	1.1	1	1.1
	WBSCR19	hypothetical protein LOC285955	A_32_P180435	1.4	1.2	1.6	1.9	2	9.8	1.4	1.5	4.4	5.9	1.1	1.4	1.1	1.7
	WBSCR19	hypothetical protein LOC285955	A_32_P177040	1.4	1.2	1.5	1.7	1.5	9.3	1.3	1.9	3.4	5.9	1.2	1.3	1.4	1.8
	WDR42A	WDR42A protein	A_24_P76725	1	1.3	1	1	1.1	5.9	1	1	1.5	5	0.9	0.9	1	1
	WDR42A		A_24_P886960	0.9	1.1	1.2	1.1	1.7	10.1	1	1.1	5.8	7	1.1	0.9	0.9	1.3
	WDR66	WD repeat domain 66	A_24_P179504	0.8	0.7	0.9	1	1.2	5.4	1	1	1.2	6.5	0.9	1.2	1.2	1.1
	WNT4	wingless-type MMTV integration site family, member 4 precursor	A_23_P382607	1	1	1.2	1.2	1.9	8.7	1.2	1.1	3.4	3.2	1.3	1.2	1.1	1.5
	XRN1	5'-3' exoribonuclease 1 isoform a	A_23_P132822	1.1	1.4	0.6	1.2	3.3	9.9	0.7	0.8	3.5	6.5	2.7	0.9	0.8	1.3
	ZFP36	zinc finger protein 36, C3H type, homolog	A_23_P39237	1.2	1.1	1.3	1.4	6.4	12	1.2	2.4	15	4.1	1.1	1.2	1.3	2.2
	ZFP36L2	butyrate response factor 2	A_23_P101960	1.3	1.4	2.3	1.5	4.9	17.6	2.1	2	19.4	10.6	1.8	1.3	1.1	2.3
	ZNF121	zinc finger protein 121	A_24_P935782	1	1.5	0.7	0.7	1.1	4.6	0.9	0.7	1.7	4.7	0.7	1.1	0.8	0.7
	ZNF222	zinc finger protein 222	A_24_P165082	0.9	1.1	0.8	0.9	1.1	4.5	0.8	0.9	1.6	5.6	0.9	0.9	0.9	1.1
	ZNF222	zinc finger protein 222	A_23_P218517	0.9	1.2	0.8	0.9	1.1	5	0.8	0.9	1.6	5.4	0.9	0.9	0.9	1.1
	ZNF222	zinc finger protein 222	A_23_P125042	0.9	1.1	0.7	0.4	1	4.2	0.6	0.7	1.2	4.9	0.6	0.8	0.8	1
	ZNF256	zinc finger protein 256	A_23_P16022	0.9	1.2	1	1	1.4	5	1.2	1.1	2.1	6	0.9	0.9	0.9	1.2
	ZNF461	gonadotropin inducible transcription repressor 1	A_23_P67424	1.1	1	1.3	1.2	1.5	5.7	1.2	1.2	2.9	4.7	1.1	1.1	1.1	1.2
	ZNF462	zinc finger protein 462	A_23_P60499	1.1	1.3	1.7	1.2	1.9	15.7	1.3	1.3	3.5	9.7	1.3	1.1	1.1	1.6
	ZNF503	zinc finger protein 503	A_23_P202484	1.2	1.4	1.8	1.5	3.4	11.4	1.8	1.5	8.2	5.5	1.5	1.5	1.2	2
	ZNF585A	zinc finger protein 585A	A_23_P90220	1	1.1	1	1.1	1.4	4.1	1	1	1.7	5.2	0.9	0.9	1	1.2
	ZNF585A		A_24_P849467	1	2.9	0.9	0.9	1.9	11.6	0.9	0.8	1.6	11.3	0.8	1	0.9	2.4
	ZNF697	ZNF697 protein	A_23_P322076	0.9	1	1.9	1.9	1.9	8.2	1.4	1.3	2.5	6.1	1.5	1.2	1.5	1.4
	ZNF704		A_24_P505790	1	1	2.1	1.6	1.9	10.3	1.7	1.5	4.6	5.5	1.6	1.4	1	1.9
	ZNF8	zinc finger protein 8	A_23_P130466	1.1	1.2	1.3	1.2	1.6	6.1	1.2	1.3	2.7	5.9	1.2	1	1.1	1.4
	ZSCAN29	zinc finger protein 690	A_23_P100092	1.1	1.4	1.6	1.3	1.6	6.5	1.5	1.4	2.7	4.8	1.4	1.3	1.2	1.5
		colon cancer-associated antigen AgSK1-2HT-ECS	A_32_P77933	0.9	0.9	1.5	1.4	2.3	22.3	1.4	1.3	7.7	14	1.3	1.3	1.3	2.7
		colon cancer-associated antigen AgSK1-2HT-ECS	A_23_P398275	0.9	0.9	1.5	1.4	2.2	16.1	1.4	1.3	5.6	10.5	1.4	1.4	1.3	2.3
		FLJ00291 protein	A_24_P932648	1.1	1.2	1.2	1.3	1.6	7.6	1.3	1.7	3.5	7.3	1	1.1	1.2	1.8
		GA repeat binding protein, beta 2	A_23_P73208	1	1.1	1	1	0.9	6.6	1.1	0.9	1.1	6	1	0.8	0.8	1.5
		golgin-like protein	A_23_P106371	1.3	1.2	1.7	1.3	1.6	9.7	1.7	1.3	4.1	5.7	1.5	1.1	1.2	1.1
		HSPC080	A_24_P917418	1.1	1	1.5	1	2.1	9.3	1.3	1.2	4.5	5.1	1.2	1.2	1	1.6
		hypothetical protein LOC147744	A_23_P107775	0.9	1.1	1.6	1.3	1.4	7.8	1.8	1.5	3.8	4.6	1.4	1	1	1.4
		hypothetical protein LOC205860	A_23_P350005	1	0.9	1.9	1.8	2	11	1.7	1.5	3.7	8.3	1.6	1.7	1.9	1.9
		hypothetical protein LOC286006	A_24_P380679	1.2	1.1	2.3	1.6	2.2	6.4	1.7	1.4	3.9	5.1	1.7	1.7	1.4	1.6
		hypothetical protein LOC440321	A_24_P264166	0.9	1.3	1.7	1.4	2	10.1	1.3	1.5	4.1	6.6	1.3	1.1	1.2	1.2
		hypothetical protein LOC54891	A_23_P142756	1	1.3	1.3	1.1	1.7	9.2	1.4	1	4	9.2	1.2	0.8	0.8	2.1
		hypothetical protein LOC80154	A_23_P129103	0.9	0.9	1.4	1.4	1.8	8.2	1.3	1.2	3.8	5.8	1.2	1.2	1.2	1.9
		KIAA1267 protein	A_24_P316381	1.2	1.4	1.9	1.4	1.8	5.8	1.9	1.7	4	4	1.3	1.3	1.2	1.2
		KIAA1267 protein	A_32_P210106	1.1	1.3	1.8	1.9	2	6	1.8	1.8	3.9	4	1.3	1.3	1.4	1.2
		KIAA1466 protein	A_24_P324581	1.8	2.1	2	1.3	6.3	8.8	1.7	1.3	6.5	3	1.5	1.4	1.6	1.4

		KIAA1466 protein	A_24_P324577	1.6	1.9	2.2	1.6	4.6	7.2	2.1	1.6	5.5	3.2	1.9	1.4	1.4	1.5
		LOC727751 protein	A_23_P320478	0.9	0.9	1.1	1.2	1.8	7.8	1.1	1.2	4	5.2	1.2	1.3	1.2	2
		MGC26597 protein	A_23_P389426	0.7	1.3	0.9	1.2	2.1	5.9	1.1	1.1	2.8	4.7	1.1	1.2	0.7	1.2
		Nedd4 binding protein 3	A_23_P58747	0.7	1.2	1.4	1.4	1.8	14	1.6	1.4	5	13.3	1.2	1.3	1.1	2.5
		PRO1995	A_24_P927090	0.8	1	1.4	1.8	3.6	20.3	1.7	1.7	9.6	7	1.4	1.6	1.3	2.8
		RBP1-like protein	A_24_P196499	1.1	1.9	1	1.1	1.2	10.1	0.9	1.2	3.1	11.7	1	0.9	1.1	1.4
		T-cell activation NFKB-like protein	A_23_P383422	0.9	1.1	1	1.1	0.9	6.5	1.3	1.2	1.8	5.1	1.1	1	0.9	1.3
		T-complex protein 1	A_23_P29110	0.8	0.7	1	1.1	1.1	10.8	1	1	3.5	5.5	1	0.9	0.8	1.1
		testes development-related NYD-SP18	A_23_P134204	5	1.2	1.1	0.9	1.2	8.2	1.2	1	2.4	6.5	1.4	1.5	1.2	1
			A_32_P87191	1.4	0.7	1.6	1.3	1.2	8.8	1.2	1.1	4	7.9	1.6	0.8	0.6	1.3
			A_32_P80295	1.5	1.3	1.5	1.4	2.1	12.6	1.4	1.4	5.2	8	1.5	1.3	1.2	2.2
			A_24_P399220	1.3	1.5	1.8	1.6	2.3	11.3	1.5	1.5	4.8	6.1	1.6	1.2	1.3	1.9
			A_32_P3564	1.2	1.3	1.4	1.5	2.6	7.2	1.6	1.6	3.5	5.1	1.5	1.3	1.2	1.7
			A_24_P264664	1.1	1.3	1.6	1.3	2.2	7	1.5	1.3	3.8	5.5	1.4	1.1	1.2	1.6
			A_32_P226205	1.2	1.6	2.1	1.3	3.2	31.6	1.3	1.3	15.7	24.2	1.6	1.1	1	2
			A_32_P106925	1	1.3	1.7	1.6	2	11.4	1.6	1.5	6.8	8.4	1.6	1.4	1.1	1.6
			A_32_P61439	1.3	1.3	1.5	1.2	1.4	12.1	1.4	1.3	2.9	6.4	1.3	1.1	1.1	1.7
			A_32_P209250	1	1.1	1.2	1	1.3	5.6	1.1	1.1	1.9	4.3	1.1	1	0.9	1.3
			A_23_P215819	1	1	1.1	1.1	1.6	7.8	1.1	1.1	3.3	6	1.1	1	1	1.3
			A_32_P126647	1	1	1.3	1.2	1.3	6.3	1.5	1.2	3.1	5.2	1.1	1	0.9	1.2
			A_32_P42989	1.5	1.3	1.8	2.5	2.5	35.4	1.4	1.5	8.7	20.2	1.4	1.7	1.3	4
			A_32_P74409	1	1	1.4	1.2	3.8	39.1	1.1	1.5	6.8	28	1.4	1.4	1.5	4
			A_32_P141184	0.9	0.9	1.3	0.8	2	4.8	1	1	2.2	6	1.3	1	1	1.3
			A_32_P59277	0.9	1.4	2.9	1.9	4	46.6	2.3	1.7	8.9	13.3	2.2	1.5	1.4	1.8
			A_23_P381979	0.9	1.2	2.2	1.4	1.8	10.8	1.9	1.3	3.9	5.1	1.8	1.1	1.1	1.7
			A_32_P2392	1.1	1.5	2.3	1.8	2	8.4	2.1	1.7	4.5	5.9	1.9	1.4	1.4	1.3
			A_32_P213948	1.1	1.1	1.8	1.4	1.5	6.1	1.7	1.4	2.5	3.3	1.6	1.2	1.2	1.1
			A_24_P272225	1.1	1.2	1.3	1.1	1.5	5.1	1.3	1.3	2.4	3.2	1.2	1	1.1	1.2
			A_24_P510502	1	1.1	1.6	1.4	1.4	9.1	1.4	1.5	3.3	5.3	1.4	1.2	1.2	1.2
			A_32_P199923	1.1	1.1	1.7	1.1	1.4	9.9	2	1.3	4.5	4.4	1.7	1.3	1	1.5
			A_32_P2766	0.9	1.2	1.6	1.3	1.6	9.6	1.6	1.5	4.8	4.1	1.2	1	0.9	1.1
			A_24_P110141	1	0.9	1.4	1.2	1.5	4.7	1.1	1.4	2.9	3.7	1.1	1	1	1.1
			A_23_P209360	0.9	1.3	1.2	1.2	1.5	4.9	1.2	1.2	2.6	3	1.2	1.1	0.9	1.1
			A_32_P234853	1	1	0.9	1.1	0.9	4.5	1.2	1	2.4	4.4	0.9	1.1	0.9	1
			A_24_P39928	0.9	0.9	1.3	1.1	0.9	6.5	0.9	1.1	2	3.1	0.8	1.1	0.9	1.1
			A_32_P128209	1.1	1.1	1.1	1.2	1.1	6.9	1.1	1.1	2	4	1	1	1.1	1
			A_24_P885873	1	1	0.7	0.9	1.1	9.2	1.1	1.5	3.2	3.6	1	1	1	0.9
			A_24_P914043	0.9	1.1	1	1.4	1.2	19.8	1	1.4	5	14.6	1.2	1.5	2.1	2.9
			A_32_P113472	0.9	1.1	1.1	1	1.7	6.1	1.1	1.1	2.3	3.8	1.1	0.8	0.7	1.3
			A_24_P924697	1	1.1	1.2	1	1.7	6.6	1.1	1	1.9	4	1.3	0.8	0.7	1.4
			A_24_P919150	0.9	0.7	1.2	1.4	2	10.5	1.7	1.6	4.3	4.2	1.3	0.9	1.2	1.3
			A_24_P718503	1	1	1.5	1.4	1.7	14.6	1.6	1.4	3.7	4.4	1.6	1.3	1.1	1.3
			A_32_P138977	1	1.3	1.3	1.6	1.1	9.8	0.9	1	4.8	4.7	1.2	1.2	0.6	1.5
			A_32_P6442	0.9	1	1.6	1.2	2.6	10	1.6	1.5	7.2	3.3	1.4	1.2	1.2	2.4
			A_32_P207802	1	1.2	3.1	2.4	4.8	17.4	2.6	2	14	5.5	2.1	1.6	1.7	2.5
			A_32_P232883	1	1	1.3	1.4	2.6	10.5	1.2	1.1	5.2	5.3	1.2	1.2	1.5	1.5
			A_32_P224345	0.8	0.7	0.9	1.1	10.8	169.9	1	1	56.1	31.3	1	0.9	1	4.2
			A_32_P13565	1	1	1.2	1.1	3.1	9.5	1.3	1.1	7.3	4.7	1.4	1.2	1.2	1.9

			A_32_P132928	1.2	1	2.3	1.5	3.7	23.5	2.1	1.6	13.2	8	1.9	1.2	1.6	3
			A_24_P332081	1	1.2	2	1.7	3.2	18.9	1.8	1.7	10.5	8.2	1.7	1.4	1.5	2.4
			A_24_P788878	1	1.4	1.4	1.3	3	15.4	1.1	1.2	9.2	6.7	1.2	1.1	0.8	2.1
			A_23_P81298	0.8	1	1.1	1	1.8	4.2	1.1	1	3.7	2.6	1	0.8	0.7	1.6
			A_24_P323522	0.8	1	2	1.7	3.9	19.6	2	1.7	17.3	7.9	1.4	1.2	1.1	2.4
			A_23_P335398	0.9	0.9	1.3	1.1	2	18.2	0.9	1	6.8	8.5	0.9	0.6	1.3	1.4
			A_32_P38782	1	1.2	2.2	1.3	2.9	12.4	1.6	1.6	7.9	5.5	1.9	1.4	1.2	1.8
			A_23_P98483	0.9	1.3	1.5	1.2	1.8	6.2	1.3	1.4	4.1	3.1	1.4	1.1	1.1	1.5
			A_24_P585428	0.8	1.3	1.3	1	1.8	5.2	1.2	1.3	5.1	2.7	1.3	0.9	1	1.2
			A_32_P127501	1.1	1.5	2.8	1.9	3	21.5	2.5	2	12.9	10.4	2.1	1.3	1.2	1.7
			A_32_P110016	0.9	0.9	1.3	1.2	1.4	4.7	1.2	1.4	3.7	2.4	1.3	0.9	0.7	1
			A_32_P221641	1	2.6	2.7	2.3	5.1	29	2.9	1.7	10.9	9	4.5	1.7	1.8	2.6
			A_24_P767972	1.2	1.3	1.1	1.5	3.1	14.4	1.7	1.3	8	4.6	1.7	1.4	1	1.4
			A_32_P184039	0.9	1.5	4.7	2.5	13.6	35.4	2.9	4	33.1	17.6	3.1	1.4	1.6	5.7
			A_24_P102283	1.3	1.5	2.7	1.8	6.2	18.1	3.5	3	13.4	10	2.5	0.9	1.2	3.8
			A_32_P165823	1.3	1.1	1.8	1.3	2.9	5.9	2.1	1.9	6	5.6	1.3	1.3	1.4	2.1
			A_32_P173955	1.2	1.5	1.4	1.2	2	7.7	2.1	1.7	4.7	3	1.3	1	1.2	1.8
			A_32_P463538	1	0.8	1.1	1.1	1.5	8	0.9	1.2	3.2	3.1	0.8	1.1	1.9	1.3
			A_24_P14776	1.8	0.7	1	1.2	1.6	10.3	1	1.5	4.3	7.6	1.2	0.9	2.6	1.5
			A_32_P6778	2	1.3	1.2	1.4	2.3	5.2	1.1	1.3	3.7	5.5	1.9	1	2	1.1
			A_32_P125803	1.6	1.6	1.1	0.9	1.3	6	1	1.3	2.7	4.1	1.6	1	1	1.2
			A_32_P104448	1.5	1.3	0.7	0.8	1.4	5.9	0.8	1.2	3.1	6.1	1	0.9	0.9	0.9
			A_32_P73991	0.8	0.7	1.2	1.1	0.8	12.4	1.4	0.7	1.2	18.3	0.8	1	0.9	1.4
			A_32_P220463	1.1	1.3	1.3	1.4	1.6	6.2	1.5	1.6	1.9	7.2	1.1	1.5	1.2	1.5
			A_32_P216015	0.8	0.7	1	1.1	1.2	5.8	1	1	1.7	7.4	1.1	1	1	1.1
			A_32_P59302	1.3	1.7	1.3	1	1.4	9.4	1.4	1.1	2.2	6.6	1.1	1.1	1.1	1
			A_32_P15081	1.2	1.4	1.1	1	1.3	13.2	1	1.2	2.2	9.5	1.1	1.2	1	1.5
			A_23_P2181	1	1	1	1	1.1	5.7	0.9	0.9	1.9	5.2	1	1.1	0.9	1
			A_32_P51855	0.9	1.2	1	1	0.9	9.3	1	1.2	2.2	5.7	1.1	0.9	0.8	1.2
			A_32_P30891	1.4	1.1	1.3	1.7	1.5	15.5	1.8	1.8	3.1	10.9	1.4	2	1.2	1.4
			A_32_P206208	0.9	0.9	1.3	1.1	0.9	6.7	1.3	1.2	1.8	5.1	1.1	1.3	1	1
			A_24_P811397	0.8	0.7	1	1.1	1	35.8	1	0.9	3	19.9	1.1	0.9	0.9	1.1
			A_24_P892464	0.9	1.1	1.1	1.1	1.6	17.6	1.5	1.3	3.5	17.5	1.4	1.3	1.2	1.8
			A_23_P5464	1.1	1.1	1.1	1.1	1.3	7.9	1.2	1.2	2.1	6.9	1.1	1.1	1.2	1.5
			A_32_P1076	0.8	0.7	0.8	0.9	1.4	8.2	0.8	0.9	2.2	8.7	1.1	0.7	1	0.9
			A_23_P42768	0.9	1	0.9	1.4	1.5	6.7	1.1	1	1.6	6.7	1.1	1	1.1	1.1
			A_32_P170454	0.9	1.2	1.4	1.4	2.3	7.4	1.3	1.3	2.5	8.3	1.2	1.2	1	1.2
			A_32_P156786	1	1.2	1.2	1.3	2.3	5.7	1.1	1.1	2.2	6	1.2	1.2	1.1	1
			A_24_P941279	0.7	1.1	1.1	1.1	1.7	5.6	1.4	1.1	2.4	5.7	1	1.2	1	1.4
			A_24_P882959	1.3	1.1	0.7	1	1.2	7.8	0.9	1.3	1.3	12	0.7	1	0.7	1.1
			A_24_P337143	1	0.9	0.8	0.8	1.4	6.2	0.7	1.2	1.4	9.5	0.6	0.6	1	1.2
			A_32_P14721	1.7	1.4	1.2	1.8	2	13.4	1.9	1.4	1.6	9.8	1.3	2.3	1.4	1.4
			A_24_P526190	2.2	1.1	1	1.4	1.2	24.5	1.2	0.9	3.4	17	1.3	0.9	1.6	2.3
			A_23_P413268	1.3	1	1.1	0.8	1.2	6.5	1.2	1	2.1	3.9	1	1.2	1.6	1.2
			A_24_P823514	1.7	1	1.4	1.2	1.8	4.5	1.2	1.1	2	4	1.3	1.1	0.9	1.1
			A_24_P95070	1	1.4	0.9	1	0.9	5.2	0.7	0.7	1.1	3.1	1	0.8	0.6	1.3
			A_32_P174285	0.9	1.6	1.3	0.9	0.9	8.4	0.9	0.9	3.6	9.5	0.9	1	1	1.6
			A_32_P192354	0.9	1	1.2	1.1	1.7	3.6	1.5	0.8	2.5	4.9	1.2	1.3	1.1	1.2
			A_32_P116957	1.2	1.1	1	1.1	1.1	5	1	1	2.6	10.5	1	1.1	1.1	1.9

			A_23_P35546	0.7	0.7	0.9	1.2	1.4	13.1	1	1	6.1	18.5	0.8	0.8	0.8	2.1
			A_24_P772488	0.7	0.6	0.9	1	1	4.4	1.1	0.9	2.8	6.9	1	0.8	1	1
			A_23_P356965	0.9	1.7	1.6	1.1	1.3	4.5	1.4	1.2	2.2	4.7	1.3	1	1	0.9
			A_24_P212875	0.8	1.2	0.7	0.8	1.8	4.4	0.8	1.2	1.3	4.8	0.8	0.6	0.9	0.7
			A_32_P8825	1.4	0.9	0.9	1.4	3.6	10.6	1.2	1.2	9.6	7.2	1.3	1.2	0.7	2.9
			A_32_P213002	2.1	2.6	2.3	1.9	7	13.7	2.3	2.1	13.4	5.9	1.8	1.1	1.5	2.6
			A_32_P102979	1.3	1.2	1.4	1.3	4	5.7	1.5	1.6	9.1	3	1.4	1	1.1	1.4
			A_32_P210038	1.2	1.2	1.6	2.5	11.7	16.7	1.7	1.7	16.3	9.5	1.3	1.1	1.4	5.1
			A_32_P143637	1.1	1.1	1.8	1.7	6.5	22.7	1.3	1.1	11.7	5.4	1.2	0.8	1.2	2.6
			A_24_P367454	0.9	1.6	1.7	2.2	6.4	25.9	0.9	2.3	22.6	12.9	1.4	0.9	1	4.5
			A_32_P111919	0.7	1.2	1.3	1.6	3.4	10.9	1.4	1.8	10.3	4.2	1.1	1.4	2.3	2.2
			A_32_P201976	1.4	1	2.3	1.8	3.9	7.8	2.3	2.5	5.8	4.3	1.3	1.2	0.8	1.3
			A_24_P252739	1.3	1	1.5	1.3	3.3	8.3	1.6	2.1	6	4.8	1	1	0.9	1.2
			A_32_P139815	1.2	1	1.5	1.2	1.9	4.1	1.2	2	2.8	2.1	1.1	1.1	1	0.7
			A_24_P230972	1	1.6	1.4	1.2	3.7	4.8	1.3	1.7	7	2	1.7	0.9	1.3	2.7
			A_32_P233405	1.5	2	1.5	1.1	2.6	5.1	1.2	1.5	4.7	3.1	1	1	1.1	1.2
			A_24_P924010	3.6	5.9	1.2	1.4	10.4	11.6	1.6	2.2	15.6	9.3	1.3	1.6	1.2	1.3
			A_32_P226556	1.2	2.8	1.9	1.6	2.3	9.5	1.5	1.3	6.9	3.2	1.7	1.4	0.9	1.8
			A_23_P6535	0.9	3.9	1.2	1.6	6.4	20.8	1.2	0.7	18.8	14.4	1.1	1.4	2	12.6
			A_24_P126406	0.4	0.5	0.9	1.1	18.2	5.7	0.8	0.8	1.4	7	0.9	1.4	1.4	0.9
D	ATP4A	ATPase, H+/K+ exchanging, alpha polypeptide	A_23_P430728	0.8	0.9	0.8	5.2	48.5	150.5	1.9	13.4	86.6	88	1	2.7	13.5	45.9
	CCL2	small inducible cytokine A2 precursor	A_23_P89431	1.9	1.2	0.9	1	5.7	3.5	0.9	1.4	6.5	4.3	1	1	1.1	5
	CCL5	small inducible cytokine A5 precursor	A_23_P152838	1.6	12	0.9	19.6	33.6	125.7	5.3	21.8	55.5	90.3	1.8	17.5	23	29.9
	CH25H	cholesterol 25-hydroxylase	A_23_P86470	1.9	0.9	0.9	6.3	888.3	3919.7	0.9	18.1	2793.6	2285.9	1.4	5	31.7	813.7
	CX3CL1	chemokine (C-X3-C motif) ligand 1	A_23_P37727	1.7	2.4	1.2	1.7	16.2	27.8	0.7	2.9	18.8	10.1	1.4	1.6	2.2	19.7
	GPR109B	G protein-coupled receptor 109B	A_23_P64721	1.6	2.3	1.5	2	85.5	226.6	1.3	3.1	37.2	70.3	1.5	4.1	10.2	42.3
	IFNB1	interferon, beta 1, fibroblast	A_23_P71774	0.7	3	1.1	13.3	243	627.9	1	66.2	353.3	321.6	0.9	9.3	31.7	180.6
	IL28A	**interleukin 28A**	**A_23_P409438**	**1.3**	**6.3**	**2.4**	**21.9**	**40.1**	**89.5**	**6.1**	**25.5**	**73.6**	**65**	**2.1**	**14.8**	**21**	**32.2**
	IL6	interleukin 6 (interferon, beta 2)	A_23_P71037	1.6	1.5	1	3.1	55.5	158.4	0.8	12.5	71.9	90.7	1	1.8	3.6	34
E	ADAD2	adenosine deaminase domain containing 2	A_23_P49136	1.2	0.9	1.4	1.5	1	14.3	1.3	1.4	1.6	2.4	1.3	1.1	1.2	1.4
	CALCB	calcitonin-related polypeptide, beta	A_24_P198178	0.9	0.8	0.7	1	1.3	4.5	0.6	0.8	0.9	5.2	0.7	1.2	1.4	0.9
	COL11A2	collagen, type XI, alpha 2 isoform 1 preproprotein	A_23_P42322	1.1	1.1	4	1.7	1.1	14	1.7	1.5	2.4	13.3	1.6	1.3	1.1	1.3
	DACT2	dapper, antagonist of beta-catenin, homolog 2	A_24_P289260	0.9	1.1	0.7	0.5	0.8	2.3	0.8	0.7	2.3	4.6	0.7	1.1	0.8	0.7
	FEZ1	zygin 1 isoform 1	A_23_P202881	1.5	0.9	0.8	0.8	0.9	5.6	0.6	0.8	1.2	4.1	0.8	1.7	1.4	1.3
	KIF25	kinesin family member 25 isoform 1	A_23_P59410	1.6	1.7	1.3	1.8	1.4	5.5	0.8	1.9	1.6	9.7	1.1	1.8	1.8	0.6
	LY6K	lymphocyte antigen 6 complex, locus K	A_32_P138348	0.9	1	1	1.1	0.8	3.6	1.2	1.1	1	5	1	1	0.8	0.9
	LY6K	lymphocyte antigen 6 complex, locus K	A_23_P397293	0.8	1	1.3	1.1	0.8	4.1	1.3	1.1	1.3	4.8	1.1	1	0.8	0.9
	OXTR	oxytocin receptor	A_23_P132619	0.8	0.8	1.5	1.2	0.8	3.4	1.3	1.2	1	5	1.5	1.1	0.7	0.9
	RBM35A	RNA binding motif protein 35A isoform 1	A_23_P259127	1.4	1.4	1	1.1	0.8	1.2	0.7	1.1	1.2	5.6	0.9	0.9	0.8	1.6
	RERG	RAS-like, estrogen-regulated, growth inhibitor	A_23_P204296	1	0.6	1.3	0.7	0.9	9.8	0.8	1.1	0.7	2.3	1.3	1.4	1	0.7
	SIRT4	sirtuin 4	A_23_P99226	0.8	0.8	1	0.8	0.8	3.2	0.5	0.8	0.9	4.6	0.6	0.9	1	0.9
	SLC22A1	solute carrier family 22 member 1 isoform b	A_23_P145569	1	0.9	0.9	1.1	0.8	1.7	1.3	1	0.9	4.1	0.8	1.1	1.2	1
	SRD5A2	3-oxo-5 alpha-steroid 4-dehydrogenase 2	A_23_P28186	0.9	1	1	1.8	1.7	6.4	0.6	1.8	1.3	5.5	1.2	1.6	1.6	0.7
	TMEM16F	transmembrane protein 16F	A_23_P53641	1.1	1.1	0.8	0.9	1.1	4.1	0.7	1	0.8	5.5	0.6	1	1.1	0.8
	UPK2	uroplakin 2	A_23_P64238	1.4	0.9	1.1	1.1	1.2	6.1	1.2	1	1.7	2.3	1.3	1.1	1	1.1
	ZNF396	zinc finger protein	A_24_P393565	1.2	1.3	1.1	0.9	1.8	5.3	0.8	1.3	2.3	4.2	0.8	1.6	1.7	1.2

	ZNF545	zinc finger protein 545	A_23_P416813	1.1	1.3	0.7	0.5	1.1	1.8	0.9	0.6	1.3	5.3	0.7	1.2	1.2	0.9
			A_32_P834726	0.8	1.2	1.3	1.7	1.1	8.7	0.7	1.5	1.4	3.9	1.5	2.3	0.9	0.9
			A_23_P93109	0.7	0.7	1	0.9	0.5	4.4	0.9	0.9	0.5	6	1.4	1	0.9	0.8
			A_23_P247	1.6	0.9	0.9	1.1	0.7	7.3	1	0.7	0.6	19.3	0.9	0.7	1.1	0.9
			A_24_P570583	1	1	1	0.9	1.2	2.2	1	1	1.3	4.9	1	0.9	0.9	0.9
			A_23_P63736	0.9	0.9	1	0.9	0.9	2.4	0.7	1.1	1.2	6.9	0.8	1	1.2	0.8
			A_32_P52386	0.9	1.4	1.5	2.7	1.5	5.8	2.1	1.4	2.3	3.4	1.5	2	1.9	1.1
			A_32_P158019	1.4	2.3	1.1	0.9	2.1	2	1	0.8	1.5	6.3	1	0.9	0.6	0.8
F	APOL1	apolipoprotein L1 isoform b precursor	A_24_P87931	6.7	7.6	1.8	1.7	19.9	38	1.6	2.3	31.5	28.2	1.6	1.7	4.2	8.1
	APOL2	apolipoprotein L2	A_23_P211488	5.6	2.5	1	1.4	14.9	25.7	1	1.8	20.6	16.8	1	1.3	3.6	6
	APOL4	**apolipoprotein L4 isoform 1**	**A_23_P380857**	**6.2**	**7.9**	**1.5**	**2.6**	**14.3**	**22.5**	**1.5**	**2.5**	**18.2**	**15**	**1.4**	**1.7**	**5.1**	**7.2**
	APOL6	**apolipoprotein L, 6**	**A_24_P941167**	**8.6**	**8.3**	**1.5**	**1.9**	**14.2**	**9.8**	**1.4**	**2.6**	**16.7**	**8.5**	**1.5**	**1.7**	**6.3**	**9**
	APOL6	**apolipoprotein L6**	**A_23_P155049**	**8.1**	**6.8**	**1.2**	**1.6**	**11.8**	**8.3**	**0.9**	**1.2**	**9.5**	**8.5**	**1.1**	**0.9**	**4.3**	**8.5**
	APOL6		**A_24_P7594**	**7.3**	**10.3**	**0.8**	**2.7**	**19.2**	**10.2**	**0.6**	**6.3**	**17.4**	**6.9**	**0.9**	**1.5**	**6.8**	**11.3**
	B2M	**beta-2-microglobulin precursor**	**A_23_P37441**	**1.7**	**5.5**	**0.6**	**0.8**	**2.8**	**12.6**	**0.6**	**0.9**	**3.6**	**12.7**	**0.7**	**0.7**	**1.4**	**4.6**
	BATF2	basic leucine zipper transcription factor, ATF-like 2	A_23_P370682	8.8	14.8	0.9	1.6	24.3	17.4	1.2	1.7	20.3	9	0.9	1.1	3.3	8.3
	BST2	bone marrow stromal cell antigen 2	A_23_P39465	8.2	21.5	1.1	1.9	16.2	24.8	1.5	2.5	18	20.9	1.3	2.6	3.5	10.6
	BTC	**betacellulin**	**A_23_P135722**	**2.3**	**5**	**1.7**	**1.5**	**3.5**	**1.9**	**1.4**	**1.5**	**3.8**	**2.2**	**1.5**	**1.4**	**1.4**	**2.7**
	C1orf38	basement membrane-induced gene isoform 1	A_24_P85775	14	14.8	0.7	1.3	27.2	7.8	1.5	1.3	16.8	7.3	0.9	0.7	1.5	2.7
	C1orf38	basement membrane-induced gene isoform 1	A_23_P873	14.2	16.6	1.2	2.4	40.9	15.5	1.5	3.4	27.7	10.2	1.2	1.5	2.1	3.6
	CA13	**carbonic anhydrase XIII**	**A_23_P381714**	**5.4**	**2.3**	**1**	**1.2**	**10.5**	**22**	**1.2**	**0.9**	**7.9**	**15.7**	**1.1**	**1.3**	**4.5**	**3.7**
	CASP1	**caspase 1 isoform alpha precursor**	**A_23_P202978**	**6.2**	**46.2**	**0.9**	**1.1**	**27.6**	**7.8**	**0.8**	**1.1**	**17.8**	**23**	**0.8**	**0.9**	**6.3**	**17.1**
	CD274	CD274 antigen	A_23_P338479	3.6	2.7	0.8	0.9	25.7	38.6	0.9	1.1	17	12.6	0.8	1	2	8.2
	CD38	**CD38 antigen**	**A_23_P167328**	**1.4**	**6**	**0.8**	**0.9**	**4.7**	**13.5**	**0.7**	**0.9**	**3.7**	**6.5**	**0.8**	**1.1**	**1.3**	**5.4**
	CEACAM1	carcinoembryonic antigen-related cell adhesion molecule 1 isoform 1 precursor	A_24_P382319	20.4	15.5	0.8	2.6	49.7	12.8	1	3.3	44.3	7.9	1.3	1.7	6.4	13.6
	CEACAM1	**carcinoembryonic antigen-related cell adhesion molecule 1 isoform 2 precursor**	**A_23_P434118**	**2.8**	**4.6**	**1.4**	**1.1**	**8.9**	**15.5**	**0.7**	**1**	**10**	**7.5**	**0.9**	**1**	**3**	**7.9**
	CFB	complement factor B preproprotein	A_23_P156687	3	7.9	0.7	0.9	26.2	38.5	0.8	1.8	42.5	15.6	0.6	0.8	1.7	6.2
	CTSS	**cathepsin S preproprotein**	**A_23_P46141**	**2.1**	**4.4**	**0.9**	**1**	**2.7**	**3.7**	**0.9**	**0.9**	**1.9**	**3.4**	**0.9**	**1.1**	**1.4**	**3.3**
	CXCL11	small inducible cytokine B11 precursor	A_23_P125278	2.9	10	1	1.9	147.8	643.8	1	9.4	321.1	284.5	1.1	2.4	10.1	96
	CXorf43	hypothetical protein LOC139324	A_23_P386364	2.8	3.7	0.5	0.6	10	33.1	0.3	0.6	8.3	22.3	0.6	0.8	1.8	4.7
	DDX58	DEAD/H (Asp-Glu-Ala-Asp/His) box polypeptide RIG-I	A_23_P20814	28.7	32	1.3	2.9	83.4	583.7	1.6	5.7	195	315.1	1.3	1.6	4.1	27.3
	DNAH3	dynein, axonemal, heavy polypeptide 3	A_24_P419286	2	1.8	0.7	1.7	7.7	2.9	1	1.6	4.2	1.9	0.9	0.7	0.7	0.9
	DTX3L	**deltex 3-like**	**A_24_P941912**	**6.1**	**7.1**	**0.9**	**1.5**	**7**	**9.4**	**0.7**	**1.7**	**7.6**	**6.3**	**0.8**	**1**	**2.7**	**4**
	DTX3L	deltex 3-like	A_23_P347040	9.8	8.6	0.9	1.3	11.6	21.6	0.8	1.3	9.1	15	0.9	1	2.1	4.1
	EIF2AK2	**eukaryotic translation initiation factor 2-alpha kinase 2**	**A_23_P142750**	**2.7**	**5.5**	**1.3**	**1.2**	**4.4**	**5.5**	**1.4**	**1.5**	**4.6**	**3.5**	**1.1**	**1.1**	**1.1**	**1.5**
	EMR1	**egf-like module containing, mucin-like, hormone receptor-like sequence 1**	**A_23_P27556**	**1.3**	**5.2**	**0.6**	**0.7**	**2.8**	**2.5**	**0.8**	**0.9**	**1.9**	**3.3**	**0.7**	**1.1**	**1.4**	**2.9**
	EXOC3L	**exocyst complex component 3-like**	**A_23_P424734**	**1.3**	**4.5**	**1.2**	**1.3**	**9.7**	**11.1**	**1.1**	**1.2**	**8.1**	**5.8**	**0.9**	**1.3**	**1.8**	**4.9**
	FAM46A	hypothetical protein LOC55603	A_23_P70660	3	2.4	1.5	1.5	8.8	13.8	1.2	1.6	14.4	10.2	1.4	1.5	1.9	2.7
	GBP1	guanylate binding protein 1, interferon-inducible, 67kD	A_32_P107372	48	41.4	1.2	1.9	128.6	340.5	1.5	1.7	136	90.2	1	1.3	18.1	70.7
	GBP1	guanylate binding protein 1, interferon-inducible, 67kD	A_23_P62890	57.4	82.6	1	1.7	50.8	426.7	1	2.7	122.2	140.5	1.1	1	14.3	64.2
	GBP3	**guanylate binding protein 3**	**A_24_P370702**	**8.4**	**11.1**	**1.2**	**1.5**	**20.9**	**12.9**	**1.2**	**1.6**	**17.9**	**10**	**1.2**	**1.1**	**6.2**	**14.4**
	GBP3	**guanylate binding protein 3**	**A_23_P51487**	**10.8**	**17.2**	**0.4**	**0.9**	**23.4**	**13**	**0.6**	**0.8**	**19.1**	**10.7**	**0.6**	**0.7**	**8.4**	**17.6**
	GBP4	guanylate binding protein 4	A_24_P45446	7.2	20.1	1	1.2	39.5	147	1.2	1.6	45.4	73.6	0.7	1.3	3.4	32.7

	GBP4	guanylate binding protein 4	A_23_P103496	49.2	143.4	0.8	2.3	225.8	303.3	1	4.5	260.1	197.8	1.4	1	17.9	187.6
	GBP5	guanylate-binding protein 5	A_23_P74290	25.7	20.1	0.7	2.4	93.8	256.7	1.4	3.4	140.5	160	1	1.3	16.5	88.5
	GMPR	guanosine monophosphate reductase	A_24_P277657	1.4	6.6	1.1	0.5	3.7	1.3	0.8	0.7	2.5	2.6	0.9	1	1	0.8
	HERC5	hect domain and RLD 5	A_23_P110196	4.3	21.4	0.7	1.5	61.6	420.3	0.8	3.5	147.3	261	0.7	1.5	4.1	40
	HLA-B	major histocompatibility complex, class I, B	A_23_P125107	1.5	5.2	0.7	0.8	4.1	18.4	0.7	0.9	5.1	10.7	0.8	0.9	1.2	4.2
	HLA-B	major histocompatibility complex, class I, B	A_24_P113674	1.6	4.3	0.8	0.9	4	16.2	0.8	1	5.2	10.4	1	0.9	1.2	3.9
	HLA-C	major histocompatibility complex, class I, C precursor	A_24_P298409	1.6	4.6	1.1	1.1	3.3	15.2	1	1.2	5	11	1.1	1.1	1.3	3.6
	HLA-C	**MHC class I antigen**	**A_23_P95917**	**1.5**	**4.6**	**0.8**	**0.9**	**3.7**	**13.9**	**0.7**	**0.9**	**4.4**	**8.8**	**0.9**	**0.9**	**1.3**	**3.5**
	HLA-C		A_23_P113716	1.5	4.3	1.1	1.1	3.5	16	1	1.2	5	11.5	1.1	1.1	1.3	3.5
	HLA-E	**major histocompatibility complex, class I, E precursor**	**A_24_P326082**	**2.2**	**4.2**	**0.8**	**0.8**	**3.4**	**11.1**	**0.8**	**0.9**	**3.4**	**6.7**	**0.8**	**0.8**	**1.1**	**2.8**
	HLA-E	**major histocompatibility complex, class I, E precursor**	**A_32_P460973**	**2.5**	**4.3**	**1**	**1**	**3.7**	**5.1**	**1**	**1.1**	**3.4**	**4.5**	**1**	**1**	**1.4**	**2.5**
	HLA-F	major histocompatibility complex, class I, F precursor	A_23_P314024	1.6	5.2	0.9	0.9	5.9	28.2	0.9	1	7	14	0.9	1	1.3	5.7
	HRASLS2	HRAS-like suppressor 2	A_23_P105012	2.1	9.8	1.2	1.3	11.3	13.1	1.1	1.4	9.7	11.1	0.8	1.2	1.9	7.3
	HRASLS2	**HRAS-like suppressor 2**	**A_24_P364263**	**2**	**6.2**	**0.9**	**1**	**4.3**	**6.6**	**1.1**	**1.1**	**3.6**	**6.2**	**1.1**	**1.1**	**1.4**	**4.2**
	HSH2D	hematopoietic SH2 domain containing	A_23_P153372	6	10.6	1	1.9	20	33.8	1	1.6	23.1	11.3	1	1.2	1.5	3.7
	IBRDC3	IBR domain containing 3	A_23_P321388	1.6	1.8	1.5	1.5	4.8	2.2	1.6	1.4	4	2	1.1	1.1	1	2.2
	IFI16	interferon, gamma-inducible protein 16	A_23_P160025	11.9	19.3	1.1	1.6	17.1	20.7	1	2	12.4	9.4	1	1	1.8	2.9
	IFI16		A_23_P217866	11.3	16.7	1.2	1.6	16.3	19.3	1.1	1.8	12.2	9.2	1.2	1.1	1.6	2.6
	IFI27	interferon, alpha-inducible protein 27	A_24_P270460	9.8	12.5	1.2	1.5	17.7	32.5	1.3	4.3	22.6	21.1	1	1.3	2.4	11.3
	IFI27	interferon, alpha-inducible protein 27	A_23_P48513	12.4	20.8	1.2	1.8	25.6	59.3	1.5	3.1	34	34.8	1.1	1.1	2.9	12.3
	IFI35	interferon-induced protein 35	A_23_P152782	2.4	7.8	0.7	0.9	6.3	3.7	0.8	1.1	5.7	3.3	0.8	0.8	1.5	2.1
	IFI44	interferon-induced, hepatitis C-associated microtubular aggregate protein	A_23_P23074	50.7	65.1	1	12.2	88.7	173.6	1.4	21	128.9	111.9	1	7	16.1	55.2
	IFI44L	histocompatibility 28	A_23_P45871	24.6	78.5	0.9	1.2	79.7	172.2	1.1	3	127.3	95.2	1	0.9	2.2	24.5
	IFI6	interferon, alpha-inducible protein 6 isoform c	A_23_P201459	14.3	45.5	1.2	2.8	37.6	56.4	1.7	4.8	43.3	43.7	1	1.4	2.7	10.4
	IFIH1	interferon induced with helicase C domain 1	A_23_P68155	16.7	30	1.1	4.3	79.8	288.2	2	8.7	150.9	191.8	1.2	3.3	8	53.8
	IFIT1	interferon-induced protein with tetratricopeptide repeats 1 isoform 2	A_23_P52266	32.1	35.9	5.6	24.4	58	121.2	16.2	35.2	94.6	76.7	4.8	14.5	11.2	33.2
	IFIT2	interferon-induced protein with tetratricopeptide repeats 2	A_23_P24004	72.6	85.4	2.4	20.5	926.4	6100.4	11.9	81.2	2569.2	3777.9	2.9	14.5	42.9	531
	IFIT2	interferon-induced protein with tetratricopeptide repeats 2	A_24_P304071	76.7	110.6	1	17.1	340.4	714.3	3.4	46.5	411.3	548.7	1.4	14.9	27.5	327
	IFIT3	interferon-induced protein with tetratricopeptide repeats 3	A_23_P35412	81.5	108.1	0.9	7.3	226.3	421.9	2.2	21.2	353.2	224.7	0.8	4.1	15.8	73.4
	IFIT5	interferon-induced protein with tetratricopeptide repeats 5	A_24_P30194	6.1	6.4	1.1	1.3	8.3	24.6	1.1	1.7	10.6	13.5	1.1	1.1	1.5	4.3
	IFIT5	interferon-induced protein with tetratricopeptide repeats 5	A_23_P63668	5.4	5.5	1.2	1.5	8.3	26	1.2	1.8	12.2	14.8	1.3	1.3	1.5	3.8
	IFITM1	interferon induced transmembrane protein 1 (9-27)	A_23_P72737	6.7	8	0.8	2.3	10	9.8	1.3	3.6	13.4	9.9	0.9	1.1	2.3	2.2
	IFITM2	interferon induced transmembrane protein 2 (1-8D)	A_24_P287043	1.8	5.4	1.1	1	3.6	1.9	1.2	1.1	4	2.6	1	1	0.8	0.7
	IFITM3	interferon-induced transmembrane protein 3 (1-8U)	A_23_P87545	2.6	9.7	1.1	1.1	6.4	5.9	1.3	1.4	8.1	6.8	1	1	1	1.2
	IFITM4P		A_24_P16124	2.2	11.5	0.9	0.9	4.4	2.5	1.1	1.1	4.9	4.1	1	0.9	0.8	0.9
	IL4I1	interleukin 4 induced 1 isoform 2	A_23_P502520	2.5	7.9	1.4	1.3	5.9	16.5	1.1	1.4	7	11.2	1.3	1	1.3	6.2
	INDO	indoleamine-pyrrole 2,3 dioxygenase	A_23_P112026	10.6	39.4	0.9	1.1	87	110.2	1	1.6	93.1	89.3	1.1	1	21.3	71
	IRF1	interferon regulatory factor 1	A_23_P41765	4.8	2.2	0.9	1.8	16.1	22.4	0.9	2.2	18.3	16.7	0.9	2	3.6	8.5
	IRF7	interferon regulatory factor 7 isoform d	A_24_P378019	8.4	13.6	1	3.9	17.7	25.2	1.3	4.9	22.2	13.9	1	1.3	2	3.7
	ISG15	interferon, alpha-inducible protein (clone IFI-15K)	A_23_P819	13.5	36.9	1.2	5.2	35.2	94	2	10.2	58.8	76.7	1.2	3.3	9.9	25.2
	ISG20	interferon stimulated gene 20kDa	A_23_P32404	2.2	6.5	1	1	9.4	38.6	1	1.3	20.4	30.4	0.9	0.9	1.8	8.2

	ISGF3G	**interferon-stimulated transcription factor 3, gamma 48kDa**	**A_23_P65442**	**14.1**	**11**	**1.9**	**3.3**	**14.4**	**14.9**	**3.2**	**5.2**	**15.3**	**11.4**	**1.4**	**1.9**	**6.9**	**6.2**
	KIAA1618	hypothetical protein LOC57714	A_24_P350124	1.7	3.5	1.6	1.5	4.6	2.9	1.6	1.7	5.6	2.2	1.5	1.2	1.3	1.6
	KLK10	kallikrein-related peptidase 10 preproprotein	A_23_P107911	2.3	4.3	1.4	1	14.9	19.9	0.9	1.8	14.7	16.4	1	1.2	2.8	16.1
	LAMP3	lysosomal-associated membrane protein 3	A_23_P29773	7.8	114.5	1.2	1.3	14.8	83	0.8	0.8	10	84.9	1.3	1.4	1.8	7.6
	LAP3	**leucine aminopeptidase 3**	**A_23_P18604**	**2.2**	**5.4**	**0.5**	**0.8**	**4.2**	**2.6**	**0.6**	**0.9**	**2.8**	**2.5**	**0.5**	**0.8**	**1**	**1.5**
	LGALS9	galectin 9 long isoform	A_32_P452655	3.2	8.8	1.3	1.5	6.8	8.2	1.3	1.5	7.8	7.6	1.3	1.2	1.4	2.5
	LGALS9	**galectin 9 long isoform**	**A_23_P116557**	**1.7**	**9.3**	**1.1**	**0.9**	**4.2**	**2.2**	**1.1**	**1.4**	**2.7**	**2.6**	**1**	**1**	**1.4**	**1**
	LMO2	LIM domain only 2	A_23_P53126	12.1	9.7	1	1.2	25	9.3	0.8	1.1	15.8	5.2	1	0.9	1.1	2.7
	MX1	myxovirus resistance protein 1	A_23_P17663	22	30.4	1.3	12.3	28.2	51.8	1.9	17.2	41.2	32	1.3	2.2	7.8	14.4
	MX2	myxovirus resistance protein 2	A_23_P6263	18.5	74.3	0.8	2	81.2	81.1	1.3	3.4	82.9	41.8	1.6	1.2	3	5.5
	MYD88	myeloid differentiation primary response gene (88)	A_23_P362659	2.7	3.5	1	1	4.3	1.2	0.9	1.2	3.3	1.3	1.1	1	1.1	1.2
	NCOA7	nuclear receptor coactivator 7	A_24_P12435	2.9	1.9	1	1.2	6.6	14.8	0.8	1.5	9.2	7.1	1.1	1.1	1.2	3.1
	NCOA7	nuclear receptor coactivator 7	A_23_P156957	3.4	2.4	1	1.2	7.7	15.9	1	3.2	12.2	7.2	1	1.1	1.2	2.7
	NLRC5	**nucleotide-binding oligomerization domains 27**	**A_23_P402892**	**8.9**	**4.9**	**1**	**1.1**	**16.2**	**3.7**	**0.9**	**1.7**	**17.5**	**3.2**	**0.9**	**1.1**	**10.3**	**7.6**
	NLRC5		**A_23_P26583**	**15.7**	**6.8**	**1.1**	**1.3**	**18.5**	**7.2**	**0.9**	**1.6**	**22.3**	**3.6**	**1**	**1**	**10.8**	**11.9**
	NMI	N-myc and STAT interactor	A_23_P154235	2.7	6.2	0.8	0.9	4.2	21	0.7	0.8	4.6	10.6	0.9	0.8	1.6	3.1
	NT5C3	**5'-nucleotidase, cytosolic III isoform 2**	**A_23_P59547**	**1.7**	**4.3**	**0.9**	**1**	**3.7**	**2.9**	**0.9**	**1**	**2.8**	**2.4**	**0.9**	**0.9**	**1.2**	**1.5**
	OAS1	2',5'-oligoadenylate synthetase 1 isoform 2	A_23_P64828	5.1	8.8	0.9	1.3	7.3	10.6	0.9	1.8	6.9	7.5	1	0.9	1.5	4.1
	OAS2	2'-5'-oligoadenylate synthetase 2 isoform 1	A_24_P343929	7.4	44	0.9	1.1	17.5	26.7	0.9	1.1	20	23.4	1	1.1	1.2	7.5
	OAS2	**2'-5'-oligoadenylate synthetase 2 isoform 1**	**A_23_P204087**	**10.5**	**30**	**1**	**1.2**	**13.5**	**19.9**	**1**	**0.7**	**8.2**	**12**	**0.7**	**0.8**	**1**	**3.7**
	OAS3	2'-5'oligoadenylate synthetase 3	A_24_P335305	2.9	10.3	0.8	1.4	8.1	12.5	0.9	1.9	8	9.6	0.8	0.9	1.4	3.5
	OAS3	2'-5'oligoadenylate synthetase 3	A_23_P47955	3.9	17.6	0.9	1.5	9.3	18.2	1.2	2.1	10.3	15.2	1	1.1	1.7	5.1
	OASL	2'-5'-oligoadenylate synthetase-like isoform a	A_23_P139786	40.8	49.6	2.1	29.7	77	187.9	11.5	41.5	114.8	135.5	2.4	24.5	33.3	58.9
	PARP12	zinc finger CCCH-type domain containing 1	A_23_P111804	4	9.4	1.1	1.4	12.7	11.9	1	1.7	12.9	6.2	1.1	1.1	2	3
	PARP14	poly (ADP-ribose) polymerase family, member 14	A_24_P161018	6.5	12.5	1.6	1.9	15.3	72.8	1.5	2.4	29.6	36.8	1.5	1.3	2.7	7
	PARP14	poly (ADP-ribose) polymerase family, member 14	A_32_P56759	5.2	8	1.1	1.3	16.8	62	0.7	2	30.2	27.4	0.7	1.3	3.6	8
	PARP9	**poly (ADP-ribose) polymerase family, member 9**	**A_23_P69383**	**10.2**	**11.3**	**1**	**2.2**	**13.9**	**11.9**	**1**	**3.4**	**14.5**	**7.4**	**1.2**	**1.1**	**3.8**	**5.2**
	PLA1A	phospholipase A1 member A	A_24_P294408	1.9	8.7	1	1.1	9.9	22.3	0.9	0.8	7.1	10.7	0.9	1.2	2.2	5.7
	PLA1A	phospholipase A1 member A	A_23_P29816	1.4	5.4	1.9	1.4	9.9	24.7	1.5	1.6	5.4	9	1.2	1.3	1.5	5.3
	PLEKHA4	pleckstrin homology domain containing, family A (phosphoinositide binding specific) member 4	A_24_P408047	3.9	8.9	1.4	2.2	23.9	79.3	1.8	4.1	43.2	46.7	1.3	1.7	3.9	16.7
	PLEKHA4	pleckstrin homology domain containing, family A (phosphoinositide binding specific) member 4	A_23_P67360	4.7	8.6	1.4	1.2	14.4	31.6	0.9	2.1	21.9	20.1	1	1.4	3.6	11.7
	PLSCR1	phospholipid scramblase 1	A_23_P69109	3.7	12.6	0.9	1.4	8.9	14.5	0.8	1.8	8.7	8.2	0.9	0.8	1.1	3.2
	PML	**promyelocytic leukemia protein isoform 1**	**A_24_P207139**	**4.5**	**5.7**	**1.3**	**1**	**6.6**	**4.5**	**0.8**	**1.5**	**6.3**	**3.1**	**1.3**	**1**	**2**	**1.5**
	PML	**promyelocytic leukemia protein isoform 6**	**A_24_P198598**	**2.7**	**4.5**	**1**	**1.1**	**4.8**	**3.6**	**1**	**1.3**	**3.9**	**2.9**	**1**	**1.2**	**1.7**	**1.6**
	PML	**promyelocytic leukemia protein isoform 6**	**A_23_P306148**	**2.7**	**4.1**	**1**	**1.1**	**5**	**3.8**	**1**	**1.4**	**4.2**	**2.9**	**1**	**1.2**	**1.6**	**1.7**
	PNPT1	**hypothetical protein**	**A_32_P76035**	**2.2**	**5.1**	**0.8**	**1**	**4.5**	**2.8**	**0.9**	**1**	**3.4**	**1.9**	**0.8**	**1.1**	**1.2**	**1.2**
	PNPT1	polyribonucleotide nucleotidyltransferase 1	A_23_P154488	2.4	4.8	1	1	5.2	7.8	1	1.1	5.1	3.1	0.9	1.1	1.2	1.2
	PPM1K	protein phosphatase 1K (PP2C domain containing)	A_24_P214598	2.5	5.7	0.7	1.2	18.3	46.7	1	1.3	28.7	27.7	0.7	0.9	1.4	6.7
	PSMB10	**proteasome beta 10 subunit proprotein**	**A_23_P140807**	**1.5**	**4.6**	**1.3**	**1.2**	**3**	**2.4**	**1.4**	**1.1**	**3.1**	**3.3**	**1.2**	**1.2**	**2.1**	**4.9**
	PSMB8	**proteasome beta 8 subunit isoform E1 proprotein**	**A_23_P250629**	**2.4**	**6.9**	**0.7**	**0.9**	**4.6**	**1.8**	**0.7**	**0.9**	**3.1**	**2.2**	**0.8**	**1**	**2.1**	**3.5**

	PSMB9	**proteasome beta 9 subunit isoform 1 proprotein**	**A_23_P111000**	**3.1**	**12**	**0.5**	**0.8**	**9.4**	**3.6**	**0.8**	**1.1**	**6.1**	**4.9**	**0.6**	**0.9**	**3.8**	**8.8**
	RARRES3	**retinoic acid receptor responder (tazarotene induced) 3**	**A_23_P1962**	**2.1**	**6**	**1.2**	**1.3**	**7.4**	**10.4**	**1.3**	**1.5**	**8**	**8.3**	**1**	**1.3**	**4.4**	**6.9**
	RASGRP3	RAS guanyl releasing protein 3 (calcium and DAG-regulated)	A_24_P54390	9.8	15.2	0.8	0.9	25.7	12.4	0.6	1.8	14.7	7.3	0.9	0.8	3.7	3.8
	REC8	**REC8 homolog**	**A_24_P344087**	**5.5**	**4.9**	**2.1**	**4.3**	**6.6**	**8.3**	**3.6**	**4.7**	**9.3**	**5.2**	**1.6**	**2.4**	**3.9**	**3.9**
	RGS22	**regulator of G-protein signalling 22**	**A_32_P125771**	**2**	**12.6**	**0.8**	**0.7**	**3.9**	**2.1**	**1.2**	**1.5**	**2.1**	**4.4**	**1**	**0.9**	**1.3**	**3**
	RNF213	chromosome 17 open reading frame 27	A_24_P923884	1.9	3.5	1.7	1.6	5.4	2.1	1.5	1.3	5.9	2.2	1.7	1.4	1.3	1.5
	RSAD2	radical S-adenosyl methionine domain containing 2	A_24_P316965	7.8	29.5	1.2	1.2	92.9	409.1	1	2.9	194.4	302.7	1	1.2	6.1	61.4
	SAMD9	sterile alpha motif domain containing 9	A_24_P175188	36.7	37	0.8	1.9	49.1	50	0.8	3.2	35.6	34.8	0.9	1.1	5	12.4
	SAMD9	sterile alpha motif domain containing 9	A_24_P175187	42.2	25.2	0.8	2.1	28.6	55.3	0.8	3.4	34.1	37.7	0.9	1.1	3.5	13.4
	SAMD9	sterile alpha motif domain containing 9	A_23_P355244	23	26.9	1	2.2	48.5	76.1	0.9	3.2	41.2	53.3	1	1.1	3.7	14.6
	SAMD9L	**sterile alpha motif domain containing 9-like**	**A_23_P145874**	**35.7**	**31.7**	**1.3**	**4.1**	**87.9**	**55.6**	**1.4**	**5.9**	**82.9**	**37.6**	**1.5**	**1.6**	**14.5**	**22.3**
	SAT1	spermidine/spermine N1-acetyltransferase	A_23_P378722	1.3	1	0.6	0.9	3.5	4.3	0.6	0.9	4.9	2.8	0.6	0.8	1.2	1.8
	SAT1	spermidine/spermine N1-acetyltransferase	A_23_P137016	1.4	1.2	0.7	1	4	5.3	0.7	1	6.3	3.4	0.7	1	1.2	2
	SIDT1	SID1 transmembrane family, member 1	A_23_P132515	4.5	9	1	1.1	15.1	2.9	1.3	1.8	9.1	1.2	0.9	1.9	2.7	2.6
	SLC15A3	**solute carrier family 15, member 3**	**A_23_P75786**	**4.9**	**14.9**	**1**	**0.4**	**15.2**	**33**	**0.7**	**0.7**	**12.9**	**17.5**	**0.9**	**0.8**	**1.7**	**7.1**
	SOCS1	suppressor of cytokine signaling 1	A_23_P420196	4.1	2.1	1.2	1.4	14.3	10.6	1.3	1.9	13.8	6.3	0.9	1.5	1.5	4.2
	SP100	**hypothetical protein**	**A_23_P209712**	**2.5**	**6.4**	**2.8**	**1.8**	**3.5**	**4.5**	**2.5**	**1.9**	**4.2**	**2.6**	**2**	**1.4**	**1.6**	**1.7**
	SP100	**nuclear antigen Sp100 isoform 2**	**A_24_P385611**	**2.9**	**5**	**0.9**	**1**	**4.4**	**5.1**	**0.8**	**1.1**	**3.8**	**3.2**	**0.8**	**0.9**	**1.2**	**1.9**
	SP100	nuclear autoantigen	A_24_P916816	5.8	7.1	2.6	3.3	10.8	11.7	2.6	3.7	11.8	5.6	1.8	1.2	1.9	3.4
	SP110	SP110 nuclear body protein isoform b	A_23_P120002	8.8	14.5	0.9	1.2	15.3	10	0.9	1.8	10.9	5.8	1	0.9	1.8	2.2
	SP140	**SP140 nuclear body protein isoform 1**	**A_24_P328504**	**3.7**	**6.8**	**1.3**	**1.5**	**5.9**	**5.5**	**0.9**	**1.2**	**4.9**	**3.5**	**1.6**	**1.1**	**2**	**3.4**
	STAT1	**signal transducer and activator of transcription 1 isoform alpha**	**A_23_P56630**	**3**	**8.3**	**0.5**	**1**	**11**	**13.1**	**0.5**	**1.1**	**6.8**	**7.7**	**0.6**	**1**	**3.7**	**4.9**
	STAT1	**signal transducer and activator of transcription 1 isoform beta**	**A_24_P274270**	**4.6**	**10.1**	**0.9**	**2.3**	**14.6**	**11.1**	**0.9**	**2.9**	**15.3**	**7.6**	**0.9**	**1.5**	**4.7**	**5.7**
	STAT2	signal transducer and activator of transcription 2	A_23_P76090	4.9	3.8	1.3	1.3	8.6	4.2	1	1.6	8.3	2.4	0.9	1.1	2.1	2.5
	TAP1	**transporter 1, ATP-binding cassette, sub-family B**	**A_23_P59005**	**4.8**	**9.2**	**1**	**1.4**	**13.6**	**12.8**	**1.1**	**1.4**	**11.5**	**9.5**	**1**	**1.4**	**3.8**	**9.3**
	TAPBPL	TAP binding protein-like	A_23_P36700	1.3	2.7	0.7	0.7	3.4	15.7	0.6	0.9	7.6	11.1	0.7	0.8	1.5	3.4
	TDRD7	tudor domain containing 7	A_23_P123672	2.7	3.1	0.9	1	5.8	20.3	0.8	1.3	9.4	12.3	1	0.8	1	2.1
	TGM2	**transglutaminase 2 isoform a**	**A_32_P86763**	**1.7**	**4.2**	**0.6**	**0.6**	**2.2**	**1.2**	**0.5**	**0.7**	**1.4**	**1.2**	**0.6**	**0.7**	**1.2**	**1.5**
	TLR3	**toll-like receptor 3**	**A_23_P29922**	**11.9**	**16.1**	**1.3**	**1.3**	**29.3**	**6.6**	**0.9**	**1.8**	**12**	**16.1**	**0.9**	**1**	**5.7**	**12.7**
	TMEM140	**hypothetical protein LOC55281**	**A_24_P372134**	**4.1**	**3.4**	**1.1**	**1**	**4.3**	**4.1**	**1**	**0.9**	**2.3**	**3.4**	**1.2**	**1**	**1.2**	**1.7**
	TMEM140	hypothetical protein LOC55281	A_23_P31177	12.1	8.5	0.9	1.1	23.9	14	1.1	1.6	14.1	10.7	1.2	0.9	3.4	4.4
	TNFSF10	tumor necrosis factor (ligand) superfamily, member 10	A_23_P121253	23.5	20.1	5.6	1.3	50.8	11.7	1.1	1.6	26.1	11.5	1.2	1.1	2.2	6.9
	TNFSF13B	tumor necrosis factor (ligand) superfamily, member 13b	A_23_P14174	6.2	13.1	0.9	1.5	17.8	19.7	1.2	1	14.5	14.1	1	1.2	2.8	4.3
	TRIM14	tripartite motif protein TRIM14 isoform alpha	A_24_P197964	2.3	8.7	0.5	1	6.4	9.4	0.7	1.2	5.6	6.5	0.6	1	1.3	2.5
	TRIM14	tripartite motif protein TRIM14 isoform alpha	A_23_P216655	2.1	7.3	0.6	1.1	7	8.6	0.8	1.5	6.3	5.6	0.7	1	1.5	2.6
	TRIM14	tripartite motif protein TRIM14 isoform alpha	A_23_P425752	1.7	4.6	1	1.2	4.9	4.9	1.1	1.3	5	3.5	1	1.2	1.2	1.6
	TRIM22	**tripartite motif-containing 22**	**A_23_P203498**	**16.1**	**42**	**0.9**	**1.4**	**57.3**	**41.8**	**1**	**1.3**	**63.1**	**36.6**	**0.8**	**0.9**	**6.6**	**19.6**
	TRIM25	tripartite motif-containing 25	A_23_P15326	2.5	2.2	1.1	1.1	4.5	11	1.2	1.2	4.8	8.3	1.1	1	1.2	1.8
	TRIM25	tripartite motif-containing 25	A_24_P936767	3.5	2.9	0.7	1.1	7.5	5.9	0.7	1.3	5.2	4.3	0.7	0.9	1.2	1.8
	TRIM34	**tripartite motif protein 34 isoform 1**	**A_24_P398323**	**2.1**	**4.1**	**0.9**	**0.9**	**4**	**1.4**	**0.8**	**0.9**	**2.3**	**1.5**	**0.8**	**0.8**	**1.5**	**1.4**
	TRIM34	**tripartite motif protein 34 isoform 3**	**A_23_P124190**	**3.4**	**7**	**2.4**	**1.8**	**5.2**	**2**	**1.6**	**1.6**	**5.1**	**1.8**	**2.2**	**1.3**	**1.6**	**2**
	TRIM38	tripartite motif-containing 38	A_24_P294851	3.6	3.3	0.7	1.2	6.4	2.3	0.9	1.3	6	1.9	0.7	1.1	1.4	1.8

	TRIM69		**A_24_P50543**	**4.1**	**3.8**	**0.9**	**0.9**	**5.1**	**4.4**	**0.7**	**1**	**3.1**	**3**	**1**	**0.7**	**1.6**	**2.9**
	UBD	**diubiquitin**	**A_23_P81898**	**6**	**12.9**	**1**	**1.2**	**7.7**	**20.3**	**0.8**	**1.1**	**5.5**	**19.2**	**1**	**0.8**	**3**	**41.6**
	UBE1L	ubiquitin-activating enzyme E1-like	A_23_P21207	3.5	21.8	1	0.8	19	8.4	0.9	0.8	24.4	8.9	0.9	0.8	2.7	7.5
	UBE2L6	**ubiquitin-conjugating enzyme E2L 6 isoform 2**	**A_23_P75741**	**2.8**	**9.2**	**0.6**	**0.8**	**4.8**	**2**	**0.6**	**0.9**	**3.4**	**2.6**	**0.7**	**1.1**	**1.8**	**2.9**
	USP18	ubiquitin specific protease 18	A_32_P132206	5.3	9.2	1.2	1.5	14.7	25.8	1.1	1.8	18.7	18	1.2	1.3	1.7	4.2
	USP18	ubiquitin specific protease 18	A_23_P132159	4.9	9.6	0.8	1.2	18.5	29.6	0.8	1.6	22.2	21.1	0.9	1	1.5	3.5
	ZNFX1	zinc finger, NFX1-type containing 1	A_24_P23034	5.7	3.2	1	1.3	7.1	15.3	0.9	1.6	9.9	11.4	1	1.2	1.7	3.7
	ZNFX1	zinc finger, NFX1-type containing 1	A_23_P68462	5.8	2.9	0.5	1.3	10.5	18.1	0.6	1.6	9.8	9.7	0.7	1.2	1.4	3.8
		hypothetical protein	A_32_P161292	2.9	5.4	0.6	0.9	10.8	25.3	1	1.5	14.5	17.8	1.1	1.1	2.8	4.2
		hypothetical protein	A_32_P6628	1.6	3.5	1.1	1	4.4	3	1	1.1	4.7	1.7	1	1	1	1.1
		hypothetical protein LOC55337	A_23_P38894	3.8	9.8	1.6	1.6	12.7	9.7	1.3	1.9	11.9	5	1.4	1.2	1.6	2
		hypothetical protein LOC55337	A_24_P236949	2.3	7.6	0.7	0.9	6	8.3	1	1.4	6.9	4.7	0.8	0.8	1.1	1.7
		hypothetical protein LOC55601	A_24_P334361	5.8	18.1	0.3	1.1	23.9	104.2	0.4	1.5	50.4	75.9	0.4	0.8	3.9	16.4
		hypothetical protein LOC55601	A_23_P41470	5.1	13.7	0.4	0.9	16.4	66.9	0.4	1.4	38.5	51.5	0.4	0.8	3	10.7
		hypothetical protein LOC79132	A_23_P38346	11.8	50.6	1.4	2.9	62.4	323.3	1.4	5.5	146.3	183.8	1.2	2	6	48.6
		hypothetical protein LOC93349	**A_23_P337753**	**2.8**	**4.3**	**1.2**	**1.1**	**6.1**	**2.7**	**0.8**	**0.8**	**4.3**	**2.8**	**0.9**	**1.1**	**2.6**	**3.2**
		leukocyte-derived arginine aminopeptidase	**A_23_P30243**	**4.3**	**4.6**	**1.1**	**1.4**	**8.3**	**11.6**	**1.2**	**1.6**	**8.8**	**11.9**	**1.1**	**1.3**	**3.1**	**5.8**
		promyelocytic leukemia protein isoform 2	A_23_P358944	5.1	4.5	1.6	1.7	9.5	7.6	1.6	1.9	9.8	4.4	1.4	1.2	1.4	2.3
		similar to galectin 9 short isoform	**A_23_P101025**	**1.4**	**7**	**1.4**	**1.2**	**3.4**	**3**	**1.7**	**1.4**	**2.7**	**2.5**	**1.6**	**1.4**	**1.1**	**1.2**
		Unknown (protein for MGC:105145)	A_24_P418044	1.7	5.4	0.9	1	4.2	17.9	0.8	1	5.2	11.4	1	1.1	1.4	4.2
		XIAP associated factor-1 isoform 1	A_23_P4286	65.7	270	1.2	2.3	277.1	345.9	1.2	3.7	225.6	209.2	1.6	1.4	7.9	77.7
		XIAP associated factor-1 isoform 1	A_23_P4283	52.8	95.9	0.9	1.5	120.5	184.2	1.1	2.7	143.6	90.8	1.4	0.9	5	38.6
			A_32_P99533	5.5	10	1.6	3.6	29.8	72.2	1.5	6.7	42.5	36.9	1.8	2	6.1	21.4
			A_24_P927166	6.4	4.2	1.5	3.3	60.2	236.6	1	6.9	126.8	103.5	1.6	1.4	6.5	28.9
			A_32_P92415	4.1	10	1.3	1.6	16.3	85.2	1.2	2.1	33.9	42.8	1.3	1.2	2.9	7.9
			A_24_P586264	3.3	6.3	0.7	1.2	22.3	47.7	1.1	1.7	34.9	33.3	0.9	1.2	1.6	8.3
			A_32_P154726	2.6	3.4	0.8	0.9	7.5	20.4	0.7	1	9.2	12.6	0.9	0.9	1.5	4.3
			A_24_P127641	5.6	8.3	1.4	1.8	16.3	36.6	1.3	2	20	16.6	1.4	1.3	2.9	7.9
			A_24_P68079	4.6	9.3	1.7	1.6	14.4	19.2	1	2	16.5	12.9	1	1.1	2.9	7.7
			A_23_P250353	4	11.1	0.7	1.2	12.2	26	0.8	1.8	16.8	22	0.9	1.1	2	8.5
			A_32_P114831	2.3	4.1	1.2	1.8	7	10.5	1.7	1.4	8	12.7	1	1.3	1.6	4.3
			A_32_P220897	2.8	2.4	1	1.1	3.6	6.8	0.8	1.5	5.4	5	1.1	0.8	1.1	2
			A_24_P829156	5.5	4.7	2.6	2.5	12.2	16.2	1.5	2.4	13.7	7.3	1.5	1.2	3.1	5.1
			A_23_P256487	3.3	3.6	0.8	0.9	24.5	52.4	0.9	1.3	20.9	27.3	0.8	0.9	2.1	12.9
			A_32_P75867	**3.3**	**5.8**	**1.7**	**1.7**	**22.2**	**23.5**	**1.2**	**3.1**	**19.3**	**13.6**	**1.8**	**2**	**7.2**	**20.1**
			A_32_P143980	**2**	**4.3**	**1.2**	**1.3**	**4**	**11.1**	**1.3**	**1.3**	**4.6**	**8.1**	**1.3**	**1.1**	**1.4**	**3.7**
			A_23_P338113	1.2	3.3	0.7	0.8	3.2	14.1	0.7	0.8	3.9	8.2	0.8	0.8	0.9	3.4
			A_23_P125109	1.5	5	0.8	0.9	4.3	22.9	0.8	0.9	5.7	13.9	0.9	1	1.2	4.7
			A_23_P373126	1.8	6.6	0.8	0.9	6.9	27	0.8	1	7.8	14.7	0.8	0.9	1.3	6.2
			A_23_P370707	1.7	5.3	0.8	0.9	7	23	0.8	1	7.4	12.9	0.8	0.9	1.5	6.3
			A_24_P860781	**1.5**	**4.6**	**0.9**	**1**	**2.5**	**12.2**	**0.9**	**0.9**	**3.4**	**8.4**	**0.9**	**1**	**1**	**3.2**
			A_23_P350295	1.1	2.3	0.9	0.9	2	10.2	0.8	0.9	2.9	7.1	0.9	0.9	1	2.5
			A_32_P54553	3.4	5.9	0.7	0.9	8.8	14.6	0.6	1.4	9.5	9.9	0.6	1	1.3	2.4
			A_23_P30069	4	17.2	1	1.5	24.9	38.8	1	2.2	34.5	22.3	0.9	1.2	2.5	4.6
			A_23_P65174	**2.3**	**4**	**1**	**1.1**	**4.8**	**6.5**	**1.1**	**1.3**	**4.5**	**3.7**	**1**	**1**	**1.5**	**1.8**
			A_23_P17837	5.3	10.7	0.9	1.9	11.9	22.3	1.8	2.9	24.5	18.4	1.1	1.8	3.4	7.9
			A_23_P384355	63.7	88.6	0.7	2.8	94.9	338.2	0.6	4.5	81.5	170.7	0.8	1	2.8	24.8
			A_24_P36898	**7.2**	**2.5**	**0.8**	**1**	**6.1**	**12.8**	**0.9**	**0.7**	**5.9**	**5.8**	**0.9**	**0.7**	**2.4**	**3.6**

			A_24_P740662	**11.5**	**8.7**	**2.2**	**4.9**	**19.6**	**26**	**2.1**	**8.1**	**28.9**	**15.7**	**1.6**	**1.9**	**7.2**	**10**
			A_24_P118892	6.3	11.9	0.9	2	14.2	13.3	0.7	1.9	9.6	9.4	0.7	1.5	1.1	1.9
			A_24_P868905	4.2	12.9	1	1.4	9.5	10.3	1.4	1.6	12.2	9.7	0.9	1.1	1.4	2.3
			A_32_P167592	2.2	7.4	1.1	1.2	4.6	3.4	1.3	1.3	5.6	4.1	1	1	0.9	0.9
			A_24_P7040	2.8	10.4	1	1	6.5	5.4	1.2	1.4	8.5	6.6	1	0.9	0.9	1.2
			A_23_P202245	2.2	13.4	1	1.2	8.8	8.6	1.1	1.1	6.3	10.2	1	0.6	0.7	1.4
			A_32_P156746	8.1	6.2	1.1	2.3	16.2	4.8	1.3	2.9	15.9	3.1	1.3	1	2.5	3.5
			A_24_P236680	3.8	3.1	1.1	1.5	7.4	3.3	1.3	1.9	5.4	2.8	1	1.2	1.5	1.7
			A_24_P15702	**2**	**4.3**	**0.5**	**0.9**	**3.8**	**1.8**	**0.5**	**1**	**1.8**	**2.3**	**0.5**	**0.9**	**1.1**	**1.4**
			A_32_P56249	**10**	**18.8**	**1.1**	**0.8**	**27.3**	**21.7**	**0.7**	**0.8**	**28.2**	**16.1**	**0.9**	**1**	**6.2**	**32**
			A_32_P171793	6.2	12.8	0.9	1.7	18.1	7.8	0.8	1.2	12.6	8.1	0.9	1.3	4.2	10.5
			A_23_P203629	**1.5**	**4.8**	**1.6**	**1.1**	**2.9**	**3.8**	**1.7**	**1.2**	**2.8**	**3.7**	**1.4**	**1.1**	**1.3**	**2.9**
			A_23_P354547	**11.5**	**8.7**	**2.1**	**7.1**	**11.7**	**10.1**	**3.8**	**7.5**	**16.2**	**5.1**	**1.5**	**3.1**	**5.1**	**5**
			A_32_P154321	**1.9**	**4.4**	**1.3**	**1.1**	**2.6**	**1.5**	**1.3**	**1.3**	**2.9**	**2.3**	**1.3**	**1**	**1.8**	**1.7**
			A_24_P15502	**1.6**	**4.4**	**1**	**1**	**2.6**	**1.8**	**1.2**	**1.2**	**3.1**	**2.3**	**1**	**1**	**0.9**	**0.8**
			A_24_P254933	2	8.1	1	1	3.6	2.6	1.2	1.3	4.4	3.8	1	1	0.9	0.9
			A_24_P306810	3.1	3.2	1.8	2.1	8.1	2.2	1.9	2.1	7.3	1.6	1.5	1	1.7	1.8
G	AVIL	advillin	A_24_P419087	1.3	1.6	1.8	2.7	3.1	5.2	2.4	3	5.2	3.1	2.1	0.9	1	1.2
	CDH15	cadherin 15 preproprotein	A_32_P25357	1.7	1.1	1	1.3	6.8	3.3	1.2	1.1	1.6	2.5	1.2	1.3	3.2	1.6
	CEBPD	CCAAT/enhancer binding protein delta	A_23_P31810	2.7	1.3	2	1.5	3.7	1.9	1.6	1.5	5.2	1.4	1.7	1	0.8	1
	CHRNA10	cholinergic receptor, nicotinic, alpha polypeptide 10	A_23_P411188	0.8	1	1.8	1.6	1.7	7.5	1.8	1.5	4.9	4.3	1.5	1.4	1.1	1.2
	DDEF1IT1	HSPC054	A_23_P146325	1.3	1.5	4.5	2.3	2.8	7.6	3.5	2.3	7.9	2.9	3.2	1.5	1.3	1.6
	FEV	FEV (ETS oncogene family)	A_23_P5460	1.2	1.2	1.6	1.5	2.4	10.9	1.7	1.2	1	1	1.2	2	1.5	2.5
	IL1B	interleukin 1, beta proprotein	A_23_P79518	1.2	1	0.8	1	1.8	4.3	0.8	1	1.6	0.8	0.9	1.1	1	3.5
	ITGB1BP2	integrin beta 1 binding protein 2	A_23_P45424	0.9	1	2.8	1.8	2.1	3.8	1.9	1.7	4.7	2	1.8	1.2	1	1.3
	MLL3	myeloid/lymphoid or mixed-lineage leukemia 3 isoform 2	A_32_P209472	0.9	1.1	2.5	2.6	2.1	11.4	2.5	2	7.6	4.4	1.5	1.5	1.2	1.8
	SATB2		A_24_P928408	1.7	1.7	3.9	3.1	2.4	7.9	3.2	2	7.1	2.6	2.4	1.4	1.5	1.2
	SOCS3	suppressor of cytokine signaling 3	A_23_P207058	2.4	1.2	1.4	1.4	4.8	1.3	1.6	1.8	4.1	0.9	1.2	1	0.8	0.7
	SSH2	hSSH-2	A_23_P395954	1.2	2	2.8	1.7	1.7	4.5	1.4	2.1	2.7	1.4	1.8	1.3	1.3	1.1
	SYNPO2		A_23_P310094	1.2	1.7	0.6	1.2	2.7	9.7	0.5	0.9	2.1	1.6	0.8	1.6	2.3	2.7
	TTC18	tetratricopeptide repeat domain 18	A_23_P326931	2.2	1	3	1.5	1.6	7.9	1.3	2.2	4.4	4.4	2.6	1.1	0.9	1.1
	ZBTB20		A_32_P179526	1.2	1.6	4.2	2.4	2.8	2.6	3.8	2.5	4.8	1.3	3.2	1.2	1.2	1.2
		hypothetical protein	A_24_P273647	0.8	1.1	1.6	1.4	1	5.2	1.3	1	2.2	2.4	1.5	1.4	0.9	0.9
		interferon epsilon 1	A_23_P302060	1.1	1.2	1.6	2.2	2	6	2.2	1.8	2.6	2	1.5	1	1.5	1.1
		KIAA1541 protein	A_24_P940218	1.1	1.1	2.6	2.1	1.9	6.4	1.9	1.7	3.7	3.9	2.2	1.8	1.5	1.5
			A_32_P98940	1.1	1.4	4.7	2.7	4.9	30.3	3.3	2.2	15.5	11.5	3.9	1.8	1.6	3.3
			A_32_P208039	1	1.2	3.9	2.2	3.3	20.3	2.7	1.8	10.3	8	2.9	1.6	1.3	2.4
			A_32_P55987	1.2	1.6	5.3	3	4.1	25.3	4.4	2.5	13.6	8.9	4.1	1.8	1.7	2.9
			A_32_P220567	1	1.1	2.4	1.7	2.2	9.4	2.1	1.9	6.2	4.1	2	1.2	1.1	1.8
			A_32_P216122	0.8	1.6	4.2	2.5	3.1	16.4	3.2	1.8	8	10.6	3.2	1.5	1.4	2.3
			A_32_P214054	0.8	1.4	3.8	2.8	2.7	11.8	3.3	2.1	5.7	6.1	3	1.7	1.3	2.1
			A_32_P15874	1	1.1	2.2	1.9	1.6	6.3	2.4	2.1	4	3.8	1.7	1.3	1.3	1.4
			A_24_P145333	0.9	1.1	2.2	1.9	1.7	4.8	1.7	1.5	4.2	2.5	2.5	1.1	1	1.3
			A_23_P24275	1.2	1.1	2.4	2.2	1.4	6.7	2.1	1.7	3.4	3.2	1.8	1.8	1.4	1.1
			A_32_P44932	1	1.2	1.9	1.6	1.3	4.8	1.9	1.6	2.4	4.7	1.6	1	1.1	1.2
			A_32_P10133	0.8	2.2	3.9	2.6	2	10.5	3.4	2.4	4.2	6	3.1	1.3	1.3	2
			A_32_P40673	1	1.5	2.1	2.3	1.5	5.1	2.5	2.1	4.1	4.4	2.5	1.2	1.1	1
			A_32_P92101	1	1.5	2.4	1.8	2	3.2	2.5	2.1	5.1	2.8	1.9	1.9	0.7	1.8

			A_32_P83973	1	1.5	4.3	2.1	2.2	6.3	3.3	2.2	5.6	2.2	2.3	1.4	1.3	1.6
			A_32_P191074	1.2	1.6	4.1	2.8	3.9	10.9	3.1	2.8	11	3.9	3.1	1.9	1.6	2
			A_24_P162128	1	1.5	4	2.1	2.8	5	2.7	2.3	6.1	2.6	2.5	1.4	1.3	1.4
			A_32_P7516	1.1	1.6	2.5	1.9	2.8	4.3	2.5	2	5.2	2	1.9	1.2	1.2	1.2
			A_23_P399292	1.1	1.6	2.6	2	3	5	2.7	2	6	2.3	1.9	1.2	1.2	1.2
			A_32_P198282	2.4	1.7	4.4	3.1	2	9.7	3.9	3	7.9	3.5	2.9	1.4	1.4	2.1
			A_32_P118220	1.1	1.3	5.2	2.5	2	9.3	4.3	2.1	5.2	4.1	2.3	1.6	1.4	1.6
			A_24_P932388	1	1.8	5.9	1.6	4	10.8	2.4	2.7	8	3.8	2.4	1.4	1.4	3.5
			A_32_P110485	1.1	1.6	2.6	2.7	3.5	8.9	1.7	3.7	4.5	2.8	1.7	1.5	1.2	1
			A_24_P204374	0.7	1	1	1.3	1.7	5.6	1.4	1.4	3	2.2	1.2	1.1	1.1	0.8
			A_32_P211048	1	3.1	5.5	2.6	1.9	9	4.7	2.5	4.1	2.8	4.7	1.7	1.6	1.3
			A_32_P129310	1.2	1.7	3.4	2	1.5	5.2	2.7	2.3	3.2	1.4	2.6	1.5	1.4	1.1
			A_32_P53976	1.5	1.7	6.3	3.3	3.3	5.4	6.8	3.3	6.4	2.1	3.1	1.7	1.5	1.7
			A_32_P198791	1.1	1.8	4.2	2.4	6.5	5.2	5.1	2.8	7.2	2.3	2.7	1.7	1.6	3
			A_23_P156408	0.8	1.3	1.5	0.8	0.8	4.3	1.2	0.9	1.1	3	2.4	0.6	0.6	1
			A_32_P158181	1.4	1.6	1.1	1.2	3.8	1.4	1.6	1.6	1.9	1.1	1.2	0.9	1.2	5.7
			A_32_P3317	1	0.8	0.6	0.7	2	2	0.5	0.8	0.7	0.6	0.6	0.8	3.8	5.2
H	ABCB6	ATP-binding cassette, sub-family B, member 6	A_24_P197196	1	0.9	1.3	1.1	1	0.2	1.4	1.2	0.7	0.4	1.1	1.1	1.2	1
	ABCB6	ATP-binding cassette, sub-family B, member 6	A_23_P5441	0.9	0.8	1.2	1.1	0.9	0.2	1.3	1.2	0.7	0.3	1.1	1	1.1	0.8
	ABCC4	ATP-binding cassette, sub-family C, member 4	A_24_P16913	1.1	0.9	0.8	0.8	0.8	0.1	0.8	0.8	0.5	0.3	1	0.9	0.8	0.7
	ABCC6	ATP-binding cassette, sub-family C (CFTR/MRP), member 6	A_23_P15272	1.3	1.4	1.6	1.3	0.9	0.2	1.3	1.1	0.7	0.3	1.5	1.4	1.1	0.8
	ABHD6	abhydrolase domain containing 6	A_23_P211850	1.1	1.3	1.4	1.2	0.9	0.2	1.2	1.1	0.7	0.5	1.4	1.4	1.4	1.1
	ACSM3	SA hypertension-associated homolog isoform 2	A_23_P317756	1.1	0.9	0.8	0.9	0.8	0.1	0.7	0.8	0.4	0.2	0.9	0.9	1	1
	ADORA2B	adenosine A2b receptor	A_23_P55477	0.9	0.9	0.9	1	0.6	0.1	0.8	0.9	0.4	0.3	0.9	1.2	0.9	0.7
	AGR2	anterior gradient 2 homolog	A_23_P31407	1.2	1.2	1.2	1.2	1.6	0.2	0.8	0.8	0.5	0.3	1.2	1.3	1.9	1.9
	AGT	**angiotensinogen preproprotein**	**A_23_P115261**	**7.5**	**2.7**	**0.8**	**0.8**	**1.7**	**0.4**	**1**	**0.8**	**0.8**	**0.3**	**0.9**	**1**	**1**	**0.7**
	AKR1C1	aldo-keto reductase family 1, member C1	A_24_P152968	1	0.8	1.1	1.2	1	0.1	1	1	0.7	0.2	1.1	1.2	1.2	0.8
	AKR1C1	aldo-keto reductase family 1, member C1	A_24_P220947	1.1	0.8	0.9	0.9	1	0.1	0.8	0.8	0.6	0.3	0.9	1.1	1.2	0.7
	AKR1C1	aldo-keto reductase family 1, member C1 (dihydrodiol dehydrogenase 1; 20-alpha (3-alpha)-hydroxysteroid dehydrogenase)	A_24_P312578	1	0.9	0.9	1	0.8	0.2	0.8	0.8	0.6	0.2	1	1.1	1	0.8
	AKR1C3	aldo-keto reductase family 1, member C3	A_23_P138541	1.1	0.7	0.8	0.9	0.7	0.1	0.7	0.8	0.5	0.2	0.8	1.1	1	0.7
	ALDH3A1	aldehyde dehydrogenase 3 family, member A1	A_23_P207213	0.7	0.5	0.5	0.5	0.6	0.1	0.6	0.6	0.5	0.2	0.5	0.7	0.7	0.6
	ALDH3A2	aldehyde dehydrogenase 3A2 isoform 2	A_23_P129896	0.9	0.7	0.9	1	0.8	0.2	0.8	1	0.6	0.2	0.9	1.2	1.1	0.9
	ANXA13	annexin A13 isoform b	A_23_P60009	1.1	0.6	0.7	0.7	0.6	0.1	0.8	0.7	0.3	0.1	0.6	0.8	1.1	0.7
	ANXA13	annexin A13 isoform b	A_23_P60006	1.3	0.7	0.8	0.8	0.6	0.1	0.7	0.7	0.2	0.1	0.8	0.7	1	0.6
	APBA2	amyloid beta A4 precursor protein-binding, family A, member 2	A_23_P146849	1	0.7	1.1	0.9	0.6	0.1	0.9	0.9	0.6	0.2	1	1.1	0.8	0.6
	APOBEC3C	apolipoprotein B mRNA editing enzyme, catalytic polypeptide-like 3C	A_23_P120931	0.9	0.9	0.7	0.8	0.8	0.2	0.7	0.7	0.6	0.3	0.7	1	0.9	0.8
	APOH	apolipoprotein H precursor	A_23_P38244	1.1	0.8	0.8	0.8	0.5	0	1	0.9	0.4	0.1	0.9	0.8	0.9	0.7
	ARL6IP5	ADP-ribosylation-like factor 6 interacting protein 5	A_23_P166640	1.3	1	0.8	0.8	0.7	0.2	0.6	0.7	0.4	0.4	0.8	1	1.1	1.2
	ATAD4	ATPase family, AAA domain containing 4	A_23_P118894	1.3	0.8	0.9	0.6	0.7	0	1	0.7	0.1	0	1	0.9	1.1	0.4
	AYTL1	hypothetical protein	A_24_P364807	1.4	1	0.8	0.8	0.9	0.2	0.9	0.9	0.4	0.3	1	1.4	1.1	1.2
	B3GNT1	UDP-GlcNAc:betaGal beta-1,3-N-acetylglucosaminyltransferase 1	A_23_P86900	1	1	1	0.8	0.6	0.1	0.8	1	0.4	0.3	1.1	1	0.8	0.6
	B3GNT3	UDP-GlcNAc:betaGal beta-1,3-N-acetylglucosaminyltransferase 3	A_23_P78980	1.1	1.1	1.3	1	1	0.2	1.1	1.1	0.6	0.3	1.3	1	1.2	1

	C12orf27		A_24_P314515	0.9	1.2	1.5	1.3	1	0.1	1.7	1.5	0.8	0.2	1.4	1.1	1.2	0.8
	C17orf58	hypothetical protein LOC284018 isoform a	A_24_P49190	1.2	1.1	0.8	0.9	0.7	0.2	0.8	0.8	0.5	0.4	0.9	1	1	1
	C18orf56	hypothetical protein LOC494514	A_24_P238499	1.1	1	0.6	0.7	0.6	0.1	0.6	0.6	0.4	0.3	0.7	0.7	0.8	0.8
	C2orf32	chromosome 2 open reading frame 32	A_23_P329353	1.3	0.9	0.8	0.8	0.7	0.1	0.7	0.8	0.5	0.3	0.8	0.9	0.9	0.8
	C4BPA	complement component 4 binding protein, alpha chain precursor	A_23_P97541	1.3	1.2	0.7	0.8	0.6	0.2	0.9	0.8	0.5	0.4	0.8	0.9	0.9	0.9
	CA12		A_23_P163338	1.3	1.1	2	1.8	0.8	0.2	1.5	1	0.4	0.2	1.6	1.5	1.6	1.1
	CA12		A_23_P163336	1.1	1.1	2.8	1.9	1.1	0.2	2.2	1.5	0.9	0.3	2.3	1.7	1.6	1.1
	CALB2	calbindin 2 full length protein isoform	A_23_P21092	1	0.8	0.9	1	0.7	0.2	0.8	0.8	0.4	0.3	0.9	1.1	1	0.7
	CD302	CD302 antigen	A_24_P396702	1.2	0.9	0.9	0.9	0.9	0.2	0.9	0.9	0.5	0.2	0.9	1	1.1	1
	CDH1	cadherin 1, type 1 preproprotein	A_23_P206359	1.2	1.7	1.2	1	0.9	0.2	0.9	0.8	0.7	0.3	1.3	1	0.8	0.8
	CDON	surface glycoprotein, Ig superfamily member	A_32_P172141	0.9	0.7	1	0.9	0.6	0.2	0.9	0.9	0.3	0.2	1	1	1	0.8
	CES1	carboxylesterase 1 isoform c precursor	A_23_P206733	0.9	0.8	0.7	0.7	0.7	0.2	0.7	0.8	0.4	0.2	0.7	0.9	0.9	0.7
	CIT	citron	A_23_P420551	0.9	0.8	0.9	0.9	0.7	0.2	1.1	1.2	0.8	0.4	0.9	0.8	0.8	0.9
	CKMT1B	creatine kinase, mitochondrial 1B precursor	A_23_P163235	0.9	0.7	0.6	0.8	0.7	0.3	0.5	0.8	0.3	0.2	0.9	0.9	1	0.8
	CMBL	carboxymethylenebutenolidase-like (Pseudomonas)	A_23_P144668	1	0.9	0.8	0.8	0.7	0.1	0.7	0.7	0.4	0.2	1	1	0.9	0.8
	CNTN1	contactin 1 isoform 1 precursor	A_23_P390700	1.1	0.7	0.6	0.7	0.9	0.2	0.5	0.7	0.4	0.1	0.6	1	1.4	1
	COL21A1	collagen, type XXI, alpha 1 precursor	A_23_P31124	2.4	0.8	0.7	0.9	0.8	0.2	0.7	0.9	0.8	0.1	1	0.7	1.5	0.8
	CORO2A	coronin, actin binding protein, 2A	A_23_P135061	1.1	1	0.9	0.9	1.1	0.2	1	1	0.8	0.3	0.9	0.9	0.9	0.9
	CPLX2	complexin 2	A_24_P391868	0.7	0.6	0.9	0.9	1	0.2	1	1	0.9	0.2	0.8	1	1	0.8
	CRYZ	crystallin, zeta	A_23_P114662	0.9	0.8	0.7	0.7	0.5	0.1	0.6	0.6	0.4	0.2	0.7	0.7	0.7	0.6
	CRYZ		A_24_P548453	0.9	0.7	0.5	0.6	0.5	0.1	0.5	0.6	0.3	0.2	0.6	0.7	0.7	0.5
	CTTNBP2	cortactin binding protein 2	A_23_P215744	1	0.8	1.5	0.9	0.3	0	1.1	0.8	0.2	0.2	1	0.7	0.4	0.4
	CXADR	coxsackie virus and adenovirus receptor precursor	A_32_P29632	0.9	1	0.6	0.7	0.7	0.2	0.5	0.7	0.4	0.4	0.7	0.7	1	0.9
	CXADR	coxsackie virus and adenovirus receptor precursor	A_24_P374943	1	1.1	0.5	0.7	0.8	0.2	0.4	0.6	0.4	0.1	0.5	0.7	1	0.6
	CYBRD1	cytochrome b reductase 1	A_23_P209564	1.1	1.1	0.8	0.8	0.7	0.2	0.6	0.7	0.5	0.3	0.9	0.8	0.9	1
	CYP24A1	cytochrome P450, family 24 precursor	A_24_P356930	0.9	1	1.5	0.9	0.8	0.2	1.2	1.1	0.9	0.4	1.4	0.7	0.8	0.9
	CYP24A1	cytochrome P450, family 24 precursor	A_23_P28815	1	1	1.6	1	0.8	0.2	1.3	1.1	1	0.4	1.5	0.7	0.9	0.9
	DHCR24	24-dehydrocholesterol reductase precursor	A_23_P379475	0.9	0.8	1.1	0.8	0.8	0.1	0.8	0.8	0.3	0.3	1	1.2	1.2	0.6
	DPYSL2	dihydropyrimidinase-like 2	A_24_P38347	1.1	0.9	0.8	0.8	0.8	0.2	0.7	0.7	0.5	0.3	0.9	0.9	1	1
	DSCR1L2	Down syndrome critical region gene 1-like 2	A_23_P391275	1.1	1.1	1.2	1	0.8	0.2	1.2	1	0.6	0.3	1.1	1	0.9	0.9
	ECH1	peroxisomal enoyl-coenzyme A hydratase-like protein	A_23_P153853	0.9	0.8	0.7	0.8	0.8	0.2	0.7	0.8	0.5	0.3	0.8	1	1	0.7
	ELL3	elongation factor RNA polymerase II-like 3	A_24_P47988	1.2	1	1.2	0.8	0.7	0.2	1.2	0.9	0.5	0.4	1.1	0.9	1	1.1
	EPHX1	epoxide hydrolase 1, microsomal (xenobiotic)	A_23_P34537	1	0.8	0.9	0.9	0.8	0.2	0.8	0.9	0.6	0.2	0.9	1.1	1	0.7
	F2R	coagulation factor II receptor precursor	A_23_P213562	0.8	1	0.5	0.5	0.7	0.2	0.4	0.6	0.3	0.3	0.5	0.6	1	1.2
	FAM64A	hypothetical protein LOC54478	A_23_P49878	0.8	0.7	0.6	0.6	0.7	0.1	0.7	0.8	0.5	0.3	0.6	0.6	0.7	0.7
	FGL1	fibrinogen-like 1 precursor	A_23_P20484	1.4	1.2	0.6	0.7	0.7	0.1	0.6	0.6	0.5	0.2	0.7	0.7	0.8	0.7
	FMO5	flavin containing monooxygenase 5	A_24_P71341	1.1	0.8	0.7	0.9	0.7	0.1	0.9	1.1	0.4	0.2	0.8	0.9	0.9	0.8
	FOXQ1	forkhead box Q1	A_32_P164246	0.8	1.2	1.3	1.1	0.7	0.1	1.2	1	0.6	0.3	1.2	1.1	0.6	0.5
	GALNT5	UDP-N-acetyl-alpha-D-galactosamine:polypeptide N-acetylgalactosaminyltransferase 5 (GalNAc-T5)	A_24_P408736	1.2	1.2	0.8	0.8	0.7	0.2	0.6	0.8	0.3	0.3	1.1	0.9	1.1	1.3
	GPX2	gastrointestinal glutathione peroxidase 2	A_23_P3038	1.1	0.8	0.9	0.9	0.9	0.2	1	0.8	0.9	0.3	1	1	1.1	1
	GRB14	growth factor receptor-bound protein 14	A_23_P154526	1	0.9	1.6	1.3	0.9	0.2	1.4	1.3	0.8	0.3	1.4	1.2	1.3	0.9
	GSTM3	glutathione S-transferase M3	A_24_P914434	1	0.8	0.8	0.9	0.7	0.2	0.8	0.8	0.5	0.3	0.9	1	0.9	0.7

	GSTO1	glutathione-S-transferase omega 1	A_24_P304051	1.1	1.2	0.8	0.9	1	0.2	0.8	0.8	0.6	0.3	0.8	0.9	1	0.8
	GSTO1	glutathione-S-transferase omega 1	A_23_P1254	1	1.2	0.7	0.8	1	0.2	0.7	0.8	0.5	0.4	0.8	0.9	1	0.8
	HHEX	hematopoietically expressed homeobox	A_23_P47034	1	1.1	0.8	0.7	0.8	0.2	0.7	0.7	0.6	0.4	0.8	0.8	0.9	0.8
	HLA-DMB	major histocompatibility complex, class II, DM beta precursor	A_32_P351968	1	0.5	0.6	0.7	0.6	0.1	0.7	0.8	0.4	0.1	0.6	0.7	0.8	0.6
	HPGD	hydroxyprostaglandin dehydrogenase 15-(NAD)	A_23_P213050	1.1	1.2	0.9	0.9	0.7	0.2	0.9	1	0.5	0.3	1	0.9	0.9	0.9
	HTRA1	HtrA serine peptidase 1	A_23_P97990	0.9	0.6	1.1	0.9	0.7	0.1	0.9	0.9	0.6	0.2	1.1	0.9	0.8	0.7
	IL6R	interleukin 6 receptor isoform 1 precursor	A_24_P379413	1.2	1	1	1	0.7	0.1	1.2	1.1	0.5	0.2	0.9	0.9	1.1	0.8
	INHBB	inhibin beta B subunit precursor	A_23_P153964	0.8	0.8	1.3	1.1	0.8	0.2	1	1	0.7	0.4	1.3	1.1	1	0.9
	KCNK3	potassium channel, subfamily K, member 3	A_23_P357724	1.4	1.3	0.9	0.9	1.3	0.2	0.7	1	0.4	0.4	1	1.2	1.3	1
	KCTD1	potassium channel tetramerisation domain containing 1	A_23_P130352	0.9	1	0.6	0.8	0.6	0.2	0.7	0.8	0.5	0.3	0.8	1	0.8	0.7
	KIAA1815	hypothetical protein LOC79956	A_23_P169154	1	0.8	0.6	0.8	0.8	0.2	0.6	0.7	0.4	0.3	0.8	0.8	1.1	0.8
	KIAA1822L	KIAA1822-like	A_23_P86059	1.1	1	1.6	1.3	1.4	0.2	1.2	1.2	0.8	0.2	1.5	1.3	1.4	0.8
	MAGEH1	melanoma antigen, family H, 1 protein	A_23_P34144	1.1	0.8	0.9	0.9	0.6	0.2	0.6	0.7	0.4	0.3	1	0.9	0.8	0.8
	MALAT1		A_24_P497244	0.9	1.2	2.1	1.5	0.9	0.2	1.8	1.6	0.9	0.3	1.8	1.3	1.3	0.9
	MALL	mal, T-cell differentiation protein-like	A_23_P102551	0.7	0.5	0.5	0.6	0.6	0.2	0.5	0.6	0.3	0.2	0.5	0.7	0.9	0.8
	MANEA	mannosidase, endo-alpha	A_23_P255663	1.2	1	0.7	0.7	0.8	0.2	0.6	0.7	0.6	0.4	0.8	0.8	1.1	1
	MANSC1	MANSC domain containing 1	A_23_P162211	1	1	0.7	0.7	0.6	0.2	0.6	0.5	0.4	0.3	0.8	0.9	1	1
	MATN2	matrilin 2 isoform b precursor	A_23_P71328	1	0.7	0.8	0.8	0.8	0.1	0.7	0.8	0.5	0.2	0.8	0.9	1	0.9
	MATN3	matrilin 3 precursor	A_23_P102058	1.1	1.2	0.6	0.7	0.7	0.2	0.6	0.6	0.4	0.4	0.7	0.8	0.9	0.9
	METTL7A	methyltransferase like 7A	A_23_P415021	1.4	0.7	1.5	1.2	0.8	0.1	1.1	0.9	0.5	0.1	1.8	0.9	0.8	0.6
	METTL7B	methyltransferase like 7B	A_24_P64653	0.9	0.8	0.6	0.7	0.6	0.2	0.7	0.7	0.4	0.3	0.8	0.8	0.9	0.7
	MGAT3		A_24_P245838	1.2	1	1.5	1.2	0.8	0.1	1	1.2	0.7	0.3	1.3	1.2	0.9	0.6
	MMP7	matrix metalloproteinase 7 preproprotein	A_23_P52761	1.3	1.3	1.1	1	0.8	0.2	0.9	0.9	0.6	0.4	1.1	0.9	0.8	0.7
	MOSC1	MOCO sulphurase C-terminal domain containing 1	A_24_P233995	0.9	0.8	1.3	1.2	0.6	0.1	1	1.2	0.6	0.3	1.2	1.1	0.9	0.6
	NMU	neuromedin U	A_23_P69537	1.2	0.9	0.8	0.8	0.8	0.1	0.9	0.8	0.5	0.2	0.9	1	0.8	0.8
	NQO1	NAD(P)H menadione oxidoreductase 1, dioxin-inducible isoform a	A_23_P206661	1	0.9	0.7	0.8	0.8	0.2	0.7	0.8	0.5	0.3	0.8	0.9	1	0.8
	NT5E	5' nucleotidase, ecto	A_24_P316430	1.2	1.7	0.4	0.6	0.9	0.2	0.7	0.8	0.9	0.7	0.5	0.6	0.7	1.1
	NTS	neurotensin/neuromedin N preproprotein	A_23_P36882	1.2	1.1	1.1	0.9	0.8	0.1	0.9	0.9	0.4	0.2	1.2	1.1	1	0.8
	OLFML2A	olfactomedin-like 2A	A_24_P220485	0.9	0.6	1.1	1	0.8	0.2	1.1	1	0.7	0.3	1.1	1	0.9	0.9
	PCYOX1L	prenylcysteine oxidase 1 like	A_23_P30275	1.2	1	1.2	1.1	0.8	0.2	1.2	1.1	0.8	0.4	1.2	1.1	0.9	1
	PDGFD	platelet derived growth factor D isoform 1 precursor	A_24_P124349	1.2	1.1	0.8	1	0.7	0.1	0.7	0.8	0.5	0.2	0.9	1	1	0.6
	PDK3	pyruvate dehydrogenase kinase, isoenzyme 3	A_23_P250478	1	0.8	0.7	0.8	0.7	0.2	0.8	0.9	0.4	0.3	0.8	0.8	1	0.9
	PDK4	pyruvate dehydrogenase kinase 4	A_24_P243749	1.4	1.3	1.1	1	0.8	0.1	1	1	0.5	0.3	1.2	0.8	1.1	1
	PDK4	pyruvate dehydrogenase kinase 4	A_23_P257087	1.2	1	0.7	0.9	0.6	0.2	0.9	1	0.4	0.2	0.9	1	1	0.7
	PF4	platelet factor 4 (chemokine (C-X-C motif) ligand 4)	A_24_P79403	1.4	0.9	1.1	1.1	0.7	0.1	1	1	0.6	0.3	1.1	1.1	1.1	0.9
	PLD1	phospholipase D1, phophatidylcholine-specific	A_24_P123190	1.1	1	1.4	1.3	0.9	0.3	0.8	1.1	0.5	0.2	1.2	0.7	2.1	1.1
	PRDM13	PR domain containing 13	A_23_P256581	1	1	1	1	0.7	0.2	0.7	0.7	0.5	0.3	1.1	1.1	0.9	0.9
	PRKACB	cAMP-dependent protein kinase catalytic subunit beta isoform 3	A_23_P371410	1.3	1.1	0.7	0.9	1	0.2	1	0.9	0.5	0.2	0.8	1	1.1	0.9
	PRKX	protein kinase, X-linked	A_23_P217339	1	0.8	1	0.9	0.7	0.2	1	0.8	0.6	0.3	1	0.9	0.9	0.9
	PRPS2	phosphoribosyl pyrophosphate synthetase 2 isoform 2	A_23_P96641	1.1	0.9	0.6	0.6	0.6	0.2	0.6	0.6	0.4	0.4	0.6	0.7	0.9	0.7
	RAB11FIP4	RAB11 family interacting protein 4 (class II)	A_24_P164549	1.2	0.8	2	1.1	0.9	0.1	1.3	1.1	0.4	0.2	1.8	1.1	1	0.6
	RAB37	RAB37, member RAS oncogene family isoform 3	A_23_P414654	1.1	0.8	1.5	1.1	1	0.2	1	1	0.6	0.2	1.5	1.1	0.9	1.1
	RALGPS1	Ral GEF with PH domain and SH3 binding motif 1	A_23_P390148	1.3	0.9	1.3	1.7	1.2	0.2	1	1.1	0.8	0.2	1.5	1.5	1.6	1.2

	RHOBTB1	Rho-related BTB domain containing 1	A_24_P158536	0.9	1	1.2	1.1	0.9	0.1	1.1	1	0.6	0.2	1.1	0.9	1	0.9
	RNASE4	ribonuclease, RNase A family, 4 precursor	A_23_P205531	1.5	0.9	0.8	0.9	1.1	0.2	0.6	0.8	0.5	0.2	1	1	1.1	0.9
	RNF128	ring finger protein 128 isoform 1	A_23_P148345	1.1	1	0.5	0.6	0.8	0.2	0.3	0.4	0.3	0.2	0.7	0.6	1.3	0.8
	RNF157	ring finger protein 157	A_32_P57810	0.9	0.8	0.9	0.9	0.7	0.2	0.8	0.8	0.5	0.3	0.9	1	0.8	0.6
	SAMD13	dnaj-like protein	A_32_P130788	0.9	0.8	0.6	0.6	0.3	0.2	0.5	0.5	0.2	0.2	0.7	0.6	0.6	0.8
	SCARA5	scavenger receptor class A, member 5 (putative)	A_23_P94103	1.1	0.9	1.3	1	1	0.2	0.9	1	0.5	0.3	1.4	1.3	1.2	1.2
	SCD5	acyl-CoA-desaturase	A_24_P385134	1.3	1	1.2	1	0.6	0.2	0.9	0.8	0.4	0.3	1.4	0.9	1	0.8
	SGCD	delta-sarcoglycan isoform 1	A_23_P147647	1.2	1.3	1	0.9	1.2	0.2	1.2	1	0.8	0.7	1.1	0.9	1.1	0.8
	SLC22A3	solute carrier family 22 member 3	A_23_P19733	1	1	0.9	0.9	0.9	0.1	0.8	0.9	0.6	0.2	1	0.9	1	0.8
	SLC22A3	solute carrier family 22 member 3	A_32_P309404	1.1	0.8	0.8	1	0.7	0.2	0.8	1	0.6	0.2	0.9	0.9	1.2	0.8
	SLC23A1	solute carrier family 23 (nucleobase transporters), member 1 isoform b	A_23_P21990	1.2	1	0.4	0.5	0.9	0.1	0.6	0.6	0.6	0.2	0.5	0.6	1	0.7
	SLC24A1	solute carrier family 24 (sodium/potassium/calcium exchanger), member 1	A_23_P205913	1.1	1	0.7	0.7	0.7	0.2	0.4	0.7	0.5	0.4	0.7	0.7	0.7	1
	SLC40A1	solute carrier family 40 (iron-regulated transporter), member 1	A_23_P102391	1.2	1.2	1.1	1.1	0.4	0.1	0.8	0.8	0.3	0.2	1.2	1.1	0.8	0.6
	SOX2	sex-determining region Y-box 2	A_23_P401055	1.1	1.2	1	0.9	0.8	0.2	1	0.9	0.5	0.3	1.1	1.1	1	1.1
	SPC25	spindle pole body component 25	A_23_P51085	1.1	0.9	0.8	0.7	0.6	0.2	1.2	0.9	0.5	0.4	0.8	0.7	0.9	0.7
	SPP1	secreted phosphoprotein 1 isoform b	A_23_P7313	1.2	1.1	1.1	1	0.9	0.2	0.7	0.8	0.5	0.2	1.1	1.1	1.3	0.9
	SRI	sorcin isoform a	A_23_P59718	1.2	0.9	0.7	0.9	0.6	0.2	0.7	0.8	0.5	0.4	0.7	0.9	0.8	0.8
	ST3GAL5	ST3 beta-galactoside alpha-2,3-sialyltransferase 5 isoform 1	A_23_P311869	0.8	0.9	0.8	0.6	0.5	0.2	0.8	0.8	0.5	0.5	0.7	0.7	0.7	1.1
	ST6GAL2	KIAA1877 protein	A_32_P126157	0.9	0.7	0.8	0.7	0.7	0.2	0.7	0.7	0.4	0.2	0.8	0.6	1.3	1.3
	ST8SIA4	**ST8 alpha-N-acetyl-neuraminide alpha-2,8-sialyltransferase 4 isoform a**	**A_23_P361984**	**4.1**	**1.6**	**0.9**	**1.2**	**3**	**1.4**	**0.9**	**1**	**1.3**	**0.6**	**1.7**	**0.8**	**2.6**	**1.6**
	SULF2	sulfatase 2 isoform a precursor	A_23_P154605	1.2	0.9	1.8	1.6	1.1	0.2	1.3	1.1	0.7	0.2	1.8	1.6	1.3	0.9
	TACSTD1	tumor-associated calcium signal transducer 1 precursor	A_23_P91081	1.3	0.9	0.9	0.9	0.8	0.1	0.8	0.8	0.5	0.2	0.9	0.9	1	0.8
	TFAP2A	transcription factor AP-2 alpha isoform a	A_32_P14187	1.4	1	1.1	0.9	0.9	0.1	0.9	0.9	0.8	0.4	1.1	1.1	1	0.7
	THRA	thyroid hormone receptor, alpha isoform 2	A_23_P207742	1.2	1.1	1.2	1.2	1	0.2	1.3	1.2	0.9	0.3	1.2	1.1	0.8	0.9
	TM4SF18	transmembrane 4 L six family member 18	A_24_P120251	1	0.9	0.7	0.7	0.7	0.2	0.7	0.8	0.5	0.3	0.7	0.7	0.8	0.7
	TM4SF4	transmembrane 4 superfamily member 4	A_23_P252432	1.1	0.7	0.6	0.7	0.5	0.1	0.7	0.8	0.4	0.2	0.7	0.6	0.7	0.5
	TRIM2	tripartite motif-containing 2	A_23_P213141	1.3	0.8	1.3	1.2	1.1	0.2	1.2	1.1	0.7	0.4	1.4	1.2	1.2	1.2
	TSC22D1	TSC22 domain family 1 isoform 1	A_23_P162739	0.9	1.1	0.7	0.8	0.7	0.2	0.6	0.7	0.5	0.3	0.7	0.8	0.8	0.8
	UGT1A6	UDP glycosyltransferase 1 family, polypeptide A6 isoform 1 precursor	A_24_P222872	1	0.7	0.7	0.7	0.5	0.1	0.5	0.7	0.3	0.2	0.7	1	1.1	0.6
	UGT1A6	UDP glycosyltransferase 1 family, polypeptide A6 isoform 1 precursor	A_23_P60599	1.2	1.1	1.2	1.2	0.7	0.2	1	1	0.6	0.4	1.3	1.2	1.2	0.9
	UGT2B11	UDP glycosyltransferase 2 family, polypeptide B11	A_23_P212968	1.1	0.5	0.6	0.8	0.8	0.2	0.7	0.8	0.9	0.2	0.7	1.1	1.1	0.7
	UPK1B	uroplakin 1B	A_24_P200219	1	0.7	0.3	0.6	0.5	0.3	0.5	0.6	0.5	0.2	0.6	0.7	0.9	0.8
	USH1C		A_23_P127818	0.9	1.2	1.7	1.1	1.6	0.2	1.9	1.8	1	0.3	1	0.8	1.1	0.9
	VAV3	vav 3 oncogene isoform 1	A_23_P201551	1.1	0.9	1.2	1	1	0.1	1	1	0.5	0.1	1.4	0.9	1.4	0.7
		hypothetical protein LOC134145	A_23_P133279	1.1	0.5	0.8	0.8	0.6	0.2	0.8	0.8	0.4	0.3	0.9	0.9	0.9	0.9
		hypothetical protein LOC25854	A_23_P416965	1.2	0.8	0.9	0.9	0.9	0.2	0.9	0.8	0.6	0.3	0.9	1	0.9	0.8
		hypothetical protein LOC54842	A_23_P28530	1.1	1	0.7	0.7	0.7	0.2	0.6	0.6	0.4	0.3	0.8	0.8	0.8	1.1
		OK/SW-CL.92	A_24_P919683	1.2	0.9	1.8	1.5	0.8	0.1	1.4	1.3	0.6	0.3	1.3	1	1.1	0.8
		phospholysine phosphohistidine inorganic pyrophosphate phosphatase	A_24_P355493	0.9	0.8	0.6	0.8	0.8	0.2	0.7	0.8	0.6	0.3	0.8	0.9	0.9	0.7
			A_32_P9924	1	1	1	1.1	0.9	0.2	0.9	1	0.6	0.3	1	1	1.1	0.9
			A_23_P46447	1	0.8	1	1	0.8	0.2	0.8	1	0.6	0.2	1	1.1	1	0.9
			A_32_P218707	1.1	0.9	1.3	1.1	1.1	0.2	1.2	1	0.8	0.4	1.2	1.2	1.3	1.3
			A_24_P451992	0.9	0.7	0.7	0.7	0.7	0.1	0.6	0.8	0.5	0.2	0.7	0.9	0.8	0.6

			A_24_P91876	1.1	0.9	1	0.9	0.9	0.2	0.8	0.8	0.5	0.3	1	1	1.1	0.9
			A_24_P35488	1.1	0.9	0.9	0.9	0.7	0.2	0.7	0.8	0.5	0.3	0.9	1	1	0.9
			A_24_P30706	1	0.8	0.7	0.8	0.7	0.2	0.7	0.8	0.4	0.3	0.8	1	0.8	0.8
			A_24_P16725	0.9	0.9	0.8	0.9	0.9	0.2	0.7	0.9	0.5	0.3	0.8	0.8	1.2	0.9
			A_24_P15845	1.1	0.8	0.6	0.7	0.9	0.2	0.6	0.7	0.5	0.3	0.7	0.9	1.2	0.8
			A_32_P95973	1.1	1	1	1.1	0.9	0.2	0.9	1.1	0.5	0.3	1.1	1.3	1.3	1
			A_32_P145502	1.1	1.2	1.1	1.2	1.1	0.2	1.1	1	0.8	0.5	1.4	1.4	1.2	1
			A_32_P16755	0.8	0.7	0.9	1	0.8	0.2	0.8	0.9	0.5	0.3	0.9	1	1	0.7
			A_24_P920388	0.9	0.9	1.1	1.5	0.9	0.2	0.9	0.9	0.5	0.3	1	1	1	0.8
			A_24_P128524	1.2	1	1.1	1.1	0.8	0.1	0.9	0.9	0.7	0.4	1	1.2	1	0.9
			A_23_P79622	1.3	1.1	1.1	1	0.8	0.2	1	0.9	0.6	0.3	1.1	1.1	0.9	0.9
			A_24_P680548	0.9	0.8	0.8	0.8	0.6	0.1	0.8	0.8	0.6	0.3	0.8	0.8	0.8	0.7
			A_24_P647163	1.1	0.9	0.8	0.8	0.6	0.1	0.8	0.8	0.5	0.2	0.9	0.8	0.8	0.7
			A_24_P15906	1.2	1.1	0.9	0.9	0.6	0.1	1	1	0.5	0.3	0.9	0.9	0.9	0.7
			A_24_P108281	1.1	0.7	0.9	0.9	0.6	0.2	1	0.8	0.5	0.4	0.8	1	0.9	0.8
			A_32_P92536	1.3	1	1.4	1.2	0.8	0.2	1.2	0.9	0.6	0.3	1.3	1	1.2	1
			A_32_P130522	1.2	1	1.1	1.1	0.9	0.2	1	0.9	0.6	0.4	1.2	1	1	1.3
			A_32_P71744	1.1	0.9	1.2	1	0.9	0.2	1	1	0.6	0.3	1.2	0.9	1.2	1.1
			A_24_P706752	1.2	0.8	1	0.9	0.8	0.2	0.9	0.9	0.6	0.3	1	1.1	1.1	1.1
			A_24_P303145	1.1	0.7	1.3	1	0.7	0.2	0.9	0.9	0.5	0.2	1.1	1.1	1	0.9
			A_23_P259561	1	0.6	0.8	0.8	0.8	0.1	0.8	1	0.4	0.2	1	0.9	1	0.7
			A_24_P118938	1	1.1	0.8	1	0.7	0.2	1	0.8	0.6	0.3	1.4	1.1	1.1	0.8
			A_32_P91491	1.2	1.2	0.8	0.8	0.8	0.1	0.9	1	0.6	0.3	0.8	0.9	1	1
			A_32_P66297	1	0.9	0.8	1	0.7	0.2	0.8	0.9	0.5	0.4	0.7	0.9	1	0.8
			A_32_P228254	1.1	1	0.7	0.7	0.5	0.2	0.7	0.7	0.4	0.4	0.9	0.7	0.8	0.7
			A_23_P75362	1.1	0.9	0.9	0.8	0.9	0.2	0.8	0.9	0.6	0.4	0.8	1	1	0.9
			A_24_P625898	0.9	1	0.5	0.6	0.5	0.2	0.5	0.6	0.4	0.4	0.6	0.7	0.7	0.8
			A_23_P213527	1.3	1.3	1.2	1	1.3	0.2	0.8	0.8	0.9	0.4	1.2	1	0.9	0.9
			A_32_P71032	0.9	0.5	0.7	0.8	0.4	0.1	0.7	0.9	0.4	0.1	0.8	0.8	0.9	0.7
			A_32_P69783	1.1	0.6	1.4	1.2	0.8	0.2	1.1	1.1	0.5	0.1	1.2	1.2	1.3	1
			A_24_P340112	1.3	0.4	1	0.9	0.6	0.2	0.9	0.7	0.3	0.1	0.9	1	0.9	1.1
			A_24_P132703	1.3	1	1.1	1.1	0.8	0.2	1.1	0.7	0.4	0.3	1.5	1.1	1	1
			A_32_P64004	0.8	1.1	0.9	1	0.8	0.1	1.1	1	0.6	0.3	0.9	0.8	0.9	0.9
			A_32_P23125	1.1	1.2	1.5	1.4	1.2	0.2	1.4	1.1	0.8	0.3	1.5	1.1	0.9	1
			A_24_P878419	1	1	1.3	1.1	0.8	0.1	1.2	1.1	0.7	0.3	1.3	1	0.8	0.7
			A_24_P213325	1	1	1.3	1.2	0.9	0.1	1.3	1.2	0.8	0.3	1.4	1.1	0.9	0.8
			A_24_P67063	1	0.9	1.3	1.2	0.9	0.1	1.2	1.2	0.8	0.3	1.2	1	0.8	0.7
			A_24_P67681	1	1	1.2	1.1	0.9	0.1	1.2	1	0.8	0.3	1.2	1	0.8	0.7
			A_23_P373119	1	1	1.3	1.1	0.9	0.1	1.2	1.1	0.7	0.2	1.3	1.1	0.9	0.8
			A_24_P871208	1.5	1.3	1.6	1.5	1	0.2	1.5	1.3	0.7	0.3	1.6	1.4	1.1	1
			A_24_P341106	1.1	1.1	1	1.1	0.8	0.1	1.1	1	0.6	0.2	1.3	1	0.8	0.7
			A_24_P24685	1.1	1.1	1.2	1.2	0.8	0.1	1.2	1.1	0.6	0.3	1.2	1	0.8	0.7
			A_24_P827794	1.3	1.1	1.2	1.2	0.8	0.2	1.1	1.2	0.7	0.4	1.3	1.1	0.8	0.7
			A_24_P475556	1.1	1	1.1	1.1	0.8	0.2	1.3	1.1	0.8	0.3	1.1	1	1	0.9
			A_24_P761490	1.1	1.2	1.4	1.1	0.8	0.2	1.5	1.3	0.9	0.4	1.3	1.1	0.9	0.8
			A_24_P109962	1.1	1.1	1.4	1.2	0.8	0.2	1.5	1.3	0.9	0.4	1.2	1	0.9	0.8
			A_23_P31681	1.1	1.1	1.2	1.3	0.8	0.2	1.3	1.3	1	0.4	1.1	0.9	0.9	0.9
			A_24_P324084	1.2	1.1	1.3	1.3	0.9	0.2	1.5	1.4	1	0.5	1.2	1.4	1.2	1
			A_24_P24982	1	1	1.1	1.2	0.8	0.2	1.3	1.2	0.9	0.5	1	1.3	1.1	0.8

			A_32_P23349	1.1	1	1.8	1.5	1	0.2	1.9	1.4	0.6	0.3	1.6	1.4	1.2	1.2
			A_23_P32737	0.8	0.8	1.2	1	0.8	0.2	1.2	1.1	0.6	0.3	1.1	0.9	0.8	0.9
			A_32_P19873	1	0.9	1.3	0.9	0.7	0.2	1.2	1.1	0.6	0.3	1.4	0.9	0.8	0.8
			A_24_P15046	1	0.9	1.4	1.3	0.8	0.2	1.1	1	0.6	0.4	1.4	1.3	0.9	1
			A_23_P15395	0.9	0.9	1.8	1.4	0.9	0.2	1.3	1.3	0.7	0.4	1.6	1.4	1.1	1
			A_32_P22350	2.3	1.7	4.7	3.9	1.6	0.1	3.4	1.9	1	0.2	2.9	2	1.4	1
			A_24_P41901	1.7	1.3	3.4	2.3	1.6	0.1	3.1	2.2	0.7	0.2	2.9	1.9	1.1	0.6
			A_32_P21350	1	1.1	3.8	2.4	0.9	0.1	3.4	2.2	1.1	0.4	3	1.6	1.2	0.8
			A_24_P26847	1	1	2.5	1.4	0.9	0.2	2.2	1.3	0.9	0.4	1.8	1.4	1	0.8
			A_32_P13337	1.2	1.2	2.1	1.6	1	0.1	2.2	1.6	1	0.2	1.7	1.2	1	0.7
			A_24_P16300	0.8	0.8	1.7	1.2	0.8	0.1	1.4	1.2	0.9	0.2	1.4	0.9	0.9	0.7
			A_23_P48080	0.8	0.9	1.5	1.3	0.9	0.2	1.4	1.3	0.7	0.3	1.2	1.2	1	0.9
			A_32_P195346	1.2	1.7	4	1.8	1.1	0.2	4.4	2.3	1	0.3	2.3	1.3	1.2	0.9
			A_24_P16378	0.9	1	1.6	1.4	0.8	0.2	1.9	1.4	0.8	0.4	1.3	1	0.9	1.1
			A_32_P54628	1.5	1.2	0.7	0.9	1.3	0.1	0.7	1.1	1.2	0.2	0.8	0.9	0.9	0.6
			A_32_P174874	1	1.1	1.3	1	1.1	0.2	1	1.4	1	0.3	1.1	1	1.2	0.9
			A_32_P3783	0.9	1.9	3.5	2.4	0.8	0.2	3.8	2.4	1	0.6	2.7	1.3	1.1	1.2
			A_24_P665185	1.3	2	4.1	2.3	1.1	0.2	3.4	2.4	1.3	0.6	3.2	1.4	1.2	1.1
			A_32_P97739	0.9	0.7	0.4	0.5	0.6	0.2	0.3	0.6	0.4	0.2	0.4	0.6	1.1	1
			A_23_P316487	0.9	0.7	0.4	0.4	0.8	0.3	0.4	0.5	0.5	0.2	0.4	0.6	1.2	0.9
			A_23_P305245	1.2	1.2	0.5	0.6	0.8	0.2	0.6	0.6	0.4	0.2	0.6	1	1.3	1.1
			A_32_P44210	1.3	0.9	1.1	0.7	1.3	0.4	0.6	0.8	0.5	0.2	1.1	0.9	1.4	1.2
			A_32_P87323	1.2	0.9	0.9	0.8	1	0.2	0.7	0.8	0.6	0.2	0.7	1.1	1.1	1
			A_32_P131998	1	0.8	0.7	0.9	1	0.2	0.8	0.8	0.5	0.3	0.7	1	1.5	1.4
			A_32_P45229	1.3	1.1	0.8	0.8	0.6	0.2	0.8	0.7	0.3	0.3	0.8	0.7	1	0.9
			A_32_P44831	1.1	0.9	0.8	0.8	0.7	0.2	0.6	0.6	0.5	0.4	0.8	1	1.1	1.2
			A_32_P11670	1.4	1	0.5	1.2	0.9	0.2	0.5	1.2	0.8	0.2	0.6	1	1	0.9
			A_23_P156996	1.3	1.4	0.9	1.2	2.3	0.2	1.1	0.9	1.8	0.4	0.8	1.3	1.4	1.2
			A_32_P203688	1.1	0.5	1	0.7	0.5	0.3	0.8	0.8	0.3	0.2	1.3	0.9	1.1	1.2
			A_23_P416305	**1**	**0.2**	**1.2**	**1**	**0.4**	**0.2**	**1.2**	**1.1**	**0.3**	**0.3**	**1**	**1.1**	**0.9**	**0.7**
			A_32_P214503	0.9	0.4	0.8	0.8	0.8	0.3	0.8	0.7	0.4	0.2	0.9	1	1.5	1.4
			A_23_P204541	1	0.6	0.6	0.8	1	0.3	0.5	0.7	0.5	0.2	0.7	0.9	1.6	1.7

[‡]Genes listed in each cluster correspond to the same genes hierarchically clustered in Figure 4.
***Rows in bold correspond to 76 additional interferon induced genes from Table S1.**
[†]Rows in blue correspond to the 17 predominantly IFN-responsive but wt HPIV1 unresponsive genes from cluster C of figure 1. 14 of those genes are found in cluster F, 1 gene in cluster C, 1 gene in cluster H, and 1 gene (RET) was not significantly differentially expressed above 4-fold between virus infections or with IFNβ treatment.

Table S3.

Table S3. Comparison of IFNB mRNA message by qPCR

		IFNB Expression (Van Cleve et al. 2006)		IFNB Expression with Taqman Assay	
Virus	Time	vs Mock	Ratio C^{F170S}:WT	vs Mock	Ratio C^{F170S}:WT
WT	24 h	5.9	**40.8**	261.7	**103.2**
C^{F170S}		240.5		27007.7	
WT	48 h	12.2	**458.3**	1227.4	**695.0**
C^{F170S}		5595.3		853061.5	

Table S4.

Symbol	Product	Agilent	6 h	24 h	6 h	12 h	24 h	48 h	6 h	12 h	24 h	48 h	6 h	12 h	24 h	48 h
AKT1	v-akt murine thymoma viral oncogene homolog 1	A_23_P2960	0.6	0.6	0.7	0.7	0.8	0.5	0.7	0.8	0.7	0.5	0.7	0.9	0.8	0.6
BAG1	BCL2-associated athanogene isoform 1L	A_23_P146654	0.9	0.9	0.8	0.8	1.1	1.1	0.8	0.9	1	0.9	0.8	0.8	0.9	1.1
BAG3	BCL2-associated athanogene 3	A_23_P52552	1.2	1.1	0.8	0.9	0.9	0.6	0.7	0.7	0.6	0.8	0.8	1	1	0.8
BAG3	BCL2-associated athanogene 3	A_23_P47077	1.1	1	0.8	0.8	0.7	0.6	0.7	0.8	0.6	0.7	0.8	0.9	0.9	0.7
BAG4	BCL2-associated athanogene 4	A_23_P146217	1.2	1.1	0.8	0.9	1	0.8	0.7	0.7	0.5	0.7	0.7	0.9	1	0.7
BCL2	B-cell lymphoma protein 2 alpha isoform	A_23_P352266	1.2	1.3	0.9	0.9	0.9	0.6	0.8	0.8	0.5	0.9	1.1	1.2	0.9	1.1
BCL2	B-cell lymphoma protein 2 beta isoform	A_23_P208132	1	1.1	1.7	1.4	1.3	2.1	1.6	1.6	1.7	1.5	1.6	1.4	1.1	1.1
BCL2A1	BCL2-related protein A1	A_23_P321703	1	1	0.8	0.9	0.9	1.5	0.9	0.9	1.1	1.3	0.8	0.9	0.8	1
BCL2A1	BCL2-related protein A1	A_23_P152002	1.2	1.4	0.9	0.8	1.8	29.3	1	0.9	3.9	13.9	0.9	1.1	1.3	5
BCL2L1	BCL2-like 1 isoform 1	A_23_P210886	0.6	0.6	0.5	0.7	0.8	0.5	0.6	0.7	0.6	0.6	0.6	0.8	0.8	0.7
BCL2L1	BCL2-like 1 isoform 2	A_24_P100130	0.8	0.9	0.5	0.8	0.7	0.5	0.7	0.8	0.7	0.9	0.6	0.8	0.7	0.7
BCL2L10	BCL2-like 10 (apoptosis facilitator)	A_23_P163209	1.5	1.1	1.9	1.4	1.1	1.2	1.4	1.2	0.9	1.4	1.6	1.5	1.4	0.8
BCL2L12	BCL2-like 12 isoform 1	A_23_P50477	0.9	0.9	1	1	1.1	1.5	1	1.1	1.4	1.6	1	1	1	1
BCL2L13	BCL2-like 13 (apoptosis facilitator)	A_24_P410389	1.4	1.4	0.8	0.6	2.6	0.8	0.6	0.7	1.3	1.4	0.5	0.9	1.2	1.2
BCL2L13	BCL2-like 13 (apoptosis facilitator)	A_24_P409494	0.9	0.9	0.7	0.9	0.9	1.4	0.9	0.9	0.8	1.2	0.7	0.9	1	1.1
BCL2L13	BCL2-like 13 (apoptosis facilitator)	A_23_P102965	1.7	1.4	1	1	2.7	2.1	1	1	1.8	1.9	1	0.8	1	1.4
BCL2L2	BCL2-like 2 protein	A_23_P418373	1	1.1	1.1	1.1	1.2	1.6	1.1	1	1.1	1.4	1.1	1	1.1	1.2
BFAR	apoptosis regulator	A_24_P184931	0.8	0.9	0.5	0.6	0.7	0.6	0.6	0.6	0.6	0.8	0.7	0.7	0.7	0.8
BFAR	apoptosis regulator	A_23_P65963	0.9	0.9	0.8	0.9	0.9	0.9	0.8	0.9	0.8	0.9	0.8	0.9	0.9	1.1
BIRC2	baculoviral IAP repeat-containing protein 2	A_24_P115774	1	1.1	0.7	0.8	1.3	3	0.7	0.8	1.4	2.5	0.8	0.9	1.1	1.6
BIRC3	baculoviral IAP repeat-containing protein 3	A_23_P98350	1.1	1.9	1	0.9	6.5	40.8	0.7	0.9	11.6	34.9	1	1	1.7	9.2
BIRC4	baculoviral IAP repeat-containing protein 4	A_23_P22460	1.2	1.4	0.8	0.9	1.4	2.4	0.9	0.9	1.3	2.4	0.9	0.9	1	1.4
BIRC5	baculoviral IAP repeat-containing protein 5 isoform 3	A_23_P118815	0.9	0.8	0.7	0.7	0.9	0.5	0.9	0.9	0.8	0.8	0.7	0.7	0.9	1
BIRC6	baculoviral IAP repeat-containing 6	A_23_P142616	1.2	1	1	0.9	1	1.2	0.9	0.9	1.1	1	0.9	0.9	1.2	1.1
BIRC7	livin inhibitor of apoptosis isoform beta	A_23_P79769	0.8	0.7	1.3	1.1	0.9	0.6	1.3	1.3	1.3	0.6	1.1	0.9	0.7	0.7
BIRC8	baculoviral IAP repeat-containing 8	A_23_P90058	0.8	0.8	0.9	1	1	1.2	1	0.9	1.2	1	1	0.9	1	1
BNIP1	BCL2/adenovirus E1B 19kD interacting protein 1 isoform BNIP1-a	A_23_P7655	0.9	0.9	1	1	1.2	1.9	1	1	1.2	2.2	1	1.2	1.1	1.2
BNIP2	BCL2/adenovirus E1B 19kD interacting protein 2	A_23_P317001	1.2	1.1	1	1.1	1.1	1.8	0.9	1	1.2	1.7	1	1	1.1	1.4
BRAF	v-raf murine sarcoma viral oncogene homolog B1	A_23_P42935	1.1	1.1	0.9	1.1	1.1	3.6	1	1.1	1.7	2.8	0.9	1	1	1.3
CFLAR	CASP8 and FADD-like apoptosis regulator	A_24_P120115	1	1.1	0.9	0.8	1.4	1.6	0.8	0.8	1.8	1.3	0.8	0.8	0.8	1.3
CFLAR	FLAME-1-delta	A_23_P209394	0.9	1.1	0.6	0.7	1.2	3.2	0.7	0.8	1.4	2.9	0.6	0.8	0.8	1.5

GDNF	glial cell derived neurotrophic factor isoform 1 preproprotein	A_24_P25544	0.8	0.7	0.8	1.1	1	1.1	1	1	1	1	1	0.8	1	0.9
GDNF	glial cell derived neurotrophic factor isoform 1 preproprotein	A_23_P167683	0.8	1	5.8	1.1	1	1.2	1	0.9	1.2	0.9	1	0.9	0.9	1
GDNF	HFK4-GDNF	A_24_P376451	1.1	1.3	1.9	1.4	1.4	2.6	1.7	1.5	2.4	1.7	1.7	1.3	1	1.3
IGF1R	IGF1R protein	A_23_P417282	1.2	0.9	1.4	1	0.9	0.4	1.2	1	0.8	0.5	1.3	1	0.9	0.8
IGF1R	insulin-like growth factor 1 receptor precursor	A_23_P205986	1	0.9	0.8	0.8	0.8	0.9	0.8	0.8	0.7	0.9	0.8	0.8	0.7	0.7
IGF1R	unknown protein	A_23_P305680	1.2	0.7	1.3	0.7	1.1	1.3	1.1	0.8	1.5	1	1	1.1	0.8	0.8
MCL1	myeloid cell leukemia sequence 1 isoform 1	A_24_P336759	1.1	1.1	0.8	0.9	2.3	2.3	0.8	1	2.9	1.7	0.8	0.9	1	1.2
MCL1	myeloid cell leukemia sequence 1 isoform 1	A_24_P336754	1.2	1.2	1.1	1.1	3.3	4.6	1.1	1.3	4.6	3.7	1	1	1.2	1.5
MCL1	myeloid cell leukemia sequence 1 isoform 1	A_24_P319635	1.4	1.4	0.6	0.9	3.8	9.2	0.7	1	5.1	8.4	0.7	0.9	1.1	1.6
NOL3	nucleolar protein 3	A_23_P206371	1	1	1.2	1.2	1.3	0.6	1.2	1.2	1.2	0.6	1.1	1.3	1.2	0.9

Table S5.

Table S5. Expression of known intrinsic apoptosis mediators after HPIV1 infection or IFN treatment			Avonex	Avonex	F170S	F170S	F170S	F170S	P(C-)	P(C-)	P(C-)	P(C-)	WT	WT	WT	WT
Symbol	Product	Agilent	6 h	24 h	6 h	12 h	24 h	48 h	6 h	12 h	24 h	48 h	6 h	12 h	24 h	48 h
APAF1	apoptotic peptidase activating factor 1 isoform c	A_23_P36611	1	1	0.9	1	0.9	1.1	1.2	0.9	0.8	1.3	1	0.8	1	1.1
BAK1	BCL2-antagonist/killer 1	A_23_P145357	1.2	0.9	0.8	0.9	1.2	0.8	1	1	0.9	0.9	0.9	1	1	1
BAX	BCL2-associated X protein isoform epsilon	A_23_P208706	0.8	0.7	0.9	1	0.9	0.5	0.9	1	0.9	0.6	0.9	1	0.9	0.9
BID	BH3 interacting domain death agonist isoform 1	A_24_P187948	1	1	0.9	1	0.9	0.6	0.9	1	0.8	0.8	0.9	0.9	1	1.2
BID	BH3 interacting domain death agonist isoform 1	A_23_P154929	1	1	0.8	0.9	0.7	0.5	0.8	0.9	0.6	0.7	0.9	0.9	1	1.2
CASP9	caspase 9 isoform alpha preproprotein	A_24_P111342	1	1	1.1	1	1	0.9	1.1	1.1	0.9	0.9	1	1	0.9	1
CASP9	caspase 9 isoform alpha preproprotein	A_23_P97309	1.1	1.2	1.3	1.2	1.2	1	1.3	1.2	1.1	1.1	1.3	1.2	1.1	1.2
DIABLO	diablo isoform 1 precursor	A_23_P47800	0.9	0.8	1	1	1	1.2	1	1	0.9	1.1	0.9	1	0.9	1
PMAIP1	phorbol-12-myristate-13-acetate-induced protein 1	A_23_P207999	2	1.4	0.6	1.1	12.6	34.2	0.7	2	24.5	21.1	0.7	1.1	1.8	5.3

Table S6.

Table S6. Genes Differentially Expressed between C^{F170S} and P(C-) infection by 2-Fold followed by $P < 0.01$ with MTC

Symbol	Product	Agilent	F170S 6	F170S 12	F170S 24	F170S 48	P(C-) 6	P(C-) 12	P(C-) 24	P(C-) 48	Ratio F170S : P(C-)[a] 6	12	24	48
ABHD6	abhydrolase domain containing 6	A_23_P211850	1.4	1.2	0.9	0.2	1.2	1.1	0.7	0.5	1.2	1	1.4	0.5
ASMTL	acetylserotonin O-methyltransferase-like	A_23_P159539	1	1	1.4	4.9	1.3	1.1	3.4	3.2	0.8	0.9	0.4	1.5
BTN2A2	butyrophilin, subfamily 2, member A2 isoform b	A_24_P337592	1.4	1.3	3.3	27.3	1.4	1.4	9	19	1	1	0.4	1.4
CASP3	caspase 3 preproprotein	A_23_P92410	0.9	1	2.3	6.3	1	1	6.5	4.1	1	1	0.3	1.6
DUSP8[b]	dual specificity phosphatase 8	A_24_P322867	1.8	2	2.7	10	1.7	1.8	7.4	5.2	1.1	1.1	0.4	1.9
FAM64A	hypothetical protein LOC54478	A_23_P49878	0.6	0.6	0.7	0.1	0.7	0.8	0.5	0.3	0.8	0.8	1.3	0.5
HIVEP2	human immunodeficiency virus type I enhancer binding protein 2	A_23_P214766	1.5	1.3	2.1	14.2	1.5	1.2	5.1	9.1	1	1	0.4	1.6
IFIT3	interferon-induced protein with tetratricopeptide repeats 3	A_23_P35412	0.9	7.3	226.3	421.9	2.2	21.2	353.2	224.7	0.4	0.3	0.6	1.9
MAP3K8	mitogen-activated protein kinase kinase kinase 8	A_23_P23947	1.4	1.4	4.1	6.6	1.2	1.8	4.7	2.9	1.1	0.8	0.9	2.3
NAV2	steerin2 protein	A_24_P933458	1.9	1.5	2.9	14.3	2.1	1.8	8.3	7.3	0.9	0.8	0.3	2
NCOA7	nuclear receptor coactivator 7	A_23_P156957	1	1.2	7.7	15.9	1	3.2	12.2	7.2	1	0.4	0.6	2.2
PRIM1	DNA primase small subunit, 49kDa	A_23_P25019	0.6	0.7	0.7	0.2	0.8	0.8	0.5	0.4	0.9	0.9	1.2	0.5
PTGS2	prostaglandin-endoperoxide synthase 2 precursor	A_24_P250922	0.8	0.9	5	12.3	0.6	1.2	7.6	4.4	1.4	0.8	0.7	2.8
PTPRG	PTPRG protein	A_32_P93493	0.9	2.6	1.3	0.2	1.1	2.3	1.8	0.4	0.8	1.1	0.7	0.4
RBM35A	RNA binding motif protein 35A isoform 1	A_23_P259127	1	1.1	0.8	1.2	0.7	1.1	1.2	5.6	1.4	1	0.6	0.2
RELB	reticuloendotheliosis viral oncogene homolog B	A_23_P55706	1.2	1.1	2.4	25.7	1.1	1	6.2	22.2	1.1	1	0.4	1.2
SIPA1L2	signal-induced proliferation-associated 1 like 2	A_23_P137470	1.4	1.2	1.7	7.7	1.1	1.2	3.8	3.7	1.2	1.1	0.5	2.1
SLC27A2	solute carrier family 27 (fatty acid transporter), member 2	A_23_P140450	0.8	0.9	0.7	0.2	0.7	0.8	0.5	0.5	1	1.1	1.3	0.4
SLC2A13	solute carrier family 2 (facilitated glucose transporter), member 13	A_23_P10211	1.1	1	1.5	14	0.9	0.9	3.5	11.3	1.2	1.1	0.4	1.2
SLCO5A1	organic anion transporter polypeptide-related protein 4	A_23_P135669	0.7	0.9	2.3	38.3	0.9	0.8	8.4	17	0.8	1.1	0.3	2.3

SPANXA1	sperm protein associated with the nucleus, X chromosome, family member A1	A_23_P96302	0.8	0.9	0.7	0.2	1.1	1	0.7	0.5	0.7	0.9	1	0.4
STK19	serine/threonine kinase 19 isoform 2	A_23_P19479	1.1	1.1	2.8	10.6	1.1	1.2	6.4	4.2	1	0.9	0.4	2.5
TNFRSF10B	tumor necrosis factor receptor superfamily, member 10b isoform 1 precursor	A_23_P169030	0.9	1	2.3	11.5	1.1	1	4.8	8.9	0.9	1	0.5	1.3
ZEB2[b]	zinc finger homeobox 1b	A_23_P142560	1.1	1.1	6.1	90.6	1	1.1	19.2	62.2	1.1	1	0.3	1.5
		A_24_P127641	1.4	1.8	16.3	36.6	1.3	2	20	16.6	1.1	0.9	0.8	2.2
		A_24_P696924	2.3	1.7	3.8	4	2	2.5	5.2	1.8	1.2	0.7	0.7	2.3
		A_32_P207802	3.1	2.4	4.8	17.4	2.6	2	14	5.5	1.2	1.2	0.3	3.1
		A_32_P51855	1	1	0.9	9.3	1	1.2	2.2	5.7	1.1	0.9	0.4	1.6

[a]Boxes indicate times post-infection at which gene expression between C^{F170S} and P(C-) infection differed by greater than 2=fold
[b]Genes shaded in gray were also identified as significantly differentially expressed between C^{F170S} and P(C-) infection by 2-fold with $P < 0.01$ simultaneously

Table S7.

Table S7. Genes Differentially Expressed by 4-fold and an ANOVA P < 0.01 with MTC[a] between C^{F170S} and P(C-) Infection

Symbol	Product	Agilent	F170S 6 hr	F170S 12 hr	F170S 24 hr	F170S 48 hr	P(C-)[b] 6 hr	P(C-) 12 hr	P(C-) 24 hr	P(C-) 48 hr	WT 6 hr	WT 12 hr	WT 24 hr	WT 48 hr
CCL5	small inducible cytokine A5 precursor	A_23_P152838	0.9	19.6	33.6	125.7	5.3	21.8	55.5	90.3	1.8	17.5	23	29.9
IFIT2	interferon-induced protein with tetratricopeptide repeats 2	A_23_P24004	2.4	20.5	926.4	6100.4	11.9	81.2	2569.2	3777.9	2.9	14.5	42.9	531
OASL	2'-5'-oligoadenylate synthetase-like isoform a	A_23_P139786	2.1	29.7	77	187.9	11.5	41.5	114.8	135.5	2.4	24.5	33.3	58.9
C20orf141		A_32_P133182	0.8	1.5	48.5	166.7	0.8	3.4	237.7	99.4	1.1	1.1	4.1	13.9
CXXC4	CXXC finger 4	A_23_P121676	1.2	0.7	2.2	35.4	1.1	1	11.2	30.5	1.8	1.1	1.1	2.8
DICER1	dicer1	A_24_P22163	1.5	1.1	2.2	25.7	1.4	1.2	9.5	13.4	1.4	1	1.1	2.7
OTUD1		A_32_P60459	0.8	0.9	7.2	150.9	0.7	1.1	29.3	102.4	0.9	0.6	1.1	7.1
PLCB4	phospholipase C beta 4 isoform a	A_23_P28898	1.3	1.7	3.6	22.5	1.5	1.7	16	23.9	1.1	1.2	1.2	1.9
SLC12A7	solute carrier family 12 (potassium/chloride transporters), member 7	A_24_P60634	1	0.8	2.4	20.4	0.8	1.1	11.8	17.7	0.9	1.2	1.3	3.1
SLC12A7	solute carrier family 12 (potassium/chloride transporters), member 7	A_23_P251855	0.7	0.9	2.4	23.8	0.7	0.9	14.6	16	0.7	0.8	1	3.4
SLC12A7	solute carrier family 12 (potassium/chloride transporters), member 7	A_23_P61688	1.7	1.3	3.6	50.1	1.5	1.5	26.5	45.1	1.5	1.3	1.5	5.1
SNPH	syntaphilin	A_23_P102706	1.4	1.2	5.2	34.9	1.3	1.5	24.9	24.5	1.5	1.2	1.2	4.7
TNFAIP6	tumor necrosis factor, alpha-induced protein 6 precursor	A_23_P165624	0.5	0.5	1	50.9	0.9	1	4.3	26.5	0.5	0.6	0.7	7
		A_24_P255384	0.9	1	1.8	52.3	0.8	1.3	13.5	31	0.9	0.9	0.9	7.3
		A_32_P95766	0.9	1.1	16	125.9	1	1	84.6	88.1	1	1	1	25.5
		A_32_P226205	2.1	1.3	3.2	31.6	1.3	1.3	15.7	24.2	1.6	1.1	1	2
FEV	FEV (ETS oncogene family)	A_23_P5460	1.6	1.5	2.4	10.9	1.7	1.2	1	1	1.2	2	1.5	2.5
SYNPO2		A_23_P310094	0.6	1.2	2.7	9.7	0.5	0.9	2.1	1.6	0.8	1.6	2.3	2.7

[a]Benjamini-Hochberg multiple testing correction (MTC)

[b]Boxes indicate time at which gene expression differed by greater than 4-fold between C^{F170S} and P(C-) infections. All 18 genes identified as significantly differentially expressed between C^{F170S} and P(C-) infection by two-way ANOVA are also present in the 43 genes identified by a paired t-test without MTC.

Table S8.

Table S8. RT-qPCR Primers

Gene Symbol	Assay ID*	TaqMan Probe Context Sequence
IRF7	Hs00242190_g1	ACCGCGGTGCAAGAGCCCAGCCCAG
IFNB1	Hs01077958_s1	TCTTCAACCAGCAGATGCTGTTTAA
MX1	Hs00182073_m1	CCTATCACCAGGAGGCCAGCAAGCG
NFKB1	Hs00231653_m1	CAAAGCAGCAGGAGCAGATCCCCTG
TRAF1	Hs01090170_m1	GCCCTTCCGGAACAAGGTCACCTTC
GAPDH	Hs99999905_m1	TTGGGCGCCTGGTCACCAGGGCTGC

*Applied Biosystems TaqMan Gene Expression Assay ID

Supplementary Information for Chapter 4

Supplementary Figure 1. Activation of components of the IFNβ enhanceosome by HPIV1 infection. Phosphorylated ATF2 (Thr 71), total ATF2, phosphorylated P38 (Thr 180 / Tyr 182), and total P38 were detected by Western blot in A549 cells (A) infected with WT, F170S, or P(C-) HPIV1 at a MOI of 5 for 48 h or (B) treated with 10 µg/mL anisomycin for 30 or 60 minutes. n.s. indicates a non-specific band.

a.

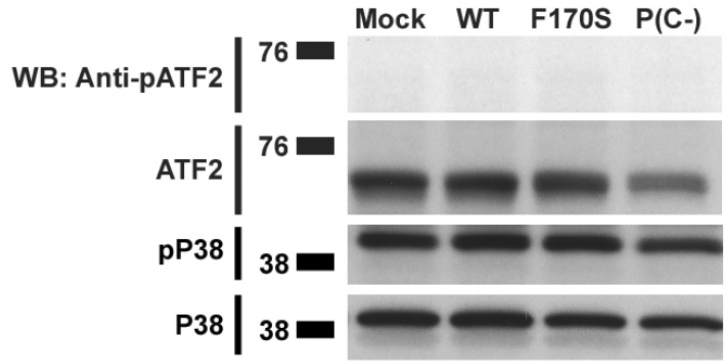

b.

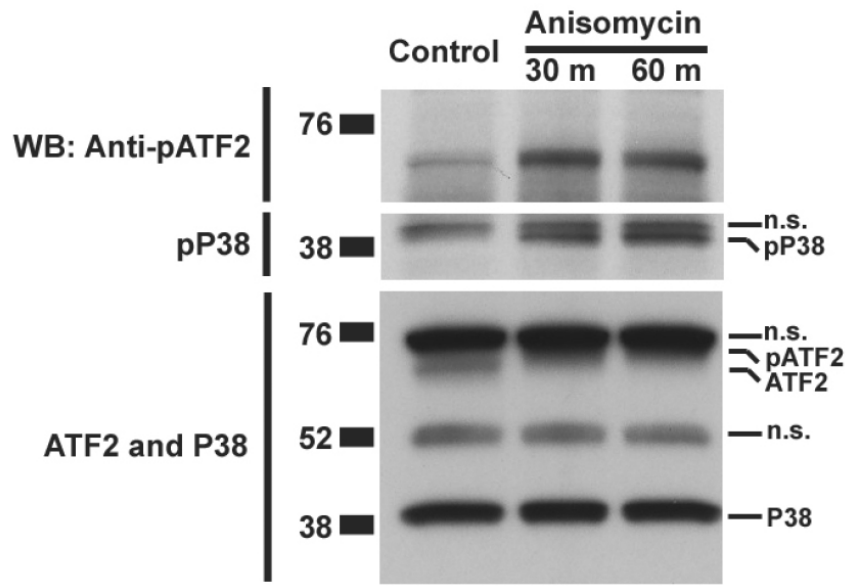

Supplementary Figure 2. Examination of C protein interaction with RIG-I pathway components. 293T cells were transfected with a Myc-tagged C expression plasmid along with (A) V5-tagged TRIM25 and/or Flag-tagged Riplet, (B) RIGI and/or MDA5, (C) IPS1 and/or TBK1, (D) TRAF3 and/or TRAF6, (E) BIRC2 and/or BIRC4, or (F) TRADD and/or FADD. Myc-tagged TRADD and Flag-tagged TRAF3 was transfected together as a positive control. Myc-tagged proteins were immuno-precipitated using immobilized anti-Myc antibodies.

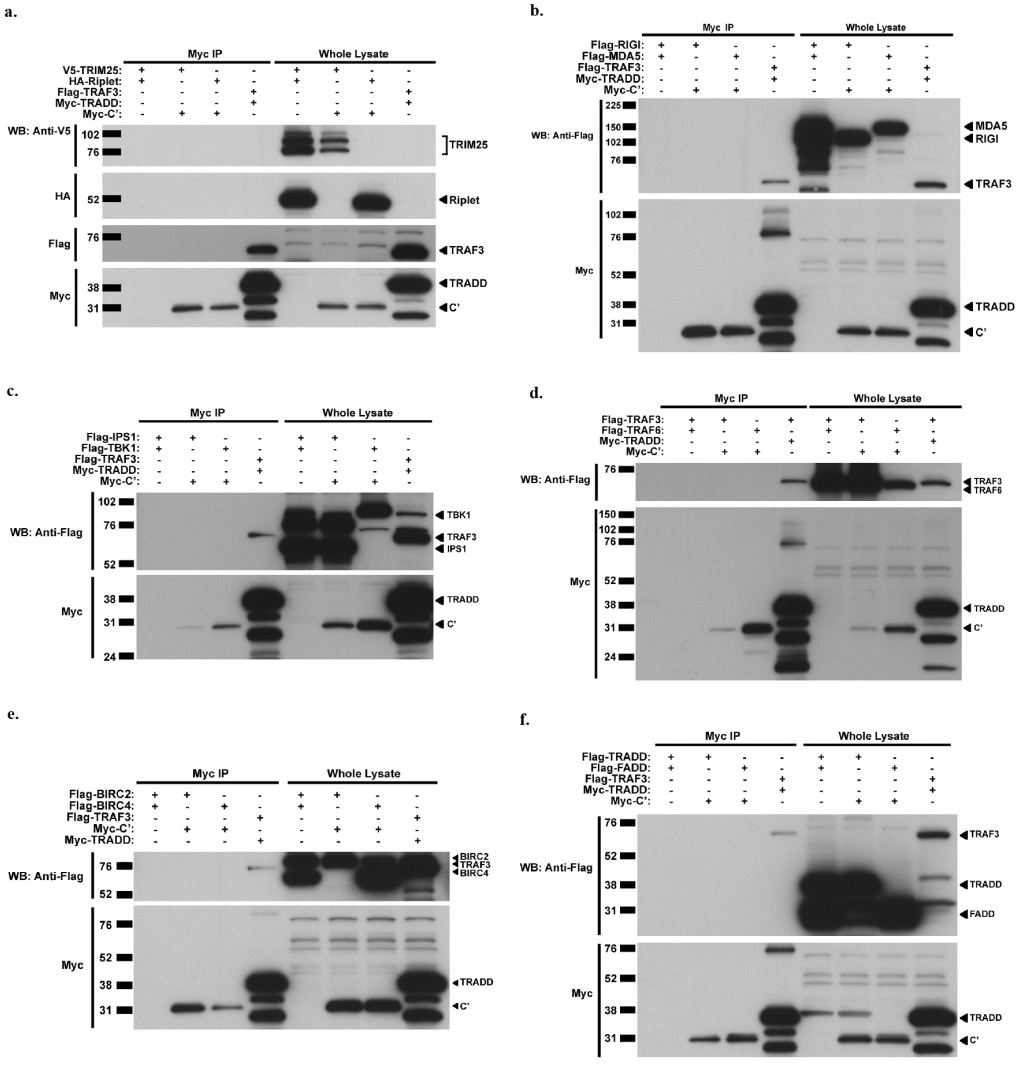

Supplementary Figure 3. Levels of viral genomic versus anti-genomic RNA levels over time during infection with WT and mutant HPIV1. HPIV1 genomic and anti-genomic RNA was distinguished using genome- and anti-genome-specific primers respectively for reverse transcription (RT) followed by real-time PCR. (A) A549 cells were infected with WT, F170S, and P(C-) HPIV1 using a MOI of 5 for 12, 24, or 48 h and genomic (left axis, intact lines) and anti-genomic RNA (right axis, dotted lines) were measured by real-time PCR, normalized to the level of WT HPIV1 anti-genome at 12 h. (B) The ratio of genomic to anti-genomic RNA from (A).

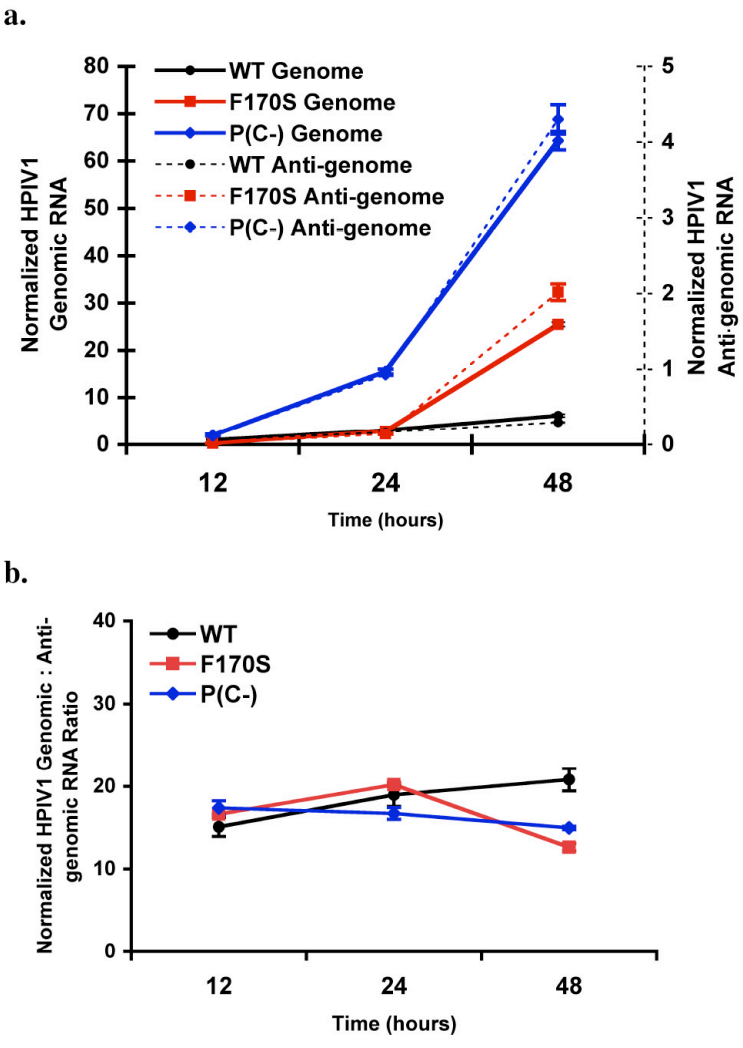

Supplementary Figure 4. Relative levels of (A) IRF3 phosphorylation, (B) IκBβ degradation, (C), P38 phosphorylation, and (D) PKR knockdown were measured by densitometry of Figure 8a and normalized to mock-infected shCON levels and to GAPDH protein expression. (E) Relative levels of C' protein expression normalized to WT HPIV1-infected shCON levels and to GAPDH.

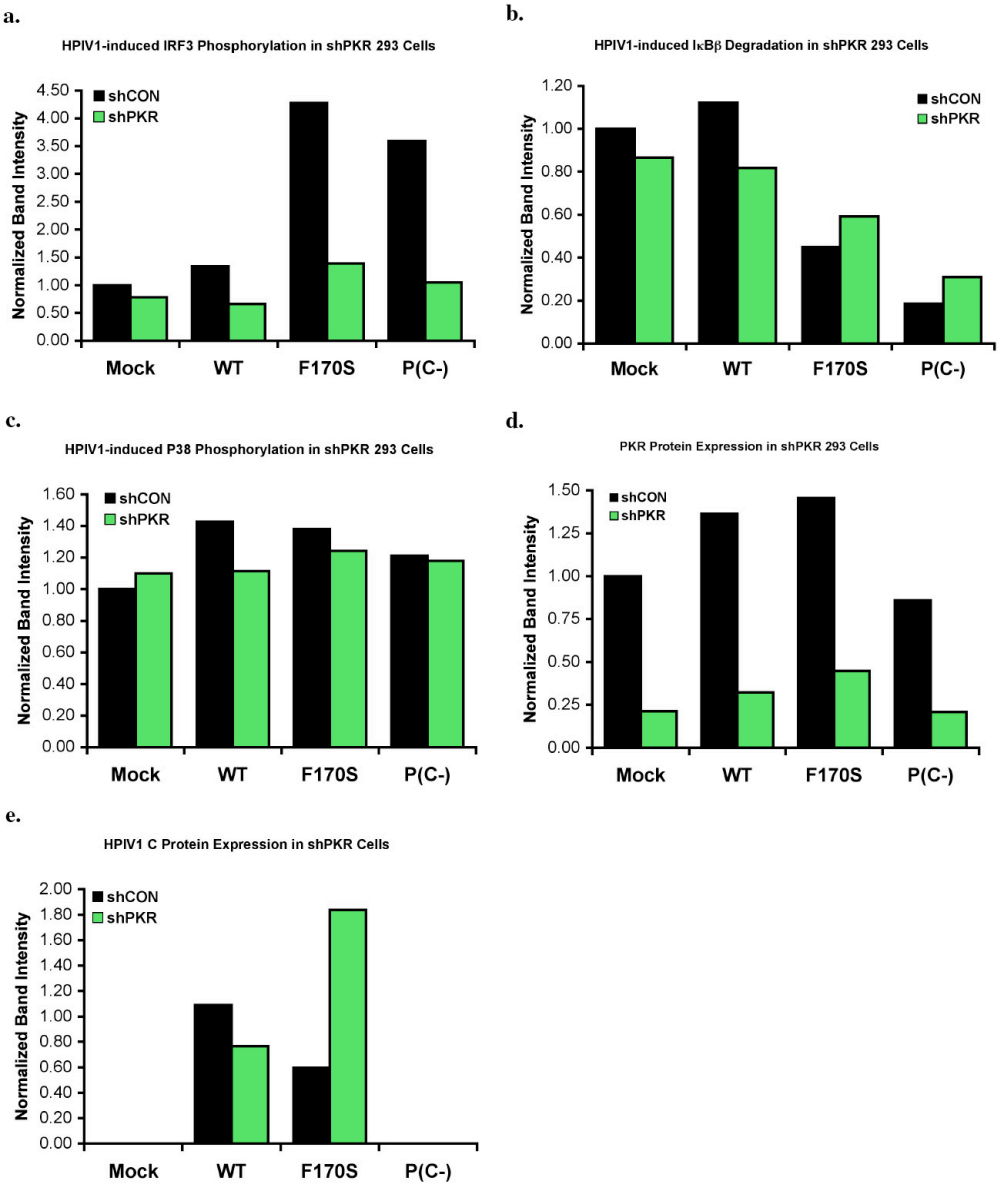

References

1. **Ahmed, M., and D. S. Lyles.** 1998. Effect of vesicular stomatitis virus matrix protein on transcription directed by host RNA polymerases I, II, and III. J Virol **72:**8413-9.

2. **Alexopoulou, L., A. C. Holt, R. Medzhitov, and R. A. Flavell.** 2001. Recognition of double-stranded RNA and activation of NF-kappaB by Toll-like receptor 3. Nature **413:**732-8.

3. **Andrejeva, J., K. S. Childs, D. F. Young, T. S. Carlos, N. Stock, S. Goodbourn, and R. E. Randall.** 2004. The V proteins of paramyxoviruses bind the IFN-inducible RNA helicase, mda-5, and inhibit its activation of the IFN-beta promoter. Proc Natl Acad Sci U S A **101:**17264-9.

4. **Baltzis, D., S. Li, and A. E. Koromilas.** 2002. Functional characterization of pkr gene products expressed in cells from mice with a targeted deletion of the N terminus or C terminus domain of PKR. J Biol Chem **277:**38364-72.

5. **Bartlett, E. J., E. Amaro-Carambot, S. R. Surman, P. L. Collins, B. R. Murphy, and M. H. Skiadopoulos.** 2006. Introducing point and deletion mutations into the P/C gene of human parainfluenza virus type 1 (HPIV1) by reverse genetics generates attenuated and efficacious vaccine candidates. Vaccine **24:**2674-84.

6. **Bartlett, E. J., E. Amaro-Carambot, S. R. Surman, J. T. Newman, P. L. Collins, B. R. Murphy, and M. H. Skiadopoulos.** 2005. Human parainfluenza virus type I (HPIV1) vaccine candidates designed by reverse genetics are attenuated and efficacious in African green monkeys. Vaccine **23:**4631-46.

7. **Bartlett, E. J., A. Castano, S. R. Surman, P. L. Collins, M. H. Skiadopoulos, and B. R. Murphy.** 2007. Attenuation and efficacy of human parainfluenza virus type 1 (HPIV1) vaccine candidates containing stabilized mutations in the P/C and L genes. Virol J **4:**67.

8. **Bartlett, E. J., A. Castano, S. R. Surman, P. L. Collins, M. H. Skiadopoulos, and B. R. Murphy.** 2007. Attenuation and efficacy of human parainfluenza virus type 1 (HPIV1) vaccine candidates containing stabilized mutations in the P/C and L genes. Virol J **4:**67.

9. **Bartlett, E. J., A. M. Cruz, J. Esker, A. Castano, H. Schomacker, S. R. Surman, M. Hennessey, J. Boonyaratanakornkit, R. J. Pickles, P. L. Collins, B. R. Murphy, and A. C. Schmidt.** 2008. Human parainfluenza virus type 1 C proteins are non-essential proteins that inhibit the host interferon and apoptotic responses and are required for efficient replication in non-human primates. J Virol.

10. **Bartlett, E. J., M. Hennessey, M. H. Skiadopoulos, A. C. Schmidt, P. L. Collins, B. R. Murphy, and R. J. Pickles.** 2008. Role of interferon in the replication of human parainfluenza virus type 1 wild type and mutant viruses in human ciliated airway epithelium. J Virol **82:**8059-70.

11. **Bartlett, E. J., M. Hennessey, M. H. Skiadopoulos, A. C. Schmidt, P. L. Collins, B. R. Murphy, and R. J. Pickles.** 2008. The role of interferon in the replication of human parainfluenza virus type 1 wild type and mutant viruses in human ciliated airway epithelium. J Virol.

12. **Belshe, R. B., F. K. Newman, E. L. Anderson, P. F. Wright, R. A. Karron, S. Tollefson, F. W. Henderson, H. C. Meissner, S. Madhi, D. Roberton, H. Marshall, R. Loh, P. Sly, B. Murphy, J. M. Tatem, V. Randolph, J. Hackell, W. Gruber, and T. F. Tsai.** 2004. Evaluation of combined live, attenuated respiratory syncytial virus and parainfluenza 3 virus vaccines in infants and young children. J Infect Dis **190:**2096-103.

13. **Billaud, G., F. Morfin, A. Vabret, A. Boucher, Y. Gillet, N. Crassard, C. Galambrun, O. Ferraris, L. Legrand, M. Aymard, B. Lina, F. Freymuth, and D. Thouvenot.** 2005. Human parainfluenza virus type 4 infections: a report of 20 cases from 1998 to 2002. J Clin Virol **34:**48-51.

14. **Bitko, V., O. Shulyayeva, B. Mazumder, A. Musiyenko, M. Ramaswamy, D. C. Look, and S. Barik.** 2007. Nonstructural proteins of respiratory syncytial virus suppress premature apoptosis by an NF-kappaB-dependent, interferon-independent mechanism and facilitate virus growth. J Virol **81:**1786-95.

15. **Bitzer, M., S. Armeanu, F. Prinz, G. Ungerechts, W. Wybranietz, M. Spiegel, C. Bernlohr, F. Cecconi, M. Gregor, W. J. Neubert, K. Schulze-Osthoff, and U. M. Lauer.** 2002. Caspase-8 and Apaf-1-independent caspase-9 activation in Sendai virus-infected cells. J Biol Chem **277:**29817-24.

16. **Bonnet, M. C., R. Weil, E. Dam, A. G. Hovanessian, and E. F. Meurs.** 2000. PKR stimulates NF-kappaB irrespective of its kinase function by interacting with the IkappaB kinase complex. Mol Cell Biol **20:**4532-42.

17. **Boonyaratanakornkit, J. B., E. J. Bartlett, E. Amaro-Carambot, P. L. Collins, B. R. Murphy, and A. C. Schmidt.** 2009. The C proteins of human

parainfluenza virus type 1 (HPIV1) control the transcription of a broad array of cellular genes that would otherwise respond to HPIV1 infection. J Virol **83:**1892-910.

18. **Bousse, T., R. L. Chambers, R. A. Scroggs, A. Portner, and T. Takimoto.** 2006. Human parainfluenza virus type 1 but not Sendai virus replicates in human respiratory cells despite IFN treatment. Virus Res **121:**23-32.

19. **Bowie, A. G., and L. Unterholzner.** 2008. Viral evasion and subversion of pattern-recognition receptor signalling. Nat Rev Immunol **8:**911-22.

20. **Buchholz, U. J., S. Finke, and K. K. Conzelmann.** 1999. Generation of bovine respiratory syncytial virus (BRSV) from cDNA: BRSV NS2 is not essential for virus replication in tissue culture, and the human RSV leader region acts as a functional BRSV genome promoter. J Virol **73:**251-9.

21. **Cadd, T., D. Garcin, C. Tapparel, M. Itoh, M. Homma, L. Roux, J. Curran, and D. Kolakofsky.** 1996. The Sendai paramyxovirus accessory C proteins inhibit viral genome amplification in a promoter-specific fashion. J Virol **70:**5067-74.

22. **Chambers, R., and T. Takimoto.** 2009. Host specificity of the anti-interferon and anti-apoptosis activities of parainfluenza virus P/C gene products. J Gen Virol **90:**1906-15.

23. **Chanock, R. M., R. H. Parrott, K. Cook, B. E. Andrews, J. A. Bell, T. Reichelderfer, A. Z. Kapikian, F. M. Mastrota, and R. J. Huebner.** 1958. Newly recognized myxoviruses from children with respiratory disease. N Engl J Med **258:**207-13.

24. **Chin, J., R. L. Magoffin, L. A. Shearer, J. H. Schieble, and E. H. Lennette.** 1969. Field evaluation of a respiratory syncytial virus vaccine and a trivalent parainfluenza virus vaccine in a pediatric population. Am J Epidemiol **89:**449-63.

25. **Chu, W. M., D. Ostertag, Z. W. Li, L. Chang, Y. Chen, Y. Hu, B. Williams, J. Perrault, and M. Karin.** 1999. JNK2 and IKKbeta are required for activating the innate response to viral infection. Immunity **11:**721-31.

26. **Collier, A. M., and W. A. Clyde, Jr.** 1977. Model systems for studying the pathogenesis of infections causing bronchiolitis in man. Pediatr Res **11:**243-6.

27. **Collins, P. L., L. E. Hightower, and L. A. Ball.** 1980. Transcriptional map for Newcastle disease virus. J Virol **35:**682-93.

28. **Colon-Ramos, D. A., P. M. Irusta, E. C. Gan, M. R. Olson, J. Song, R. I. Morimoto, R. M. Elliott, M. Lombard, R. Hollingsworth, J. M. Hardwick, G. K. Smith, and S. Kornbluth.** 2003. Inhibition of translation and induction of apoptosis by Bunyaviral nonstructural proteins bearing sequence similarity to reaper. Mol Biol Cell **14:**4162-72.

29. **Cook, M. K., B. E. Andrews, H. H. Fox, H. C. Turner, W. D. James, and R. M. Chanock.** 1959. Antigenic relationships among the newer myxoviruses (parainfluenza). Am J Hyg **69:**250-64.

30. **Counihan, M. E., D. K. Shay, R. C. Holman, S. A. Lowther, and L. J. Anderson.** 2001. Human parainfluenza virus-associated hospitalizations among children less than five years of age in the United States. Pediatr Infect Dis J **20:**646-53.

31. **Counihan, M. E., D. K. Shay, R. C. Holman, S. A. Lowther, and L. J. Anderson.** 2001. Human parainfluenza virus-associated hospitalizations among children less than five years of age in the United States. Pediatr Infect Dis J **20:**646-53.

32. **Curran, J., and D. Kolakofsky.** 1989. Scanning independent ribosomal initiation of the Sendai virus Y proteins in vitro and in vivo. EMBO J **8:**521-6.

33. **Curran, J., J. B. Marq, and D. Kolakofsky.** 1992. The Sendai virus nonstructural C proteins specifically inhibit viral mRNA synthesis. Virology **189:**647-56.

34. **de Breyne, S., R. S. Monney, and J. Curran.** 2004. Proteolytic processing and translation initiation: two independent mechanisms for the expression of the Sendai virus Y proteins. J Biol Chem **279:**16571-80.

35. **De Maeyer, E., and J. De Maeyer-Guignard.** 1998. Type I interferons. Int Rev Immunol **17:**53-73.

36. **Der, S. D., A. Zhou, B. R. Williams, and R. H. Silverman.** 1998. Identification of genes differentially regulated by interferon alpha, beta, or gamma using oligonucleotide arrays. Proc Natl Acad Sci U S A **95:**15623-8.

37. **Durbin, A. P., W. R. Elkins, and B. R. Murphy.** 2000. African green monkeys provide a useful nonhuman primate model for the study of human parainfluenza virus types-1, -2, and -3 infection. Vaccine **18:**2462-9.

38. **Eisen, M. B., P. T. Spellman, P. O. Brown, and D. Botstein.** 1998. Cluster analysis and display of genome-wide expression patterns. Proc Natl Acad Sci U S A **95:**14863-8.

39. **Elco, C. P., J. M. Guenther, B. R. Williams, and G. C. Sen.** 2005. Analysis of genes induced by Sendai virus infection of mutant cell lines reveals essential roles of interferon regulatory factor 3, NF-kappaB, and interferon but not toll-like receptor 3. J Virol **79:**3920-9.

40. **Elmore, S.** 2007. Apoptosis: a review of programmed cell death. Toxicol Pathol **35:**495-516.

41. **Fitzgerald, K. A., S. M. McWhirter, K. L. Faia, D. C. Rowe, E. Latz, D. T. Golenbock, A. J. Coyle, S. M. Liao, and T. Maniatis.** 2003. IKKepsilon and TBK1 are essential components of the IRF3 signaling pathway. Nat Immunol **4:**491-6.

42. **Forster, J., G. Ihorst, C. H. Rieger, V. Stephan, H. D. Frank, H. Gurth, R. Berner, A. Rohwedder, H. Werchau, M. Schumacher, T. Tsai, and G. Petersen.** 2004. Prospective population-based study of viral lower respiratory tract infections in children under 3 years of age (the PRI.DE study). Eur J Pediatr **163:**709-16.

43. **Fulginiti, V. A., J. J. Eller, O. F. Sieber, J. W. Joyner, M. Minamitani, and G. Meiklejohn.** 1969. Respiratory virus immunization. I. A field trial of two inactivated respiratory virus vaccines; an aqueous trivalent parainfluenza virus vaccine and an alum-precipitated respiratory syncytial virus vaccine. Am J Epidemiol **89:**435-48.

44. **Gack, M. U., R. A. Albrecht, T. Urano, K. S. Inn, I. C. Huang, E. Carnero, M. Farzan, S. Inoue, J. U. Jung, and A. Garcia-Sastre.** 2009. Influenza A virus

NS1 targets the ubiquitin ligase TRIM25 to evade recognition by the host viral RNA sensor RIG-I. Cell Host Microbe **5:**439-49.

45. **Gack, M. U., Y. C. Shin, C. H. Joo, T. Urano, C. Liang, L. Sun, O. Takeuchi, S. Akira, Z. Chen, S. Inoue, and J. U. Jung.** 2007. TRIM25 RING-finger E3 ubiquitin ligase is essential for RIG-I-mediated antiviral activity. Nature **446:**916-920.

46. **Garcia-Sastre, A., and C. A. Biron.** 2006. Type 1 interferons and the virus-host relationship: a lesson in detente. Science **312:**879-82.

47. **Garcin, D., J. Curran, M. Itoh, and D. Kolakofsky.** 2001. Longer and shorter forms of Sendai virus C proteins play different roles in modulating the cellular antiviral response. J Virol **75:**6800-7.

48. **Garcin, D., J. Curran, and D. Kolakofsky.** 2000. Sendai virus C proteins must interact directly with cellular components to interfere with interferon action. J Virol **74:**8823-30.

49. **Garcin, D., M. Itoh, and D. Kolakofsky.** 1997. A point mutation in the Sendai virus accessory C proteins attenuates virulence for mice, but not virus growth in cell culture. Virology **238:**424-431.

50. **Garcin, D., M. Itoh, and D. Kolakofsky.** 1997. A point mutation in the Sendai virus accessory C proteins attenuates virulence for mice, but not virus growth in cell culture. Virology **238:**424-31.

51. **Garcin, D., J. B. Marq, S. Goodbourn, and D. Kolakofsky.** 2003. The amino-terminal extensions of the longer Sendai virus C proteins modulate pY701-Stat1 and bulk Stat1 levels independently of interferon signaling. J Virol **77:**2321-9.

52. **Geiss, G., G. Jin, J. Guo, R. Bumgarner, M. G. Katze, and G. C. Sen.** 2001. A comprehensive view of regulation of gene expression by double-stranded RNA-mediated cell signaling. J Biol Chem **276:**30178-82.

53. **Gitlin, L., L. Benoit, C. Song, M. Cella, S. Gilfillan, M. J. Holtzman, and M. Colonna.** Melanoma differentiation-associated gene 5 (MDA5) is involved in the innate immune response to Paramyxoviridae infection in vivo. PLoS Pathog **6:**e1000734.

54. **Goodbourn, S., L. Didcock, and R. E. Randall.** 2000. Interferons: cell signalling, immune modulation, antiviral response and virus countermeasures. J Gen Virol **81:**2341-64.

55. **Gosselin-Grenet, A. S., J. B. Marq, L. Abrami, D. Garcin, and L. Roux.** 2007. Sendai virus budding in the course of an infection does not require Alix and VPS4A host factors. Virology **365:**101-12.

56. **Gotoh, B., K. Takeuchi, T. Komatsu, and J. Yokoo.** 2003. The STAT2 activation process is a crucial target of Sendai virus C protein for the blockade of alpha interferon signaling. J Virol **77:**3360-70.

57. **Gotoh, B., K. Takeuchi, T. Komatsu, J. Yokoo, Y. Kimura, A. Kurotani, A. Kato, and Y. Nagai.** 1999. Knockout of the Sendai virus C gene eliminates the viral ability to prevent the interferon-alpha/beta-mediated responses. FEBS Lett **459:**205-10.

58. **Gottlieb, J., T. F. Schulz, T. Welte, T. Fuehner, M. Dierich, A. R. Simon, and I. Engelmann.** 2009. Community-acquired respiratory viral infections in lung transplant recipients: a single season cohort study. Transplantation **87:**1530-7.

59. **Grandvaux, N., M. J. Servant, B. tenOever, G. C. Sen, S. Balachandran, G. N. Barber, R. Lin, and J. Hiscott.** 2002. Transcriptional profiling of interferon regulatory factor 3 target genes: direct involvement in the regulation of interferon-stimulated genes. J Virol **76:**5532-9.

60. **Grandvaux, N., B. R. tenOever, M. J. Servant, and J. Hiscott.** 2002. The interferon antiviral response: from viral invasion to evasion. Curr Opin Infect Dis **15:**259-67.

61. **Greenberg, D. P., R. E. Walker, M. S. Lee, K. S. Reisinger, J. I. Ward, R. Yogev, M. M. Blatter, S. H. Yeh, R. A. Karron, C. Sangli, L. Eubank, K. L. Coelingh, J. M. Cordova, M. J. August, H. B. Mehta, W. Chen, and P. M. Mendelman.** 2005. A bovine parainfluenza virus type 3 vaccine is safe and immunogenic in early infancy. J Infect Dis **191:**1116-22.

62. **Gubbay, O., J. Curran, and D. Kolakofsky.** 2001. Sendai virus genome synthesis and assembly are coupled: a possible mechanism to promote viral RNA polymerase processivity. J Gen Virol **82:**2895-903.

63. **Hall, C. B., R. G. Douglas, Jr., R. L. Simons, and J. M. Geiman.** 1978. Interferon production in children with respiratory syncytial, influenza, and parainfluenza virus infections. J Pediatr **93:**28-32.

64. **Hartman, A. L., B. H. Bird, J. S. Towner, Z. A. Antoniadou, S. R. Zaki, and S. T. Nichol.** 2008. Inhibition of IRF-3 activation by VP35 is critical for the high level of virulence of ebola virus. J Virol **82:**2699-704.

65. **Hartman, A. L., L. Ling, S. T. Nichol, and M. L. Hibberd.** 2008. Whole-genome expression profiling reveals that inhibition of host innate immune

response pathways by Ebola virus can be reversed by a single amino acid change in the VP35 protein. J Virol **82:**5348-58.

66. **Hasan, M. K., A. Kato, M. Muranaka, R. Yamaguchi, Y. Sakai, I. Hatano, M. Tashiro, and Y. Nagai.** 2000. Versatility of the accessory C proteins of sendai virus: contribution to virus assembly as an additional role. J Virol **74:**5619-28.

67. **Hausmann, S., J. B. Marq, C. Tapparel, D. Kolakofsky, and D. Garcin.** 2008. RIG-I and dsRNA-induced IFNbeta activation. PLoS One **3:**e3965.

68. **Heikkinen, T., M. Thint, and T. Chonmaitree.** 1999. Prevalence of various respiratory viruses in the middle ear during acute otitis media. N Engl J Med **340:**260-4.

69. **Henderson, F. W., A. M. Collier, M. A. Sanyal, J. M. Watkins, D. L. Fairclough, W. A. Clyde, Jr., and F. W. Denny.** 1982. A longitudinal study of respiratory viruses and bacteria in the etiology of acute otitis media with effusion. N Engl J Med **306:**1377-83.

70. **Hershey, J. W.** 1991. Translational control in mammalian cells. Annu Rev Biochem **60:**717-55.

71. **Heylbroeck, C., S. Balachandran, M. J. Servant, C. DeLuca, G. N. Barber, R. Lin, and J. Hiscott.** 2000. The IRF-3 transcription factor mediates Sendai virus-induced apoptosis. J Virol **74:**3781-92.

72. **Ho Sui, S. J., J. R. Mortimer, D. J. Arenillas, J. Brumm, C. J. Walsh, B. P. Kennedy, and W. W. Wasserman.** 2005. oPOSSUM: identification of over-

represented transcription factor binding sites in co-expressed genes. Nucleic Acids Res **33:**3154-64.

73. **Honda, K., A. Takaoka, and T. Taniguchi.** 2006. Type I interferon [corrected] gene induction by the interferon regulatory factor family of transcription factors. Immunity **25:**349-60.

74. **Horikami, S. M., J. Curran, D. Kolakofsky, and S. A. Moyer.** 1992. Complexes of Sendai virus NP-P and P-L proteins are required for defective interfering particle genome replication in vitro. J Virol **66:**4901-8.

75. **Horikami, S. M., R. E. Hector, S. Smallwood, and S. A. Moyer.** 1997. The Sendai virus C protein binds the L polymerase protein to inhibit viral RNA synthesis. Virology **235:**261-70.

76. **Hornung, V., J. Ellegast, S. Kim, K. Brzozka, A. Jung, H. Kato, H. Poeck, S. Akira, K. K. Conzelmann, M. Schlee, S. Endres, and G. Hartmann.** 2006. 5'-Triphosphate RNA is the ligand for RIG-I. Science **314:**994-7.

77. **Hou, S., P. C. Doherty, M. Zijlstra, R. Jaenisch, and J. M. Katz.** 1992. Delayed clearance of Sendai virus in mice lacking class I MHC-restricted CD8+ T cells. J Immunol **149:**1319-25.

78. **Hromas, R., S. J. Collins, D. Hickstein, W. Raskind, L. L. Deaven, P. O'Hara, F. S. Hagen, and K. Kaushansky.** 1991. A retinoic acid-responsive human zinc finger gene, MZF-1, preferentially expressed in myeloid cells. J Biol Chem **266:**14183-7.

79. **Hui, D. S., J. Woo, E. Hui, A. Foo, M. Ip, K. W. To, E. S. Cheuk, W. Y. Lam, A. Sham, and P. K. Chan.** 2008. Influenza-like illness in residential care homes:

a study of the incidence, aetiological agents, natural history and health resource utilisation. Thorax **63:**690-7.

80. **Irie, T., N. Nagata, T. Igarashi, I. Okamoto, and T. Sakaguchi.** Conserved charged amino acids within Sendai virus C protein play multiple roles in the evasion of innate immune responses. PLoS One **5:**e10719.

81. **Irie, T., N. Nagata, T. Yoshida, and T. Sakaguchi.** 2008. Paramyxovirus Sendai virus C proteins are essential for maintenance of negative-sense RNA genome in virus particles. Virology **374:**495-505.

82. **Irie, T., N. Nagata, T. Yoshida, and T. Sakaguchi.** 2008. Recruitment of Alix/AIP1 to the plasma membrane by Sendai virus C protein facilitates budding of virus-like particles. Virology **371:**108-20.

83. **Itoh, M., H. Hotta, and M. Homma.** 1998. Increased induction of apoptosis by a Sendai virus mutant is associated with attenuation of mouse pathogenicity. J Virol **72:**2927-34.

84. **Itoh, M., Y. Isegawa, H. Hotta, and M. Homma.** 1997. Isolation of an avirulent mutant of Sendai virus with two amino acid mutations from a highly virulent field strain through adaptation to LLC- MK2 cells. J Gen Virol **78:**3207-15.

85. **Itoh, M., Y. Isegawa, H. Hotta, and M. Homma.** 1997. Isolation of an avirulent mutant of Sendai virus with two amino acid mutations from a highly virulent field strain through adaptation to LLC-MK2 cells. J Gen Virol **78 (Pt 12):**3207-15.

86. **Iwane, M. K., K. M. Edwards, P. G. Szilagyi, F. J. Walker, M. R. Griffin, G. A. Weinberg, C. Coulen, K. A. Poehling, L. P. Shone, S. Balter, C. B. Hall, D. D. Erdman, K. Wooten, and B. Schwartz.** 2004. Population-based surveillance

for hospitalizations associated with respiratory syncytial virus, influenza virus, and parainfluenza viruses among young children. Pediatrics **113:**1758-64.

87. **Janeway, C. A., Jr.** 1989. Approaching the asymptote? Evolution and revolution in immunology. Cold Spring Harb Symp Quant Biol **54 Pt 1:**1-13.

88. **Jenner, R. G., and R. A. Young.** 2005. Insights into host responses against pathogens from transcriptional profiling. Nat Rev Microbiol **3:**281-94.

89. **Karron, R. A., R. B. Belshe, P. F. Wright, B. Thumar, B. Burns, F. Newman, J. C. Cannon, J. Thompson, T. Tsai, M. Paschalis, S. L. Wu, Y. Mitcho, J. Hackell, B. R. Murphy, and J. M. Tatem.** 2003. A live human parainfluenza type 3 virus vaccine is attenuated and immunogenic in young infants. Pediatr Infect Dis J **22:**394-405.

90. **Karron, R. A., and P. L. Collins.** 2007. Chapter 42. Parainfluenza Viruses, p. 1497-1526. *In* D. M. Knipe and P. M. Howley (ed.), Fields Virology, Fifth ed, vol. 1. Lippincott Williams & Wilkins, Philadelphia.

91. **Karron, R. A., M. Makhene, K. Gay, M. H. Wilson, M. L. Clements, and B. R. Murphy.** 1996. Evaluation of a live attenuated bovine parainfluenza type 3 vaccine in two- to six-month-old infants. Pediatr Infect Dis J **15:**650-4.

92. **Karron, R. A., M. Makhene, K. Gay, M. H. Wilson, M. L. Clements, and B. R. Murphy.** 1996. Evaluation of a live attenuated bovine parainfluenza type 3 vaccine in two- to six-month-old infants. Pediatr Infect Dis J **15:**650-654.

93. **Karron, R. A., P. F. Wright, F. K. Newman, M. Makhene, J. Thompson, R. Samorodin, M. H. Wilson, E. L. Anderson, M. L. Clements, B. R. Murphy,**

and et al. 1995. A live human parainfluenza type 3 virus vaccine is attenuated and immunogenic in healthy infants and children. J Infect Dis **172:**1445-50.

94. **Kasel, J. A., A. L. Frank, W. A. Keitel, L. H. Taber, and W. P. Glezen.** 1984. Acquisition of serum antibodies to specific viral glycoproteins of parainfluenza virus 3 in children. J Virol **52:**828-32.

95. **Kash, J. C., E. Muhlberger, V. Carter, M. Grosch, O. Perwitasari, S. C. Proll, M. J. Thomas, F. Weber, H. D. Klenk, and M. G. Katze.** 2006. Global suppression of the host antiviral response by Ebola- and Marburgviruses: increased antagonism of the type I interferon response is associated with enhanced virulence. J Virol **80:**3009-20.

96. **Kato, A., C. Cortese-Grogan, S. A. Moyer, F. Sugahara, T. Sakaguchi, T. Kubota, N. Otsuki, M. Kohase, M. Tashiro, and Y. Nagai.** 2004. Characterization of the amino acid residues of sendai virus C protein that are critically involved in its interferon antagonism and RNA synthesis down-regulation. J Virol **78:**7443-54.

97. **Kato, A., Y. Ohnishi, M. Kohase, S. Saito, M. Tashiro, and Y. Nagai.** 2001. Y2, the smallest of the Sendai virus C proteins, is fully capable of both counteracting the antiviral action of interferons and inhibiting viral RNA synthesis. J Virol **75:**3802-10.

98. **Kato, H., O. Takeuchi, S. Sato, M. Yoneyama, M. Yamamoto, K. Matsui, S. Uematsu, A. Jung, T. Kawai, K. J. Ishii, O. Yamaguchi, K. Otsu, T. Tsujimura, C. S. Koh, C. Reis e Sousa, Y. Matsuura, T. Fujita, and S. Akira.**

2006. Differential roles of MDA5 and RIG-I helicases in the recognition of RNA viruses. Nature **441:**101-5.

99. **Kawai, T., K. Takahashi, S. Sato, C. Coban, H. Kumar, H. Kato, K. J. Ishii, O. Takeuchi, and S. Akira.** 2005. IPS-1, an adaptor triggering RIG-I- and Mda5-mediated type I interferon induction. Nat Immunol **6:**981-8.

100. **Kingsbury, D. W., and R. W. Darlington.** 1968. Isolation and properties of Newcastle disease virus nucleocapsid. J Virol **2:**248-55.

101. **Kohl, A., R. F. Clayton, F. Weber, A. Bridgen, R. E. Randall, and R. M. Elliott.** 2003. Bunyamwera virus nonstructural protein NSs counteracts interferon regulatory factor 3-mediated induction of early cell death. J Virol **77:**7999-8008.

102. **Kolakofsky, D., T. Pelet, D. Garcin, S. Hausmann, J. Curran, and L. Roux.** 1998. Paramyxovirus RNA synthesis and the requirement for hexamer genome length: the rule of six revisited. J Virol **72:**891-9.

103. **Komada, H., S. Kusagawa, C. Orvell, M. Tsurudome, M. Nishio, H. Bando, M. Kawano, H. Matsumura, E. Norrby, and Y. Ito.** 1992. Antigenic diversity of human parainfluenza virus type 1 isolates and their immunological relationship with Sendai virus revealed by using monoclonal antibodies. J Gen Virol **73:**875-84.

104. **Komatsu, T., K. Takeuchi, J. Yokoo, and B. Gotoh.** 2004. C and V proteins of Sendai virus target signaling pathways leading to IRF-3 activation for the negative regulation of interferon-beta production. Virology **325:**137-48.

105. **Koyama, A. H., H. Irie, A. Kato, Y. Nagai, and A. Adachi.** 2003. Virus multiplication and induction of apoptosis by Sendai virus: role of the C proteins. Microbes Infect **5:**373-8.

106. **Kozak, M.** 1987. At least six nucleotides preceding the AUG initiator codon enhance translation in mammalian cells. J. Mol. Biol. **196:**947-950.

107. **Kumar, A., Y. L. Yang, V. Flati, S. Der, S. Kadereit, A. Deb, J. Haque, L. Reis, C. Weissmann, and B. R. Williams.** 1997. Deficient cytokine signaling in mouse embryo fibroblasts with a targeted deletion in the PKR gene: role of IRF-1 and NF-kappaB. EMBO J **16:**406-16.

108. **Kurotani, A., K. Kiyotani, A. Kato, T. Shioda, Y. Sakai, K. Mizumoto, T. Yoshida, and Y. Nagai.** 1998. Sendai virus C proteins are categorically nonessential gene products but silencing their expression severely impairs viral replication and pathogenesis. Genes Cells **3:**111-24.

109. **Kurotani, A., K. Kiyotani, A. Kato, T. Shioda, Y. Sakai, K. Mizumoto, T. Yoshida, and Y. Nagai.** 1998. Sendai virus C proteins are categorically nonessential gene products but silencing their expression severely impairs viral replication and pathogenesis. Genes Cells **3:**111-124.

110. **Latorre, P., T. Cadd, M. Itoh, J. Curran, and D. Kolakofsky.** 1998. The various Sendai virus C proteins are not functionally equivalent and exert both positive and negative effects on viral RNA accumulation during the course of infection. J Virol **72:**5984-93.

111. **Le May, N., S. Dubaele, L. Proietti De Santis, A. Billecocq, M. Bouloy, and J. M. Egly.** 2004. TFIIH transcription factor, a target for the Rift Valley hemorrhagic fever virus. Cell **116:**541-50.

112. **Le Mercier, P., D. Garcin, E. Garcia, and D. Kolakofsky.** 2003. Competition between the Sendai virus N mRNA start site and the genome 3'-end promoter for viral RNA polymerase. J Virol **77:**9147-55.

113. **Lee, J. Y., J. A. Marshall, and D. S. Bowden.** 1994. Characterization of rubella virus replication complexes using antibodies to double-stranded RNA. Virology **200:**307-12.

114. **Levy, D. E., and A. Garcia-Sastre.** 2001. The virus battles: IFN induction of the antiviral state and mechanisms of viral evasion. Cytokine Growth Factor Rev **12:**143-56.

115. **Li, X., B. Gold, C. O'HUigin, F. Diaz-Griffero, B. Song, Z. Si, Y. Li, W. Yuan, M. Stremlau, C. Mische, H. Javanbakht, M. Scally, C. Winkler, M. Dean, and J. Sodroski.** 2007. Unique features of TRIM5alpha among closely related human TRIM family members. Virology **360:**419-33.

116. **Li, X. D., L. Sun, R. B. Seth, G. Pineda, and Z. J. Chen.** 2005. Hepatitis C virus protease NS3/4A cleaves mitochondrial antiviral signaling protein off the mitochondria to evade innate immunity. Proc Natl Acad Sci U S A **102:**17717-22.

117. **Lin, L., and S. L. Peng.** 2006. Coordination of NF-kappaB and NFAT antagonism by the forkhead transcription factor Foxd1. J Immunol **176:**4793-803.

118. **Liu, P., M. Jamaluddin, K. Li, R. P. Garofalo, A. Casola, and A. R. Brasier.** 2007. Retinoic acid-inducible gene I mediates early antiviral response and Toll-

like receptor 3 expression in respiratory syncytial virus-infected airway epithelial cells. J Virol **81:**1401-11.

119. **Loo, Y. M., J. Fornek, N. Crochet, G. Bajwa, O. Perwitasari, L. Martinez-Sobrido, S. Akira, M. A. Gill, A. Garcia-Sastre, M. G. Katze, and M. Gale, Jr.** 2008. Distinct RIG-I and MDA5 signaling by RNA viruses in innate immunity. J Virol **82:**335-45.

120. **Maniatis, T., J. V. Falvo, T. H. Kim, T. K. Kim, C. H. Lin, B. S. Parekh, and M. G. Wathelet.** 1998. Structure and function of the interferon-beta enhanceosome. Cold Spring Harb Symp Quant Biol **63:**609-20.

121. **Marie, I., J. E. Durbin, and D. E. Levy.** 1998. Differential viral induction of distinct interferon-alpha genes by positive feedback through interferon regulatory factor-7. EMBO J **17:**6660-9.

122. **Marx, A., T. J. Torok, R. C. Holman, M. J. Clarke, and L. J. Anderson.** 1997. Pediatric hospitalizations for croup (laryngotracheobronchitis): biennial increases associated with human parainfluenza virus 1 epidemics. J. Infect. Dis. **176:**1423-1427.

123. **Matsuoka, Y., J. Curran, T. Pelet, D. Kolakofsky, R. Ray, and R. W. Compans.** 1991. The P gene of human parainfluenza virus type 1 encodes P and C proteins but not a cysteine-rich V protein. J Virol **65:**3406-10.

124. **McAllister, C. S., and C. E. Samuel.** 2009. The RNA-activated protein kinase enhances the induction of interferon-beta and apoptosis mediated by cytoplasmic RNA sensors. J Biol Chem **284:**1644-51.

125. **McAllister, C. S., A. M. Toth, P. Zhang, P. Devaux, R. Cattaneo, and C. E. Samuel.** Mechanisms of protein kinase PKR-mediated amplification of beta interferon induction by C protein-deficient measles virus. J Virol **84:**380-6.

126. **McAuliffe, J. M., S. R. Surman, J. T. Newman, J. M. Riggs, P. L. Collins, B. R. Murphy, and M. H. Skiadopoulos.** 2004. Codon substitution mutations at two positions in the L polymerase protein of human parainfluenza virus type 1 yield viruses with a spectrum of attenuation in vivo and increased phenotypic stability in vitro. J Virol **78:**2029-36.

127. **McLean, J. E., A. Ruck, A. Shirazian, F. Pooyaei-Mehr, and Z. F. Zakeri.** 2008. Viral manipulation of cell death. Curr Pharm Des **14:**198-220.

128. **Michallet, M. C., E. Meylan, M. A. Ermolaeva, J. Vazquez, M. Rebsamen, J. Curran, H. Poeck, M. Bscheider, G. Hartmann, M. Konig, U. Kalinke, M. Pasparakis, and J. Tschopp.** 2008. TRADD Protein Is an Essential Component of the RIG-like Helicase Antiviral Pathway. Immunity.

129. **Moeller, K., I. Duffy, P. Duprex, B. Rima, R. Beschorner, S. Fauser, R. Meyermann, S. Niewiesk, V. ter Meulen, and J. Schneider-Schaulies.** 2001. Recombinant measles viruses expressing altered hemagglutinin (H) genes: functional separation of mutations determining H antibody escape from neurovirulence. J Virol **75:**7612-20.

130. **Moscona, A., and R. W. Peluso.** 1991. Fusion properties of cells persistently infected with human parainfluenza virus type 3: participation of hemagglutinin-neuraminidase in membrane fusion. J Virol **65:**2773-7.

131. **Murakami, M., T. Towatari, M. Ohuchi, M. Shiota, M. Akao, Y. Okumura, M. A. Parry, and H. Kido.** 2001. Mini-plasmin found in the epithelial cells of bronchioles triggers infection by broad-spectrum influenza A viruses and Sendai virus. Eur J Biochem **268:**2847-55.

132. **Muroi, M., and K. Tanamoto.** 2008. TRAF6 distinctively mediates MyD88- and IRAK-1-induced activation of NF-kappaB. J Leukoc Biol **83:**702-7.

133. **Murphy, B. R., S. L. Hall, A. B. Kulkarni, J. E. Crowe, Jr., P. L. Collins, M. Connors, R. A. Karron, and R. M. Chanock.** 1994. An update on approaches to the development of respiratory syncytial virus (RSV) and parainfluenza virus type 3 (PIV3) vaccines. Virus Res **32:**13-36.

134. **Murphy, B. R., G. A. Prince, P. L. Collins, K. Van Wyke Coelingh, R. A. Olmsted, M. K. Spriggs, R. H. Parrott, H. W. Kim, C. D. Brandt, and R. M. Chanock.** 1988. Current approaches to the development of vaccines effective against parainfluenza and respiratory syncytial viruses. Virus Res **11:**1-15.

135. **Murphy, B. R., D. D. Richman, E. G. Chalhub, C. P. Uhlendorf, S. Baron, and R. M. Chanock.** 1975. Failure of attenuated temperature-sensitive influenza A (H3N2) virus to induce heterologous interference in humans to parainfluenza type 1 virus. Infect Immun **12:**62-68.

136. **Nagai, Y.** 1995. Virus activation by host proteinases. A pivotal role in the spread of infection, tissue tropism and pathogenicity. Microbiol Immunol **39:**1-9.

137. **Newman, J. T., J. M. Riggs, S. R. Surman, J. M. McAuliffe, T. A. Mulaikal, P. L. Collins, B. R. Murphy, and M. H. Skiadopoulos.** 2004. Generation of recombinant human parainfluenza virus type 1 vaccine candidates by importation

of temperature-sensitive and attenuating mutations from heterologous paramyxoviruses. J Virol **78:**2017-28.

138. **Newman, J. T., S. R. Surman, J. M. Riggs, C. T. Hansen, P. L. Collins, B. R. Murphy, and M. H. Skiadopoulos.** 2002. Sequence analysis of the Washington/1964 strain of human parainfluenza virus type 1 (HPIV1) and recovery and characterization of wild-type recombinant HPIV1 produced by reverse genetics. Virus Genes **24:**77-92.

139. **Nolan, S. M., M. H. Skiadopoulos, K. Bradley, O. S. Kim, S. Bier, E. Amaro-Carambot, S. R. Surman, S. Davis, M. St Claire, R. Elkins, P. L. Collins, B. R. Murphy, and A. Schaap-Nutt.** 2007. Recombinant human parainfluenza virus type 2 vaccine candidates containing a 3' genomic promoter mutation and L polymerase mutations are attenuated and protective in non-human primates. Vaccine **25:**6409-22.

140. **Oshiumi, H., M. Matsumoto, K. Funami, T. Akazawa, and T. Seya.** 2003. TICAM-1, an adaptor molecule that participates in Toll-like receptor 3-mediated interferon-beta induction. Nat Immunol **4:**161-7.

141. **Oshiumi, H., M. Matsumoto, S. Hatakeyama, and T. Seya.** 2009. Riplet/RNF135, a RING finger protein, ubiquitinates RIG-I to promote interferon-beta induction during the early phase of viral infection. J Biol Chem **284:**807-17.

142. **Panne, D., T. Maniatis, and S. C. Harrison.** 2004. Crystal structure of ATF-2/c-Jun and IRF-3 bound to the interferon-beta enhancer. EMBO J **23:**4384-93.

143. **Parrott, R. H., A. Vargosko, A. Luckey, H. W. Kim, C. Cumming, and R. Chanock.** 1959. Clinical features of infection with hemadsorption viruses. N Engl J Med **260:**731-8.

144. **Pestka, S., J. A. Langer, K. C. Zoon, and C. E. Samuel.** 1987. Interferons and their actions. Annu Rev Biochem **56:**727-77.

145. **Peters, K., S. Chattopadhyay, and G. C. Sen.** 2008. IRF-3 activation by sendai virus infection is required for cellular apoptosis and avoidance of persistence. J Virol **82:**3500-8.

146. **Pfaffl, M. W.** 2001. A new mathematical model for relative quantification in real-time RT-PCR. Nucleic Acids Res **29:**e45.

147. **Pichlmair, A., O. Schulz, C. P. Tan, T. I. Naslund, P. Liljestrom, F. Weber, and C. Reis e Sousa.** 2006. RIG-I-mediated antiviral responses to single-stranded RNA bearing 5'-phosphates. Science **314:**997-1001.

148. **Pichlmair, A., O. Schulz, C. P. Tan, J. Rehwinkel, H. Kato, O. Takeuchi, S. Akira, M. Way, G. Schiavo, and C. Reis e Sousa.** 2009. Activation of MDA5 requires higher-order RNA structures generated during virus infection. J Virol **83:**10761-9.

149. **Pickles, R. J., D. McCarty, H. Matsui, P. J. Hart, S. H. Randell, and R. C. Boucher.** 1998. Limited entry of adenovirus vectors into well-differentiated airway epithelium is responsible for inefficient gene transfer. Journal of virology **72:**6014-23.

150. **Pierrou, S., M. Hellqvist, L. Samuelsson, S. Enerback, and P. Carlsson.** 1994. Cloning and characterization of seven human forkhead proteins: binding site specificity and DNA bending. EMBO J **13:**5002-12.

151. **Porotto, M., M. Murrell, O. Greengard, and A. Moscona.** 2003. Triggering of human parainfluenza virus 3 fusion protein (F) by the hemagglutinin-neuraminidase (HN) protein: an HN mutation diminishes the rate of F activation and fusion. J Virol **77:**3647-54.

152. **Power, U. F., K. W. Ryan, and A. Portner.** 1992. The P genes of human parainfluenza virus type 1 clinical isolates are polycistronic and microheterogeneous. Virology **189:**340-3.

153. **Ray, R., B. J. Glaze, and R. W. Compans.** 1988. Role of individual glycoproteins of human parainfluenza virus type 3 in the induction of a protective immune response. J Virol **62:**783-7.

154. **Reed, G., P. H. Jewett, J. Thompson, S. Tollefson, and P. F. Wright.** 1997. Epidemiology and clinical impact of parainfluenza virus infections in otherwise healthy infants and young children < 5 years old. J Infect Dis **175:**807-13.

155. **Reid, S. P., L. W. Leung, A. L. Hartman, O. Martinez, M. L. Shaw, C. Carbonnelle, V. E. Volchkov, S. T. Nichol, and C. F. Basler.** 2006. Ebola virus VP24 binds karyopherin alpha1 and blocks STAT1 nuclear accumulation. J Virol **80:**5156-67.

156. **Sakaguchi, T., A. Kato, F. Sugahara, Y. Shimazu, M. Inoue, K. Kiyotani, Y. Nagai, and T. Yoshida.** 2005. AIP1/Alix is a binding partner of Sendai virus C protein and facilitates virus budding. J Virol **79:**8933-41.

157. **Sakai, K., Y. Kawaguchi, Y. Kishino, and H. Kido.** 1993. Electron immunohistochemical localization in rat bronchiolar epithelial cells of tryptase Clara, which determines the pneumotropism and pathogenicity of Sendai virus and influenza virus. J Histochem Cytochem **41:**89-93.

158. **Samuel, C. E.** 2001. Antiviral actions of interferons. Clin Microbiol Rev **14:**778-809.

159. **Samuel, C. E.** 2001. Antiviral actions of interferons. Clin Microbiol Rev **14:**778-809, table of contents.

160. **Sanda, C., P. Weitzel, T. Tsukahara, J. Schaley, H. J. Edenberg, M. A. Stephens, J. N. McClintick, L. M. Blatt, L. Li, L. Brodsky, and M. W. Taylor.** 2006. Differential gene induction by type I and type II interferons and their combination. J Interferon Cytokine Res **26:**462-72.

161. **Sandelin, A., W. Alkema, P. Engstrom, W. W. Wasserman, and B. Lenhard.** 2004. JASPAR: an open-access database for eukaryotic transcription factor binding profiles. Nucleic Acids Res **32:**D91-4.

162. **Santoro, M. M., T. Samuel, T. Mitchell, J. C. Reed, and D. Y. Stainier.** 2007. Birc2 (cIap1) regulates endothelial cell integrity and blood vessel homeostasis. Nat Genet **39:**1397-402.

163. **Sato, M., H. Suemori, N. Hata, M. Asagiri, K. Ogasawara, K. Nakao, T. Nakaya, M. Katsuki, S. Noguchi, N. Tanaka, and T. Taniguchi.** 2000. Distinct and essential roles of transcription factors IRF-3 and IRF-7 in response to viruses for IFN-alpha/beta gene induction. Immunity **13:**539-48.

164. **Schjerven, H., P. Brandtzaeg, and F. E. Johansen.** 2003. Hepatocyte NF-1 and STAT6 cooperate with additional DNA-binding factors to activate transcription of the human polymeric Ig receptor gene in response to IL-4. J Immunol **170:**6048-56.

165. **Schlee, M., A. Roth, V. Hornung, C. A. Hagmann, V. Wimmenauer, W. Barchet, C. Coch, M. Janke, A. Mihailovic, G. Wardle, S. Juranek, H. Kato, T. Kawai, H. Poeck, K. A. Fitzgerald, O. Takeuchi, S. Akira, T. Tuschl, E. Latz, J. Ludwig, and G. Hartmann.** 2009. Recognition of 5' triphosphate by RIG-I helicase requires short blunt double-stranded RNA as contained in panhandle of negative-strand virus. Immunity **31:**25-34.

166. **Schultz-Cherry, S., N. Dybdahl-Sissoko, G. Neumann, Y. Kawaoka, and V. S. Hinshaw.** 2001. Influenza virus ns1 protein induces apoptosis in cultured cells. J Virol **75:**7875-81.

167. **Seth, R. B., L. Sun, C. K. Ea, and Z. J. Chen.** 2005. Identification and characterization of MAVS, a mitochondrial antiviral signaling protein that activates NF-kappaB and IRF 3. Cell **122:**669-82.

168. **Skiadopoulos, M. H., S. R. Surman, J. M. Riggs, C. Orvell, P. L. Collins, and B. R. Murphy.** 2002. Evaluation of the replication and immunogenicity of recombinant human parainfluenza virus type 3 vectors expressing up to three foreign glycoproteins. Virology **297:**136-52.

169. **Skiadopoulos, M. H., T. Tao, S. R. Surman, P. L. Collins, and B. R. Murphy.** 1999. Generation of a parainfluenza virus type 1 vaccine candidate by replacing

the HN and F glycoproteins of the live-attenuated PIV3 cp45 vaccine virus with their PIV1 counterparts. Vaccine **18:**503-10.

170. **Skiadopoulos, M. H., L. Vogel, J. M. Riggs, S. R. Surman, P. L. Collins, and B. R. Murphy.** 2003. The genome length of human parainfluenza virus type 2 follows the rule of six, and recombinant viruses recovered from non-polyhexameric-length antigenomic cDNAs contain a biased distribution of correcting mutations. J Virol **77:**270-9.

171. **Slobod, K. S., J. L. Shenep, J. Lujan-Zilbermann, K. Allison, B. Brown, R. A. Scroggs, A. Portner, C. Coleclough, and J. L. Hurwitz.** 2004. Safety and immunogenicity of intranasal murine parainfluenza virus type 1 (Sendai virus) in healthy human adults. Vaccine **22:**3182-6.

172. **Smith, C. B., R. H. Purcell, J. A. Bellanti, and R. M. Chanock.** 1966. Protective effect of antibody to parainfluenza type 1 virus. N Engl J Med **275:**1145-52.

173. **Spann, K. M., K. C. Tran, B. Chi, R. L. Rabin, and P. L. Collins.** 2004. Suppression of the induction of alpha, beta, and lambda interferons by the NS1 and NS2 proteins of human respiratory syncytial virus in human epithelial cells and macrophages. J Virol **78:**4363-9.

174. **Spann, K. M., K. C. Tran, and P. L. Collins.** 2005. Effects of nonstructural proteins NS1 and NS2 of human respiratory syncytial virus on interferon regulatory factor 3, NF-kappaB, and proinflammatory cytokines. J Virol **79:**5353-62.

175. **Spriggs, M. K., B. R. Murphy, G. A. Prince, R. A. Olmsted, and P. L. Collins.** 1987. Expression of the F and HN glycoproteins of human parainfluenza virus type 3 by recombinant vaccinia viruses: contributions of the individual proteins to host immunity. J Virol **61:**3416-23.

176. **Stojdl, D. F., B. D. Lichty, B. R. tenOever, J. M. Paterson, A. T. Power, S. Knowles, R. Marius, J. Reynard, L. Poliquin, H. Atkins, E. G. Brown, R. K. Durbin, J. E. Durbin, J. Hiscott, and J. C. Bell.** 2003. VSV strains with defects in their ability to shutdown innate immunity are potent systemic anti-cancer agents. Cancer Cell **4:**263-75.

177. **Stollar, B. D., and V. Stollar.** 1970. Immunofluorescent demonstration of double-stranded RNA in the cytoplasm of Sindbis virus-infected cells. Virology **42:**276-80.

178. **Strahle, L., D. Garcin, P. Le Mercier, J. F. Schlaak, and D. Kolakofsky.** 2003. Sendai virus targets inflammatory responses, as well as the interferon-induced antiviral state, in a multifaceted manner. J Virol **77:**7903-13.

179. **Strahle, L., J. B. Marq, A. Brini, S. Hausmann, D. Kolakofsky, and D. Garcin.** 2007. Activation of the beta interferon promoter by unnatural Sendai virus infection requires RIG-I and is inhibited by viral C proteins. J Virol **81:**12227-37.

180. **Takahasi, K., M. Yoneyama, T. Nishihori, R. Hirai, H. Kumeta, R. Narita, M. Gale, Jr., F. Inagaki, and T. Fujita.** 2008. Nonself RNA-Sensing Mechanism of RIG-I Helicase and Activation of Antiviral Immune Responses. Mol Cell **29:**428-40.

181. **Takeuchi, K., T. Komatsu, Y. Kitagawa, K. Sada, and B. Gotoh.** 2008. Sendai virus C protein plays a role in restricting PKR activation by limiting the generation of intracellular double-stranded RNA. J Virol **82:**10102-10.

182. **Talon, J., C. M. Horvath, R. Polley, C. F. Basler, T. Muster, P. Palese, and A. Garcia-Sastre.** 2000. Activation of interferon regulatory factor 3 is inhibited by the influenza A virus NS1 protein. J Virol **74:**7989-96.

183. **Taniguchi, T., and A. Takaoka.** 2002. The interferon-alpha/beta system in antiviral responses: a multimodal machinery of gene regulation by the IRF family of transcription factors. Curr Opin Immunol **14:**111-6.

184. **Tao, T., F. Davoodi, C. J. Cho, M. H. Skiadopoulos, A. P. Durbin, P. L. Collins, and B. R. Murphy.** 2000. A live attenuated recombinant chimeric parainfluenza virus (PIV) candidate vaccine containing the hemagglutinin-neuraminidase and fusion glycoproteins of PIV1 and the remaining proteins from PIV3 induces resistance to PIV1 even in animals immune to PIV3. Vaccine **18:**1359-66.

185. **Tapparel, C., S. Hausmann, T. Pelet, J. Curran, D. Kolakofsky, and L. Roux.** 1997. Inhibition of Sendai virus genome replication due to promoter-increased selectivity: a possible role for the accessory C proteins. J Virol **71:**9588-99.

186. **Tapparel, C., D. Maurice, and L. Roux.** 1998. The activity of Sendai virus genomic and antigenomic promoters requires a second element past the leader template regions: a motif (GNNNNN)3 is essential for replication. J Virol **72:**3117-28.

187. **Terenzi, F., D. J. Hui, W. C. Merrick, and G. C. Sen.** 2006. Distinct induction patterns and functions of two closely related interferon-inducible human genes, ISG54 and ISG56. J Biol Chem **281:**34064-71.

188. **Thanos, D., and T. Maniatis.** 1995. NF-kappa B: a lesson in family values. Cell **80:**529-32.

189. **Thomas, L. R., A. Henson, J. C. Reed, F. R. Salsbury, and A. Thorburn.** 2004. Direct binding of Fas-associated death domain (FADD) to the tumor necrosis factor-related apoptosis-inducing ligand receptor DR5 is regulated by the death effector domain of FADD. J Biol Chem **279:**32780-5.

190. **Tojima, Y., A. Fujimoto, M. Delhase, Y. Chen, S. Hatakeyama, K. Nakayama, Y. Kaneko, Y. Nimura, N. Motoyama, K. Ikeda, M. Karin, and M. Nakanishi.** 2000. NAK is an IkappaB kinase-activating kinase. Nature **404:**778-82.

191. **Tsai, K. S., and R. G. Thomson.** 1975. Bovine parainfluenza type 3 virus infection: virus replication in bovine embryonic cell cultures and virion separation by rate-zonal centrifugation. Infect Immun **11:**770-82.

192. **Van Cleve, W., E. Amaro-Carambot, S. R. Surman, J. Bekisz, P. L. Collins, K. C. Zoon, B. R. Murphy, M. H. Skiadopoulos, and E. J. Bartlett.** 2006. Attenuating mutations in the P/C gene of human parainfluenza virus type 1 (HPIV1) vaccine candidates abrogate the inhibition of both induction and signaling of type I interferon (IFN) by wild-type HPIV1. Virology **352:**61-73.

193. **Vlieghe, D., A. Sandelin, P. J. De Bleser, K. Vleminckx, W. W. Wasserman, F. van Roy, and B. Lenhard.** 2006. A new generation of JASPAR, the open-

access repository for transcription factor binding site profiles. Nucleic Acids Res **34:**D95-7.

194. **Vulliemoz, D., and L. Roux.** 2001. "Rule of six": how does the Sendai virus RNA polymerase keep count? J Virol **75:**4506-18.

195. **Wang, Q., D. R. Nagarkar, E. R. Bowman, D. Schneider, B. Gosangi, J. Lei, Y. Zhao, C. L. McHenry, R. V. Burgens, D. J. Miller, U. Sajjan, and M. B. Hershenson.** 2009. Role of double-stranded RNA pattern recognition receptors in rhinovirus-induced airway epithelial cell responses. J Immunol **183:**6989-97.

196. **Wang, X., M. Li, H. Zheng, T. Muster, P. Palese, A. A. Beg, and A. Garcia-Sastre.** 2000. Influenza A virus NS1 protein prevents activation of NF-kappaB and induction of alpha/beta interferon. J Virol **74:**11566-73.

197. **Weber, F., A. Bridgen, J. K. Fazakerley, H. Streitenfeld, N. Kessler, R. E. Randall, and R. M. Elliott.** 2002. Bunyamwera bunyavirus nonstructural protein NSs counteracts the induction of alpha/beta interferon. J Virol **76:**7949-55.

198. **Weber, F., G. Kochs, and O. Haller.** 2004. Inverse interference: how viruses fight the interferon system. Viral Immunol **17:**498-515.

199. **Weber, F., V. Wagner, S. B. Rasmussen, R. Hartmann, and S. R. Paludan.** 2006. Double-stranded RNA is produced by positive-strand RNA viruses and DNA viruses but not in detectable amounts by negative-strand RNA viruses. J Virol **80:**5059-64.

200. **Wei, C., J. Li, and R. E. Bumgarner.** 2004. Sample size for detecting differentially expressed genes in microarray experiments. BMC Genomics **5:**87.

201. **Westaway, E. G., J. M. Mackenzie, M. T. Kenney, M. K. Jones, and A. A. Khromykh.** 1997. Ultrastructure of Kunjin virus-infected cells: colocalization of NS1 and NS3 with double-stranded RNA, and of NS2B with NS3, in virus-induced membrane structures. J Virol **71:**6650-61.

202. **Whitlow, Z. W., J. H. Connor, and D. S. Lyles.** 2008. New mRNAs are preferentially translated during vesicular stomatitis virus infection. J Virol **82:**2286-94.

203. **Wilkins, C., and M. Gale, Jr.** Recognition of viruses by cytoplasmic sensors. Curr Opin Immunol **22:**41-7.

204. **Won, S., T. Ikegami, C. J. Peters, and S. Makino.** 2007. NSm protein of Rift Valley fever virus suppresses virus-induced apoptosis. J Virol **81:**13335-45.

205. **Wright, P. F., M. R. Ikizler, R. A. Gonzales, K. N. Carroll, J. E. Johnson, and J. A. Werkhaven.** 2005. Growth of respiratory syncytial virus in primary epithelial cells from the human respiratory tract. J Virol **79:**8651-4.

206. **Wyatt, L. S., B. Moss, and S. Rozenblatt.** 1995. Replication-deficient vaccinia virus encoding bacteriophage T7 RNA polymerase for transient gene expression in mammalian cells. Virology **210:**202-5.

207. **Xu, L. G., Y. Y. Wang, K. J. Han, L. Y. Li, Z. Zhai, and H. B. Shu.** 2005. VISA is an adapter protein required for virus-triggered IFN-beta signaling. Mol Cell **19:**727-40.

208. **Yang, M. R., S. R. Lee, W. Oh, E. W. Lee, J. Y. Yeh, J. J. Nah, Y. S. Joo, J. Shin, H. W. Lee, S. Pyo, and J. Song.** 2008. West Nile virus capsid protein

induces p53-mediated apoptosis via the sequestration of HDM2 to the nucleolus. Cell Microbiol **10:**165-76.

209. **Yang, Y. L., L. F. Reis, J. Pavlovic, A. Aguzzi, R. Schafer, A. Kumar, B. R. Williams, M. Aguet, and C. Weissmann.** 1995. Deficient signaling in mice devoid of double-stranded RNA-dependent protein kinase. EMBO J **14:**6095-106.

210. **Yie, J., K. Senger, and D. Thanos.** 1999. Mechanism by which the IFN-beta enhanceosome activates transcription. Proc Natl Acad Sci U S A **96:**13108-13.

211. **Yin, H. S., R. G. Paterson, X. Wen, R. A. Lamb, and T. S. Jardetzky.** 2005. Structure of the uncleaved ectodomain of the paramyxovirus (hPIV3) fusion protein. Proc Natl Acad Sci U S A **102:**9288-93.

212. **Yoneyama, M., and T. Fujita.** 2007. Function of RIG-I-like receptors in antiviral innate immunity. J Biol Chem **282:**15315-8.

213. **Yoneyama, M., M. Kikuchi, K. Matsumoto, T. Imaizumi, M. Miyagishi, K. Taira, E. Foy, Y. M. Loo, M. Gale, Jr., S. Akira, S. Yonehara, A. Kato, and T. Fujita.** 2005. Shared and unique functions of the DExD/H-box helicases RIG-I, MDA5, and LGP2 in antiviral innate immunity. J Immunol **175:**2851-8.

214. **Yoneyama, M., M. Kikuchi, T. Natsukawa, N. Shinobu, T. Imaizumi, M. Miyagishi, K. Taira, S. Akira, and T. Fujita.** 2004. The RNA helicase RIG-I has an essential function in double-stranded RNA-induced innate antiviral responses. Nat Immunol **5:**730-7.

215. **Yoon, C. H., E. S. Lee, D. S. Lim, and Y. S. Bae.** 2009. PKR, a p53 target gene, plays a crucial role in the tumor-suppressor function of p53. Proc Natl Acad Sci U S A **106:**7852-7.

216. **Young, D. F., L. Didcock, S. Goodbourn, and R. E. Randall.** 2000. Paramyxoviridae use distinct virus-specific mechanisms to circumvent the interferon response. Virology **269:**383-90.

217. **Yount, J. S., L. Gitlin, T. M. Moran, and C. B. Lopez.** 2008. MDA5 participates in the detection of paramyxovirus infection and is essential for the early activation of dendritic cells in response to Sendai Virus defective interfering particles. J Immunol **180:**4910-8.

218. **Zamanian-Daryoush, M., T. H. Mogensen, J. A. DiDonato, and B. R. Williams.** 2000. NF-kappaB activation by double-stranded-RNA-activated protein kinase (PKR) is mediated through NF-kappaB-inducing kinase and IkappaB kinase. Mol Cell Biol **20:**1278-90.

219. **Zhang, L., M. E. Peeples, R. C. Boucher, P. L. Collins, and R. J. Pickles.** 2002. Respiratory syncytial virus infection of human airway epithelial cells is polarized, specific to ciliated cells, and without obvious cytopathology. J Virol **76:**5654-66.

220. **Zhirnov, O. P., T. E. Konakova, T. Wolff, and H. D. Klenk.** 2002. NS1 protein of influenza A virus down-regulates apoptosis. J Virol **76:**1617-25.